The evolution of cavitation resistance in conifers

Maximilian Larter

THESE

Pour obtenir le grade de

DOCTEUR DE L'UNIVERSITE DE BORDEAUX

Spécialité : Ecologie évolutive, fonctionnelle et des communautés

Ecole doctorale: Sciences et Environnements

Evolution de la résistance à la cavitation chez les conifères

The evolution of cavitation resistance in conifers

Maximilian LARTER

Directeur : Sylvain DELZON (DR INRA)
Co-Directeur : Jean-Christophe DOMEC (Professeur, BSA)

Soutenue le 22/07/2016
Devant le jury composé de :
Rapporteurs :
Mme Amy ZANNE, Prof., George Washington University
Mr Jordi MARTINEZ VILALTA, Prof., Universitat Autonoma de Barcelona
Examinateurs :
Mme Lisa WINGATE, CR INRA, UMR ISPA, Bordeaux
Mr Jérôme CHAVE, DR CNRS, UMR EDB, Toulouse

Title: The evolution of cavitation resistance in conifers

Abstract

Forests worldwide are at increased risk of widespread mortality due to intense drought under current and future climate change. In particular, conifer species seem extremely vulnerable to mortality due to hydraulic failure or embolism. The main objective of this thesis was to examine conifer resistance to embolism in an evolutionary framework. Firstly, we uncovered 9-fold variation in resistance to embolism across 250 species from the 7 conifer families, culminating in a new world record in *Callitris tuberculata* (P_{50} = -18.8 MPa). We demonstrated the evolutionary relationship between increased embolism resistance and the anatomy of bordered pits. By combining this unprecedented physiological dataset with a time-calibrated phylogeny of over 300 species, we retraced conifer diversification and the evolution of embolism resistance. We discovered multiple evolutionary dynamics with several conifer lineages shifting to higher rates of speciation and trait evolution. We found that conifers with high drought resistance diversified more rapidly, especially crown groups of Cupressaceae composed of the *Cupressus-Juniperus* clade and the *Callitris* clade. Within this last group, diversification rates increased over the course of the aridification of Australia over the last 30 million years. We show how their xylem has been shaped by drought, becoming more resistant to embolism, but crucially we found no trade-off with water transport efficiency or construction costs. This work greatly expands our understanding of how vascular plants have evolved to cope with extreme drought.

Key words: embolism, drought, evolution, conifer, xylem, climate change

Titre: Evolution de la résistance à la cavitation chez les conifères

Résumé

Les forêts du monde entier sont menacées de mortalités importantes lors de sécheresses intenses liés au changement climatique. Les conifères en particulier semblent extrêmement vulnérables à la mort par dysfonctionnement hydraulique de leur système vasculaire ou embolie. Le principal objectif de cette thèse est d'étudier la résistance à l'embolie des conifères dans un cadre évolutif. Premièrement, nous avons mis en évidence que la résistance à l'embolie varie d'un facteur neuf sur plus de 250 espèces parmi les 7 familles de conifères, atteignant un nouveau record du monde avec *Callitris tuberculata* (P_{50} = -18.8 MPa). Nous avons montré le lien évolutif entre cette résistance et l'anatomie des ponctuations aréolées. En combinant cette base de données unique avec une phylogénie calibrée de plus de 300 espèces, nous avons retracé la diversification des conifères et l'évolution de leur résistance à l'embolie. Nous avons découvert que plusieurs lignées de conifères ont brusquement changé de dynamiques évolutives, avec l'accélération de la spéciation et de l'évolution de résistance à l'embolie. En outre, les conifères plus résistants se sont diversifié plus rapidement, notamment les genres *Cupressus*, *Juniperus* et *Callitris* (Cupressaceae). La diversification de ces derniers s'est accélérée avec l'aridification de l'Australie sur les derniers 30 Millions d'années. Nous montrons que leur xylème a été façonné par la sécheresse, devenant plus résistant à l'embolie mais surtout sans compromettre l'efficience du transport de l'eau ou augmenter son coût de construction. Cette thèse élargit notre compréhension de l'évolution des plantes vasculaire face aux sécheresses intenses.

Mots clés: embolie, sécheresse, évolution, conifères, xylème, changement climatique

BIOGECO

[Biodiversité, gènes et communautés, UMR 1202, 33610 Pessac, France]

Résumé substantiel

I. Introduction/contexte :

Le changement du climat causé par l'activité humaine va entraîner, au cours des décennies à venir, des sécheresses et des canicules plus intenses, plus fréquentes et plus longues, avec des conséquences lourdes pour les écosystèmes du monde entier (Stocker et al., 2013). On dénombre notamment de nombreux épisodes de mortalités importantes d'arbres (notamment de conifères) dans les forêts à travers le monde (Allen et al., 2010). Ceci pourrait entrainer des conséquences importantes sur l'activité économique de ces régions, leur biodiversité et plus largement sur les cycles de l'eau et du carbone. Chez les arbres, il semble que le dysfonctionnent hydraulique lié au phénomène de « cavitation » est la cause majeure de mortalité lors de sècheresses intenses (Anderegg et al., 2016), seul ou en interaction avec d'autres phénomènes (McDowell et al., 2008; Sala et al., 2010). D'après la théorie de « Cohésion-Tension », le mouvement de l'eau dans les plantes est gouverné par l'évaporation d'eau par les stomates qui créé une dépression et tire l'eau à travers le système vasculaire : le xylème (Dixon, 1914; Tyree and Zimmermann, 2002). Ce mécanisme met sous tension la colonne d'eau dans la plante (pression négative, en MegaPascals), qui est maintenue en cet état métastable par les fortes liaisons hydrogène entre les molécules d'eau. Lorsque la demande évaporative augmente lors de sécheresses, la vaporisation de l'eau à cause de la tension excessive (ou « cavitation ») crée des embolies qui viennent boucher les éléments conducteurs de sève (trachéides et vaisseaux), limitant l'apport en eau aux parties aériennes (Tyree and Sperry, 1989).

Il existe un seuil de réduction de la conductance du xylème au-delà duquel les arbres sont incapables de survivre (Brodribb et al., 2010; Urli et al., 2013) : chez les conifères, on mesure P_{50} (MPa), la pression à laquelle 50% des trachéides sont « embolisés ». Ce paramètre directement lié à valeur sélective des espèces varie largement entre espèces au sein du taxon des conifères (Maherali et al., 2004), mais cette variation n'est pas uniformément distribuée. Par exemple, le genre *Pinus* et plus largement à l'échelle de la famille, les Pinaceae montrent très peu de variabilité pour ce trait (Delzon et al., 2010). Au sein des espèces, il semble qu'il y'ait relativement peu de différentiation génétique, ce qui indique des contraintes évolutives (Lamy et al., 2011). A l'opposé, les Cupressaceae peuvent être très vulnérables (*Taxodium distichum*) ou très résistants (*Callitris columellaris*) (Pittermann et al., 2012).

Il apparaît donc un besoin crucial de mieux comprendre le fonctionnement des plantes lors de sècheresses extrêmes, afin de mieux prédire l'impact du changement climatique sur les écosystèmes forestiers. De plus, étudier l'évolution du xylème et de sa capacité à résister à la cavitation peut nous permettre de comprendre comment certains groupes d'espèces sont devenus exceptionnellement

résistants. L'objectif de cette thèse est donc d'examiner la résistance à la cavitation des conifères dans un contexte évolutif. Pour cela, nous avons allié une stratégie d'échantillonnage et de phénotypage d'un maximum d'espèces de conifères couvrant l'ensemble de la diversité taxonomique de ce groupe et des outils de la biologie comparative utilisant la phylogénétique.

Quels groupes de conifères ont évolué vers un xylème extrêmement résistant à la cavitation ? Quelles modifications au niveau du xylème sont liées à cette évolution (anatomie des ponctuations aréolées, dimensions des trachéides, densité du bois, conductance hydraulique) ? Quel est le rôle du climat dans cette évolution et à quel moment a-t-elle eu lieu ? Pour répondre à ces questions, cette thèse est organisée en trois parties : i) nous présentons d'abord la grande variabilité de l'écophysiologie des conifères grâce à une base de données sans précèdent; puis ii) dans une seconde partie, grâce à une nouvelle phylogénie pour plus de 300 espèces de conifères, nous montrons l'existence de plusieurs dynamiques évolutives chez les conifères, avec un lien entre résistance à la cavitation et diversification et iii) dans la dernière partie, nous détaillons la radiation évolutive du genre *Callitris* lors de l'aridification du continent Australien, accompagné d'une transition remarquable vers un xylème adapté aux conditions de sécheresses extrêmes.

II. La variabilité globale de l'écophysiologie des conifères

Nous avons mesuré P_{50} de plus de 270 espèces de conifères (des sept familles et 63 sur 70 genres existante – Chapitre 1) avec la technique du CAVITRON (Cochard et al., 2005). Ce paramètre de résistance à la cavitation varie d'un facteur dix, de -1.6 à -18.8 MPa. La majeure partie de cette variabilité est limitée aux Cupressaceae, Taxaceae et Podocarpaceae, et nous avons trouvé très peu de variation pour ce trait au sein des Pinaceae et Araucariaceae. Les espèces du biome méditerranéen sont par ailleurs les plus résistantes, bien qu'une large variation soit évidente au sein de chaque biome (à part le biome boréal). La théorie prévoit qu'une forte résistance à la cavitation est liée à un coût de construction du bois plus important, pour résister aux fortes tensions présentes dans le xylème. Nous avons vérifié cette hypothèse avec un lien entre densité du bois et P_{50} – en fait, une forte résistance à la sécheresse implique un bois plus dense, mais le corolaire n'est pas vrai, puisqu'il existe des espèces vulnérables à bois extrêmement dense. Par contre, il n'y a pas de réduction de la conductivité du xylème avec l'augmentation de la résistance à la cavitation. Ces relations sont maintenues lorsque l'on tient compte de la proximité phylogénétique des espèces. A l'échelle des conifères, l'évolution de ce trait ne semble pas être contrainte, puisque nous avons découvert peu de signal phylogénétique, c'est-à-dire que les espèces proches sont moins similaires qu'attendu sous un modèle évolutif simple. Nous avons découvert en Australie le record du monde de résistance à la cavitation, *Callitris tuberculata*, qui a évolué pour atteindre une barrière physique limitant le transport de la sève chez les arbres à la limite

du désert (Chapitre 2). Sa P_{50} de -18,8 MPa indique qu'il est capable de transporter de l'eau à des pressions proches du point de vaporisation de l'eau à température ambiante. Enfin, grâce à des observations au microscope électronique à balayage nous avons mis en évidence une corrélation entre évolution de la résistance à la cavitation et l'anatomie fine du xylème (Chapitre 3). Chez les conifères, les pores entre trachéides comportent une membrane poreuse (margo) et un épaississement central (le torus) qui est dévié pour venir se plaquer sur l'ouverture du pore lorsque la pression devient intenable dans un des trachéides (Pittermann et al., 2005). La ponctuation agit alors comme une valve, empêchant la propagation de l'embolie. Nous avons montré que l'évolution d'une forte résistance à la cavitation est liée à une évolution du degré de recouvrement du pore par le torus (l'efficacité de l'effet « valve »).

III. Evolution de la résistance à la sécheresse et diversification des conifères.

Pour replacer cette variabilité écophysiologique dans un contexte évolutif, nous avons établi une phylogénie moléculaire de 300 espèces de conifères, en utilisant des séquences de plusieurs gènes disponibles sur des banques de données en ligne (Chapitre 4). Les branches de cette phylogénie ont ensuite été transformées pour représenter des millions d'années en utilisant des fossiles datés comme points de calibration. En se basant sur ce travail, nous avons ensuite modélisé la diversification des conifères et l'évolution de P_{50} en utilisant une méthode Bayésienne (BAMM ; Rabosky et al., 2013; Rabosky, 2014) qui évalue des modèles complexes ou chaque portion de la phylogénie peut appartenir à une dynamique macro-évolutive propre. Nous avons découvert de multiples dynamiques de diversification, avec par exemple une forte augmentation du renouvellement de certaines lignées de Pinaceae (plus forts taux de spéciation et d'extinction au sein du groupe *Picea*-*Pinus*) depuis 150 millions d'années. En parallèle, la famille des Podocarpaceae a vu son taux de diversification nettement augmenter il y a 70 millions d'années. Ceci est probablement grâce à sa compétitivité face à la domination des plantes à fleurs à cette période, via une augmentation de sa surface photosynthétique (Biffin et al., 2012). Enfin, nous avons mis en évidence deux sauts de diversification parallèles dans les « groupes-couronnes » de la famille : Cupressaceae, dans l'hémisphère nord (sous-familles Cupressoidae) et l'hémisphère Sud (sous-famille Callitroidae). Ces dynamiques évolutives de diversification accélérées sont apparues il y a environ 50 millions d'années, ce qui correspond à une période de refroidissement et de modification des régimes hydriques au niveau global. Nous montrons aussi que sur cette même période, le taux d'évolution de la résistance à la cavitation de ces deux groupes a explosé, notamment sur les dernières 30 millions d'années. Ces résultats semblent confirmer que la résistance à la cavitation a conféré à ces deux groupes écologiquement similaires un fort succès évolutif leur permettant se diversifier en colonisant les milieux arides qui ont commencé à apparaître à partir de la fin de l'Eocène. Ce lien a ensuite été confirmé en utilisant un autre modèle

(QUASSE ; FitzJohn, 2012) qui a confirmé le lien étroit dans notre étude entre un taux de diversification élevé et une forte résistance à la cavitation.

IV. La radiation évolutive de *Callitris* face à l'aridification de l'Australie

Le groupe-couronne de la sous-famille Callitroidae comprend une vingtaine d'espèces (des genres *Callitris*, *Actinostrobus* et *Neocallitropsis*) distribuées à travers l'Australie et la Nouvelle-Calédonie. Avec le record du monde de résistance à la cavitation à la limite du désert Australien et des espèces tropicales de forêt humide, ce groupe est un candidat idéal pour étudier en détail l'évolution du xylème lors d'une radiation évolutive vers les milieux arides. Nous avons donc mesuré pour toutes les espèces de ce groupe la résistance à la cavitation, la conductance hydraulique du xylème et différents paramètres anatomiques du xylème (Chapitre 5). Grâce à une nouvelle phylogénie, nous montrons que la diversification de ce groupe suit l'aridification de l'Australie, d'abord graduellement aux alentours de 30 millions d'années, puis très rapidement au cours des dernières 15 millions d'années. En parallèle, la résistance à la cavitation s'est décuplée, pour passer d'environ -4 MPa chez les espèces de Nouvelle-Calédonie à plus de -15 MPa chez plusieurs espèces du continent Australien. Grâce à des données climatiques pour toutes ces espèces, nous avons mis en évidence le rôle important du climat pour l'évolution du xylème (P_{50}, dimensions des trachéides) sans toutefois affecter la densité du bois ou l'efficience de transport de l'eau. Une nouvelle fois, nous n'avons trouvé aucune influence de la résistance à la cavitation sur la densité du bois d'une part ou la conductance hydraulique d'autre part. Il semble donc que ces espèces sont capables de développer une forte résistance à l'embolie sans affecter par ailleurs la performance de leur xylème, probablement grâce à des adaptations au niveau des ponctuations.

Conclusions et perspectives

Dans cette thèse, nous avons largement élargit notre connaissance du fonctionnement des conifères lors de sècheresses intenses, fournissant des données concrètes pour mieux modéliser et prédire la réponse des écosystèmes forestiers aux changements du climat. Nous avons clarifié les liens entre différents traits émergents du xylème, avec l'absence de relation entre résistance à la cavitation et efficience du transport de l'eau. Bien qu'une relation semble exister entre densité du bois et P_{50}, celle-ci n'est pas valable pour tous les conifères. La seule chose que l'on puisse dire est qu'il existe un seuil de densité de bois en dessous duquel une forte résistance à la cavitation ne peut exister. Grâce à la phylogénétique et à des approches de biologie évolutive, nous avons de plus montré le rôle de la sécheresse dans l'évolution des conifères, notamment chez les Cupressaceae, chez qui l'évolution de la résistance à la sécheresse au cours des dernières 50 millions d'années est accompagnée d'une rapide diversification. D'autres facteurs sont nécessaires pour expliquer la diversification des autres familles,

tels que l'apparition des Angiospermes pour les Podocarpaceae. La rapidité du changement climatique moderne pourrait fortement limiter la possibilité d'adaptation, et l'avenir semble incertain pour les nombreuses espèces de conifères déjà menacés d'extinction actuellement et à l'aire de répartition restreinte.

Bibliographie

Allen CD, Macalady AK, Chenchouni H, Bachelet D, McDowell N, Vennetier M, Kitzberger T, Rigling A, Breshears DD, Hogg EH (Ted), Gonzalez P, Fensham R, Zhang Z, Castro J, Demidova N, Lim J-H, Allard G, Running SW, Semerci A, Cobb N (2010) A global overview of drought and heat-induced tree mortality reveals emerging climate change risks for forests. Forest Ecology and Management **259**: 660–684

Anderegg WRL, Klein T, Bartlett M, Sack L, Pellegrini AFA, Choat B (2016) Meta-analysis reveals that hydraulic traits explain cross-species patterns of drought-induced tree mortality across the globe. Pnas. doi: 10.1073/pnas.1525678113

Biffin E, Brodribb TJ, Hill RS, Thomas P, Lowe AJ (2012) Leaf evolution in Southern Hemisphere conifers tracks the angiosperm ecological radiation. Proceedings Biological sciences / The Royal Society **279**: 341–8

Brodribb TJ, Bowman DJMS, Nichols S, Delzon S, Burlett R (2010) Xylem function and growth rate interact to determine recovery rates after exposure to extreme water deficit. The New phytologist **188**: 533–42

Cochard H, Damour G, Bodet C, Tharwat I, Poirier M, Améglio T (2005) Evaluation of a new centrifuge technique for rapid generation of xylem vulnerability curves. Physiologia Plantarum **124**: 410–418

Delzon S, Douthe C, Sala A, Cochard H (2010) Mechanism of water-stress induced cavitation in conifers: bordered pit structure and function support the hypothesis of seal capillary-seeding. Plant, cell & environment **33**: 2101–11

Dixon HH (1914) Transpiration and the ascent of sap in plants. MacMillan, London

FitzJohn RG (2012) Diversitree : comparative phylogenetic analyses of diversification in R. Methods in Ecology and Evolution **3**: 1084–1092

Lamy J-B, Bouffier L, Burlett R, Plomion C, Cochard H, Delzon S (2011) Uniform Selection as a Primary Force Reducing Population Genetic Differentiation of Cavitation Resistance across a Species Range. PLoS ONE **6**: e23476

Maherali H, Pockman WT, Jackson RB (2004) Adaptive variation in the vulnerability of woody plants to xylem cavitation. Ecology **85**: 2184–2199

McDowell N, Pockman WT, Allen CD, Breshears DD, Cobb N, Kolb T, Plaut J, Sperry J, West A, Williams DG, Yepez E a (2008) Mechanisms of plant survival and mortality during drought: why do some plants survive while others succumb to drought? The New phytologist **178**: 719–39

Pittermann J, Sperry JS, Hacke UG, Wheeler JK, Sikkema EH (2005) Torus-Margo Pits Help Conifers Compete with Angiosperms. Science **310**: 1924–1924

Pittermann J, Stuart SA, Dawson TE, Moreau A (2012) Cenozoic climate change shaped the evolutionary ecophysiology of the Cupressaceae conifers. Proceedings of the National Academy of Sciences of the United States of America **109**: 9647–52

Rabosky DL (2014) Automatic detection of key innovations, rate shifts, and diversity-dependence on phylogenetic trees. PloS one **9**: e89543

Rabosky DL, Santini F, Eastman J, Smith SA, Sidlauskas B, Chang J, Alfaro ME (2013) Rates of speciation and morphological evolution are correlated across the largest vertebrate radiation. Nature communications **4**: 1958

Sala A, Piper F, Hoch G (2010) Physiological mechanisms of drought-induced tree mortality are far from being resolved. The New phytologist **186**: 274–81

Stocker TF, Qin D, Plattner G-K, Tignor MM, Allen SK, Boschung J, Nauels A, Xia Y, Bex V, Midgley PM (2013) IPCC, 2013: Climate Change 2013: The Physical Science Basis. Contribution of Working Group I to the Fifth Assessment Report of the Intergovernmental Panel on Climate Change. Cambridge University Press, Cambridge, United Kingdom and New York, NY, USA

Tyree MT, Sperry JS (1989) Vulnerability of xylem to cavitation and embolism. Annual Review of Plant Biology **40**: 19–36

Tyree MT, Zimmermann MH (2002) Xylem Structure and the Ascent of Sap. Springer Science & Business Media

Urli M, Porté AJ, Cochard H, Guengant Y, Burlett R, Delzon S (2013) Xylem embolism threshold for catastrophic hydraulic failure in angiosperm trees. Tree physiology **33**: 672–83

Foreword

The work for this thesis was done within the BIOGECO research unit, and was supported by a competitive grant through the doctoral school program. The *Callitris* project (and my two month trip to Australia) was financed by a mobility grant from the LabEx COTE (ANR-10-LABX-45), and I obtained a grant from Western Sydney University (the Hawkesbury Institute for the Environment). This thesis is based on published articles (or in preparation) and is therefore mostly in English, but a substantial abstract is available in French.

Avant-propos

Cette thèse a été réalisée au sein de l'UMR BIOECO, et financée par une bourse ministérielle via le concours de l'école doctorale. J'ai effectué une mobilité de deux mois (mai-juillet 2014) en Australie grâce au soutien du LabEx COTE (ANR-10-LABX-45) et une bourse d'accueil pour jeunes chercheurs de Western Sydney University – Hawkesbury Institute for the Environment. J'ai fait le choix de rédiger une thèse sur articles, c'est-à-dire que le texte est composé des articles publiés ou en préparation, donc en anglais. Un résumé présentant le contexte et les objectifs de la thèse, ainsi que la méthodologie adoptée et les principaux résultats est néanmoins disponible en français.

Acknowledgements

Bon, bah voilà on dirait que c'est la bonne. « Enfin », comme diraient certain(e)s. Je ne fais pas trop dans le cérémonial, mais ça fait quand même un petit quelque chose. Y'a un paquet de gens à remercier, alors je vais pas y'aller par quatre chemins.

Sylvain, depuis les premiers cours avec toi en master, j'ai eu le feeling que tu faisais des trucs super cools, avec la patate et le sourire et j'ai pas été déçu. Mon stage de M2 paraît bien loin maintenant… mais j'aime toujours autant ce projet, qui a quand même pas mal évolué quand même. J'apprécie les petites discussions à la volée autour d'un café (ou en allant en chercher un), nos échanges à l'arrache par mail, et nos réunions improvisées, décalées, et qui finalement débordent et décalent la journée de tout le monde. J'en sors toujours la tête plus claire que quand j'y suis rentré, et je crois que j'ai toujours appris quelque chose. On verra quand ça sera bouclé pour de bon (et que tout sera publié…), mais j'ai l'impression que ça a bien fonctionné au final. Merci, donc, pour tout ça !

JC, tu as suivis de loin ce projet, qui était depuis le début plus celui de Sylvain. Je te remercie quand même chaleureusement pour les longues discussions qu'on a pu avoir de temps en temps, et la bouteille de bourbon que tu m'as ramené au tout début (je l'ai encore, faudra qu'on l'ouvre ensemble !). Et j'espère sincèrement qu'on puisse « vraiment » bosser ensemble un jour.

Annabel, j'ai trouvé, quand tu reviens je t'appelerai *jefe* (dis-moi que c'est pas pris, ça aussi) ! Tu m'as accueilli au labo chaleureusement alors que c'était pas forcément joué d'avance. Pour toutes les discussions à la rien avoir, et parfois à la avoir, pour ton amour du *Boss* du NJ, et pour les repas autour de ton dessous-de-toit, milles mercis. Tu gères, j'espère que tu reviendras des States requinquée, et j'oublie pas que je te dois toujours une publi…

Je ne vais pas faire un paragraphe par tête du labo non plus, donc à l'ancienne, et commençant par un ancien, JB je te remercie pour ton influence pendant mon stage, qui a surement aidé à me pousser à rempiler pour la thèse; Pauline pour nos collaborations – bon courage avec tous tes poulets ; Pim, mon basque préféré, pour ton sourire et les discussions « ru'by » ; Nadège et Nastasia pour votre accueil quand je pointe le bout de mon nez dans le bureau et les discussions folles sur la science, les burgers, et autres... Au labo (mais pas que) la folle équipe de Régis et Gaëlle, vous assurez toujours, merci pour les coups de main, les dépannages et tout ça. Petit

clin d'œil à Frédo à la densito, merci pour la réception chaleureuse à chaque fois dans ton atelier et ton aide plus que précieuse sur des centaines d'échantillons !

To all the other people in the lab I can't think of at the minute, many thanks for all the brilliant exchanges about science and other stuff, the coffee and croissants, or weird (lovely) biscuits (?) from the Spanish contingent, *muchísimas gracias* Torres, Noelia, Marta, you rock! Tim it was lovely having you around, thanks for the help on the "world record" paper, and I hope we can do some crazy *Callitris* stuff soon (science I mean).

A huge thank you to all the people who made my trip to Australia possible, especially Sebastian. We're going to get some more good papers out this project, just you wait! Also, I'll send you some drafts soon, haha! Anita, I can't thank you enough for driving around Australia with me, and I hope I can repay the favour someday.

It goes without saying, thanks to all my family, mum and dad especially for their unwavering faith that I wasn't a complete f*** up. Huge hugs to you guys, I love you. Alex et Agathe pour avoir supporté de m'héberger chez vous, puis chez nous, gros bisous et milles merci! Et oui merci et bisous à toi aussi, Fred ! Pour quoi ? Pour m'avoir donné le goût du doux liquide ambré venu d'Ecosse, pardi ! Héhé…

Enfin, last but not least, the hugest thanks to my lovely beautiful, you that make me so much better, push me on, and put up with all my crazy moments. This was only possible thanks to you, so you deserve a massive chunk of credit. I promise I'll buy you a goat (or two) to make up for it all, the late nights, the early mornings, leaving you to go to Australia, the "don't worry I'm nearly done" 's and all that. I love you!! (and rambam !)

Table of contents

Introduction

1. Climate change and drought-induced tree mortality by hydraulic failure

Anthropogenic climate change is challenging ecosystems across the world, forcing natural populations to adapt, migrate, or face extinction (Walther et al., 2002). The impacts of the changing climate are already evident in ecosystems across the planet, with coral-reef dieback due to ocean acidification and temperature rise (Hoegh-Guldberg et al., 2007), droughts affecting many terrestrial ecosystems (Allen et al., 2010; Zhao and Running, 2010) and extreme climatic events (droughts, heatwaves and storms) severely impacting human communities globally, through failing crops, cardiovascular and respiratory health issues and spreading of infectious diseases, storm damage and extensive flooding (Patz et al., 2005). As key members of forest ecosystems and important carbon sinks, tree species are the focal point of much research into the impact of climate change, and into patterns of species adaptability or migration capacity (Pearson, 2006; Aitken et al., 2008; Delzon et al., 2013). Visible worldwide, drought is having a dramatic impact on forest species, with high mortality rates recorded for example in western North-America (van Mantgem et al., 2009) or Canadian boreal forests (Peng et al., 2011), but also at a global scale across all eco-regions (Allen et al., 2010; Settele et al., 2014; Bennett et al., 2015; Fig. 1).

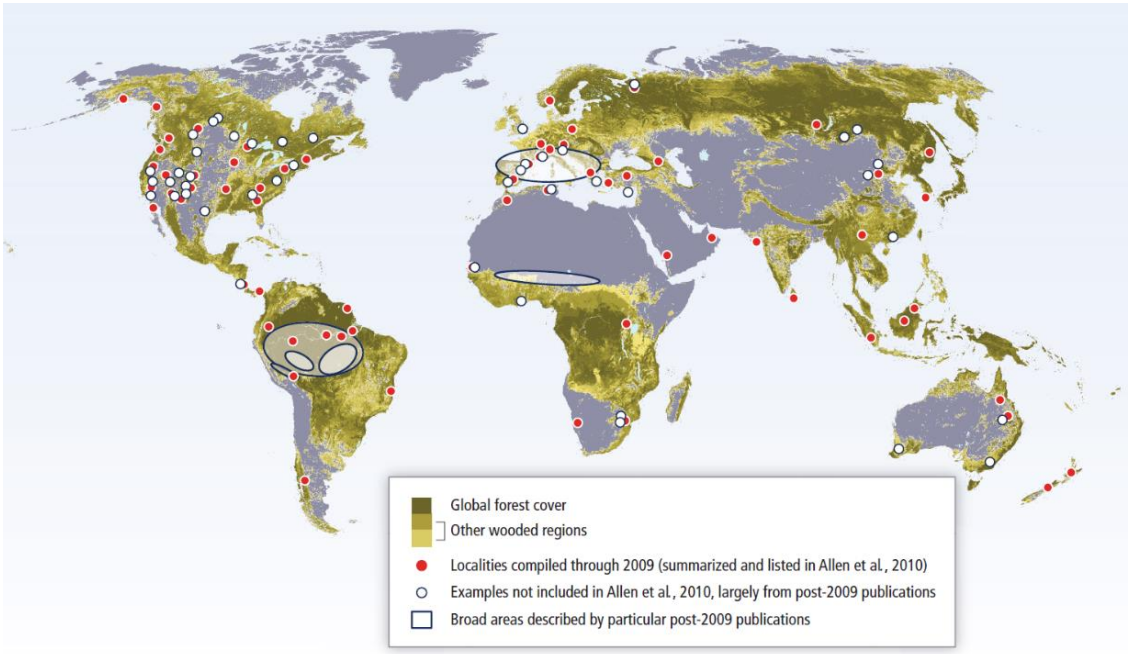

Figure 1. Forest ecosystems with reported drought or heat-induced mortality (since 1970), reproduced from (Settele et al., 2014). Background colours represent forest cover (grey is no forest cover). Red dots are taken from (Allen et al., 2010), white dots are compiled and listed in (Settele et al., 2014).

Worryingly, many regions are projected to suffer from more frequent, prolonged, and severe drought episodes (Stocker et al., 2013). These events can negatively impact photosynthesis and growth rates, potentially turning forests into carbon sources, and generally affecting the water and carbon cycles (Bonan, 2008; Kurz et al., 2008; Anderegg et al., 2015c). There is therefore an urgent need to further our knowledge and understanding of plants' response to drought, for example to improve modelling of their future distributions, predict areas of high mortality, plan ahead by selecting species and/or varieties in managed forests, and to assist in breeding programs for the forestry industry.

Response to prolonged water-stress involves mechanisms both passive and active at whole-plant, organ, cellular, and molecular levels, and therefore is necessarily complex and varies within a plant and between individuals and species (Levitt, 1980; Fang and Xiong, 2015). Although there is considerable debate as to what exactly kills a tree during drought (Sala et al., 2010; Anderegg et al., 2015b), catastrophic failure of the water-transport system due to drought-induced xylem embolism is emerging as the major driver of tree mortality (Anderegg et al., 2012; Anderegg and Anderegg, 2013; Balducci et al., 2014; Anderegg et al., 2015a; Rowland et al., 2015; Anderegg et al., 2016). Another leading cause is described as the "carbon-starvation" hypothesis (McDowell et al., 2008), which refers to the depletion of a plants' non-structural carbohydrate (NSC) reserves since plants cannot assimilate carbon at a high enough rate during drought (due to stomatal closure). However, recent studies have shown that i) trees subjected to drought die sooner than starved trees (Hartmann et al., 2013) and ii) tree mortality can be predicted exclusively using loss of vascular transport capacity due to embolism (Anderegg et al., 2015a) precise monitoring of the dynamics of NSC reserves in plants is challenging, and their exact role in survival during and/or after drought is unclear (Hartmann, 2015). Furthermore, there remains much disagreement between NSC measurement methods and even between labs using the same method on the same samples (Quentin et al., 2015). Additionally, complex interactions between hydraulic failure and carbon starvation are likely, and investigations into plant mortality during drought are further confounded by biotic attacks (Mitchell et al., 2013; Dickman et al., 2014; Sevanto et al., 2014; Gaylord et al., 2015; Hartmann et al., 2015). In contrast, there is strong evidence of a direct link between plant death and dramatic failure of water transport (Brodribb and Cochard, 2009; Brodribb et al., 2010; Urli et al., 2013), which is both well understood and is routinely measured worldwide to quantify plant drought-resistance (Sperry and Tyree, 1988; Cochard et al., 2013; Lens et al., 2013).

The upward flow of water through vascular tissue (xylem) in plants is driven by evaporation of water at the leaf surface, a process called transpiration. The depression caused by the surface-tension of each air/sap meniscus in the leaves creates a water-potential gradient throughout the plant (Fig. 2), gradually pulling up the water-column in the plant as water is lost to the atmosphere through evaporation. This is known as the Cohesion-Tension theory (Tyree, 1997; Angeles et al., 2004), because 1) this passive water-transport mechanism induces negative pressure - or tension - within the xylem sap, and 2) this transmission of tension through the plant is enabled by the cohesive forces (hydrogen bonds) that bind water molecules to each other and to the cell walls.

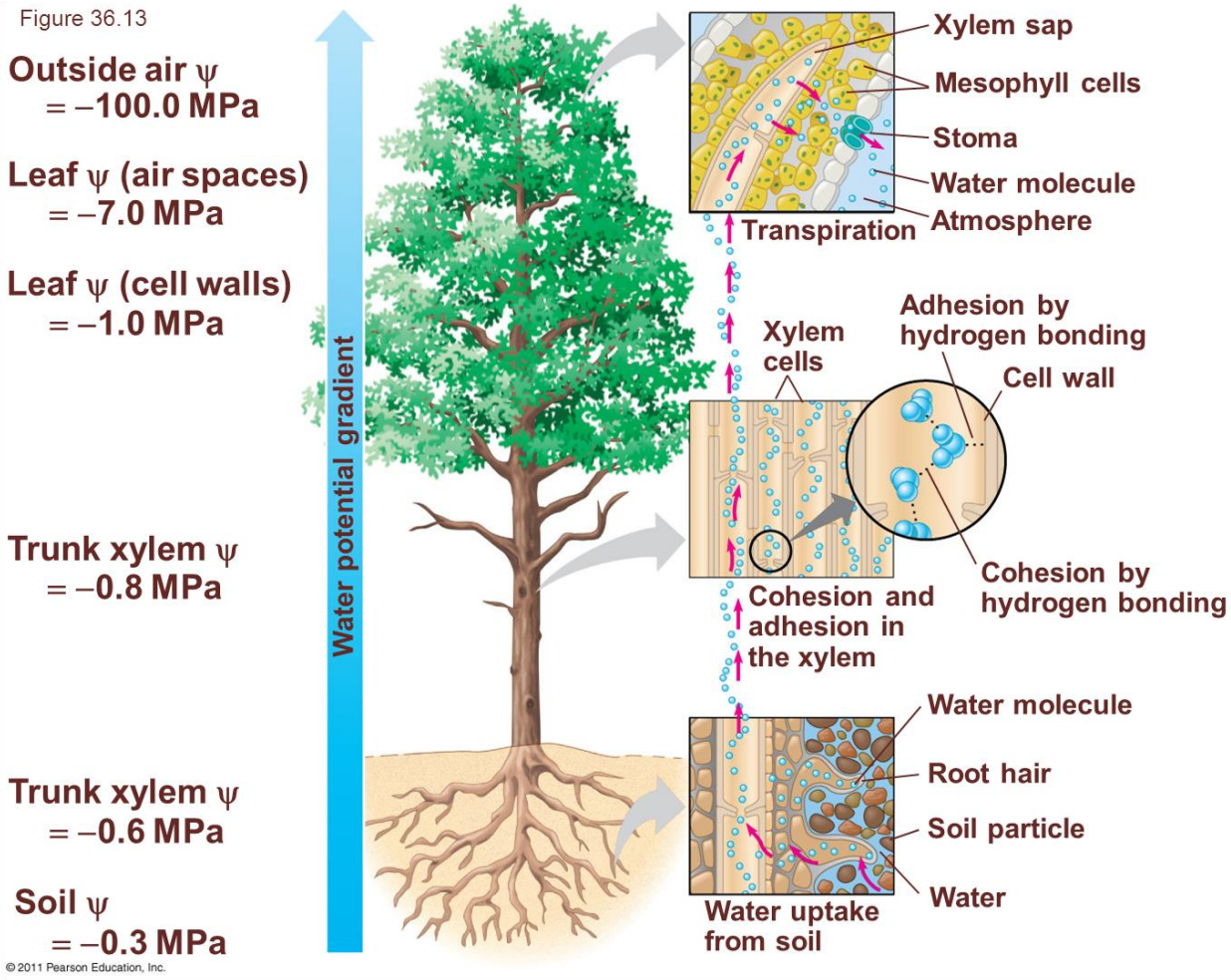

Figure 2. Water transport in plants and the Cohesion-Tension theory (© 2011 Pearson Education, Inc.). Evaporative demand (highly negative water-potentials) from the air drives evaporation in the stomatal chambers (top right). The negative water pressure gradient (left, blue arrow) is transmitted downwards through the water column in the xylem (right), to the finest root hairs that take in water from the soil (bottom right).

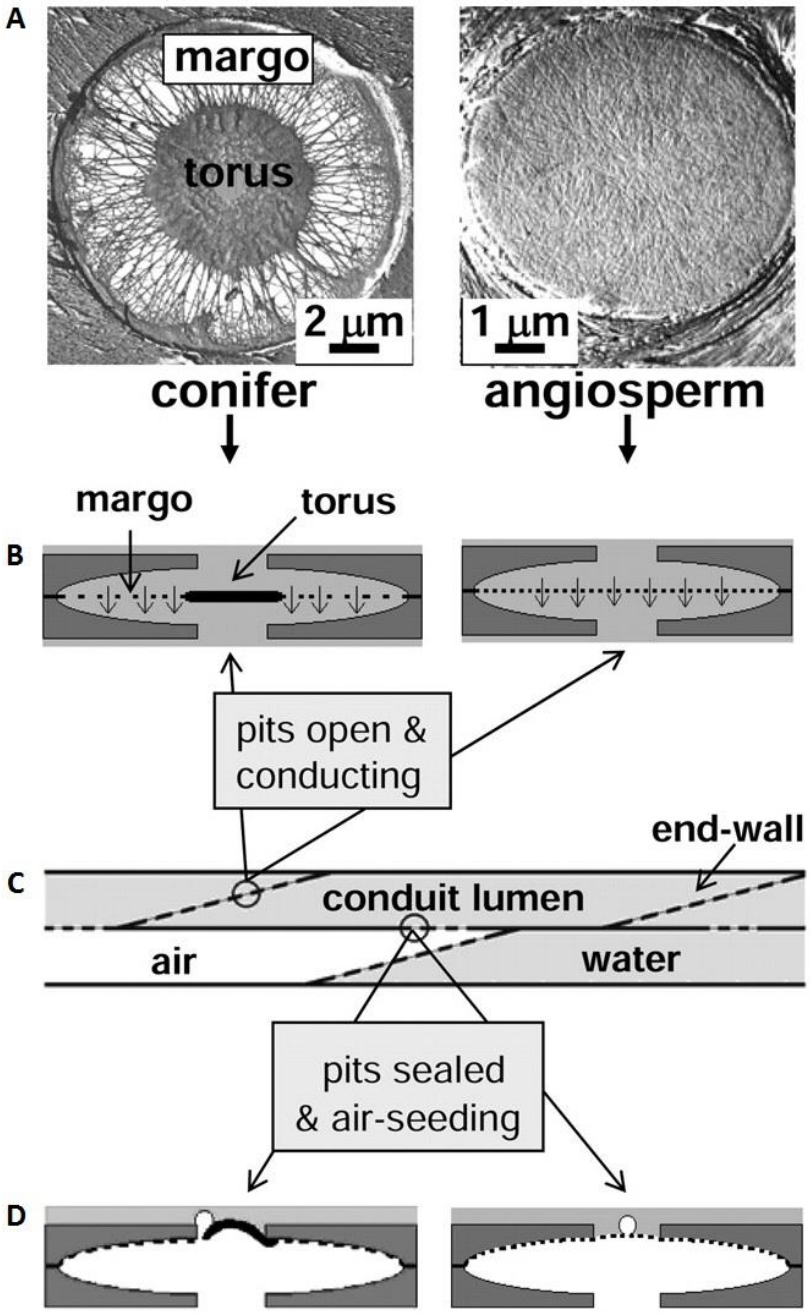

Figure 3: Comparison of pit structure, water-flow and air-seeding in Conifers (left) and Angiosperms (right). Reproduced from Pittermann et al., 2005. **A**. SEM images of torus-margo pits in conifers and homogenous membrane in Angiosperms. **B**. Cross-section schematic view of the position of the membranes between two functional elements, with arrows showing water flow through the membrane pores. **C**. Network of conducting cells, with one air-filled element. **D**. Membranes in their deflected "sealed" position between the conducting elements and the air-filled "embolized" one, showing the locations of air-seeding.

While this process enables plants to extract water from dry soils, and move it to tens of meters above the ground against the pull of gravity, it depends entirely on maintaining an intact vascular network filled with water in a metastable liquid state, and therefore relies "on an inherently vulnerable transport system" as "any break in the column necessarily disrupts water flow" (Tyree and Sperry, 1989). Indeed, air-bubbles can be drawn into conductive xylem elements from neighbouring air-filled spaces or cells, according to the "air-seeding hypothesis"

(Cochard et al., 2009). When so-called "cavitation" occurs, the small initial gas-bubble spreads to fill the entire cell, which is then air-filled, or embolized, and therefore no longer functional, thus reducing the plant's overall capacity to feed water to its aerial organs (Sperry and Tyree, 1988). We note here that throughout this thesis we use "cavitation" and "embolism" interchangeably, as if the terms were synonyms; cavitation refers to the initial air-bubble inception and expansion, whereas embolism refers to the final results, i.e. an air-filled conduit. During drought, with increased evaporative demand at the leaf and lower (more negative) soil water-potential, xylem tension increases, leading to increasing numbers of cavitation events, drastically reducing hydraulic conductance (Sperry and Sullivan, 1992). At short time-scales,

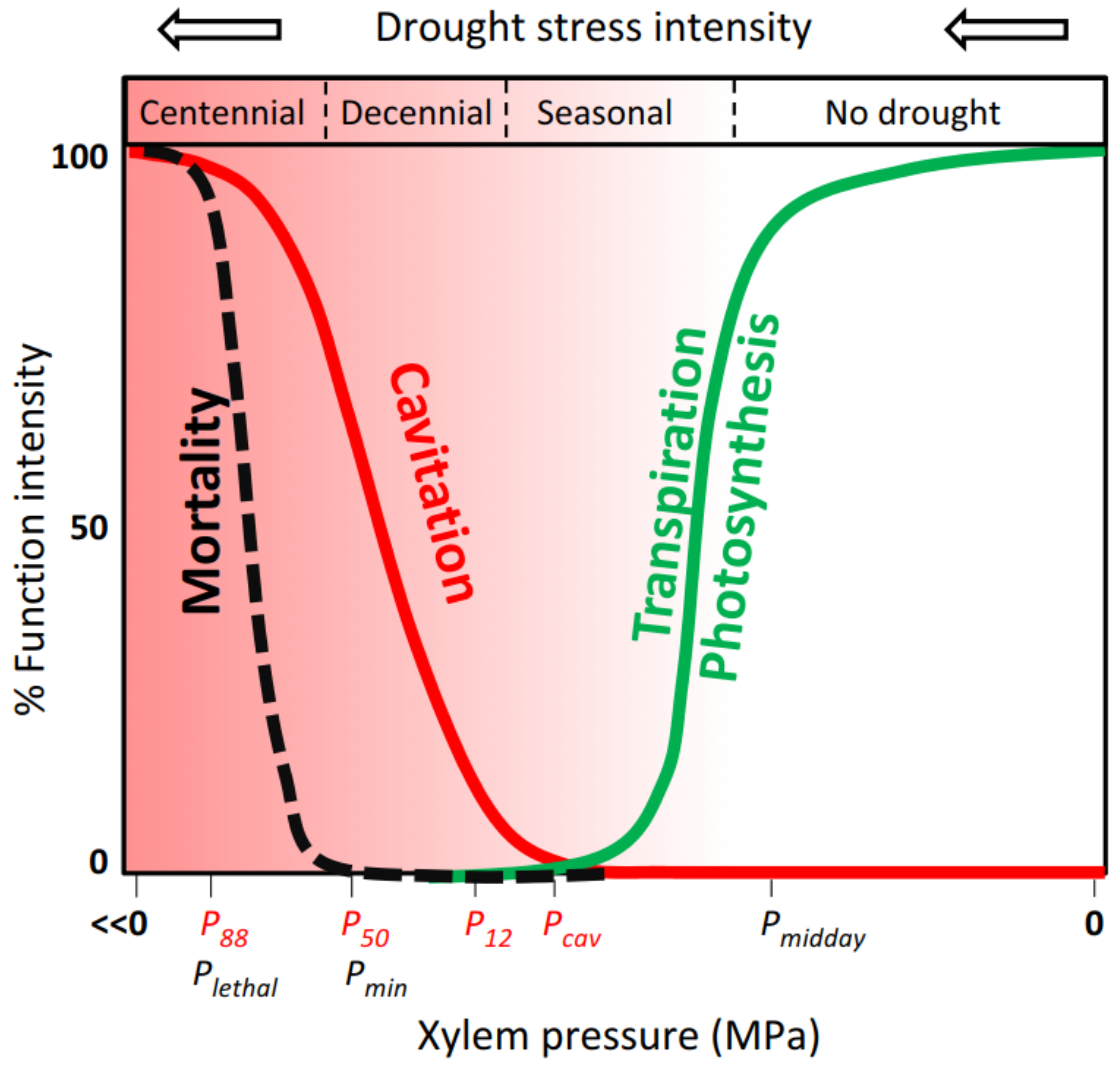

Figure 4: Gas exchange functions and xylem cavitation across varying levels of drought. In normal conditions (right, xylem pressure close to 0), xylem pressure is maintained at healthy levels by regulation of stomatal conductance (green curve). During seasonal drought, gas exchange stops but low levels of cavitation are observed. Exceptional years (decennial, centennial) cause further lowering of xylem pressure into values inducing low levels of embolism, until P_{50} is reached (P_{88} for angiosperms). Reproduced from (Delzon and Cochard, 2014).

plants regulate water-loss to avoid water-potentials that could cause grievous injury to their water-transport system due to embolism (Brodribb et al., 2003). Plants go to extreme lengths to protect their xylem, shedding leaves to reduce transpiration, and stopping photosynthesis for long periods – leading to death from lack of carbon-assimilation (Plaut et al., 2012). Recent views place hydraulic failure as a rare event, occurring during prolonged, exceptional drought, well after regular gas-exchange has ceased (see Figure 4; Delzon and Cochard, 2014). Some authors have suggested that plants can recover relatively easily from embolism and experience daily cycles of refilling (Brodersen et al., 2010; Zufferey et al., 2011; Knipfer et al., 2016). However, the precise mechanisms involved, conditions required remain elusive and natural selection for a loss of vascular function at daily peak evaporative demand seems counter-intuitive (Zwieniecki and Holbrook, 2009; Rockwell et al., 2014). Furthermore, recent controversies regarding measurement artefacts causing severe overestimation of species embolism levels (Wheeler et al., 2013; Torres-Ruiz et al., 2015; Pivovaroff et al., 2016) have called a great deal of evidence for refilling into question.

Plants have evolved to prevent these problems, with for example a multitude of inter-connected conductive elements that translate into a multitude of pathways for water to ascend the tree, minimizing the impact of the loss of a few conductive elements to embolism. Also, water flows from one element to another through pores (pits) with a membrane (margo) that acts as a barrier to air bubbles and prevents the spread of embolism throughout the xylem. Additionally, conifers possess a central thickening of the membrane (the torus) that acts as a valve to isolate the air-filled tracheids from the rest of the system (Bailey, 1916). In vessel-bearing species (Angiosperms), cavitation occurs as air-bubbles are pulled through the porous membrane, whereas in Gymnosperms, the torus prevents this leakage (see Fig. 3). In this case, an imperfect seal between the torus and the pit-aperture is the probable location of air-leakage in conifer bordered-pits (Delzon et al., 2010; Pittermann et al., 2010). This seems to confer increased resistance to drought-induced cavitation to coniferous species, that are generally less vulnerable than Angiosperms (Maherali et al., 2004; Choat et al., 2012).

Resistance to drought-induced cavitation is related to fitness, since it seems to give trees increased chance of survival in case of severe drought. For example, in the southwestern USA, a mixed conifer forest suffered high mortality rates in the wake of a drought period in the early 2000s. The more cavitation-resistant *Juniperus monosperma* was hardly affected while more vulnerable *Pinus edulis* was decimated (Breshears et al., 2009). Previous work has highlighted a wide cavitation resistance range in tree species (Maherali et al., 2004; Delzon et al., 2010),

and this variation seems to be linked to their ecology, with species from arid regions more resistant to cavitation than mesic species (Brodribb and Hill, 1999; Maherali et al., 2004), justifying the use of cavitation resistance as a metric of plants' adaptation to water-stress. There is good evidence that there is a level of drought beyond which plants cannot recover even with the return of sufficient hydration, with mortality well correlated with the water-potential inducing 50% loss of conductance to emboli (Blackman et al., 2009; Brodribb and Cochard, 2009; Brodribb et al., 2010; Anderegg et al., 2012; Choat et al., 2012; Urli et al., 2013). P_{50} can be considered a more appropriate predictor of mortality than other measurements of water status (turgor loss point or stomatal response) because per cent loss of conductance is a meaningful representation of xylem desiccation.

With the increased understanding of plant water-transport and its' potential flaws, techniques were developed to keep track of plants' physiological state. For example, water-status of a leaf is routinely measured by imposing positive pressure on the leaf using a "pressure bomb" (Scholander et al., 1964; Tyree, 1972), and observing the point when water starts bubbling out of the cut extremity of the twig/petiole, which is equivalent to the (negative) leaf water pressure. Xylem dysfunction, or cavitation, was first quantified using the acoustic method: as the sap ruptures, energy is released as acoustic emissions – from audible "clicks" to ultrasound emissions (Milburn and Johnson, 1966; Tyree and Sperry, 1989) – which can be tracked to draw the dynamics of loss of conductance in the sample. More recent methods involve directly monitoring water-flow decrease as stress is imposed to a plant or sample (leaf, branch, or root). Drought-stress can be slowly induced by letting the sample or plant dehydrate ("bench dehydration technique"), or the process can be accelerated by using centrifugal force (static or flow-centrifuge techniques) to induce negative pressure in the xylem analogous to that experienced by the plant during drought. By visualizing percent loss of conductance of the xylem as a function of xylem pressure (MPa), one obtains a so-called vulnerability curve (generally a sigmoid), from which one can derive estimates of a sample's "cavitation resistance" – notably from the inflexion point, i.e. the pressure at which 50% of total hydraulic conductance is lost (P_{50} – in megaPascals), and the slope of the curve (S – in $\%.MPa^{-1}$). Some of these methods are more or less prone to biases or artefacts, prompting a recent debate about which is the "benchmark" or reference method, notably because of difficulties caused by open-vessels in the sample (Cochard et al., 2013; Wheeler et al., 2013; Rockwell et al., 2014; Torres-Ruiz et al., 2014; Wang et al., 2014; but see Jacobsen and Pratt, 2012; Sperry et al., 2012). Recently, non-destructive "un-biased" methods are slowly unravelling these issues (Bouche et al., 2015;

Cochard et al., 2015; Torres-Ruiz et al., 2015; Brodribb et al., 2016; Choat et al., 2016). As leaves are the organs the most exposed to highly negative water-potentials, they could act as fuses for the water-transport system, "cavitating" early at the onset of drought conditions to protect the more costly tissues in the branches (Tyree et al., 1993; Tyree and Zimmermann, 2013). However, recent results show similar resistance to cavitation of the xylem in branches and leaves in *Pinus pinaster* (Bouche et al., 2015), and in any case very strong relationship between branch P_{50} and leaf P_{50} exists (Tim Brodribb, *pers. comm.*, Bartlett et al. *in prep*). A recent study reported very low intra-tree (branch, trunk and root) variability for P_{50} in several conifer species (Bouche et al., 2016). All cavitation resistance measurements and values reported in this thesis are therefore measured on branches, using a single method, the so-called Cavitron (or in-situ flow-centrifuge method) that has been shown to be accurate in conifers (Cochard et al., 2010; Choat et al., 2016; Pivovaroff et al., 2016).

The rate at which cavitation occurs varies widely between species (Maherali et al., 2004; Delzon et al., 2010), with vulnerable species rapidly losing conductance at moderate tensions (P_{50} around -2 to -0.5 MPa), whereas some species can withstand high xylem tensions before embolism starts to occur (P_{50} < -4 MPa). However, a study comparing severity of drought experienced by trees (i.e. the lowest water-potentials observed seasonally) to levels of drought inducing death by hydraulic failure (i.e. P_{50}) found global convergence in tree vulnerability to drought across ecosystems (Choat et al., 2012), i.e. wet and dry forest have an equally limited hydraulic safety margin regarding lethal levels of drought. This worrying state of affairs has led a major push towards understanding tree hydraulic function (and dysfunction) in recent years, building on theoretical understanding of water transport through vascular tissues (Dixon and Joly, 1895; Dixon, 1914; Tyree, 2003; Tyree and Zimmermann, 2013), and advances in techniques to measure accurately and rapidly a plant's intrinsic resistance to drought (see a review of methods in Cochard et al. (2013). On the one hand, Northern Hemisphere coniferous species tend to be dominant or abundant forest species, and widespread mortality could lead to great loss of biodiversity and would dramatically affect some of the worlds' largest terrestrial carbon sinks - notably the huge boreal forests – adding a positive feedback effect on the greenhouse effect (Anderegg et al., 2015c). Furthermore, some conifers are among the most economically important tree species in the world, not least in the Aquitaine region (France), where maritime pine forms one of Europe's largest managed forests, covering about 10 000 square kilometres. On the other hand, in many parts of the world (Mexico, South-East Asia and South-East China, New Caledonia) conifers are in high diversity but often with extremely

reduced distributions and are often local endemics (Eckenwalder, 2009). A third of all conifer species are considered endangered (IUCN, 2015), and many examples of forest die-back implicate coniferous species (Martínez-Vilalta and Piñol, 2002; Bigler et al., 2007; van Mantgem et al., 2009; Peng et al., 2011; McDowell et al., 2015).

2. Conifers

Conifers are an ancient group of vascular seed-plants that first appeared nearly 300 million years ago, and are the largest surviving group of gymnosperms (which also include Cycads, Gnetophytes and *Ginkgo*), with over 600 species grouped in 7 families (Pinaceae, Araucariaceae, Podocarpaceae, Taxaceae, Cephalotaxaceae, Sciadopityaceae, and Cupressaceae), and around 80 genera (Farjon, 2010). Some remarkable conifers include the tallest trees in the world (*Sequoia sempervirens*), the most massive (*Sequoiadendron giganteum*), some of the oldest living organisms (either as a single tree – *Pinus longaeva*, or as a resprouting stump – *Picea abies*). Over their long history, they have evolved to occur in some of the wettest environments (in tropical rainforests in south-east Asia, New Caledonia) and some of driest deserts (*Cupressus dupreziana* in the Sahara, or *Callitris* in the Australian desert), stretch far into the Arctic circle (e.g. *Larix gmelinii* in the Taymyr Peninsula in Siberia) and into the upper reaches of the Himalaya (*Juniperus tibetica* in Southeastern Tibet at 4900m - Miehe et al., 2007). Such ecological ubiquity is matched by an equal measure of morphological and physiological variation. Conifer leaves go from long needles (Pinaceae) to small triangular scales (Cupressaceae) and broad flattened "leaves" (Podocarpaceae). While most conifers are evergreen, some species are deciduous (mainly *Taxodium* and *Larix*), and one species - *Parasitaxus usta* - is a root parasite, its exclusive host being another conifer, *Falcatifolium taxoides*. Despite their global presence, their distributions reveal a strong biogeographic signal reflecting their ancient history, with only the Cupressaceae family spanning the equator, the other families being restricted to either hemisphere. Conifer diversity is not uniformly distributed, either spatially or taxonomically. Their diversity reveals patterns of high abundance but limited diversity in high latitudes and low abundance but high diversity in sub-tropical to tropical areas (Enright and Hill, 1995; Farjon, 2010). Furthermore, most conifer species are part of a handful of genera (e.g. *Pinus*, *Podocarpus*, *Abies*, *Juniperus*), and some small geographic regions host a remarkable number of conifer species, for example New Caledonia (43 endemic species) or Mexico (~50 pine species).

Recent work using phylogenetics has aimed at explaining some of these biogeographic and diversification patterns. Leslie et al. (2012) found that Northern Hemisphere (NH) conifer clades are younger than their Southern Hemisphere (SH) counterparts, likely due to climatic upheavals being more frequent and severe in the NH, whereas pockets of stable favourable climate have been maintained in the SH. Cardoso et al. (Cardoso et al., 2015) found support for increased speciation rates in high altitude NH clades. Conifers produce separate (male) pollen cones and (female) seed cones, which tend to be woody and scaly (the ancestral state), but derived "fleshy" cones have evolved separately several times (in Taxaceae, Podocarpaceae and *Juniperus*). A large majority of conifers with fleshy cones also have derived dioecy (separate male and female plants), and monoecy (the plesiomorphic state with one plant bearing both types of cones) has been retained in most lineages with "dry" scaly cones and wind-dispersed seeds. However, no relationship between breeding system (monecy vs dioecy) or dispersal (wind/gravity vs animal-dispersed) and diversification rates has been found (Leslie et al., 2013). At a family level, Podocarp lineages with flattened leaves diversified while facing competition for light during the rise of the Angiosperms (Biffin et al., 2012), while their scale-leaved counterparts' diversification rates remained constant. More generally, conifers are thought to have been gradually excluded by competition with Angiosperms into less favourable ecosystems, notably poorer, drier and colder environments over the last 100 million years (Bond, 1989), among other hypotheses (Augusto et al., 2014). For example, Cupressaceae crown groups are hypothesized to have diversified into dry environments during the later Eocene (Pittermann et al., 2012).

Across such an old and diverse clade, fitness-related traits should show signals of adaptive evolution, with clades exposed to a dry climate evolving drought-tolerance adaptations such as increased cavitation resistance. When the world enters a drier climatic cycle, developing a significant evolutionary innovation (such as a new strategy to face drought) could even lead to adaptive radiations, by opening up new niche space to diversify into. Previous work has indeed shown evolutionary convergence for this trait, with multiple lineages independently evolving increased cavitation resistance, both in Angiosperms and Conifers (Maherali et al., 2004; Pittermann et al., 2012). However this variation seems to be limited to some clades, with for example the pine genus (*Pinus*) showing low variation for cavitation resistance (Delzon et al., 2010), indicating some form of evolutionary stasis. A study of North-American junipers revealed a degree of phylogenetic conservatism, with closely-related species having more

similar trait values than expected by chance (Willson et al., 2008) which in turn reflects some form of evolutionary constraint on P_{50}.

Cavitation resistance is one of several inter-connected hydraulic traits, with demonstrated trade-offs at various levels between P_{50} and mechanical strength and water-transport efficiency: selective forces acting on one of these traits will be balanced by opposite forces selecting for another trait, which could reduce variation and evolution of cavitation resistance. As water is transported through the xylem at high tensions, huge forces are applied to cell walls which could lead to their collapse under sufficient strain. Reinforced cell walls, i.e. increased wall thickness versus lumen diameter, are better at resisting implosion due to high xylem tension but reduce water flow, both by a reduction in total transporting area and by reducing conductivity of inter-conduit pores (Sperry, 2003; Sperry et al., 2006).

Resistance to hydraulic failure by cavitation seems to come from anatomical adjustments at areas of possible air-leakage within pit structures, e.g. reducing pore size in pit membranes in Angiosperms and improving the valve-effect efficiency of the torus structure in Conifers - both of which lead to a parallel increase in resistivity to water-flow (Hacke and Sperry, 2001). Functional trade-offs are hypothesized to maintain a certain susceptibility to xylem cavitation, as developing a "safe" xylem is balanced against competitive needs, for example water-transport efficiency and lower wood construction cost, especially in wetter climates (Tyree et al., 1994; Hacke et al., 2006; Pittermann et al., 2006a; Pittermann et al., 2006b; Sperry et al., 2008). This would contribute to explain the relatively narrow safety-margin observed on a global sample of tree species (Choat et al., 2012) between levels of drought routinely experienced by species on the one hand and the lethal threshold that induces irreversible damage to the xylem on the other. Although there is evidence for a simple relationship between xylem efficiency and xylem safety across a broad sample of angiosperms and gymnosperms (Gleason et al., 2015), there are no species that have attained both high safety and high efficiency while somewhat paradoxically, some species seem to maintain vulnerability and remain relatively inefficient.

At an intra-specific level, cavitation resistance has shown a surprising lack of scaling with the environment even for species with very wide distributions. For example, one study found no significant effect of climatic aridity on P_{50} whereas other traits (such as branch leaf-to-sapwood area ratio) were plastic over the wide range of *Pinus sylvestris* (Martínez-Vilalta et al., 2009). When comparing populations from the whole climatic range of maritime pine (*P.*

pinaster), (Lamy et al., 2011) found less genetic differentiation for cavitation resistance (Qst) than expected under genetic drift (neutral markers, Fst), with the authors concluding that the trait is likely canalized, suggesting genetic constraints on cavitation resistance variation in this species. Little is known about the genetic determinism of cavitation resistance, although work on model species such as Arabidopsis (Tixier et al., 2013), and search for QTLs (Quantative Trait Loci – Lamy, 2012) offer some leads to follow in the future. Because cavitation resistance is related to the fine anatomy of the xylem, notably at the inter-tracheid pit level, it is probably associated to the genetic architecture of cell and cell-wall development, and therefore is likely under strong genetic regulation, as random changes can have disastrous consequences for growth, water-transport efficiency and mechanical support. A gene implicated in determining P_{50} could be implicated in other traits (pleiotropy), and a multitude of genes could also interact to establish this phenotype (polygenic trait) - such complex genetic networks necessarily limit the impact of a single mutation on a single gene, therefore reducing the variability on which natural (and artificial) selection can act. It is worth noting however that recent results for *Fagus sylvatica*, a widespread angiosperm species, go against this trend (Schuldt et al., 2015), which is in keeping with the observation that within-species variation for P_{50} is higher in Angiosperms than Gymnosperms (Anderegg, 2015).

3. Evolutionary biology

Examining cavitation resistance at a macro-evolutionary scale releases some of these constraints, notably by integrating over millions of years of cumulative changes and multiple evolutionary strategies displayed in various lineages, each evolving independently across the planet. However, reconstructing past evolution and understanding processes that shaped clades millions of years ago based on data from extant species poses many challenges.

For example, relationships between extant species are not always clear, and placement of fossils with certainty in lineages is sometimes tricky. Traits of interest are not always directly measurable on fossil specimens (for soft tissues for example) and fossils can be incomplete or ambiguous, completely lacking for some lineages or at least coverage can be biased toward some clades because of the peculiar conditions required for fossil conservation. Thankfully, following the emergence of the field of phylogenetics, evolutionary biology has been able to overcome some of these hurdles, with the development of models of diversification and trait evolution based on phylogenetic trees. Some authors point out nonetheless some obvious limitations of “tree thinking”, such as trying to infer processes when only observing patterns (Losos, 2011).

Box 1. Phylogeny workflow

This box describes the general process behind constructing a time-calibrated phylogeny for a group of species. I discuss some of the choices I made and the software I used to build the phylogenies in this thesis.

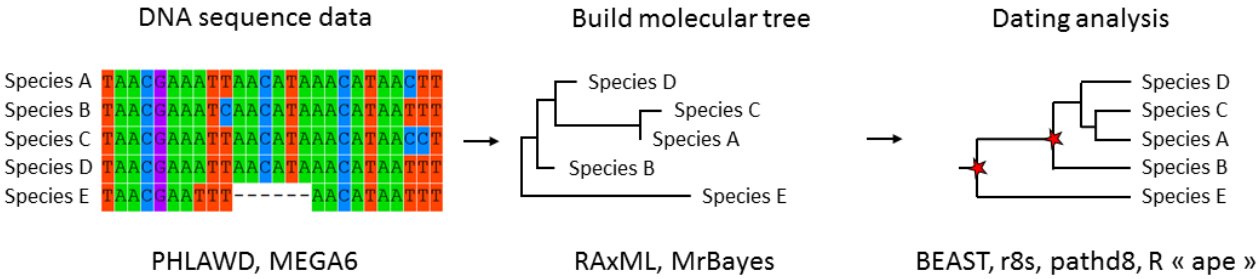

DNA sequence data

Sometimes the only option is to obtain fresh samples (leaves for example) and perform DNA extraction and sequencing, which is becoming increasingly quick and cost-effective. Some groups of well-studied species and genes are already sequenced and online in databases such as Genbank (Benson et al., 2011). The choice of which genetic regions to sequence (or download) is not trivial: depending on the scope of the study, a gene with slow rates of evolution can be a good choice for a large scale study of distant species, or give too little resolution in a group of closely related species. Conversely, a fast evolving non-coding region (intergenic spacers for example) could be so diverged they are impossible to align and compare for distant species, but useful to resolve infra-generic relationships. Once the sequences are obtained, they must first be aligned to be allow comparison of each position across all species - various alignment programs exist, the more commonly used are for example Muscle, ClustalW and MAFFT. The sequence alignment must be manually checked to remove errors with an editing program like MEGA (Tamura et al., 2011). Multiple sets of sequences can be constructed, thus increasing the data used for estimation of the phylogenetic relationships between the taxa.

Molecular tree building:

Two main families of phylogenetic analysis are commonly used, that use either maximum likelihood or Bayesian inference. Both these inference methods are based around a similar principle: finding a tree (with topology and branch lengths) and a substitution model parameters that are a "good" fit to the sequence data, measured by their likelihood given the data. The substitution model simply describes the rates of transition between nucleotides (A to T, C to G for example) in the form of a rate matrix.

BOX 1. PHYLOGENY WORKFLOW (CONTINUED)

Maximum likelihood software - such as RAxML (Stamatakis et al., 2005) – produce a quick starting tree, estimate the substitution model parameters from the data, then try and improve the likelihood score of the model by modifying the tree using a stepwise algorithmic procedure. Statistical support for clades is evaluated by bootstrapping, which is usually performed by resampling sites from the nucleotide sequences.

Bayesian inference methods use Markov Chain Monte Carlo (MCMC) to rapidly generate a large series of candidate models that provide an approximation (or sample) of the posterior probability density of the model. The frequency of a topology in the sample converges to the posterior probability of that given topology. The proportion of trees in the sample that contain a given clade gives an estimate of the posterior probability of the clade: BI produce a summary tree topology that includes clades supported by high posterior probabilities. MrBayes (Ronquist et al., 2012) and BEAST (Drummond and Rambaut, 2007) are the most used BI phylogenetic programs.

Fossil calibration and dating:

These phylogenetic trees (phylograms) have branch lengths in units of molecular distance, for example in substitutions per million sites. Evolutionary inferences need transformed trees where the branches are proportional to time, or chronograms.

The molecular clock hypothesis states that molecular evolution (the accumulation of mutations) occurs at a steady rate over time and lineages. First proposed for protein sequence evolution in the 60s, evidence from DNA sequences shows that various factors (such as generation time) can affect clock rates in different lineages of a tree, which explained initial discrepancies between time estimates obtained from dated phylogenies with a global molecular clock and ages estimated from the fossil record. More recent models “relax” the assumptions of the molecular clock to allow rates to vary across the tree, while also assuming that neighbouring branches are likely have relatively similar rates. Different methods have been developed to implement molecular clocks, using independent historical data to calibrate certain nodes in the tree (usually fossil information), and then to model rates across the tree (Kumar, 2005; Anderson, 2007; Ho and Duchêne, 2014). BEAST allows simultaneous estimation of tree topology and node ages, and implements various relaxed clock models. The penalized-likelihood method is implemented in r8s and the R package “ape” (Sanderson, 2002; Kim and Sanderson, 2008; Paradis, 2013).

Evolutionary theory states that all living things on earth share common ancestry (Darwin, 1859), therefore their relatedness can be determined by examining heritable traits, notably by observing and comparing their DNA sequences. For example, human and chimpanzee (our closest relative) DNA sequences are highly similar, much more for example than between human and cat. Over the last decades, rising availability of DNA data and the combined advances in modelling molecular evolution and computing power have enabled the construction of large phylogenetic trees, retracing with varying degrees of confidence the relationships between living organisms (see Box 1).

The branching patterns within time-calibrated phylogenies give insight into the tempo of diversification within the clade, for example long branches (with no bifurcations) indicate low speciation and/or high extinction and multiple bifurcations over a few million years imply a burst of speciation (Nee et al., 1992; Nee et al., 1994). Simple models for bifurcating phylogenies exist, such as the constant rate birth-death model (BD), governed simply by a speciation rate - i.e. the probability at any given time that a given lineage will split, giving rise to two daughter lineages – and an extinction rate – i.e. the probability of a lineage at any time going extinct. More recently, models that allow rates to vary across the tree, or where rates depend on various factors (e.g. the environment, trait values, or lineage diversity) have been developed (see Stadler, 2013). These models can be fit to empirical phylogenies, usually by maximizing the likelihood of the data under various models. For example, given a BD model, at any point of the phylogeny we can estimate the likelihood that some speciation and extinction rates will result in the observed branching pattern, descendant extant species and their trait values. Working backwards through the tree towards the root, the model likelihood is obtained for the whole tree, and can be for example be compared to alternative models using likelihood ratios or Akaike's Information Criterion (AIC).

Similarly, by combining phylogenies with trait data for extant species, one can reconstruct trait evolution throughout the clade (Felsenstein, 1985). For example, one of the simplest and most used models is Brownian Motion (BM). Derived from the stochastic motion of molecules in a gas, BM describes evolution as a random process where at any time, a lineage's trait value can increase or decrease by a random amount, drawn from a normal distribution, centred on 0 and of variance σ^2. When a lineage split occurs, trait values in the descendant lineages start evolving independently. These random changes in character states are governed σ^2, which describes the rate of character evolution under the model. Knowing the phylogeny and trait data of a clade, one can estimate the best BM model parameters using maximum likelihood. BM is

a general model that is suitable for cases where trait evolution occurs due to genetic drift, directional selection with dynamic optimums, or where stasis is followed by quick bursts of rapid evolution (O'Meara et al., 2006). Extensions to this model include the Ornstein-Uhlenbeck (OU) model, where the BM random process is pulled towards an optimum value (which is the same for all lineages), which is appropriate for modelling traits under global directional selection. Across large clades with diverse life-histories and ecologies, it seems reasonable that a single BM model may not always be appropriate to capture the diversities of evolutionary dynamics that can exist. More complex models have recently been developed which fit models with shifts between multiple evolutionary processes: different lineages can belong to different evolutionary dynamics (Alfaro et al., 2009; Eastman et al., 2011; Beaulieu et al., 2012; Thomas and Freckleton, 2012; Rabosky et al., 2014).

A common ancestor, living in an ancestral ecological niche, gives rise to closely related species are necessarily ecologically similar (Darwin, 1859). Traits in related species tend to be more similar than expected, simply because these species share evolutionary history, which across clades can lead to spurious trait correlations. Phylogeny therefore needs to be accounted for when investigating evolutionary relationships between traits (Felsenstein, 1985). One simple method for correcting for phylogeny is the PIC method (Phylogenetically Independent Contrasts), where the relationship is investigated not on species trait values, but on contrasts, calculated at each node of the phylogeny, between each pair of species/clades. This removes phylogenetic correlation as the difference between trait values represents the variance accumulated on the independent evolutionary pathways since the divergence at the most recent ancestor. Among more recent methods increasingly being used are the Phylogenetic Generalized Least Squares (PGLS; Revell, 2010). This phylogenetically informed regression uses the λ transformation to correct the error structure of the regression for phylogenetic signal induced by similarity of trait values in related species. This is more robust than PICs since it does not overcorrect for phylogeny when trait evolution deviates from BM (an assumption of PICs).

Finally, because in many cases diversification and trait evolutionary dynamics are inter-dependent, models have been developed where a lineages' speciation and extinction rates are dependent on character states (Maddison et al., 2007; Fitzjohn et al., 2009; Fitzjohn, 2010; FitzJohn, 2012). For example, (Pyron and Wiens, 2013) showed that tropical amphibian lineages were more diverse than their temperate cousins, due to increased speciation and reduced extinction rates (similar trends have been found for mammals (Rolland et al., 2014)).

These methods enable us to identify major drivers of diversification, either morphological or anatomical traits or ecological factors.

By combining ecophysiology and evolutionary biology, this thesis breaks ground by bridging a gap between disciplines, and shines a new light on conifer evolution. Understanding how species have become so remarkably adapted to their sometimes extreme environments can help us predict how they will respond to future environmental challenges.

4. Objectives

The main objective of this thesis was to examine conifer drought-resistance in an evolutionary framework, combining plant physiology, ecology and evolutionary biology to understand how this clade has been shaped by exposure to severe drought. This work is organized into three parts: the first aims to expand our knowledge of the breadth and diversity of conifer ecophysiology, while the second offers an evolutionary perspective on conifer cavitation resistance and its role the diversification of Conifers. The final part is a detailed investigation into the evolution of the most cavitation-resistant genus, the Australian cypress-pines *Callitris*.

Part I. Drought adaptation of conifer hydraulics: wide global variation in ecophysiology and xylem anatomy

Although our global understanding of plant function during drought stress has advanced greatly over the last decades, the full scale of the variation in species responses to drought is unknown, prompting the need for a systematic approach, covering the largest possible taxonomic and ecological scale. Given the current climatic context, a further emphasis was placed on identifying species and/or genera with affinities for dry environments, to better understand species survival under the effects of extreme drought.

Chapter 1: Global Variation of Drought-Tolerance in Conifers - Delzon et al. (*in prep*)

We took advantage of new high-throughput measurement techniques to screen a large number of species spanning all conifer families (90% of genera), in the aim to construct a global conifer cavitation-resistance database. Our working hypothesis was that wide variation in P_{50} existed in conifers, and that since species tend to be well adapted to their environments, a fitness related trait such as cavitation resistance would track species climate. We found amazing 10-fold variation in species P_{50}, which was mainly concentrated in the Podocarpaceae, Cephalotaxaceae and Cupressaceae families. However, the pattern is reversed in the Pinaceae family, with very little variation. Species from the Mediterranean biome tend to be more resistant than species

from the temperate and boreal biomes, although there is wide variation within each biome. We found support for a trade-off between construction costs and safety from cavitation, but no associated reduction in hydraulic conductivity.

Chapter 2: Extreme Aridity Pushes Trees to Their Physical Limits (Larter et al., Plant Physiology, 2015)

One major question we wanted to answer was how far tree species can go to limit the risk of embolism during drought? As part of a wider sampling project of the genus *Callitris*, *Callitris tuberculata* (Western Australia) was found to be the most resistant to cavitation tree species ever measured. With a range expanding into some of the driest parts of Australia, this species can survive xylem tensions extremely close to the physical limit of liquid water transport.

Chapter 3: A broad survey of hydraulic and mechanical safety in the xylem of conifers (Bouche, Larter et al. 2014, Journal of Experimental Botany).

We looked at the fine anatomy of xylem across a wide sample of species, and found a strong relationship between cavitation resistance and various inter-tracheid pit level traits linked to the efficiency of sealing of the pit aperture by the torus when it is deflected. A trade-off was also evidenced between cavitation resistance and construction costs, with wider tracheid walls in resistant species, likely due to increased mechanical stress under higher tensions in xeric species.

Part II. The evolution of cavitation-resistance and its role in the diversification of Conifers

Previous work has shown either evolutionary lability or strong constraints for cavitation resistance evolution. Taking advantage of this unprecedented physiological database, and by adopting macro-evolutionary modelling approaches, we examined the evolutionary patterns in cavitation resistance and the diversification of Conifers.

Chapter 4: Drought and the evolution of cavitation resistance drives Conifer diversification (Larter, Delzon et al., in prep.)

At both a global scale and across geological time, this study aims at examining conifer ecophysiology in an evolutionary framework. How and when did drought tolerant conifer lineages appear and diversify? Can we find a link between ecophysiology and diversification? After building a time-calibrated phylogeny for over 300 conifer species, we implemented several diversification and trait evolution models. We identify several bursts of diversification

across conifer taxa, notably in Pinaceae, Podocarpaceae, and twice in Cupressaceae. We show that multiple conifer clades have independently and rapidly evolved towards increased cavitation resistance, and demonstrate a link between increased cavitation resistance and lineage speciation and extinction dynamics.

Part III. Adaptive radiation of *Callitris*: linking hydraulics, xylem anatomy and climate across the driest continent on Earth

Chapter 4: The evolution of Callitris xylem driven by climate during an adaptive radiation

The *Callitris* genus radiated across Australian dry environments over the last 30 million years. Occupying both wet and extremely dry areas, and displaying the full range of cavitation resistance, this group offers a unique perspective into the evolution of plants to cope with extreme xylem pressure drops during drought. Within a phylogenetic framework, we found a strong role of aridity in determining xylem hydraulic traits such as cavitation resistance and tracheid dimensions, but no effect on hydraulic conductance. We found no evidence of a safety-efficiency trade-off. Using a time-calibrated phylogeny, we find that the radiation of Callitris coincides with increasing trends of aridity across the Australian continent.

Part I: Drought adaptation of conifer hydraulics: wide global variation in ecophysiology and xylem anatomy

Chapter 1: Global Variation of Drought-Tolerance in Conifers (Sylvain Delzon, Maximilian Larter et al., in prep.)

Global Variation of Drought-Tolerance in Conifers

Summary

Conifers are one of the most ecologically and economically important plant Orders that exhibits wide variation in key functional traits spanning approximately 300 Million years of evolution. Of particular interest given their longevity and stature, is the evolution of stress tolerance in the water-transport system. Using the newly developed CAVITRON technique, an extensive dataset has been developed for cavitation resistance (P_{50}, the negative pressure inducing 50% loss of hydraulic conductance), a fitness-related trait critical for plant survival during severe drought. We analyzed the global variation in cavitation resistance, wood density, and hydraulic conductivity across 277 conifer species from the seven extant conifer families growing in the four main biomes. P_{50} widely varied across species and genera (from -1.6 to -18.8 MPa) and within all biomes, except in the boreal forest. Using a time-calibrated molecular phylogeny, we find low phylogenetic signal and that convergent evolution of high resistance to cavitation occurred in several lineages. Much of the present day variation was associated with crown groups within *Cupressaceae*, whereas *Pinaceae* exhibited a strong evolutionary stasis. There was no evidence for correlated evolution between hydraulic conductivity and P_{50}, but a significant trend to increasing wood density with cavitation resistance, suggesting an evolutionary basis for a trade-off between safety and construction cost. These findings provide a global and integrative understanding of the macro-evolution and cross-species variation in a core fitness-related trait in conifers.

Introduction

Conifers are a very important component of terrestrial ecosystems and grow under widely differing conditions of climate and soil. They currently occur from dry woodlands (*Cupressus*) to boreal forests (*Picea*) in the Northern hemisphere and from semi-arid woodland (*Callitris*) to rainforests (*Podocarpus*) in the Southern hemisphere. They dominate many forests in the northern hemisphere (e.g. Taiga and coniferous temperate forests) and are of high timber and

horticultural value, providing all the world's softwood timber for construction and housing in temperate regions. The fossil record indicates that the conifers evolved towards the end of the Carboniferous, approximately 300 million years ago, and were a diverse and ecologically important component of the vegetation until the Late Mesozoic (Hill, 2005). Since the Cretaceous, conifers have declined in diversity and relative abundance while angiosperms have gradually expanded their distribution and their diversity (Lidgard and Crane, 1988; Bond, 1989; Enright and Hill, 1995; Augusto et al., 2014). Extant conifers tend to be most predominant in harsh ecosystems (cold, dry, nutrient-poor and after catastrophic disturbance) and consist of seven families (*Araucariaceae, Cephalotaxaceae, Cupressaceae, Pinaceae, Podocarpaceae, Sciadopityaceae and Taxaceae*) comprising about 630 species (Farjon and Page, 2001) of which 28% are threatened (IUCN, 2015).

Global evidence of drought-induced forest dieback has been reported recently (van Mantgem et al., 2009; Allen et al., 2010), especially in conifer woodlands and forests (Breshears et al., 2005; Bigler et al., 2007; Peng et al., 2011; Sánchez-Salguero et al., 2012). These examples of drought-related tree mortality have grown more frequent during the past decade and suggest that no forest type or climate zone is invulnerable to rapid change in climate. However, mortality rate is highly variable among species, with significant differences recorded in conifer species growing in the same site (Breshears et al., 2005). Accumulating observational and experimental evidence suggests that the vulnerability of water transport systems to drought-induced embolism is causally linked to survival and may be responsible for inter-specific differences in mortality (Davis et al., 2002; Maherali et al., 2004; Cochard et al., 2008; Brodribb and Cochard, 2009; Brodribb et al., 2010). For instance, the massive drought-related die-off in North American pinyon-juniper woodlands was confined largely to the cavitation vulnerable *Pinus edulis*, rather than the co-occurring and cavitation resistant *Juniperus monosperma* (Breshears et al., 2005). The same pattern was reported in southern European woodland (Sánchez-Salguero et al., 2012) with a higher drought-related impact in more vulnerable (*Pinus sylvestris*, P_{50}=-3.2 MPa) than more resistant species to cavitation (*Pinus halepensis*, P_{50} is around -5 MPa, (Delzon et al., 2010; David-Schwartz et al., 2016). Global surveys of cavitation resistance in woody species also show that xeric species are more resistant to embolism than mesic species (Maherali et al., 2004; Cochard et al., 2008; Choat et al., 2012), which suggests that the ecological distribution of plants is affected by their ability to withstand embolism. To further predict variation in mortality responses among ecosystems and species, more detailed, specific physiological insights are now needed, especially about drought-induced failure of the

hydraulic system given that drought frequency and severity will likely increase in many regions in the future (Jentsch et al., 2007; Coumou and Rahmstorf, 2012; Stocker et al., 2013).

Associations between vulnerability to cavitation resistance and aridity suggest that natural selection has shaped its evolution (Maherali et al., 2004). Nevertheless, the well-known trade-off between transport efficiency (i.e. hydraulic conductance) and xylem safety (i.e. cavitation resistance) is commonly invoked to explain the evolution of the large range in cavitation resistance among species (Tyree et al., 1994; Tyree and Zimmermann, 2002). Xylem conductivity and tracheid size are potentially constrained by hydraulic safety considerations, such as resistance to freezing-induced cavitation, to conduit implosion and to water stress-induced cavitation (see (Sperry et al., 2008 for an authoritative overview). Xylem cavitation and embolism is caused by air sucked into conduits at high water tension through porous walls and is therefore intimately linked to the anatomy of pit membranes (Jarbeau et al., 1995; Cochard et al., 2009; Delzon et al., 2010). Increasing porosity of pit membranes makes water transport more efficient, but it also makes transporting elements more vulnerable to air-seeding. For the uniformly porous pit membrane of angiosperms, where greater safety from air-seeding cavitation through inter-vessel pits occurs when the total area of pits decreases (Wheeler et al., 2005), selection for greater pit membrane porosity may constrain the evolution of cavitation resistance. In tracheid-bearing conifers, however, resistance to air-seeding only depends on how airtight the torus-pit aperture seal is (Delzon et al., 2010). It is therefore unlikely that a trade-off between transport efficiency and xylem safety occurs among species.

Wood density, which describes the proportion of the xylem that is tissue and cell walls (i.e., conduit walls) and the space within cell walls (i.e., lumen area and wall porosity), might be indirectly linked to cavitation resistance in conifers. Hydraulic failure also occurs when negative pressures overcome the ability of the xylem conduit walls to resist implosion (collapse), the strength of the conduit being proportional to how thick the xylem wall is relative to the lumen diameter. Trees must therefore develop thicker xylem walls and/or smaller conduit diameters to prevent xylem wall collapse under negative pressure (Hacke et al., 2001), resulting in subsequent increases in xylem construction costs and wood density. Previous studies have indeed reported a correlation between cavitation resistance and wood density across conifer species (Hacke and Sperry, 2001; Jacobsen et al., 2005; Delzon et al., 2010), but too few species were examined to provide a global pattern.

Relative to angiosperms, few conifer species have been investigated to date (Delzon et al., 2010; Pittermann et al., 2010) and extensive measurements of cavitation resistance are needed

to better characterize the global variation and the evolution of this traits over the conifer taxa. This was not possible prior to the development of a new device, the so-called CAVITRON (Cochard et al., 2005) and the set-up of high-throughput phenotyping platforms that allow characterization of cavitation resistance (P_{50}, xylem pressure inducing 50% loss of hydraulic conductance) by measuring a vulnerability curve on a branch sample in less than 15 min. This new technology allows us to screen a lot of species, but also populations and genotypes in order to assess the intra-specific variability for this trait (Lamy et al., 2011).

In this study, we investigated the variability of cavitation resistance among 277 conifer species from the seven extant families, growing in the four main biomes in both hemispheres and tested the extent to which interspecific variation is due to convergent evolution or trait conservatism. We then analyzed the relationship between cavitation resistance traits, hydraulic conductance (transport efficiency) and wood anatomy taking phylogeny into account. We hypothesized that (i) cavitation resistance of conifer species strongly reflects phylogenetic history with a high degree of conservation within clades as conifers are considered to be highly conservative in their morphology, with a number of species being referred to as "living fossils" (Prager et al., 1976; Niklas, 1997)), (ii) the variability of cavitation resistance should be highest in the *Cupressaceae* because this family inhabits a diversity of regions in both hemispheres and grows in some of the driest and wettest environments of the planet, and (iii) that a global trade-off forces higher wood density with increasing cavitation resistance, but that in conifers no safety-efficiency trade-off exists. Exploring the relationship between phylogenetic history and interspecific variation in cavitation resistance may help us to explain the distributions and the successful survival of conifers during extreme drought.

Methods

Plant material

From 2005 to 2015, we sampled 276 conifer species among the seven existing *Pinophyta* families: *Araucariaceae* (n=28), *Cephalotaxaceae* (n=5), *Cupressaceae* (n=85), *Pinaceae* (n=93), *Podocarpaceae* (n=54), *Sciadopityaceae* (n=1) and *Taxaceae* (n=10) (Farjon, 2010). Samples were collected in Royal Botanic gardens (Kew London, Sydney and Hobart) and Bedgebury National Pinetum (UK) during the winter-spring period at which time plants should have been experiencing minimal water stress. One or two branches were sampled in three to ten mature individuals per species. Only straight branches 40 cm long were selected in the upper

part of the crown using a telescopic pool-pruner or a slingshot. Immediately after the sampling in the morning, needles were removed and stems were wrapped up with damp paper and conditioned with plastic bags to avoid transpiration. Then, samples were brought back to the high-throughput phenotyping platform (http://sylvain-delzon.com/caviplace, University of Bordeaux, France) and kept refrigerated at 4°C until measurements were taken.

Hydraulic and wood density traits

Xylem cavitation was assessed with the CAVITRON, a centrifuge technique following the procedure described by Cochard (Cochard, 2002; Cochard et al., 2005). Centrifugal force was used to establish negative pressure in the xylem and to provoke water stress-induced cavitation, using a custom-built honeycomb aluminium rotor (Precis 2000, Bordeaux, France) mounted on a high-speed centrifuge (Sorvall $RC5_{c+}$, USA). This technique enables measurement of the hydraulic conductance (k_i) of a branch under negative pressure. Xylem pressure (P_i) was first set to a reference pressure (-0.5 MPa) and hydraulic conductance (k_i) was determined by measuring the flux of a reference ionic solution (10 mmol dm^{-3} KCl and dm^{-3} mmol dm^{-3} $CaCl_2$ in deionized water) through the sample. The centrifugation speed was then set to a higher value for three minutes to expose the sample at a more negative pressure. For each pressure step, hydraulic conductance (ki) was determined by measuring displacement speed of the air-water meniscus at the downstream extremity of the branch. This measurement was performed with a calibrated CCD camera (Scout sca640, Basler, Germany) coupled with custom software (Cavisoft version 3.2, BIOGECO, University of Bordeaux). This software is also used for associated data acquisition and computation of conductance and vulnerability curves. Conductance was measured four times for each step, and the average was used to compute the percent loss of xylem conductance (PLC in %). PLC was determined at each pressure step following the equation:

$$PLC = 100 \times \left(1 - \frac{k_i}{k_{\max}}\right) \qquad \text{Eqn 1}$$

where k_{max} corresponds to the maximum hydraulic conductance measured at low speed. The procedure was repeated for at least eight pressure steps with a -0.5 or -1 MPa step increment until PLC reached at least 90%. Rotor velocity was monitored with a 10 rpm resolution electronic tachymeter and xylem pressure was adjusted to about -0.02 MPa. The percent loss of xylem conductance as a function of xylem pressure (MPa) represents the sample's vulnerability

curve (VC). A sigmoid function (Pammenter and Vander Willigen, 1998) was fitted to the VC from each sample using the following equation:

$$PLC = \frac{100}{\left[1 + \exp\left(\frac{S}{25} * \left(P - P_{50}\right)\right)\right]} \quad \text{Eqn 2}$$

where P_{50} (MPa) is the xylem pressure inducing 50% loss of conductance and S (% MPa^{-1}) is the slope of the vulnerability curve at the inflexion point. P_{50} is a measure of the resistance to embolism of the sample, whereas S indicates the rate at which embolism occurs with increasing levels of drought. The xylem-specific hydraulic conductance (k_s) was estimated from k_{max} and the sapwood area of the branch, defining the transport efficiency.

Wood density was measured with an indirect-reading X-ray densitometer (Polge, 1966) on the samples used for cavitation measurements (226 species in total). Two orthogonal (longest and shortest axes) radial density profiles were obtained by analyzing the scanned images with WinDENDRO software (Guay et al., 1992). For each sample, we derived three parameters from the distribution of wood density values (after removing the values corresponding to the pith), the mean value (D_{mean}), the 10^{th} percentile (D_{min}) and the 90^{th} percentile (D_{max}). A cross-validation was done using the classical direct gravimetric method (water displacement) on a sub-sample (60 species). A 27-cm-long segment was submerged in water to measure its fresh volume by water displacement using an analytical balance. Then, samples were dried in an oven at 70 °C until constant weight to determine their dry masses. The linear relationship between mean densities resulting from the X-ray scans and gravimetric densities was positive and highly significant (R^2=0.67; P<0.0001).

Construction of phylogenetic trees

Sequences for 314 Gymnosperm species were retrieved from GENBANK (Benson et al., 2011) using the PHLAWD pipeline (Smith et al., 2009). To build a phylogeny for all species in the P50 dataset, we obtained sequences for chloroplast genes rbcL and matK, nuclear gene phyP, and to provide further resolution within genera, we used the largely used ITS1–5.8S–ITS2 ribosomal DNA region. Due to high sequence variability in the ITS regions, we separated the large conifer families resulting in 5 separate alignments (Pinaceae, Araucariaceae, Podocarpaceae, Taxaceae-Cephalotaxaceae and Cupressaceae). We used three Cycad species (*Cycas micronesica*, *Zamia furfuracea*, and *Encephalartos ferox*) as outgroup based on the sister-relationship between Cycads and conifers, the higher confidence in their early fossil

record for calibration (Leslie et al., 2012), and the uncertainty surrounding the phylogenetic placement of *Ginkgo biloba* (Wang and Ran, 2014). All alignments were then manually checked and trimmed using MEGA6 (Tamura et al., 2011), and concatenated into a multi-gene dataset using Mesquite (Maddison and Maddison, 2015). A full maximum likelihood tree search was conducted using RAxML (Stamatakis, 2006) with 1000 bootstrap replicates. The single best tree was used to construct a time-tree using *chronos*:ape in R, using a relaxed clock model and specifying a set of fossil 15 calibration points used in Leslie *et al.*, 2012. More detailed information on the phylogenetic reconstruction and dating analysis can be found in Larter et al. (in prep.).

Data analysis

Variations of trait values (P_{50}, S, k_s and wood density) among taxonomic group and biomes were assessed using a one-way analysis of variance. In order to put the amount of trait conservatism into a taxonomic context, we performed a taxonomically nested analysis of variance. Lastly, to explore this taxonomic variation at a finer scale, we also computed the coefficient of variation (CV) of cavitation resistance traits for each taxonomic group and biome with eight or more species. Statistical analyses were conducted using the SAS software (version 9.2 SAS Institute, Cary, NC, USA). Cavitation resistance values (P_{50}) were converted to positive to aid interpretation of results (an increase in P_{50} means an increase in resistance). To evaluate bivariate trait relationships, we conducted cross-species Spearman correlations, to account for non-linearity of the relationships.

Additionally, conifer species are phylogenetically related and share some degree of evolutionary history. They therefore cannot be considered as statistically independent, since closely-related species necessarily resemble each other (Felsenstein, 1985; Harvey and Pagel, 1991). PGLS accounts for phylogeny in regressions by reducing the weight of data-points that share common ancestors (Symonds and Blomberg, 2014). We log-transformed all variables prior to the linear regression analysis.

Several comparative methods are commonly used to investigate phylogenetic signal, i.e. to test whether close species tend to have similar trait values. We used two metrics: Pagel's λ and Blomberg's K (Pagel, 1999; Blomberg et al., 2003; Revell et al., 2008; Revell, 2010; Kamilar et al., 2013). λ takes values between zero and one, and is a transformation parameter of the interior branches of the tree, reducing (to zero) or maximizing (λ = 1) the shared evolutionary pathways between species. A value of λ = 0 implies that trait evolution is independent from the

phylogeny, whereas λ = 1 indicates perfect phylogenetic dependence, i.e. that the trait has evolved according to Brownian motion (BM). λ was estimated by maximum likelihood optimization and tested both against 0 and 1 using likelihood ratio tests λ. *K* varies on the interval [0; +*inf*]. A *K* value of 1 implies a BM model of evolution, with *K* values <1 indicating less similarity between close species than expected under BM (low phylogenetic signal), and *K*>1 indicating the reverse. Significance of phylogenetic signal is tested by comparing the variance of phylogenetic independent contrasts (PICs, Felsenstein, 1985) of the original data to the variance of PICs over 999 permutations of trait values.

We performed PGLS and phylogenetic signal tests in the R statistical environment (R Core Team, 2015). We implemented phylogenetic generalized least-squares (PGLS) regressions using *pgls* {caper} (Orme, 2013), and calculated phylogenetic signal using both *fitContinuous:geiger* (Harmon *et al.*, 2008) and *phylosig:phytools* (Revell, 2012).

Results

Inter-specific variation

In the present study, 63 out of the 70 extant genera were sampled corresponding at least to 80% of the generic diversity within the three largest families (*Cupressaceae*, *Pinaceae* and *Podocarpaceae*). Cavitation resistance (P_{50}) varied widely within the conifer taxa with a mean P_{50} of -5.18 ± 0.18 MPa (mean ± SE). The "bois bouchon" (*Retrophyllum minus*) from New Caledonia was the least resistant to cavitation (P_{50} = -1.58 MPa), while the semi-arid australian conifer *Callitris tuberculata* was the most resistant species ever measured (P_{50} = -18.82 MPa). The distribution of cavitation resistance across species was skewed and nonnormal (skewness = -1.78, Shapiro-Wilk test= 0.79, p = 0.0001; Fig. 1 bottom inset), with 50% of the species having a P_{50} ranging between -3 and -6 MPa. The variation in P_{50} was primarily attributable to genera within a family (59%) whereas species only explained 23 % of the variance. The more cavitation resistant genera were *Tetraclinis*, *Actinostrobus*, *Callitris*, *Cupressus*, *Platycladus*, *Juniperus*, *Diselma*, *Cupressocyparis*, *Widdringtonia* (Fig. 1) and all belong to the *Cupressaceae* family. However, most of the *Cupressaceae* previously included in *Taxodiaceae* were highly vulnerable to cavitation; P_{50} ranged between -2.3 to -3.4 MPa for *Taxodium*, *Glyptostrobus*, *Metasequoia*, *Athrotaxis* and *Taiwana*. Therefore, the highest variability of cavitation resistance was observed within the *Cupressaceae* family (7-fold, CV=52%, Fig. S1, Table S1). In contrast, within the *Araucariaceae*, *Cephalotaxaceae*, *Taxaceae* and *Pinaceae* families, P_{50} only varied by less than 2.5-fold (CV=14-18%; Table S1;

Fig. S1). Within the latter family, *Cedrus* species were the more cavitation resistant (e.g. *Cedrus deodara* P_{50} = -6.69 MPa) whereas all the *Pinus* species (CV=13%) ranged between -5.03 MPa

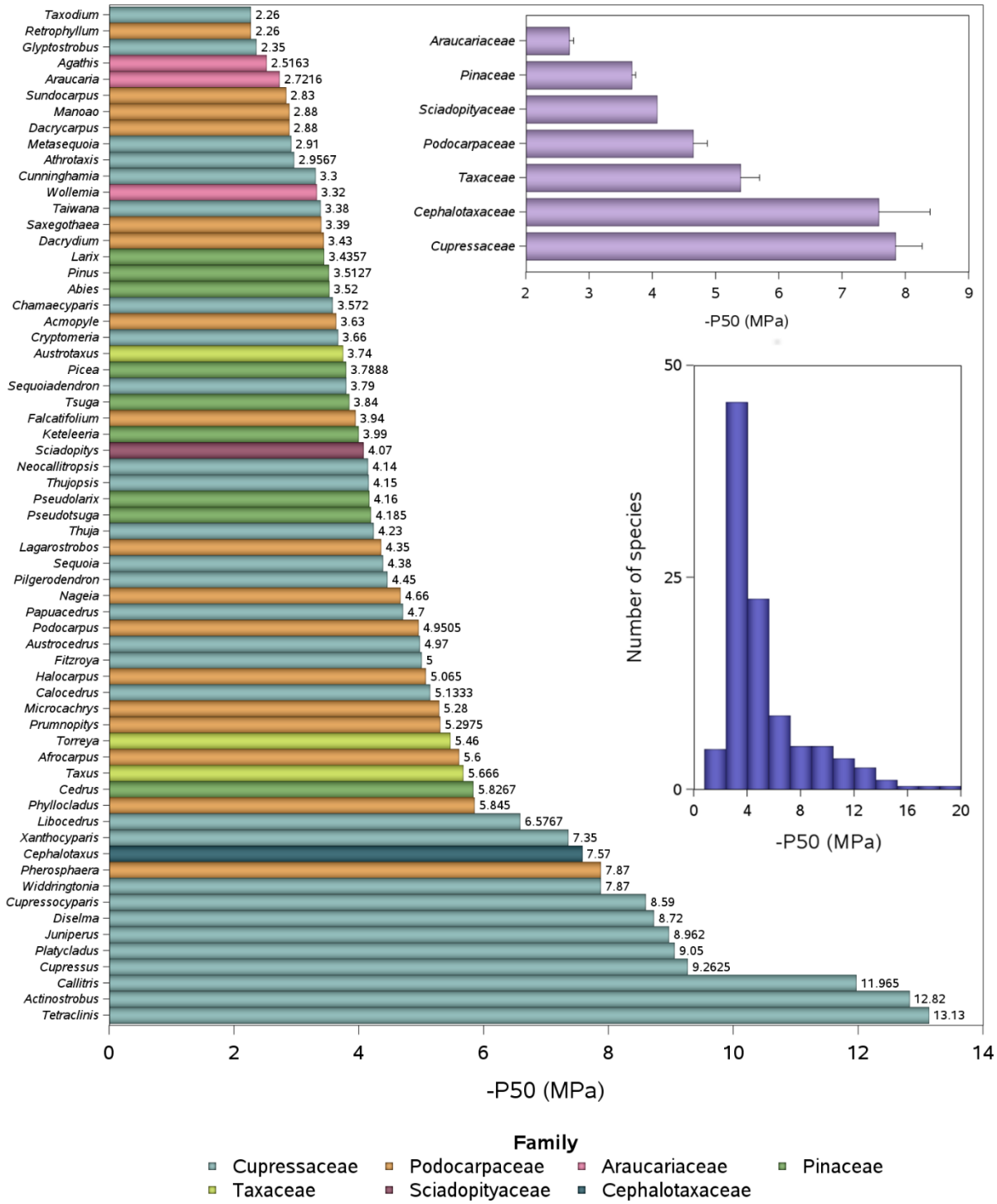

Figure 1. Cavitation resistance (P_{50}, xylem pressure inducing 50% loss in hydraulic conductance) of 63 conifer genera. Mean value of P_{50} for each family is shown in the upper inset. Frequency distribution of species cavitation resistance is shown in the lower inset. Vulnerability curves were measured in 276 species using the CAVITRON technique (n=3-7 specimen per species).

(the Mediterranean pine *Pinus halepensis*) and -2.7 MPa (the high elevation pines *Pinus densata* from China and *P. wallichiana* from the Himalaya, Fig. S1). The *Podocarpaceae* exhibited an intermediate variability with a CV of 28 %. Overall, the *Cupressaceae* and *Cephalotaxaceae* (n=4 only) families had the most negative P_{50} (the more resistant to cavitation) whereas the *Araucariaceae* and *Pinaceae* family had the least negative mean values (the more vulnerable **to cavitation; Fig. 1 inset, p<0.0001).**

Conifers from the southern hemisphere (mean P_{50} = -5.50 MPa, n=80) were significantly more cavitation resistant than those from the northern hemisphere (mean P_{50} = -4.74 MPa, n=123, p=0.0465). Cavitation resistance of conifers also dramatically varied within biomes, about five-fold in mediterranean, temperate and tropical biomes, whereas the variability was rather low (1.5-fold; Fig. 2) in the boreal biome consisting mainly of *Pinaceae* (larch, spruce, fir and pine). Mean P_{50} values of species occurring in the mediterranean biome were significantly more negative (P_{50} = -8.13 MPa; p<0.0001, Fig. 2) than those in the temperate and tropical biomes (P_{50} = -4.41 MPa and P_{50} = -4.60 MPa, respectively). Species from the boreal forest were the more vulnerable to cavitation with a mean P_{50} of -3.41 MPa (Fig 2). Finally, among the five different leaf shapes of conifers, species with scale-like leaves were significantly more cavitation resistant than those from the other groups (Fig. S2).

The slope of the vulnerability curve (*S*) also dramatically varied among species (17-fold) from 8 % MPa^{-1} for *Diselma archeri* to 206 % MPa^{-1} for *Pinus pumila*; species from the *Cupressaceae* and *Cephalotaxaceae* families having the smallest slope and therefore embolized very slowly (Fig. S3). Wood density varied slightly across species (2.5-fold), with an overall mean of 0.57 g cm^{-3}. The maximum was 0.83 g cm^{-3} for *Pherosphaera hookerianana*, and the minimum was 0.33 g cm^{-3} for *Pinus devoniana*. Finally, xylem specific hydraulic conductance (k_s) varies 50-fold across conifers. High and low values of were found within each family (Fig. S3): for instance *Pinus leiophylla* (Pinaceae; k_s = 0.0022 $m^2.MPa^{-1}$ s^{-1}), *Callitris intratropica* (Cupressaceae; k_s = 0.0013 m^2 MPa^{-1} s^{-1}) or *Afrocarpus mannii* (Podocarpaceae; k_s = 0.0011 m^2 MPa^{-1} s^{-1}) have among the highest k_s values, and whereas *Libocedrus bidwillii* (Cupressaceae; k_s = 0.000083 m^2 MPa^{-1} s^{-1}), *Microcachrys tetragona* (Podocarpaceae; k_s = 0.000085 m^2 MPa^{-1} s^{-1}) and *Pinus bungeana* (Pinaceae; k_s = 0.000098 m^2 MPa^{-1} s^{-1}) are among the least efficient.

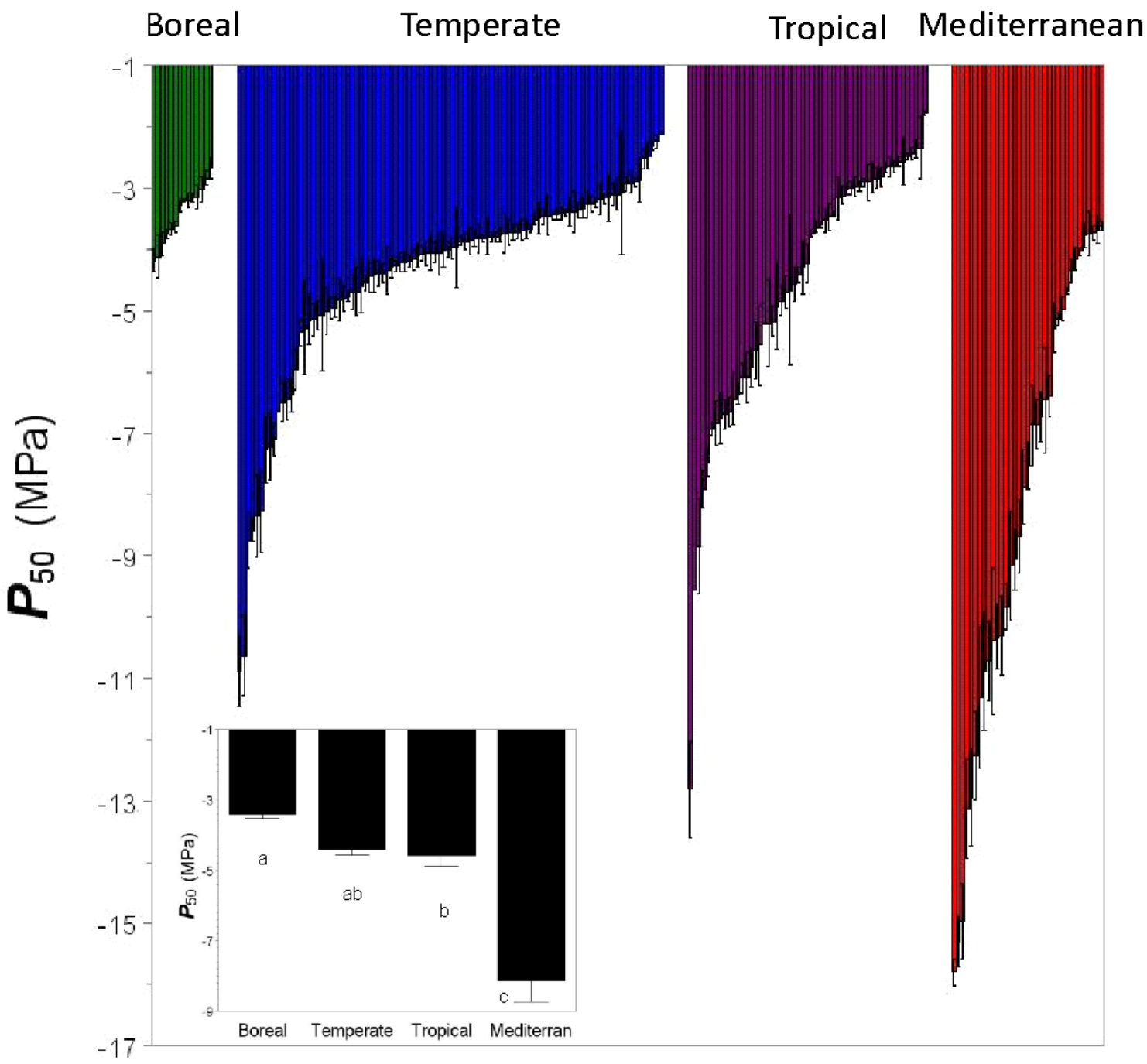

Figure 2. The distribution of cavitation resistance (P_{50}, xylem pressure inducing 50% loss in hydraulic conductance) for the 276 species studied ranked by magnitude within the four main biomes. The mean P_{50} for each biome is shown in the inset.

Phylogenetic signal

Phylogenetic signal indices showed greater trait convergence than conservatism for hydraulic traits in the Pinales. We found higher variation in traits than expected under the Brownian motion evolution model (as tested by the K statistic) (Table 1). K values range from 0.04 (for

k_s) to 0.2 (for *S*), which indicates that related species were more dissimilar than expected under BM. The PIC variance test (proposed by Blomberg et al., 2003) was significant except for k_s, meaning the distribution of trait values at the tips of the phylogeny is non-random (again, except for hydraulic conductance k_s).

These results are corroborated by λ values, which are all less than 1, i.e. closely related species show trait values more different than expected under the BM model (Table 1). For all traits except k_s, λ was significantly different from 0, indicating an intermediate level of phylogenetic signal.

Table 1. Phylogenetic signal in hydraulic traits in Conifers, using Blomberg's K (Blomberg et al. 2003) and Pagel's λ (Pagel, 1999). Bold font indicates significant deviation from 0 (no signal) and 1 (Brownian Motion model, λ only).

			λ	**log-likelihood scores**		
	K	**p**	**(p vs 0; p vs 1)**	**λ**	**λ = 0**	**λ = 1**
P_{50}	**0.06**	**0.04**	0.77 (**<0.001**; **<0.001**)	-522.4	-628.4	-741.8
S	**0.20**	**<0.001**	0.85 (**<0.001**; **<0.001**)	-1133.3	-1292.9	-1251.0
k_s	0.04	0.54	0.01 (0.77; **<0.001**)	1514.2	1514.2	1359.3
ρ	**0.11**	**<0.001**	0.69 (**<0.001**; **<0.001**)	266.6	227.1	178.5

P_{50}: xylem pressure inducing 50% loss of hydraulic conductance
S: slope of the vulnerability curve
k_s: xylem specific hydraulic conductance
ρ: wood density

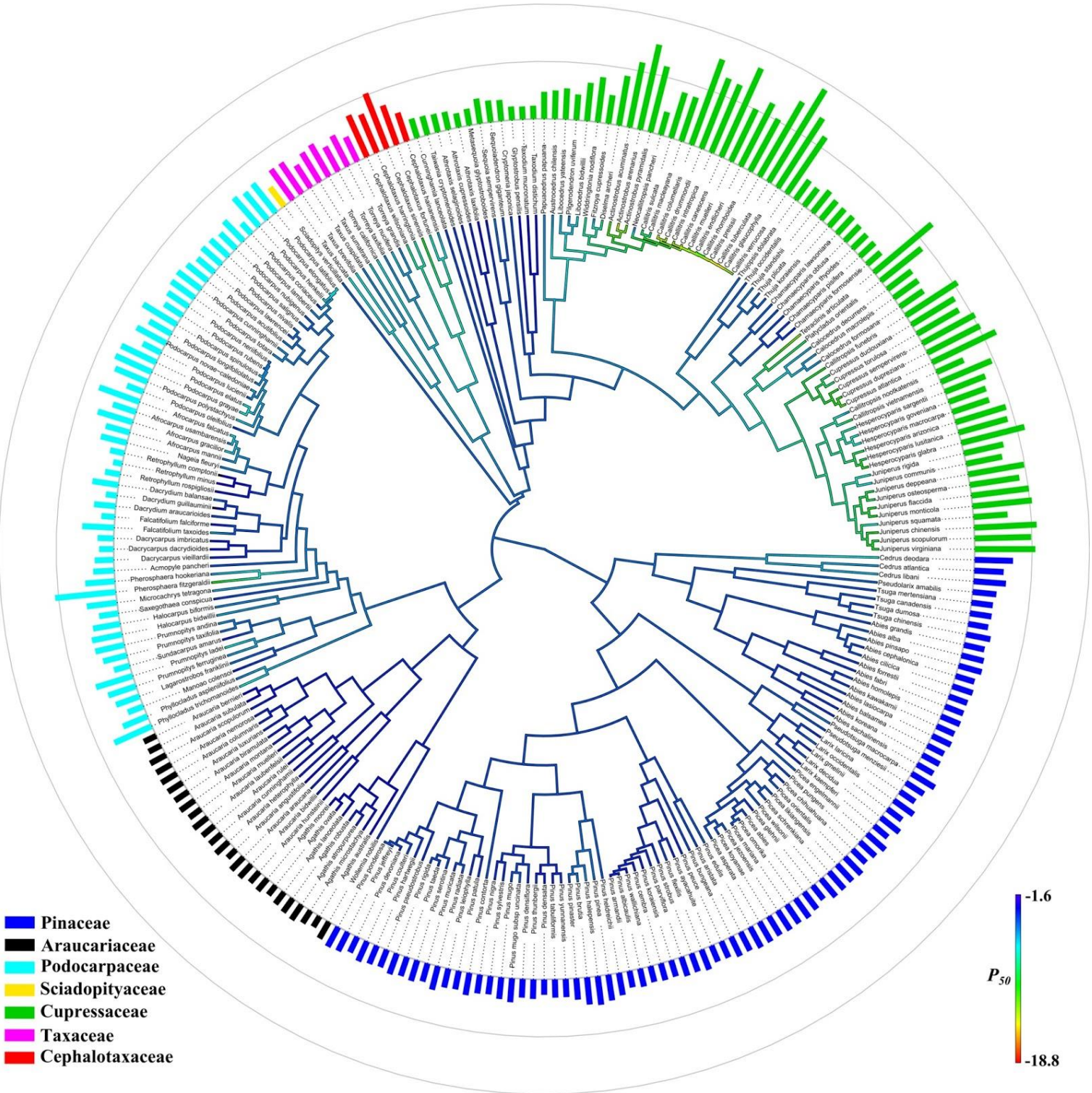

Figure 3. Phylogeny of 252 conifer species and their cavitation resistance (bars represent P_{50}, pressure inducing 50% loss of hydraulic conductance, coloured by family). From the inside out, the gray circles indicate P_{50} values of -10 MPa and -20 MPa. Branches are coloured according to maximum likelihood reconstructed P_{50} values.

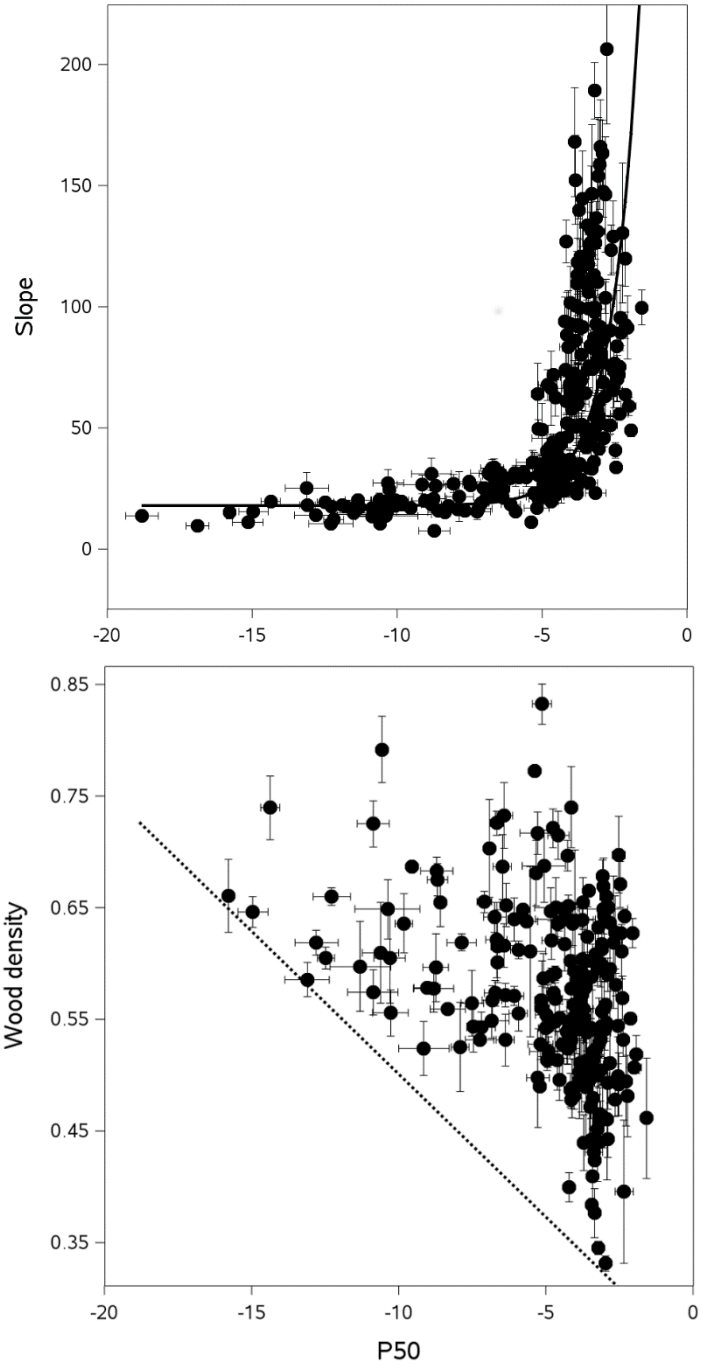

Figure 4. Cavitation resistance (P50) versus mean values of vulnerability curve slope (top panel) and wood density for conifer branches (bottom panel). The curve in the top panel is the best fit of a non-linear model. In the bottom panel, the dotted line suggests a boundary below which data are excluded because of conduit implosion. Error bars represent SE.

The extent to which interspecific variation in traits is due to convergent evolution or trait conservatism can also be illustrated by mapping traits onto the phylogeny of *Pinophyta*. The distribution of P_{50} along the phylogeny (Fig. 3) reveals that high resistance to cavitation has evolved several times in the *Cupressaceae*. For instance, distantly related genera such as *Callitris*, *Cupressus*, *Juniperus* and *Tetraclinis* have all evolved toward a more resistant xylem (low values for both P_{50} and S (Fig. S3)). Moreover, Figure 3 highlights the very low variability

in *Pinaceae* relative to the other lineages (top side of the figure). No clear pattern was found for k_s and wood density (Fig. S3).

Correlation between traits

We found a strong negative correlation between P_{50} and S (s = -0.78; Fig. 4b, Table 2), showing that the rate of embolism decreases as cavitation resistance increases and that species with P_{50} lower than -6 MPa always embolise very slowly (low S values). This tight relationship is confirmed by the PGLS analysis (Table 2).

Despite the huge observed ranges of P_{50} and k_s, no correlation between specific hydraulic conductivity (k_s) and cavitation resistance traits (P_{50} and S) was observed as determined by either cross-species correlations or the PGLS analyses (Table 2). k_s was only weakly correlated with wood density in the Spearman correlation analysis, and not correlated once phylogeny was considered using PGLS (see Table 2).

Table 2: Relationships between hydraulic traits through Spearman correlations, linear regressions and PGLS among cavitation resistance traits (P_{50} and S), xylem specific conductivity (k_s) and wood density (ρ) within the conifer taxa. P_{50} values were converted to positive values for an easier interpretation of the correlation (increasing P_{50} means increasing cavitation resistance), and all data was log-transformed for the regression analysis. Bold font indicates statistical significance at α = 0.05. **n** is the number of species included in the analysis. **λ** is the phylogenetic signal found in the regression's residual error.

		Spearman Correlations			**Linear regressions**			**PGLS regressions**				
		n	**s**	**p**	**Coef.**	**R^2**	**p**	**n**	**λ (95% CI)**	**Coef.**	**R^2**	**p**
P_{50}	***S***	276	-0.79	**<0.0001**	-1.18	0.61	**<0.001**	252	0.76 (0.60; 0.86)	-0.74	0.33	**<0.001**
	k_s	246	-0.0062	0.92	0.06	0.00	0.42	223	0.13 (-; 0.54)	-0.01	0.00	0.92
	ρ	225	0.37	**<0.0001**	1.15	0.14	**<0.001**	210	0.5 (-; 0.67)	0.79	0.10	**<0.001**
S	***k_s***	246	0.042	0.51	0.04	0.00	0.42	223	0.22 (-; 0.56)	0.16	0.01	0.07
	ρ	225	-0.42	**<0.0001**	-0.09	0.20	**<0.001**	210	0.56 (0.34; 0.74)	-0.08	0.06	**<0.001**
k_s	**ρ**	196	-0.18	**0.01**	-1.20	0.08	**<0.001**	182	0.00 (-; 0.32)	-1.25	0.09	**<0.001**

However, greater wood density was associated with increasing cavitation resistance and flatter vulnerability curves (s = 0.37 and s = -0.42 respectively; Fig. 4a and Table 2). The lower boundary of the data was closely correlated with the limit of wood density under which tracheid elements may experience implosion (Hacke et al., 2001): resistant species are exposed to much higher xylem tension, and therefore cannot have low wood density These relationships hold when phylogeny is taken into account (Table 2), indicating that these traits are evolutionarily linked.

Discussion

It is commonly assumed that the rate of evolution of conifers has been slow, mainly because of the lack of gross morphological differences between some Mesozoic conifer fossils and their living relatives (e.g. *Metasequoia*, *Wollemia*, *Araucaria*) and their homogeneous wood showing much less variability than in angiosperms (Greguss and others, 1955). Yet, our results provide a new functional perspective of the evolutionary history of this major lineage. Phylogenetic signal indices across the whole conifer phylogeny show convergent evolution for hydraulic traits in the Pinales, with close relatives showing less similarity than expected under Brownian motion. However, this overall trend of homoplasy arose predominantly from the divergence between families (with species from different families evolving toward similar phenotypes), whereas low variation was generally found within families (closely related species were phenotypically similar at this taxonomic level). Genus indeed explained the largest amount of the variance in cavitation resistance (more than 60%). In addition, the study of cavitation resistance from the emergence of the conifers revealed that much of the present day variation was associated with drought resistant clades in Cupressaceae. The *Cupressaceae* evolved toward a more cavitation resistant xylem over time as they might be outcompeted by fast-growing angiosperms in wet and nutrient-rich environments (Bond, 1989; Berendse and Scheffer, 2009)whereas the *Pinaceae* exhibited a strong evolutionary stasis. The comparison of P_{50} values among conifer families supported our initial hypothesis that *Pinaceae* are more vulnerable to xylem embolism and show less variability in this trait than other conifers. These results indicate that is important to consider the variation among different conifer lineages, rather than treating them as one gymnosperm functional group.

Different families, different evolutionary histories

While cavitation resistance varies over a large range (from -1.5 to -18.8 MPa), more than half of the studied conifer species presented a P_{50} between -3 and -5 MPa. The variability of this trait appeared to be family dependent and was much higher in *Cupressaceae* and

Podocarpaceae (CV = 52 % and 28 %, respectively) than in all the other families (CV < 18%). In addition, there was a marked evolution toward more drought resistant xylem in *Cupressaceae*, and little or no diversification for P_{50} in other families. *Cupressaceae* species widely occur in both hemispheres from wet habitats (*Athrotaxis*, *Metasequoia*, *Taxodium* and *Taiwania*) to very arid woodlands (*Actinostrobus*, *Callitris*, *Cupressus*, *Juniperus*, *Platycladus* and *Tetraclinis* Brodribb and Hill, 1997; Brodribb and Hill, 1999) while for instance species from the *Pinaceae* family mostly inhabit temperate climates in the Northern hemisphere. The evolution toward a higher resistance to water stress-induced cavitation in Cupressoid and Callitroid clades of the *Cupressaceae* (*Juniperus*, *Cupressus* and *Callitris*) might help explain the successful survival of these genera during drought (Pittermann et al., 2012) and could contribute to the rapid expansion of these drought-resistant species into arid lands (Adams and Demeke, 1993, Jackson et al. 2002) Though more modestly, *Podocarpaceae* also exhibited variability in resistance to cavitation that reflects a range of habitats from equatorial rainforest to Mediterranean climates in Africa and Australia. However, further phylogenetic analyses are required to test the hypothesis whether this family evolved toward a less cavitation resistant xylem to persist in angiosperm-dominated equatorial forests. A recent study showed for example that the ancestral foliage state in *Podocarpaceae* featured imbricate leaves and that a shift to flattened leaves and wet habitats occurred in all the larger clades at the same time angiosperms were radiating (Biffin et al., 2012)). This pattern seemingly contrasts with the broad trend towards drought tolerance - and small scale-like leaves - in *Cupressaceae*, and probably explains the lack of a trend in P_{50} for Podocarps over time.

In contrast, the *Pinaceae* exhibited very low variability between species and genera, with exception of *Cedrus* which presented higher resistance to cavitation than the other genera. Cavitation resistance was remarkably stable within the *Pinus* genus, showing strong evidence of persistent similarity of function among closely related taxa in this lineage. The high vulnerability to embolism of pines compared to other conifers had been reported in previous studies (e.g. Delucia et al., 2000; Piñol and Sala, 2000; Martínez-Vilalta and Piñol, 2002). Slow anatomical and physiological evolution is a characteristic feature of *Pinaceae* and has been ascribed to their slow chromosomal evolution (Prager et al., 1976). It is also worth noticing that comparative genomics has revealed a high degree of macro-synteny (conservation of gene content) and collinearity (conservation of gene order across genetic linkage maps) in the Pinaceae (Pelgas et al., 2006; Pavy et al., 2012; de Miguel et al., 2015). However, although diversification for P_{50} in *Pinaceae* was small, they exhibit higher adaptation than angiosperms

(Buschiazzo et al., 2012). One spectacular example of ecophysiological evolution was recently reported for the Vietnamese pine (*Pinus krempfii*) which has evolved broad leaves, i.e. flattened needles, to compete for light with evergreen angiosperm trees in tropical forests (Brodribb and Feild, 2008).

The lack of evolution of cavitation resistance in Pinaceae could be associated with several factors, including stabilizing selection for an optimal P_{50} value or constrained by a lack of genetic variation for cavitation resistance within populations. Though estimates of selection on *Pinaceae* populations are rare, recent evidence indicates that there is no genetic differentiation among populations from contrasted environments and limited additive genetic variance in *Pinus pinaster* (Lamy et al., 2011). Furthermore, a comparison of the distribution of neutral markers and quantitative genetic differentiation suggests that population differentiation was lower than expected from genetic drift alone, which means that (i) natural selection favoured the same mean phenotype in different environments maintaining ancestral traits (consequence of uniform selection) or (ii) cavitation resistance is canalized. Similar lack of differentiation have been published for other pine species, i.e. P. hartwegii (Sáenz-Romero et al., 2013) and P. halepensis (N. MartinStPaul, pers. com.). This result is consistent with the hypothesis that absence or paucity of genetic variation may constrain the evolution of cavitation resistance, suggesting that the history of this trait in the *Pinaceae* might have been guided in part by restrictions on genetic variation rather than insufficient time since an evolutionary divergence or phylogenetic niche conservatism (Lusk, 2008).

This evolutionary stasis is notably different from the pattern observed in *Cupressaceae* and might be attributed to different strategies of drought adaptation among clades. Many *Pinaceae* avoid dehydration through isohydric stomatal regulation, and typically close stomata at leaf water potentials higher than -2 MPa (Lopushinsky, 1969; DeLucia et al., 1988; Green and Mitchell, 1992). In addition, several *Pinaceae* respond to growth in arid conditions by reducing the leaf:sapwood area ratio, which increases whole plant hydraulic conductivity (Margolis et al., 1995; Mencuccini and Grace, 1995; Delucia et al., 2000; Delzon et al., 2004). This change reduces the free energy required to extract water from soils, and keeps water potential gradients from dropping to levels which cause cavitation (Mencuccini and Grace, 1995; Maherali and DeLucia, 2001). In contrast, *Cupressaceae* species growing in dry habitats can sustain more negative water potential and have a wide safety margin (tolerance strategy) (Meinzer et al., 2009). If *Pinaceae* have evolved dehydration avoidance as a means to cope with drought, then populations may not experience selection for xylem that is more resistant to water stress induced

cavitation. Another confirmation of this strategic dichotomy between these two groups of conifers is the divergence in stomatal closure mechanism, with Pinaceae sealing their stomata tighly using abscissic acid, whereas cavitation resistant Cupressaceae species let leaf desication passively seal stomata (Brodribb et al., 2014). The latter therefore allow lower water-potentials through leaky stomata, in exchange of more rapid recovery of function following re-watering. They have therefore evolved to more negative P50 to avoid risk of xylem embolism during prolonged drought, while Pinaceae and other clades using abscissic acid favour avoiding the risk of embolism.

Hydraulic safety *vs*. efficiency trade-off in conifers

The possibility of a trade-off between cavitation resistance (safety) and xylem hydraulic conductivity (efficiency) was tested but no evidence of an inverse relationship between P_{50} and k_s was found within the conifer taxa. In a meta-analysis including both angiosperm and conifer species, Maherali et al. (2004) found that the significant relationship between k_s and P_{50} was primarily driven by the structural difference between the two lineages. If the two clades are considered separately (or a phylogenetically independent contrast analysis is performed), no correlation was observed as in our study focusing only on a wide sample of conifers and taking phylogeny into account using PGLS. This result confirms that the size of conduits and therefore transport efficiency are not constrained by the need to avoid of water-stress induced cavitation in tracheid-bearing species (Brodribb and Hill, 1999; Kavanagh et al., 1999)). Hydraulic conductivity (efficiency) is determined by both lumen and end-wall resistances; the latter contributed 64% to total xylem resistance to water-flow in tracheid-bearing species (Pittermann et al., 2006a; Sperry et al., 2006). According to the pit area hypothesis, resistance to cavitation increased with decreasing total pit area between conduits (Wheeler et al., 2005). However, the mode of air-seeding in the torus-margo pits of conifer tracheids does not appear to follow this hypothesis but rather the valve effect theory (Delzon et al., 2010), for which the Achilles' heel of conifer conduits is the adhesion of the torus to the pit border (seal capillary-seeding; Bouche et al. 2014). Moreover, the porosity of the torus itself might be another air-seeding mechanism in tracheids (torus-capillary-seeding; Jansen et al. 2012). To tightly seal the pit aperture, the torus must be both fully impermeable and wider than the pit aperture. Therefore, safety from cavitation constrains torus size and structure but not the amount of pit membrane, the size of tracheid or the margo porosity. Therefore, there is no evidence that protection against air-

seeding in conifer tracheids is linked to conduit size and transport efficiency (Pittermann et al., 2006a).

Conifer wood consists mostly of tracheids, and conduit reinforcement can be achieved with minimum investment at the tissue level. P_{50} was significantly correlated with wood density, with resistant species to cavitation having a denser wood. Correlated evolution between wood density and cavitation resistance in conifers suggests a trade-off between safety and construction cost. The high values of wood density always observed for cavitation-resistant species (P_{50}<-8 MPa) which experience more negative water potential *in natura* (Choat et al., 2012) suggest that the evolution of thick and lignified cell walls is a prerequisite for conduits to resist to implosion under negative pressure(Sperry et al., 2006). However, the high variability of wood density among species that are vulnerable to cavitation (-2 MPa < P50 <-6 MPa, see Fig. 4), together with the lack of relationship between these two traits at the intraspecific level(Lamy et al., 2012), demonstrate that the use of wood density as a proxy of drought tolerance is not generally good practice. Moreover, there was a slight but significant correlated evolution between transport efficiency and wood density, which suggests that transport efficiency may be constrained more by conduit implosion under negative xylem water potential than by water-stress induced cavitation *per se*. However, given that changes in the ratio of cell wall thickness to lumen size (thickness-to-span ratio) with cavitation resistance have been reported among few conifer species (Hacke et al., 2001; Sperry et al., 2006; Willson et al., 2008), tracheid diameter and wall-thickness need to be investigated over a broad range of conifers to properly test this hypothesis.

Conclusion

Conifer trees are on average over 3-fold more resistant to cavitation than angiosperm trees ($P_{50angio}$ = -1.94 MPa reported in Maherali et al. 2004). The evolution of their vascular system - with the appearance of the torus-margo pit membrane - allows conifers to enhance the ability of the pit to prevent air-seeding between tracheids (i.e. the torus has the capacity to act as a valve by sealing the pit aperture (Delzon et al., 2010; Pittermann et al., 2010). Our results, together with recent studies demonstrate that the living conifers are not relicts, but (i) are relatively recent (most Cenozoic crown group conifers are significantly younger than their angiosperms counterparts (Crisp and Cook, 2011) and (ii) have evolved a vascular system with a sophisticated inter-conduit pit that much more efficiently prevents water-stress embolism than vessel pits in angiosperms, while crucially not penalizing water-transport efficiency. This

evolutionary innovation in conifer xylem opened up a range of cavitation resistance that has been inaccessible to their sister group, the angiosperms. However, the lack of evolutionary change for cavitation resistance in the Pinaceae lineage, likely due to genetic constraints on macroevolution, might restrict their ability to adapt their vascular system to environmental changes. Our results show how a combination of an extensive ecophysiological dataset for a core fitness-related trait and phylogenetic approaches can lead to a greater perception of the evolutionary history of this Order. This study offers insights both into how conifers have responded to climate change in the past and how future climate change may affect them.

Acknowledgements

We thank the Royal Botanic Gardens, Kew, the Bedgebury National Pinetum in UK, the Royal Botanic Garden Sydney and the Royal Tasmanian Botanical Gardens in Australia for supporting research work with their living collections. The "*Cavitating the conifers of the world*" project has been supported by INRA (innovative project), the Facility of Excellence Awards (Equipex Xyloforest), the TRANZFOR program (Australia-EU), the SYNTHESYS Project http://www.synthesys.info/ which is financed by European Community Research Infrastructure Action under the FP7 "Capacities" Program.", and the Royal Society International Joint Project between RBG Kew and INRA.

References

Adams RP, Demeke T (1993) Systematic relationships in Juniperus based on random amplified polymorphic DNAs (RAPDs). Taxon 553–571

Allen CD, Macalady AK, Chenchouni H, Bachelet D, McDowell N, Vennetier M, Kitzberger T, Rigling A, Breshears DD, Hogg EH (Ted), Gonzalez P, Fensham R, Zhang Z, Castro J, Demidova N, Lim J-H, Allard G, Running SW, Semerci A, Cobb N (2010) A global overview of drought and heat-induced tree mortality reveals emerging climate change risks for forests. Forest Ecology and Management **259**: 660–684

Augusto L, Davies TJ, Delzon S, De Schrijver A (2014) The enigma of the rise of angiosperms: can we untie the knot? Ecology letters **17**: 1326–38

Benson DA, Karsch-Mizrachi I, Lipman DJ, Ostell J, Sayers EW (2011) GenBank. Nucleic acids research **39**: D32–7

Berendse F, Scheffer M (2009) The angiosperm radiation revisited, an ecological explanation for Darwin's "abominable mystery". Ecology letters **12**: 865–72

Biffin E, Brodribb TJ, Hill RS, Thomas P, Lowe AJ (2012) Leaf evolution in Southern Hemisphere conifers tracks the angiosperm ecological radiation. Proceedings Biological sciences / The Royal Society **279**: 341–8

Bigler C, Gavin DG, Gunning C, Veblen TT (2007) Drought induces lagged tree mortality in a subalpine forest in the Rocky Mountains. Oikos **116**: 1983–1994

Blomberg SP, Garland T, Ives AR (2003) Testing for phylogenetic signal in comparative data: behavioral traits are more labile. Evolution; international journal of organic evolution **57**: 717–45

Bond WJ (1989) The tortoise and the hare: ecology of angiosperm dominance and gymnosperm persistence. Biological Journal of the Linnean Society **36**: 227–249

Breshears DD, Cobb NS, Rich PM, Price KP, Allen CD, Balice RG, Romme WH, Kastens JH, Floyd ML, Belnap J, Anderson JJ, Myers OB, Meyer CW (2005) Regional vegetation die-off in response to global-change-type drought. Proceedings of the National Academy of Sciences of the United States of America **102**: 15144–8

Brodribb T, Hill RS (1999) The importance of xylem constraints in the distribution of conifer species. New Phytologist **143**: 365–372

Brodribb T, Hill RS (1997) Light response characteristics of a morphologically diverse group of southern hemisphere conifers as measured by chlorophyll fluorescence. Oecologia **110**: 10–17

Brodribb TJ, Bowman DJMS, Nichols S, Delzon S, Burlett R (2010) Xylem function and growth rate interact to determine recovery rates after exposure to extreme water deficit. The New phytologist **188**: 533–42

Brodribb TJ, Cochard H (2009) Hydraulic failure defines the recovery and point of death in water-stressed conifers. Plant physiology **149**: 575–84

Brodribb TJ, Feild TS (2008) Evolutionary significance of a flat-leaved Pinus in Vietnamese rainforest. The New phytologist **178**: 201–9

Brodribb TJ, McAdam S a M, Jordan GJ, Martins SC V (2014) Conifer species adapt to low-rainfall climates by following one of two divergent pathways. Proc Natl Acad Sci U S A. doi: 10.1073/pnas.1407930111

Buschiazzo E, Ritland C, Bohlmann J, Ritland K (2012) Slow but not low: genomic comparisons reveal slower evolutionary rate and higher dN/dS in conifers compared to angiosperms. BMC evolutionary biology **12**: 8

Choat B, Jansen S, Brodribb TJ, Cochard H, Delzon S, Bhaskar R, Bucci SJ, Feild TS, Gleason SM, Hacke UG, Jacobsen AL, Lens F, Maherali H, Martínez-Vilalta J, Mayr S, Mencuccini M, Mitchell PJ, Nardini A, Pittermann J, Pratt RB, Sperry JS, Westoby M, Wright IJ, Zanne AE (2012) Global convergence in the vulnerability of forests to drought. Nature **491**: 752–5

Cochard H (2002) A technique for measuring xylem hydraulic conductance under high negative pressures. Plant, Cell and Environment **25**: 815–819

Cochard H, Barigah ST, Kleinhentz M, Eshel A (2008) Is xylem cavitation resistance a relevant criterion for screening drought resistance among Prunus species? Journal of Plant Physiology **165**: 976–982

Cochard H, Damour G, Bodet C, Tharwat I, Poirier M, Améglio T (2005) Evaluation of a new centrifuge technique for rapid generation of xylem vulnerability curves. Physiologia Plantarum **124**: 410–418

Cochard H, Hölttä T, Herbette S, Delzon S, Mencuccini M (2009) New insights into the mechanisms of water-stress-induced cavitation in conifers. Plant physiology **151**: 949–54

Coumou D, Rahmstorf S (2012) A decade of weather extremes. Nature Climate Change **2**: 491–496

Crisp MD, Cook LG (2011) Cenozoic extinctions account for the low diversity of extant gymnosperms compared with angiosperms. The New phytologist **192**: 997–1009

David-Schwartz R, Paudel I, Mizrachi M, Shklar G, Delzon S, Cochard H, Lukyanov V, Badel E, Capdeville G, Cohen S (2016) Evidence for genetic differentiation in vulnerability to embolism in Pinus halepensis. Front. Plant Sci.

Davis SD, Ewers FW, Sperry JS, Portwood K a, Crocker MC, Adams GC (2002) Shoot dieback during prolonged drought in Ceanothus (Rhamnaceae) chaparral of California: a possible case of hydraulic failure. American journal of botany **89**: 820–8

Delucia EH, Maherali H, Carey E V (2000) Climate-driven changes in biomass allocation in pines. Global Change Biology **6**: 587–593

DeLucia EH, Schlesinger WH, Billings WD (1988) Water relations and the maintenance of Sierran conifers on hydrothermally altered rock. Ecology 304–311

Delzon S, Douthe C, Sala A, Cochard H (2010) Mechanism of water-stress induced cavitation in conifers: bordered pit structure and function support the hypothesis of seal capillary-seeding. Plant, cell & environment **33**: 2101–11

Delzon S, Sartore M, Burlett R, Dewar R, Loustau D (2004) Hydraulic responses to height growth in maritime pine trees. Plant, Cell & Environment **27**: 1077–1087

Enright NJ, Hill RS (1995) Ecology of the southern conifers. Smithsonian Institution Press,

Washington, D.C.

Farjon A (2010) A Handbook of the World's Conifers (2 Vols.). BRILL

Felsenstein J (1985) Phylogenies and the comparative method. American Naturalist 1–15

Green TH, Mitchell RJ (1992) Effects of nitrogen on the response of loblolly pine to water stress I. Photosynthesis and stomatal conductance. New Phytologist **122**: 627–633

Greguss P, others (1955) Identification of living gymnosperms on the basis of xylotomy. Identif. living gymnosperms basis xylotomy.

Guay R, Gagnon R, Morin H (1992) A new automatic and interactive tree ring measurement system based on a line scan camera. The Forestry Chronicle **68**: 138–141

Hacke UG, Sperry JS (2001) Functional and ecological xylem anatomy. Perspectives in Plant Ecology, Evolution and Systematics **4**: 97–115

Hacke UG, Sperry JS, Pockman WT, Davis SD, McCulloh KA (2001) Trends in wood density and structure are linked to prevention of xylem implosion by negative pressure. Oecologia **126**: 457–461

Harvey PH, Pagel MD (1991) The Comparative Method in Evolutionary Bology.

Hill K (2005) Diversity and evolution of gymnosperms. *In* RJ Henry, ed, Plant Divers. Evol. Cabi, Cambridge, MA, pp 25–44

IUCN (2015) The IUCN Red List of Threatened Species. Version 2015-4. <http://www.iucnredlist.org>

Jackson RB, Banner JL, Jobbágy EG, Pockman WT, Wall DH (2002) Ecosystem carbon loss with woody plant invasion of grasslands. Nature **418**: 623–626

Jacobsen AL, Ewers FW, Pratt RB, Iii WAP, Davis SD (2005) Do Xylem Fibers Affect Vessel Cavitation Resistance ? 1. **139**: 546–556

Jarbeau JA, Ewers FW, Davis SD (1995) The mechanism of water-stress-induced embolism in two species of chaparral shrubs. Plant, Cell & Environment **18**: 189–196

Jentsch A, Kreyling J, Beierkuhnlein C (2007) A new generation of climate-change experiments: events, not trends. Frontiers in Ecology and the Environment **5**: 365–374

Kamilar JM, Cooper N, B PTRS (2013) Phylogenetic signal in primate behaviour, ecology and life history. Philosophical transactions of the Royal Society of London Series B, Biological sciences **368**: 20120341

Kavanagh KL, Bond BJ, Aitken SN, Gartner BL, Knowe S (1999) Shoot and root vulnerability to xylem cavitation in four populations of Douglas-fir seedlings. Tree Physiology **19**: 31–37

Lamy J-B, Bouffier L, Burlett R, Plomion C, Cochard H, Delzon S (2011) Uniform Selection as a Primary Force Reducing Population Genetic Differentiation of Cavitation Resistance across a Species Range. PLoS ONE **6**: e23476

Lamy JB, Lagane F, Plomion C, Cochard H, Delzon S (2012) Micro-evolutionary patterns of juvenile wood density in a pine species. Plant Ecology **213**: 1781–1792

Leslie AB, Beaulieu JM, Rai HS, Crane PR, Donoghue MJ, Mathews S (2012) Hemisphere-scale differences in conifer evolutionary dynamics. Proceedings of the National Academy of Sciences of the United States of America **109**: 16217–21

Lidgard S, Crane PR (1988) Quantitative analyses of the early angiosperm radiation. Nature **331**: 344–346

Lopushinsky W (1969) Stomatal closure in conifer seedlings in response to leaf moisture stress. Botanical Gazette 258–263

Lusk C (2008) Constraints on the evolution and geographical range of Pinus. New Phytologist **178**: 1–3

Maddison WP, Maddison DR (2015) Mesquite: a modular system for evolutionary analysis.

Maherali H, DeLucia EH (2001) Influence of climate-driven shifts in biomass allocation on water transport and storage in ponderosa pine. Oecologia **129**: 481–491

Maherali H, Pockman WT, Jackson RB (2004) Adaptive variation in the vulnerability of woody plants to xylem cavitation. Ecology **85**: 2184–2199

van Mantgem PJ, Stephenson NL, Byrne JC, Daniels LD, Franklin JF, Fulé PZ, Harmon ME, Larson AJ, Smith JM, Taylor AH, Veblen TT (2009) Widespread increase of tree mortality rates in the western United States. Science (New York, NY) **323**: 521–4

Margolis H, Oren R, Whitehead D, Kaufmann MR (1995) Leaf Area Dynamics. Ecophysiology of coniferous forests 181

Martínez-Vilalta J, Piñol J (2002) Drought-induced mortality and hydraulic architecture in pine populations of the NE Iberian Peninsula. Forest Ecology and Management **161**: 247–256

Meinzer FC, Johnson DM, Lachenbruch B, McCulloh KA, Woodruff DR (2009) Xylem hydraulic safety margins in woody plants: Coordination of stomatal control of xylem tension with hydraulic capacitance. Functional Ecology **23**: 922–930

Mencuccini M, Grace J (1995) Climate influences the leaf area/sapwood area ratio in Scots pine. Tree Physiology **15**: 1–10

de Miguel M, Bartholomé J, Ehrenmann F, Murat F, Moriguchi Y, Uchiyama K, Ueno S, Tsumura Y, Lagraulet H, de Maria N, others (2015) Evidence of intense chromosomal shuffling during conifer evolution. Genome biology and evolution **7**: 2799–2809

Niklas KJ (1997) The evolutionary biology of plants. University of Chicago Press

Orme D (2013) The caper package : comparative analysis of phylogenetics and evolution in R. R package version 05, 2 1–36

Pagel M (1999) Inferring the historical patterns of biological evolution. Nature **401**: 877–84

Pammenter NW, Vander Willigen C (1998) A mathematical and statistical analysis of the curves illustrating vulnerability of xylem to cavitation. Tree physiology **18**: 589–593

Pavy N, Pelgas B, Laroche J, Rigault P, Isabel N, Bousquet J (2012) A spruce gene map infers ancient plant genome reshuffling and subsequent slow evolution in the gymnosperm lineage leading to extant conifers. Bmc Biology **10**: 84

Pelgas B, Beauseigle S, Acheré V, Jeandroz S, Bousquet J, Isabel N (2006) Comparative genome mapping among Picea glauca, P. mariana$\times$ P. rubens and P. abies, and correspondence with other Pinaceae. Theoretical and Applied Genetics **113**: 1371–1393

Peng C, Ma Z, Lei X, Zhu Q, Chen H, Wang W, Liu S, Li W, Fang X, Zhou X (2011) A drought-induced pervasive increase in tree mortality across Canada's boreal forests. Nature Climate Change **1**: 467–471

Piñol J, Sala A (2000) Ecological implications of xylem cavitation for several Pinaceae in the Pacific Northern USA. Functional Ecology **14**: 538–545

Pittermann J, Choat B, Jansen S, Stuart SA, Lynn L, Dawson TE (2010) The relationships between xylem safety and hydraulic efficiency in the Cupressaceae: the evolution of pit membrane form and function. Plant physiology **153**: 1919–31

Pittermann J, Sperry JS, Hacke UG, Wheeler JK, Sikkema EH (2006) Inter-tracheid pitting and the hydraulic efficiency of conifer wood: The role of tracheid allometry and cavitation protection. American Journal of Botany **93**: 1265–1273

Pittermann J, Stuart SA, Dawson TE, Moreau A (2012) Cenozoic climate change shaped the evolutionary ecophysiology of the Cupressaceae conifers. Proceedings of the National Academy of Sciences of the United States of America **109**: 9647–52

Polge H (1966) Établissement des courbes de variation de la densité du bois par exploration densitométrique de radiographies d ' échantillons prélevés à la tarière sur des arbres vivants Applications dans les domaines Technologique et Physiologique. Annales des sciences forestières **23**: 215

Prager EM, Fowler DP, Wilson AC (1976) Rates of evolution in conifers (Pinaceae). Evolution 637–649

R Core Team (2015) R: A language and environment for statistical computing 3.12.

Revell LJ (2010) Phylogenetic signal and linear regression on species data. Methods in Ecology and Evolution **1**: 319–329

Revell LJ (2012) phytools: An R package for phylogenetic comparative biology (and other things). Methods in Ecology and Evolution **3**: 217–223

Revell LJ, Harmon LJ, Collar DC (2008) Phylogenetic signal, evolutionary process, and rate. Systematic biology **57**: 591–601

Sáenz-Romero C, Lamy J-B, Loya-Rebollar E, Plaza-Aguilar A, Burlett R, Lobit P, Delzon S (2013) Genetic variation of drought-induced cavitation resistance among Pinus hartwegii populations from an altitudinal gradient. Acta Physiologiae Plantarum **35**: 2905–2913

Sánchez-Salguero R, Navarro-Cerrillo RM, Camarero JJ, Fernández-Cancio Á (2012) Selective drought-induced decline of pine species in southeastern Spain. Climatic Change **113**: 767–785

Smith SA, Beaulieu JM, Donoghue MJ (2009) Mega-phylogeny approach for comparative biology: an alternative to supertree and supermatrix approaches. BMC evolutionary biology **9**: 37

Sperry JS, Hacke UG, Pittermann J (2006) Size and function in conifer tracheids and

angiosperm vessels. American Journal of Botany **93**: 1490–1500

Sperry JS, Meinzer FC, McCulloh KA (2008) Safety and efficiency conflicts in hydraulic architecture: scaling from tissues to trees. Plant, Cell & Environment **31**: 632–645

Stamatakis A (2006) RAxML-VI-HPC: maximum likelihood-based phylogenetic analyses with thousands of taxa and mixed models. Bioinformatics (Oxford, England) **22**: 2688–90

Stocker TF, Qin D, Plattner G-K, Tignor MM, Allen SK, Boschung J, Nauels A, Xia Y, Bex V, Midgley PM (2013) IPCC, 2013: Climate Change 2013: The Physical Science Basis. Contribution of Working Group I to the Fifth Assessment Report of the Intergovernmental Panel on Climate Change. Cambridge University Press, Cambridge, United Kingdom and New York, NY, USA

Symonds MRE, Blomberg SP (2014) A primer on Phylogenetic Generalised Least Squares. *In* LZ Garamszegi, ed, Mod. Phylogenetic Comp. Methods Their Appl. Evol. Biol. Springer Berlin Heidelberg, p 553

Tamura K, Peterson D, Peterson N, Stecher G, Nei M, Kumar S (2011) MEGA5: molecular evolutionary genetics analysis using maximum likelihood, evolutionary distance, and maximum parsimony methods. Molecular biology and evolution **28**: 2731–9

Tyree MT, Davis SD, Cochard H (1994) Biophysical perspectives of xylem evolution: is there a tradeoff of hydraulic efficiency for vulnerability to dysfunction? IAWA journal **15**: 335–360

Tyree MT, Zimmermann MH (2002) Xylem Structure and the Ascent of Sap. Springer Science & Business Media

Wang XQ, Ran JH (2014) Evolution and biogeography of gymnosperms. Molecular Phylogenetics and Evolution **75**: 24–40

Wheeler JK, Sperry JS, Hacke UG, Hoang N (2005) Inter-vessel pitting and cavitation in woody Rosaceae and other vessel led plants: A basis for a safety versus efficiency trade-off in xylem transport. Plant, Cell and Environment **28**: 800–812

Willson CJ, Manos PS, Jackson RB (2008) Hydraulic traits are influenced by phylogenetic history in the drought-resistant, invasive genus Juniperus (Cupressaceae). American journal of botany **95**: 299–314

Supplementary information

Table 1: Coefficient of variation (CV) of the studied traits for each family (with a number of species >8) and biome. Taxa or biomes with low magnitude of variance (CV<20%) are in bold.

		CV			
		P_{50}	S	k_s	ρ
Family	*Araucariaceae*	**14**	28	54	**12**
	Cephalotaxaceae	**17**	**18**	68	**-**
	Cupressaceae	52	65	62	**13**
	Pinaceae	**18**	38	52	**15**
	Podocarpaceae	28	51	50	**9**
	Taxaceae	**13**	45	19	**16**
Biome	Boreal	**14**	32	57	**10**
	Mediterranean	47	78	57	**12**
	Temperate	38	62	59	**14**
	Tropical	46	72	56	**15**

P_{50}: xylem pressure inducing 50% loss of hydraulic conductance; S: slope of the vulnerability curve; k_s: xylem-specific hydraulic conductance; ρ: total wood density

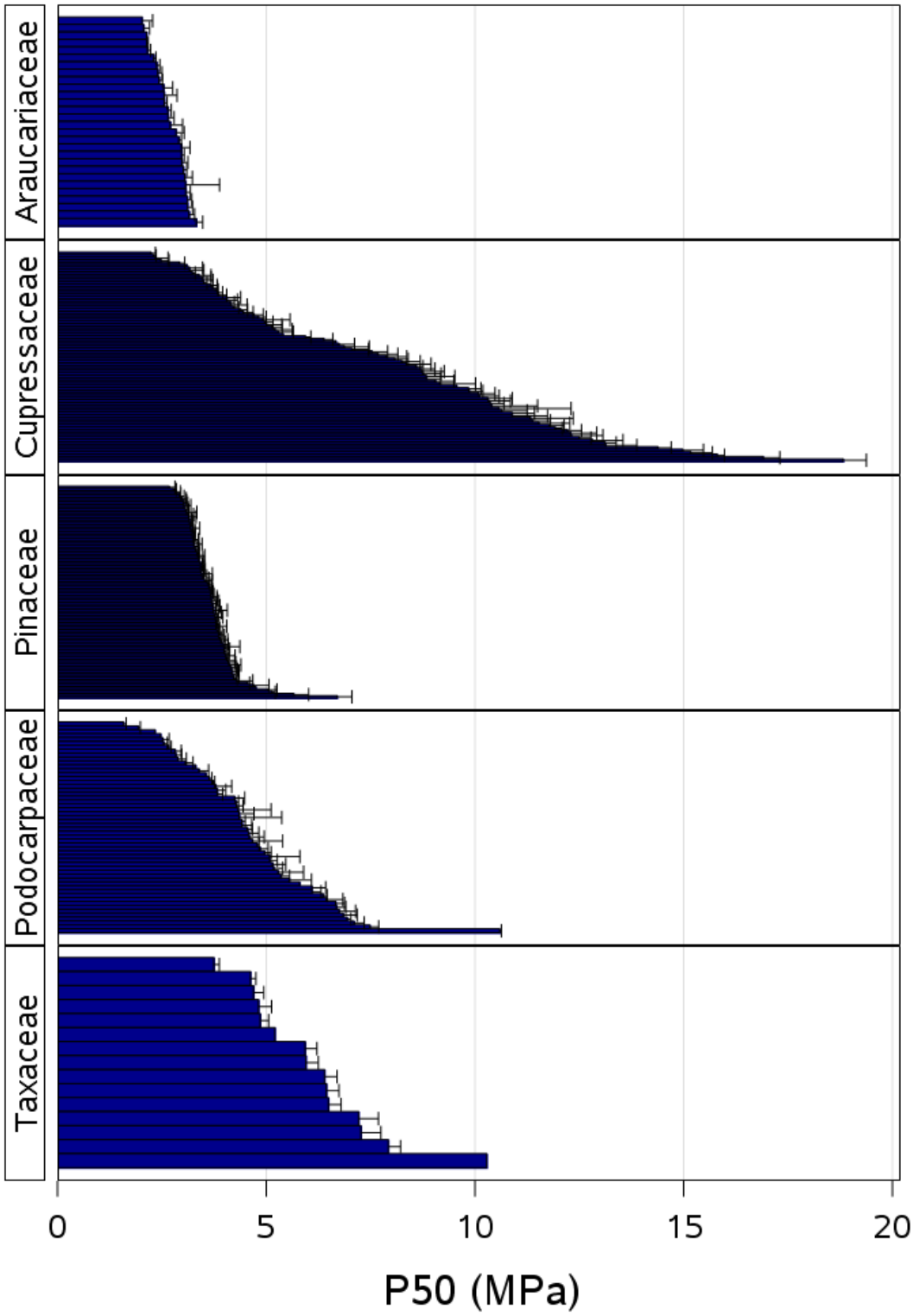

Figure S1. Variability of cavitation resistance (P_{50}, xylem pressure inducing 50% loss in hydraulic conductance) across species within the five largest families (Araucariaceae, Cupressaceae, *Pinaceae Podocarpaceae* and Taxaceae (including Cephalotaxaceae)).

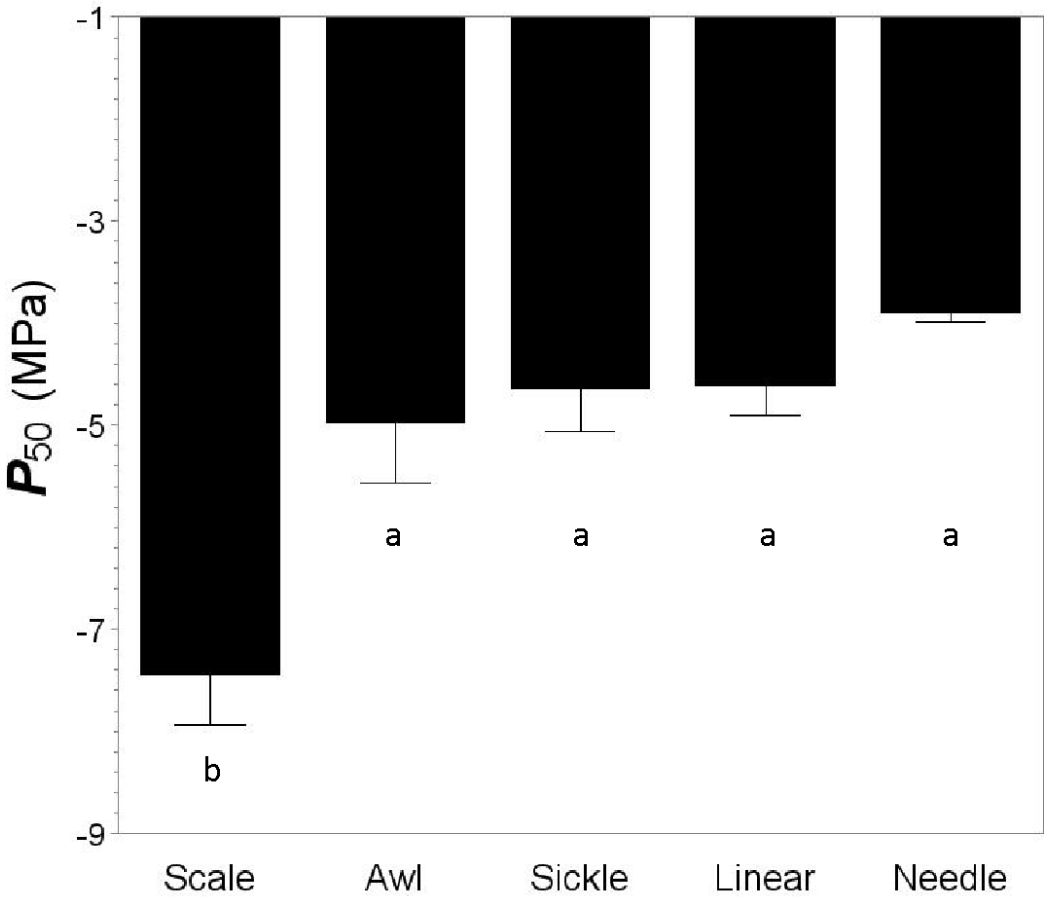

Figure S2. Mean value of xylem pressure inducing 50% loss in conductance (P_{50}) for each type of leaf shape. Error bars represent SE.

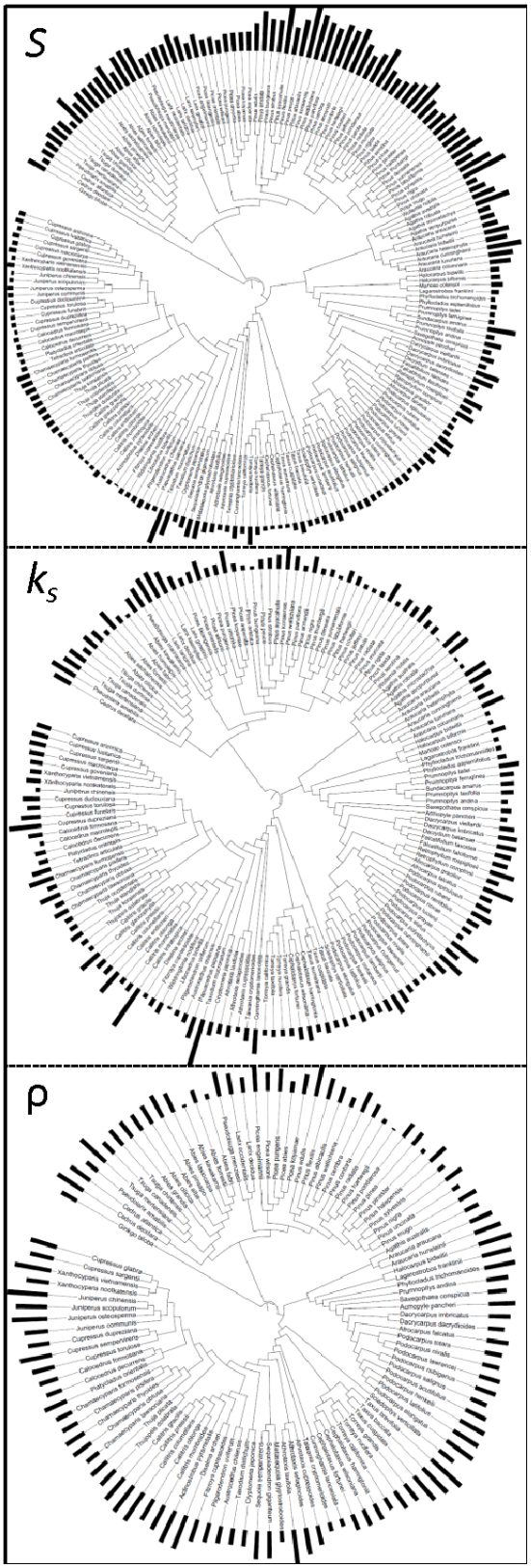

Figure S3. Values of cavitation resistance (*S*, slope of the vulnerability curve), transport efficiency (k_s, xylem specific hydraulic conductance) and wood density (ρ) are mapped onto the phylogenetic tree of conifers (black bars). Nodes are listed in a clockwise manner.

Chapter 2: Extreme Aridity Pushes Trees To Their Physical Limits. Maximilian Larter, Tim J. Brodribb, Sebastian Pfautsch, Régis Burlett, Hervé Cochard, and Sylvain Delzon. (Plant Physioloy, 2015)

Scientific Correspondence

Extreme Aridity Pushes Trees to Their Physical Limits

Maximilian Larter, Tim J. Brodribb, Sebastian Pfautsch, Régis Burlett, Hervé Cochard, and Sylvain Delzon*

Institut National de la Recherche Agronomique, Biodiversité, Gènes and Communautés-Unité Mixte de Recherche 1202, F–33610 Cestas, France (M.L., R.B., S.D.); Université de Bordeaux, Biodiversité, Gènes and Communautés-Unité Mixte de Recherche 1202, F–33615 Pessac, France (M.L., R.B., S.D.); School of Biological Science, University of Tasmania, Hobart, Tasmania 7001, Australia (T.J.B.); Hawkesbury Institute for the Environment, University of Western Sydney, Penrith, New South Wales 2751, Australia (S.P.); and Institut National de la Recherche Agronomique, Clermont University, Unité Mixte de Recherche 547 Physique et Physiologie Intégratives de l'Arbre Fruitier et Forestier, F–63100 Clermont-Ferrand, France (H.C.)

ORCID IDs: 0000-0002-4390-4195 (S.P.); 0000-0001-8289-5757 (R.B.); 0000-0003-3442-1711 (S.D.).

Drought-induced hydraulic failure is a leading cause of mortality of trees (McDowell et al., 2008; Anderegg et al., 2012) and has become a major concern in light of future climate predictions, with forests across the world showing signs of vulnerability to intense and prolonged drought events (Allen et al., 2010). We show here that Callitris tuberculata, a conifer species from extremely dry areas of Western Australia, is the most cavitation resistant tree species in the world to date (mean xylem pressure leading to 50% loss of hydraulic function [P_{50}] = 218.8 MPa). Hydraulic conductance is maintained in these plants at pressures remarkably close to the practical limit of water metastability, suggesting that liquid water transport under the cohesion-tension theory has reached its operational boundary.

Coping with desiccation is one of the greatest challenges faced by plant life on land, and the evolution of specialized tissue for the transport of water played a key role in the colonization of continents (Black and Pritchard, 2002; Sperry, 2003). As well as evolving mechanisms to reduce water loss (e.g. stomata and waxy leaf surfaces), land plants also have to provide their aerial organs with water to fuel photosynthesis, supply metabolism, and control leaf temperature through transpiration, even when water availability is low. Driven by competition for limited resources, plants have perfected their vascular systems over hundreds of millions of years, enabling vertical transport of water to heights in excess of 100 m above the ground and resulting in the dominance of trees across a wide range of terrestrial ecosystems. However, trees are excluded from extremely dry and cold climates; we propose here that an absolute limit for water transport in trees exists, set by the physical properties of liquid water, restricting the existence of woody non succulent trees in dry deserts.

[1]This work was supported by the French National Research Agency in the framework of the Investments for the Future Program within the COTE Cluster of Excellence (grant no. ANR–10–LABX–45) and by the Hawkesbury Institute for the Environment, University of Western Sydney, through its Research Exchange Program.

* Address correspondence to sylvain.delzon@u-bordeaux.fr. S.D. conceived the original screening and research plans; S.D. and S.P. supervised the experiments; M.L. performed most of the experiments; R.B. provided technical assistance to M.L.; M.L. and S.D. designed the experiments and analyzed the data; M.L. wrote the article with contributions of all the authors; S.D., S.P., H.C., and T.J.B. supervised and complemented the writing.

The movement of water against gravity in trees is driven by a remarkably simple process, described by the tension-cohesion theory (Tyree and Sperry, 1989; Tyree, 1997; Sperry, 2003). Evaporation at the leaf surface causes water in the plant to move up through a specialized transport tissue and drives water uptake from the soil. This leads water in the xylem to be stretched at negative pressures. However, cohesive forces due to hydrogen bonds bind water molecules together and also onto cell walls, sufficiently to maintain water in a liquid yet metastable state prone to sudden vaporization by cavitation. In moist soils, these pressures are moderate, typically above 22 MPa, but during drought, they decrease considerably, as plants are forced to extract water from drying soil, which reduces the stability of the water column. Below a specific pressure threshold, cavitation events occur when airwater menisci located at pores between xylem conduits break (Tyree, 1997; Cochard et al., 2009; Mayr et al., 2014), vaporizing sap, reducing xylem conductance, and eventually leading to plant death by desiccation (Brodribb et al., 2010; Urli et al., 2013). The xylem pressure at which cavitation occurs, leading to 50% loss of hydraulic function (P_{50}), is a trait that varies widely across species (Delzon et al., 2010; Bouche et al., 2014) and links with climate: xeric species are more resistant to cavitation than species that occupy more mesic habitats (Brodribb and Hill, 1999; Maherali et al., 2004; Choat et al., 2012; Pittermann et al., 2012). Conifers are generally more resistant to cavitation than angiosperms (Maherali et al., 2004; Choat et al., 2012), likely due to the presence of a pressure-activated safety valve that reduces the spread of air between xylem cells (Bouche et al., 2014). The most cavitation-resistant trees known

804 Plant Physiology, July 2015, Vol. 168, pp. 804–807, www.plantphysiol.org

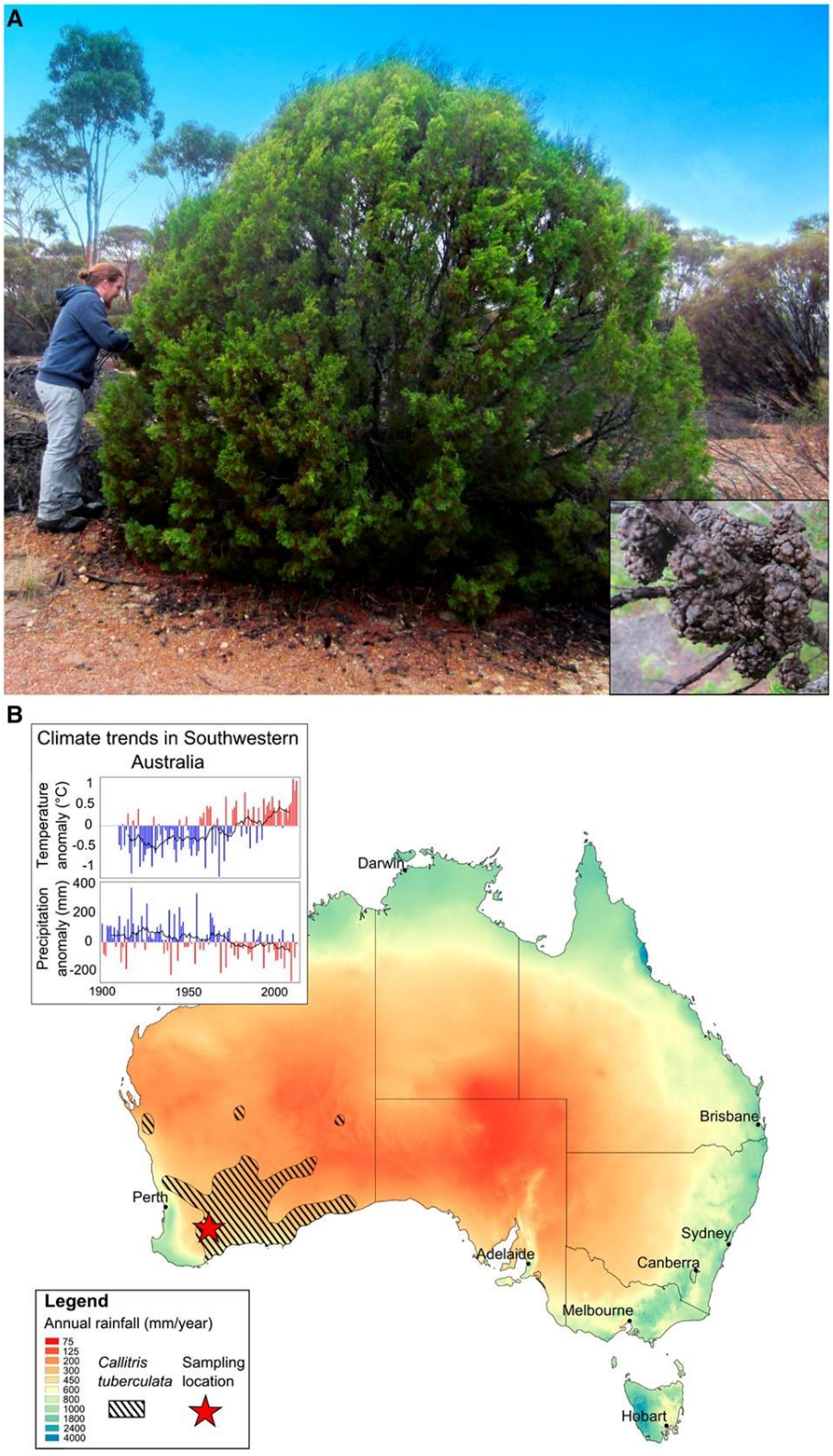

Figure 1. *C. tuberculata* appearance, distribution range, and climate. A, C. tuberculata from the sampled population near Lake Grace in Western Australia. The inset shows a close-up view of the tuberculate female cones of this species (photograph by A. Wesolowski). B, Map of Australia showing C. tuberculata's distribution (hatched area; the red star is the sampling location). Background colors represent mean annual precipitations. The inset at top left shows annual rainfall and temperature anomalies over the 20th century compared with the average (1961–1990) for southwestern Australia. Red bars highlight hot and/or dry years, and the black line indicates the 10-year moving average.

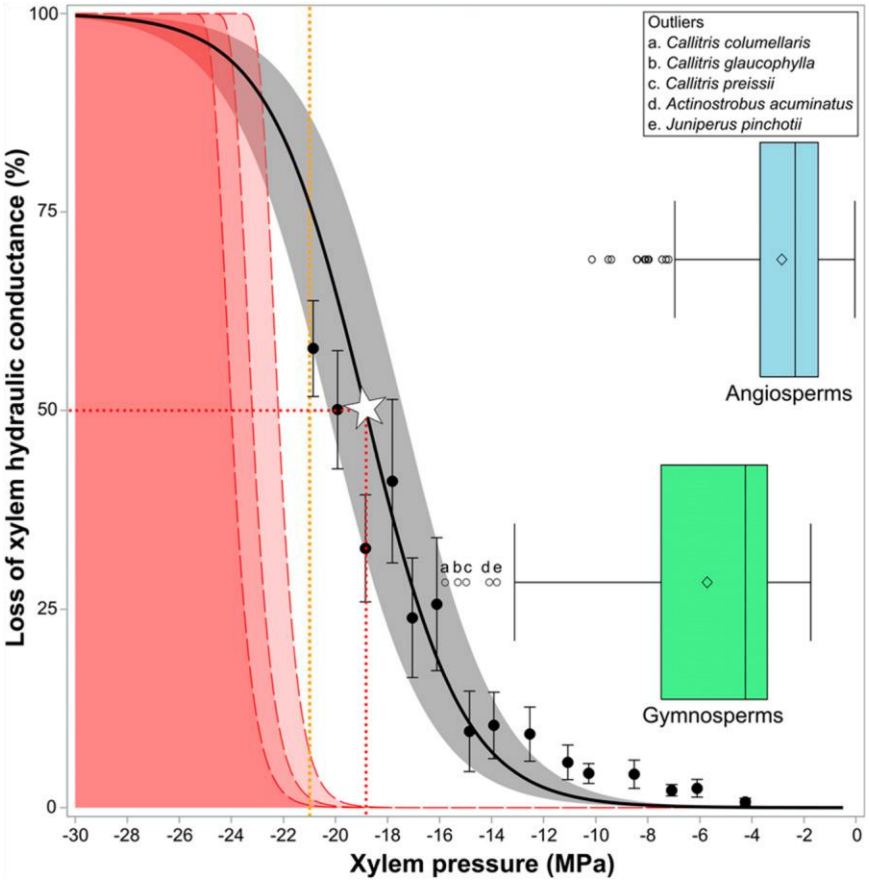

Figure 2. Vulnerability curve for C. tuberculata. Points show average loss of conductance ±SE for 15 pressure classes across all individuals. The black line is the Pammenter model for the species average P_{50} (white star) and slope; the gray shaded area shows 95% confidence limits for the mean. The orange vertical line represents the maximum speed of the centrifuge. The red dashed curves and the red shaded area show bulk cavitation probability curves at 20˚C, 30˚C, and 40˚C (from left to right). Box plots show the distribution of published P_{50} values for 384 angiosperm species (light blue) and 160 gymnosperm species (green). Outliers are detailed in the inset at top right.

to date are conifers of the genus *Callitris* from Australia and New Caledonia, in particular *Callitris columellaris*, displaying a P_{50} of 16 MPa (Brodribb et al., 2010). Here, we present the record cavitation resistance of *Callitris tuberculata* (Cupressaceae; Fig. 1; Supplemental Materials and Methods S1). This tree species is common in extremely arid ecosystems of southwestern Australia, where its range stretches far into the Great Victoria Desert (Fig. 1B). In this area, the climate is dry and hot, with most rainfall occurring during a short wet season (Supplemental Fig. S1). At its most extreme margin, the average annual rainfall is below 180 mm, and annual evapotranspiration can exceed rainfall 10 times, presumably making this species one of the most drought-tolerant trees in the world.

Our results show that this species from the desert tree line produces a previously unparalleled P_{50} of -18.8 ± 0.6 MPa (n = 9; Fig. 2; Supplemental Fig. S2; Supplemental Table S1), making it, to our knowledge, the most drought resistant tree ever measured. At -21 MPa, the lowest pressure we could achieve with our device (thus extending the experimental xylem pressure range by nearly 20%, from -17.3 MPa; Brodribb et al., 2010), around 25% to 50% of xylem conduits were still functional, with the final cavitation events predicted to occur at about -25 MPa. Could evolution push xylem pressure to more extreme values to enable this species to colonize even drier habitats? Strikingly, physics' answer is no, as *C. tuberculata* has reached the operational limit of water metastability.

According to the classical nucleation theory (Debenedetti, 1996), homogenous water cavitation occurs at pressures below -120 MPa at ambient temperature, as has been verified by experiments using microscopic liquid water inclusions in quartz (Zheng et al., 1991; Azouzi et al., 2013). Conversely, other experimental data suggest that bulk cavitation occurs heterogenously on ubiquitous impurities at much higher pressures, from -20 to -30 MPa, depending on the method used to induce negative pressure, water purity, and water temperature (for review, see Caupin et al., 2012). Consistently, in recent experiments based on a synthetic tree (Wheeler and Stroock, 2008; Vincent et al., 2012), bulk cavitation occurs rapidly at tensions of around -22 MPa. The presence of impurities, dissolved minerals, and nutrients in xylem sap (Buhtz et al., 2004; Krishnan et al., 2011) leads us to speculate that bulk cavitation in tree xylem will likely occur at similar pressures, setting an absolute physical limit for water transport in trees during drought.

Drought stress has pushed this species to evolve the most resistant xylem, to the point that *C. tuberculata* is able to potentially maintain water flow up to the limit of physical properties of liquid water. Already growing in an environment severely limited by water

availability, its adaptation to future conditions (i.e. by lowering P_{50}) may be restricted by reaching this physical boundary. Indeed, in southwestern Australia, a strong trend toward a drier and warmer climate has been evidenced over the 20th century (Fig. 1B, inset). This could lead to a contraction of forest at the desert margin, but it also offers the possibility of a range expansion into historically wetter regions to the southwest.

Hydraulic failure is one of the main hypotheses to explain tree death following prolonged periods of drought (Anderegg et al., 2012). Experiments have shown that, after reaching cavitation levels of around 50% in conifers or 90% in angiosperms, trees cannot recover (Brodribb et al., 2010; Urli et al., 2013). Furthermore, a recent study showed that trees in all ecosystems function with similarly narrow safety margins regarding this threshold to cavitation (Choat et al., 2012). Like southwestern Australia, many regions are projected to suffer from increasingly frequent and severe droughts (Stocker et al., 2013), highlighting the need to better understand the physiological responses of trees to drought stress to improve predictions of the impact of climate change on forests and woodlands. Our results suggest that *C. tuberculata* is an ideal candidate for further investigations, for example into xylem anatomy modifications allowing the evolution of increased cavitation resistance. Evolution toward xylem safety from cavitation leads to a tolerance strategy, allowing plants to maintain limited function even in stressed conditions. We have discovered an absolute limit to this evolutionary path due to water metastability in the xylem, explaining why trees tend to be excluded from the most arid ecosystems.

Supplemental Data

The following supplemental materials are available.

Supplemental Figure S1. Climate data.

Supplemental Figure S2. Vulnerability curves for all individuals.

Supplemental Table S1. Hydraulic traits for Callitris spp. individuals.

Supplemental Materials and Methods S1. Detailed description of data collection and analysis.

Received February 12, 2015; accepted May 30, 2015; published June 1, 2015.

LITERATURE CITED

Allen CD, Macalady AK, Chenchouni H, Bachelet D, McDowell N, Vennetier M, Kitzberger T, Rigling A, Breshears DD, Hogg EH, et al (2010) A global overview of drought and heat-induced tree mortality reveals emerging climate change risks for forests. For Ecol Manage 259: 660–684

Anderegg WR, Berry JA, Smith DD, Sperry JS, Anderegg LD, Field CB (2012) The roles of hydraulic and carbon stress in a widespread climateinduced forest die-off. Proc Natl Acad Sci USA 109: 233–237

Azouzi ME, Ramboz C, Lenain JF, Caupin F (2013) A coherent picture of water at extreme negative pressure. Nat Phys 9: 38–41

Black M, Pritchard HW, editors (2002) Desiccation and Survival in Plants: Drying without Dying. CABI Publishing, Wallingford, UK

Bouche PS, Larter M, Domec JC, Burlett R, Gasson P, Jansen S, Delzon S (2014) A broad survey of hydraulic and mechanical safety in the xylem of conifers. J Exp Bot 65: 4419–4431

Brodribb T, Hill RS (1999) The importance of xylem constraints in the distribution of conifer species. New Phytol 143: 365–372

Brodribb TJ, Bowman DJ, Nichols S, Delzon S, Burlett R (2010) Xylem function and growth rate interact to determine recovery rates after exposure to extreme water deficit. New Phytol 188: 533–542

Buhtz A, Kolasa A, Arlt K, Walz C, Kehr J (2004) Xylem sap protein composition is conserved among different plant species. Planta 219: 610–618

Caupin F, Arvengas A, Davitt K, Azouzi MM, Shmulovich KI, Ramboz C, Sessoms DA, Stroock AD (2012) Exploring water and other liquids at negative pressure. J Phys Condens Matter 24: 284110

Choat B, Jansen S, Brodribb TJ, Cochard H, Delzon S, Bhaskar R, Bucci SJ, Feild TS, Gleason SM, Hacke UG, et al (2012) Global convergence in the vulnerability of forests to drought. Nature 491: 752–755

Cochard H, Hölttä T, Herbette S, Delzon S, Mencuccini M (2009) New insights into the mechanisms of water-stress-induced cavitation in conifers. Plant Physiol 151: 949–954

Debenedetti PG (1996) Metastable Liquids: Concepts and Principles. Princeton University Press, Princeton, NJ

Delzon S, Douthe C, Sala A, Cochard H (2010) Mechanism of water-stress induced cavitation in conifers: bordered pit structure and function support the hypothesis of seal capillary-seeding. Plant Cell Environ 33: 2101–2111

Krishnan HB, Natarajan SS, Bennett JO, Sicher RC (2011) Protein and metabolite composition of xylem sap from field-grown soybeans (Glycine max). Planta 233: 921–931

Maherali H, Pockman WT, Jackson RB (2004) Adaptive variation in the vulnerability of woody plants to xylem cavitation. Ecology 85: 2184–2199

Mayr S, Kartusch B, Kikuta S (2014) Evidence for air-seeding: watching the formation of embolism in conifer xylem. J Plant Hydraul 1: e-0004

McDowell N, Pockman WT, Allen CD, Breshears DD, Cobb N, Kolb T, Plaut J, Sperry J, West A, Williams DG, et al (2008) Mechanisms of plant survival and mortality during drought: why do some plants survive while others succumb to drought? New Phytol 178: 719–739

Pittermann J, Stuart SA, Dawson TE, Moreau A (2012) Cenozoic climate change shaped the evolutionary ecophysiology of the Cupressaceae conifers. Proc Natl Acad Sci USA 109: 9647–9652

Sperry JS (2003) Evolution of water transport and xylem structure. Int J Plant Sci 164: S115–S127

Stocker TF, Qin D, Plattner GK, Tignor MM, Allen SK, Boschung J, Nauels A, Xia Y, Bex V, Midgley PM (2013) IPCC, 2013: Climate Change 2013: The Physical Science Basis. Cambridge University Press, Cambridge, UK

Tyree MT (1997) The cohesion-tension theory of sap ascent: current controversies. J Exp Bot 48: 1753–1765

Tyree MT, Sperry JS (1989) Vulnerability of xylem to cavitation and embolism. Annu Rev Plant Biol 40: 19–36

Urli M, Porté AJ, Cochard H, Guengant Y, Burlett R, Delzon S (2013) Xylem embolism threshold for catastrophic hydraulic failure in angiosperm trees. Tree Physiol 33: 672–683

Vincent O, Marmottant P, Quinto-Su PA, Ohl CD (2012) Birth and growth of cavitation bubbles within water under tension confined in a simple synthetic tree. Phys Rev Lett 108: 184502

Wheeler TD, Stroock AD (2008) The transpiration of water at negative pressures in a synthetic tree. Nature 455: 208–212

Zheng Q, Durben DJ, Wolf GH, Angell CA (1991) Liquids at large negative pressures: water at the homogeneous nucleation limit. Science 254: 829–832

Supplemental material:

Materials and Methods:

Sampling

As part of investigations into record cavitation-resistant conifers, we collected samples (branches of about 40 cm) from a population of *Callitris tuberculata* near Lake Grace (WA, Australia) in July 2014. They were immediately wrapped in wet paper towels with foliage removed, and sent for measurement at the BIOGECO lab at INRA - University of Bordeaux (France; http://sylvain-delzon.com/?page_id=536) where they were kept in dark, damp and refrigerated conditions until measurements were conducted.

Vulnerability curves

Cavitation resistance was estimated with the flow-centrifuge technique, based on the Cavitron method (Cochard *et al.*, 2005), in which centrifugation is used to induce negative pressure in the xylem of the sample and conductance is monitored during spinning (as measured by the water flow through the stem). Samples were cut to length (27 cm), then bark was removed and the ends were re-cut with a clean razor blade. We used a specially designed centrifuge rotor, reinforced to allow previously unattainable speeds of above 13000 rpm. We thus reached a record maximum speed of 15000 rpm, which induces xylem pressure of around -21 MPa. Maximum conductance is estimated at low speed (high pressure), then we gradually increase rotation speed, repeatedly measuring conductance at least 3 times at each pressure step. As xylem pressure is forced to more negative values, cavitation events occur, leading to a drop in hydraulic conductance, which is classically represented as so-called vulnerability curves, percent loss of conductance (or PLC) as a function of pressure. Each individual vulnerability curve was fit using the Pammenter model (Pammenter and Vander Willigen, 1998), with P_{50} derived as the pressure leading to a 50% decrease in conductance (Supplemental Fig. S2). This procedure has been extensively described elsewhere, see for example Methods in Delzon et al. (2010) and Jansen et al. (2012). Individual P_{50} and other parameters for each individual are presented in Supplemental Table S1. Conductance measurements for all individuals were pooled and binned into 15 pressure classes, to create an average vulnerability curve (Fig. 1). The shaded area in Fig. 1 represents the 95% confidence interval for the mean obtained with the CLM option in the Means Procedure in SAS. All statistical analyses was conducted using SAS software (SAS 9.4 Institute, Cary, NC, USA).

This method also enables estimation of xylem specific conductivity, a measure of xylem capacity to transport water. No significant correlation with xylem safety from cavitation was

found within this population of *C. tuberculata* (regression analysis r^2=0.035; P=0.63), indicating absence of a functional trade-off between safety and efficiency.

Cavitation resistance data

We extracted published measurements of cavitation resistance from Choat et al. (2012) and Bouche et al. (2014) of both Angiosperm and Gymnosperm species to allow comparison of *Callitris tuberculata* to other species. These datasets are available online respectively from the Nature and Journal of Experimental Botany websites.

Bulk cavitation curves

Bulk heterogeneous cavitation curves for temperatures of 20, 30 and 40°C (likely to occur in the xylem of *C. tuberculata* during summer drought) were constructed based on equation 12 in Herbert et al. (2006).

Climate data

Annual temperature and precipitation deviation from the 1961-1990 average was obtained from the Australian Bureau of Meterology (http://www.bom.gov.au). *Callitris tuberculata* occurrences were downloaded from the Global Biodiversity Information Facility (GBIF; http://www.gbif.org), and used to outline an approximate distribution range. Climate layers were then obtained from Worldclim (Hijmans *et al.*, 2005) (http://www.worldclim.org) and the Global Aridity Index and PET datasets (http://www.cgiar-csi.org/data/global-aridityand-pet-database), and data for each location was extracted in QGIS 2.4.0 (Quantum, 2011) using the point-sampling tool. We show here the average monthly precipitations and maximum daily temperature for all locations obtained from GBIF (Supplemental Fig. S1).

Literature cited :

Bouche PS, Larter M, Domec J-C, Burlett R, Gasson P, Jansen S, Delzon S. 2014. A broad survey of hydraulic and mechanical safety in the xylem of conifers. Journal of experimental botany.

Choat B, Jansen S, Brodribb TJ, *et al.* 2012. Global convergence in the vulnerability of forests to drought. Nature **491**, 752–755.

Cochard H, Damour G, Bodet C, Tharwat I, Poirier M, Améglio T. 2005. Evaluation of a new centrifuge technique for rapid generation of xylem vulnerability curves. Physiologia Plantarum **124**, 410–418.

Delzon S, Douthe C, Sala A, Cochard H. 2010. Mechanism of water-stress induced cavitation in conifers: bordered pit structure and function support the hypothesis of seal capillary-seeding. Plant, cell & environment **33**, 2101–2111.

Herbert E, Balibar S, Caupin F. 2006. Cavitation pressure in water. Physical Review E **74**, 041603.

Hijmans RJ, Cameron SE, Parra JL, Jones PG, Jarvis A. 2005. Very high resolution interpolated climate surfaces for global land areas. International Journal of Climatology **25**, 1965–1978.

Jansen S, Lamy J-B, Burlett R, Cochard H, Gasson P, Delzon S. 2012. Plasmodesmatal pores in the torus of bordered pit membranes affect cavitation resistance of conifer xylem. Plant, cell & environment.

Pammenter NW, Vander Willigen C. 1998. A mathematical and statistical analysis of the curves illustrating vulnerability of xylem to cavitation. Tree physiology **18**, 589–593.

Quantum G. 2011. Development Team, 2012. Quantum GIS Geographic Information System. Open Source Geospatial Foundation Project. [http://qgis.osgeo.org].

Figure S1. Climate diagram of average monthly precipitations and maximum temperatures for *Callitris tuberculata*'s estimated range. Black bars represent monthly precipitations, and the red curve shows maximum temperatures.

Figure S2. Vulnerability curves for nine individual trees of *Callitris tuberculata*. Each point represents mean value of percent loss of hydraulic conductance over at least three measurements of hydraulic conductance (bars represent ± standard error). Lines represent the Pammenter model fit to each individual curve, and dashed lines show were the model was expanded beyond experimental data.

Table S1. Cavitation resistance parameters for each individual. P_{50}, P_{12}, and P_{88} are, respectively, the xylem pressure inducing 50%, 12% and 88% loss of xylem hydraulic conductance. *S* is the slope of the vulnerability curve at P_{50}. *ks* is the specific xylem conductivity, a standardized measurement of the samples' capacity to transport water.

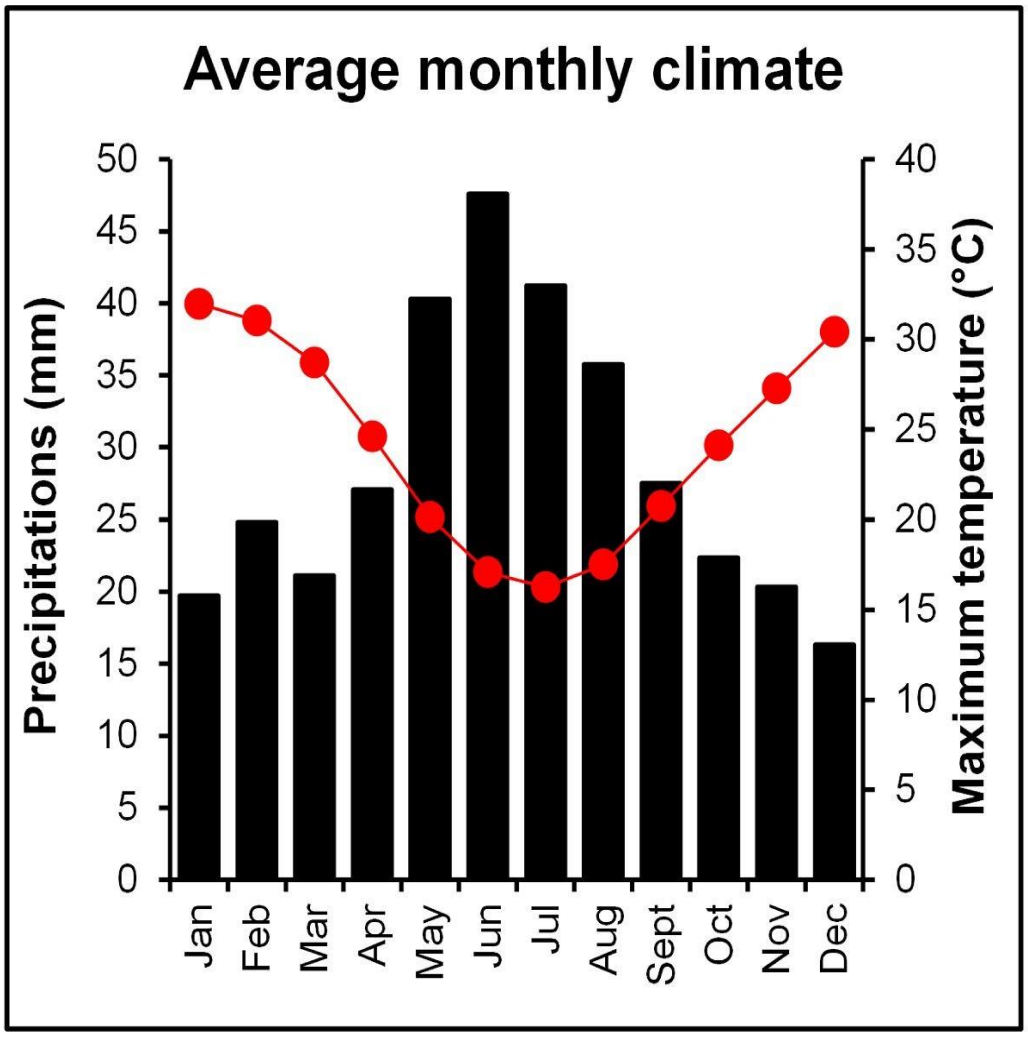

Figure S1. Climate diagram of average monthly precipitations and maximum temperatures for *Callitris tuberculata*'s estimated range. Black bars represent monthly precipitations, and the red curve shows maximum temperatures.

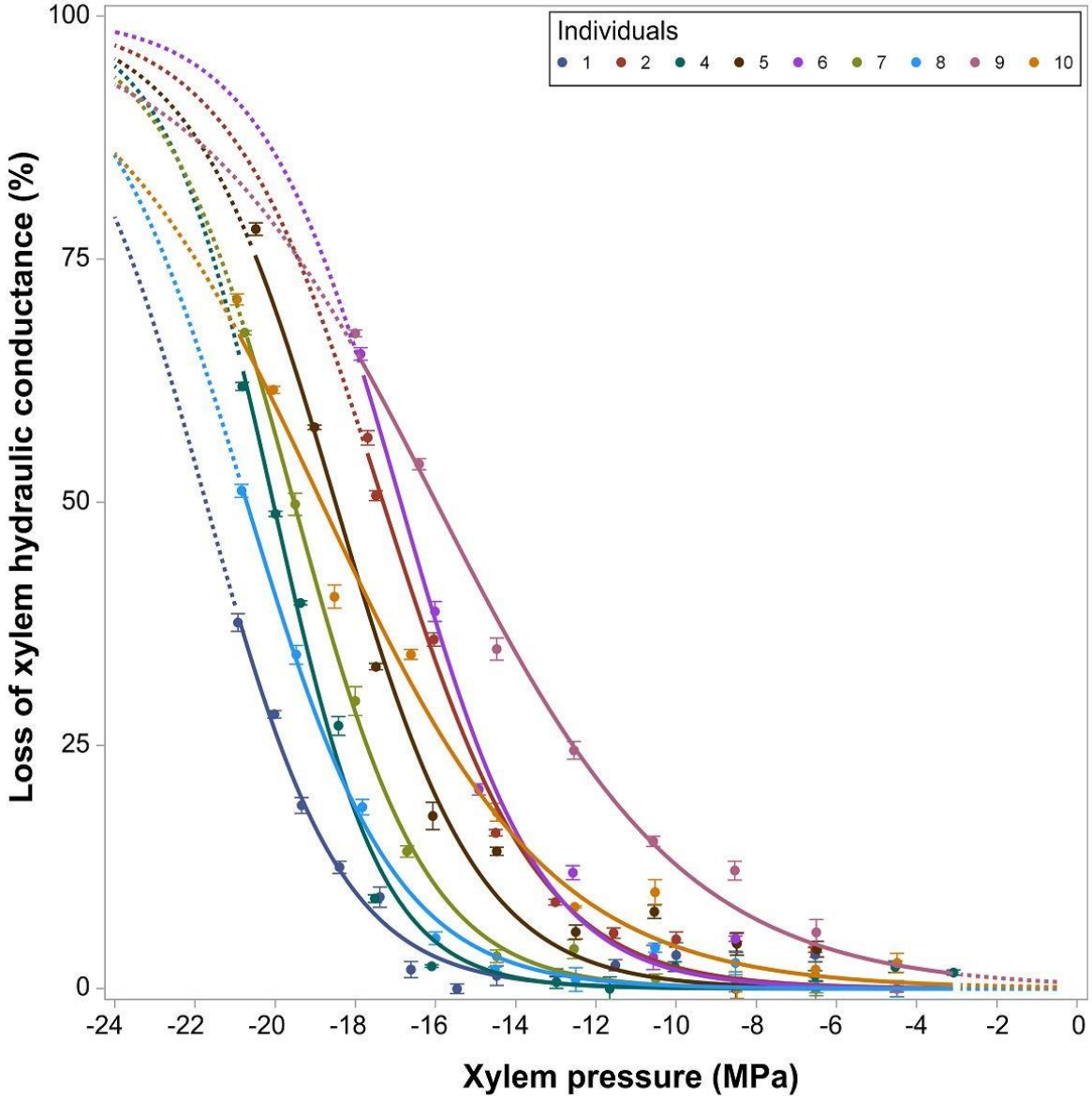

Figure S2. Vulnerability curves for nine individual trees of *Callitris tuberculata*. Each point represents mean value of percent loss of hydraulic conductance over at least three measurments of hydraulic conductance (bars represent ± standard error). Lines represent the Pammenter model fit to each individual curve, and dashed lines show were the model was expanded beyond experimental data.

Supplemental Table S1. Cavitation resistance parameters for each individual. P_{50}, P_{12} and P_{88} are respectively, the xylem pressure inducing 50%, 12% and 88% loss of xylem hydraulic conductance. S is the slope of the vulnerability curve at P_{50}. ks is the specific xylem conductivity, a standardized measurment of the samples' capacity to transport water.

Individual	P_{50} (MPa)	P_{12} (MPa)	P_{88} (MPa)	S (%.MPa^{-1})	ks (kg.m^{-1}.s^{-1}.MPa^{-1})
1	-21.73	-18.35	-25.11	14.80	0.000390
2	-17.31	-13.45	-21.17	12.96	0.000359
4	-20.05	-17.33	-22.76	18.42	0.000261
5	-18.50	-14.92	-22.07	13.99	0.000468
6	-16.87	-13.38	-20.35	14.34	0.000344
7	-19.53	-16.22	-22.84	15.10	0.000566
8	-20.71	-17.03	-24.39	13.58	0.000329
9	-15.99	-9.77	-22.20	8.04	0.000484
10	-18.85	-13.13	-24.56	8.75	0.000226
Average	-18.84	-14.84	-22.83	13.33	0.000381

Chapter 3: A broad survey of hydraulic and mechanical safety in the xylem of conifers.

Pauline S. Bouche, Maximilien Larter, Jean-Christophe Domec, Régis Burlett, Peter Gasson, Steven Jansen and Sylvain Delzon. (Journal of Experimental Botany, 2014)

Journal of Experimental Botany Advance Access published June 10, 2014

Journal of Experimental Botany doi:10.1093/jxb/eru218
This paper is available online free of all access charges (see http://jxb.oxfordjournals.org/open_access.html for further details)

RESEARCH PAPER

A broad survey of hydraulic and mechanical safety in the xylem of conifers

Pauline S. Bouche[1,2,3], Maximilien Larter[2,3], Jean-Christophe Domec[4,5], Régis Burlett[3], Peter Gasson[6], Steven Jansen[1] and Sylvain Delzon[2,3,*]

1 Institute for Systematic Botany and Ecology, Ulm University, Ulm, Germany
2 INRA, UMR BIOGECO, F-33610 Cestas, France
3 University of Bordeaux, UMR BIOGECO, 33405 Talence, France
4 Bordeaux Sciences Agro, University of Bordeaux, 33175 Gradignan, France
5 INRA, UMR TCEM, F-33140 Villenave d'Ornon, France
6 Jodrell Laboratory, Royal Botanic Garden, Kew, Richmond, Surrey, TW9 3DS, UK

* To whom correspondence should be addressed. E-mail: sylvain.delzon@u-bordeaux1.fr

Received 6 February 2014; Revised 14 April 2014; Accepted 22 April 2014

Abstract

Drought-induced forest dieback has been widely reported over the last decades, and the evidence for a direct causal link between survival and hydraulic failure (xylem cavitation) is now well known. Because vulnerability to cavitation is intimately linked to the anatomy of the xylem, the main objective of this study was to better understand the xylem anatomical properties associated with cavitation resistance. An extensive data set of cavitation resistance traits and xylem anatomical properties was developed for 115 conifer species, with special attention given to the micro-morphology of bordered pits. The ratio of torus to pit aperture diameter, so-called torus overlap, increased with increasing cavitation resistance, while the flexibility of the margo does not seem to play a role, suggesting that air-seeding is located at the seal between the aspirated torus and pit aperture. Moreover, punctured tori were reported in various Pinaceae species. Species resistant to cavitation had thicker tracheid walls, while their lumen diameter (conduit size) was only slightly reduced, minimizing the impact on hydraulic conductance. The results also demonstrated (i) the existence of an indirect trade-off between hydraulic safety and mechanical strength; and (ii) a consistency between species distribution and xylem anatomy: species with a wide torus overlap and high valve effects are found in arid environments such as the Mediterranean region.

Key words: Cavitation resistance, hydraulic efficiency, mechanical strength, seal capillary-seeding, torus–margo pit, xylem anatomy, wall implosion.

Introduction

Evidence for drought-induced forest dieback has been reported worldwide (Bigler *et al.*, 2007; Van Mantgem *et al.*, 2009; Allen *et al.*, 2010; Peng *et al.*, 2011; SanchezSalguero *et al.*, 2012). There is growing evidence that all forest types or climate zones are equally vulnerable to drought events, even in currently mesic environments (Allen *et al.*, 2010; Choat *et al.*, 2012). Although gymnosperms seem to be on average more resistant to cavitation (Maherali *et al.*, 2004; S. Delzon *et al.*, unpublished data) and have greater hydraulic safety margins *per se* than angiosperms (Choat *et al.*, 2012), they are also not immune to drought-induced mortality (Breshears *et al.*, 2005; Sanchez-Salguero *et al.*, 2012; Hartmann *et al.*, 2013).

Resistance to cavitation is a crucial trait in trees to cope with drought stress (Cochard and Delzon, 2013) in addition to, for example, rooting depth, internal water storage, and changes in biomass allocation or leaf anatomy. Indeed,

substantial evidence of a direct causal link between drought resistance and cavitation resistance has been highlighted in both conifers (Brodribb and Cochard, 2009; Brodribb *et al.*, 2010) and angiosperms (Barigah *et al.*, 2013; Urli *et al.*, 2013). Global surveys of cavitation resistance in woody species have not surprisingly shown that species from xeric climates are more resistant to embolism than species from wet climates (Maherali *et al.*, 2004; Cochard *et al.*, 2008; Choat *et al.*, 2012). Incorporation of phylogenetic information strengthened these adaptive inferences and suggests that cavitation resistance-related traits are under natural selection (Maherali *et al.*, 2004; Willson *et al.*, 2008; Pittermann *et al.*, 2010). Hence, there is convincing evidence that the geographical distribution of many tree species is determined by their ability to resist droughtinduced embolism (Engelbrecht *et al.*, 2007; Choat *et al.*, 2012; Delzon and Cochard, 2014).

Drought-induced embolism occurs in the xylem, in which water is transported under tension (Tyree and Zimmerman, 2002). While the exact mechanisms remain unknown, drought-induced embolism formation is thought to occur via air leakage from an embolized conduit (non-functional) to a functional conduit. When the pressure in the xylem is sufficiently negative, the rupture of an air–sap meniscus allows propagation of air bubbles through porous interconduit pit membranes (Crombie *et al.*, 1985; Cochard *et al.*, 1992; Jarbeau *et al.*, 1995; Tyree and Zimmerman, 2002). Cavitation resistance would therefore be influenced by the structure and function of bordered pits. Accordingly, variation in xylem anatomy, conduit characteristics, and bordered pits has been associated with cavitation resistance in both angiosperms (Sperry and Hacke, 2004; Jansen *et al.*, 2009; Lens *et al.*, 2011) and conifers (Hacke *et al.*, 2004; Domec *et al.*, 2006; Delzon *et al.*, 2010).

Cavitation in angiosperms occurs by air-seeding at the pit membrane level. Under well-hydrated conditions, the pit membrane separating two functional vessels is in a relaxed position (i.e. unaspirated) and sap flows through the pores of the membrane. When water stress occurs, the pressure difference between an embolized and functional vessel leads to the rupture of an air–sap meniscus located within the pit. Embolism formation in angiosperms seems to depend on the size of the largest pores in the pit membranes (Choat *et al.*, 2003, 2004; Christman *et al.*, 2009). In conifers, the inter-tracheid pits are morphologically characterized by a centrally located torus and a porous margo region. When the pressure difference in xylem increases, the deflection of the torus against the pit aperture seals off the embolized tracheid (Liese and Bauch, 1967; Bailey, 1913). This so-called 'valve effect' prevents the spread of air into the functional xylem and may depend on the torus diameter relative to pit aperture diameter (Hacke *et al.*, 2004; Domec *et al.*, 2006; Delzon *et al.*, 2010). How does cavitation occur in torus–margo pits? Different mechanisms of air-seeding have been proposed to explain cavitation in conifers (for a review, see Cochard, 2006). Recent studies demonstrated that as for angiosperms, cavitation occurs by rupture of an air–sap meniscus in the vicinity of the pit membrane (Sperry and Hacke, 2004; Cochard *et al.*, 2009), but the exact location of where the meniscus breaks is unknown. Two mechanisms are likely: (i) air bubbles pass through pores at the edge of the torus when the torus and the inner wall of the pit membrane are not perfectly sealed (seal capillary-seeding hypothesis; Cochard *et al.*, 2009; Delzon *et al.*, 2010; Pittermann *et al.*, 2010); and (ii) the torus structure is not fully impermeable, meaning that air bubbles may pass through tiny pores (torus capillary-seeding hypothesis; Jansen *et al.*, 2012). According to recent studies, the first is more likely in most conifer families, while the second may be an additional mechanism in Pinaceae (Jansen *et al.*, 2012). Additional anatomical observations of bordered pits in a broader range of conifers are believed to provide further details about how embolism formation occurs in gymnosperms.

Conifer tracheids are involved not only in water transport but also in mechanical support of the plant. The length of a tracheid, its diameter, and the thickness of its wall are factors contributing to mechanical strength. Based on measurements and theoretical estimations, cavitation resistance is correlated to the 'thickness to span' ratio of tracheids (Hacke *et al.*, 2001; Sperry *et al.*, 2006; Domec *et al.*, 2009; Arbellay *et al.*, 2012). Higher absolute resistance to cavitation is associated with lower negative sap pressure and requires stronger tracheids with a higher thickness to span ratio to resist to mechanical stress. An increase in the thickness to span ratio, probably due to reduced lumen diameter (Pittermann *et al.*, 2006*b*; Sperry *et al.*, 2006), thus also enhances the resistance to water stress. The physiological consequences of this trade-off between hydraulic safety and mechanical strength has received considerable attention (Baas *et al.*, 2004; Domec *et al.*, 2006, 2009; Pittermann *et al.*, 2006*a*, *b*, 2011; Choat *et al.*, 2007). Therefore, conduit structure is potentially constrained by safety considerations (Sperry *et al.*, 2008). In this study, the linkage between xylem anatomy and resistance to drought-induced cavitation was assessed using a large database of 115 conifer species. By broadly sampling across conifer phylogeny and four major terrestrial biomes, the objectives were (i) to better understand how xylem anatomical properties associated with air-seeding influence the mechanical strength of the xylem; and (ii) to assess the evolutionary trends of xylem anatomy in the selected taxa. It was hypothesized (i) that the anatomy and functional properties of pit pairs strongly influence cavitation resistance in conifer species—more specifically it was believed that the valve effect (product of torus–aperture overlap and margo flexibility) plays a major role in cavitation resistance; and (ii) that increased cavitation resistance is associated with higher mechanical strength.

Materials and methods

Plant material

Anatomical observations and cavitation measurements were conducted on 60 conifer species. Additional data were retrieved from Delzon *et al.* (2010) and Jansen *et al.* (2012) (40 and 15

Table 1. Taxonomic diversity of conifers and species studied (following Farjon et al., 2008).

Family	Genera	Genera sampled	Species	Species sampled
Araucariaceae	3	3	41	9
Cephalotaxaeae	1	1	11	3
Cupressaceae	30	25	133	43
Pinaceae	11	7	228	35
Podocarpaceae	19	14	186	19
Sciadopityaceae	1	1	1	1
Taxaceae	5	2	23	5
Total	70	53	627	115

species, respectively) and completed by measuring novel characteristics. A total of 115 species, including seven families and 45 genera (see Table 1, and Supplementary Table S1 available at *JXB* online), were used to test the relationship between cavitation resistance and anatomical traits. All anatomical observations have been carried out on material that had previously been used for measuring cavitation resistance. These observations were limited to one individual for most species and, in cases where several samples were available, the sample that was closest to the average P_{50} value; that is, the xylem pressure inducing 50% loss of hydraulic conductance, was selected. Although the intraspecific variability in pit anatomy can be considerable between organs (roots showed dramatic differences in conduit and pit anatomical properties compared with branches; Domec *et al.*, 2008; Jansen *et al.*, 2009; Schoonmaker *et al.*, 2010), here it was assumed that intraspecific variation was smaller than interspecific variation (Matzner *et al.*, 2001; Maherali *et al.*, 2004; Martinez-Vilalta *et al.*, 2009). Moreover, to avoid any additional intra-organ variability, only anatomical features in the xylem of young branches were measured.

Microscope techniques

Light microscopy Four to five transverse sections were cut for each sample with a sliding microtome, stained with safranin (1%), and fixed on a microscope slide. Sections were observed with a light microscope (DM2500, Leica, Germany) at the University of Bordeaux. Five photos per section were taken with a digital camera (DFC290, Leica, Germany), and analysed with WinCell (Regent Inst., Canada). *Scanning electron microscopy (SEM)* SEM observations were conducted at Ulm University with a Hitachi cold-field emission scanning electron microscope and with a benchtop scanning electron microscope at the University of Bordeaux (PhenomG2 pro; FEI, The Netherlands). For the Hitachi SEM, thin (1 µm) radial sections were cut in different parts of the stem, air-dried, coated with platinum using a sputter coater (Emitech Ltd; Ashford, UK) for 2 min at 10 mA, and observed under 2 kV. For the benchtop SEM, samples of 5–8 mm long were cut with a razor blade in a radial direction. After drying for 24 h in an oven at 70 °C, the samples were fixed on stubs, coated with gold using a sputter coater (108 Auto; Cressington, UK) for 40 s at 20 mA, and observed under 5 kV.

Transmission electron microscopy (TEM) A transmission electron microscope was used to obtain ultrastructural details of pit membranes for 33 species. One stem per species was cut into 1 mm_3 blocks and dehydrated in an ethanol series. The ethanol was gradually replaced with LR White resin (London Resin Co., Reading, UK) over several days (for more details, see Jansen *et al.*, 2012). Then, transverse ultrathin (between 60 nm and 90 nm) sections were cut using a diamond knife and collected on 100 mesh copper grids. The ultrathin sections were manually stained with uranyl acetate and lead citrate. Observations were carried out with a JEOL JEM-1210 transmission electron microscope (Jeol, Tokyo, Japan) at 80 kV accelerating voltage, and digital images were taken using a MegaView III camera (Soft Imaging System, Münster, Germany).

Xylem anatomical features

All anatomical features related to tracheids and bordered pits (see Table 2) were based on earlywood, which is responsible for most of the hydraulic conductance (Domec and Gartner, 2002). Based on light microscopy images (×200 magnification), the tracheid lumen diameter (D_T; the simple average of the equivalent circle diameter) and the thickness of the double wall between neighbouring conduits (T_W) were measured. Pit membrane diameter (D_{PM}), aperture diameter (D_{PA}), and torus diameter (D_{TO}) were measured using SEM (Fig. 1). The distance between two pit borders (L_{PB}; Fig. 1), the number of margo pores (N_{MP}), the mean and maximum diameter of margo pores (D_{MP}, D_{MPmax}), and the mean diameter of pores in the torus (D_{TP}) (Fig. 2) were measured using SEM images. Because the L_{PB} parameter varies depending on the distribution of pits in tracheids, a constant distribution of pits along the entire length of a tracheid was assumed for these measurements. Average values for all anatomical features were determined based on a minimum of 20 measurements. All anatomical measurements were conducted using ImageJ freeware (W.S. Rasband, ImageJ, US National Institutes of Health, Bethesda, MD, USA, http://imagej.nih.gov/ij/, 1997–2012).

Xylem anatomical properties

The following functional properties of pit membranes and tracheids (Table 2) were estimated from anatomical measurements to investigate micro-morphological variation in relation to embolism formation.

Seal capillary seeding The margo flexibility [$F=(D_{PM}-D_{TO})/D_{TO}$], the torus overlap [$O=(D_{TO}-D_{PA})/D_{TO}$], and the valve effect ($V_{EF}=F\times O$) were estimated following Delzon *et al.* (2010). D_{PM} is the pit membrane diameter, D_{PA} the pit aperture diameter, and D_{TO} is the torus diameter.

Margo and torus capillary seeding pressure The pressure difference between two adjacent tracheids required to break the air–water meniscus in the margo was calculated following the Young–Laplace equation:

$$P_{MC} = -[4\cos\tau(\alpha)] / D_{MP}$$

where τ (0.0728 N m_{-1} at 20 °C) is the surface tension of water, α is the contact angle between the microfibrils and the meniscus (assumed equal to 0°), and D_{MP} is the average diameter of the margo pores.

The pressure difference required to break the air–water meniscus in the torus when it is already sealed against the pit aperture was calculated as:

$$P_{TC}D_{TP} = -[4\cos\tau(\alpha)] / D_{TO}$$

where D_{TP} is the mean diameter of a pore in the torus.

Torus deflection

The pressure difference required to aspirate the pit membrane onto the pit border was estimated according to Domec *et al.* (2006):

$$P_{TD}N\, e_A r D_{PM} = -(2\ \mathrm{MOE} e_A) / (\pi r\, D_{PM})$$

where N is the number of margo strands, which was assigned to the average value of 55 and 200 strands per pit (Domec *et al.*, 2006).

Table 2. Anatomical traits and functional properties with reference to their acronym, definition, microscope technique units, and number of measurements

Acronym	Definition	Technique	Unit	Minimum number of measurements
Anatomical features				
D_T	Tracheid lumen diameter : the simple average of the equivalent circle diameter	LM or TEM	µm	30
D_{MP}	Margo pore diameter	SEM	nm	50
D_{MPmax}	Maximum margo pore diameter	SEM	nm	50
D_{PA}	Pit aperture diameter (horizontal diameter at its widest point)	SEM or TEM	µm	20
D_{PM}	Pit membrane diameter (horizontal diameter at its widest point)	SEM or TEM	µm	20
D_{TO}	Torus diameter (horizontal diameter at its widest point)	SEM or TEM	µm	20
D_{TP}	Torus pore diameter	SEM	nm	20
N_{MP}	Number of pores in a margo	SEM	-	-
L_{PB}	Distance between pit adjacent borders	SEM	µm	20
T_{TW}	Tracheid wall thickness measured as the double wall between two adjacent tracheids	LM or TEM	µm	30
Functional traits				
D_H	Hydraulic diameter = $\Sigma D_T^5/\Sigma D_T^4$	-	µm	-
F	Flexibility of the margo = $(D_{PM} - D_{TO})/D_{TO}$	-	-	-
L_E	Ligament efficiency	-	-	-
O	Torus overlap = $(D_{TO} - D_{PA})/D_{TO}$	-	-	-
P_{WI}	Wall implosion pressure	-	MPa	-
P_{MC}	Margo capillary seeding pressure	-	MPa	-
P_{RS}	Rupture stretching pressure	-	MPa	-
P_{TC}	Torus capillary-seeding pressure	-	MPa	-
P_{TD}	Torus deflection pressure	-	MPa	-
R_{PA}	Pit aperture resistivity	-	MPa s m^{-3}	-
R_{MP}	Margo pore resistivity	-	MPa s m^{-3}	-
R_P	Total pit resistivity	-	MPa s m^{-3}	-
$T_W D_T^{-}$	Thickness to span ratio	-	MPa s m^{-3}	-
V_{EF}	Valve effect = O x F	-	-	-

MOE is the modulus of elasticity of the strands (taken at 3.5 GPa; Domec *et al.*, 2006) and e_A is the margo spoke strain at aspiration (e_A=0.03D_{PM}/D_{PM}–D_{TO}).

Rupture stretching The pressure difference needed to break strands of the margo was estimated following Domec *et al.* (2006):

$$P_{RS}=-2JN[(D_{PM}/2r)/\pi(D_{TO}/2+(D_{PA}/2)^2]-P_{TD}$$

where J is the tension of a strand between the aspirated position and stretched position when the torus goes through the pit aperture and no longer covers the whole aperture [J=0.0147(e_S–e_A) MOE] and e_S is the margo spoke strain in the stretched position [e_S=(D_{TO}–D_{PA}+0.03D_{PM})/(D_{PM}–D_{TO})].

Pit hydraulic resistance The hydraulic trade-off associated with cavitation resistance was quantified by calculating the pit aperture resistivity (R_{PA}), margo resistivity (R_M), and total pit resistance (R_P) following Hacke *et al.* (2004) and Pittermann *et al.* (2010):

$$R_{PA}=[128T_{PA}\upsilon/(\pi D_{PA})^4+24\upsilon/D_{PA}^3]$$

where υ is the viscosity of the water (0.001 Pa.s at 20°C) and T_{PA} is the thickness of a single pit border calculated from the double wall thickness (T_{PA}=81% of T_W; Domec *et al.*, 2008).

$$R_M = [24\upsilon/(N_{MP}D_{MP})^3]f(h)$$

where N_{MP} is the number of pores in the margo and $f(h)$ is the function of h, the proportion of the margo occupied by pores [h=$N_{MP}\pi(N_{MP}/2)^2/\pi(D_{PM}/2)^2$]. The total pit resistance R_P equals the sum of R_{PA} and R_M (R_P=R_{PA}+R_M).

The thickness to span ratio was also estimated as it reflects the tracheid contribution to conductance. It corresponds to T_W/D_T, where T_W is the double wall thickness and D_T the tracheid lumen diameter (the simple average of the equivalent circle diameter).

Xylem failure by theoretical conduit implosion The conduit implosion pressure was defined as the pressure difference across the tracheid wall required to cause bending stress to exceed the wall strength. It was estimated using methods described by Domec *et al.* (2008):

$$P_{WI}=(\omega/\beta)(T_W/D_T)^2 L_E (I_H/I_S)$$

where ω is the strength of the wall material assumed to be 80 MPa (Hacke *et al.*, 2001), and β is a coefficient taken as 0.25. The moment ratio, I_H/I_S, represents the ratio of the second moment of area of a wall with pit chamber (I_H) to that of a solid wall with no pit chamber present (I_S). Hacke *et al.* (2004) showed that I_H/I_S does not change with air-seeding pressure, and is on average ~0.95 in conifers. The ligament efficiency [L_E=1–$D_{PA}/(D_{PM}+L_{PE})$] quantifies the spatial distribution of the pit aperture in the wall.

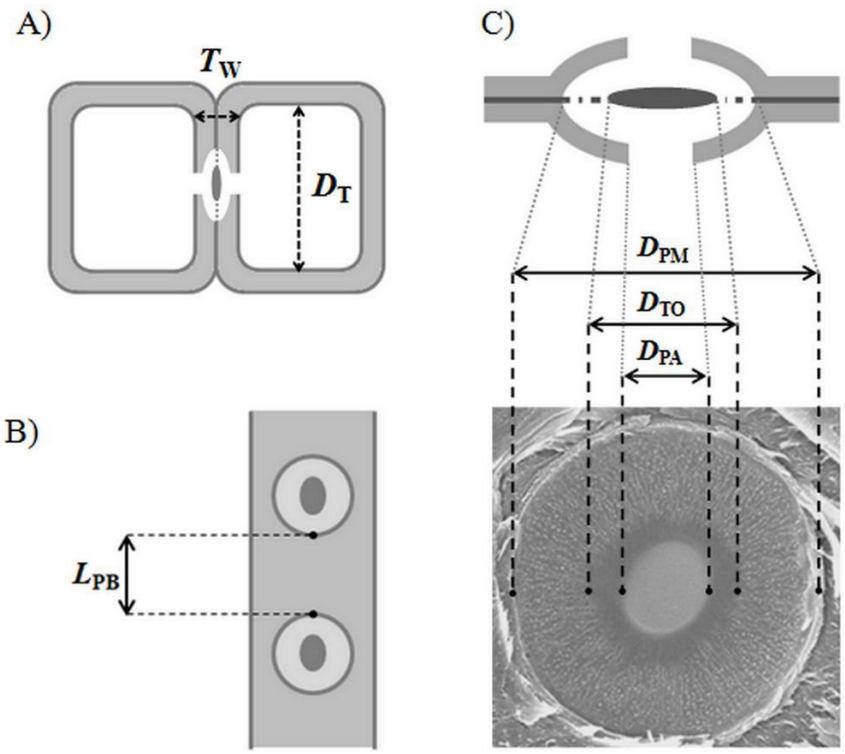

Fig. 1. Tracheid and pit membrane structure. (A) Transverse view of two adjacent tracheids. T_W, double wall thickness; D_T, tracheid lumen diameter. (B) Radial view of a pitted wall. L_{PB}, distance between two adjacent pit borders. (C) Transverse (top) and radial (bottom) view of a bordered pit membrane. D_{PM}, pit membrane diameter; D_{TO}, torus diameter; D_{PA}, pit aperture diameter.

Cavitation resistance

Cavitation resistance data were retrieved from Delzon *et al.* (2010; unpublished data). Data analyses were carried out for several cavitation traits, P_{50} (xylem pressure inducing 50% loss of hydraulic conductance), S (slope of the vulnerability curves) (Pammenter and Vander Willigen, 1998), P_{12} (xylem air entry), and P_{88} (xylem pressure at which 88% of conductivity is lost) (for more details, see Domec and Gartner, 2001). As similar results were found for all cavitation parameters, it was decided to present the relationship between anatomical traits and P_{50} for simplicity. However, xylem air entry pressure (P_{12}) was also used to test whether cavitation occurs before or after torus deflection.

Data analysis

Cross-species correlations between xylem anatomical traits and cavitation resistance were tested with a Pearson correlation coefficient (r) and a Spearman correlation coefficient (s) for nonlinear data. In addition, the species distribution in the four major biomes was retrieved from Delzon *et al*. (unpublished data), and variations of anatomical traits among biomes were assessed using a one-way analysis of variance (ANOVA). Data and statistical analyses were conducted using the SAS software (version 9.3 SAS Institute, Cary, NC, USA).

Phylogeny can induce bias when testing for correlations in pairs of traits within a group of species. Because of shared evolutionary history between related species, the assumption of independence of classical statistical tests and correlations is disregarded (Felsenstein, 1985; Harvey and Pagel, 1991; Garland *et al.*, 1992). The phylogenetically independent contrast method (or PIC; Felsenstein, 1985) is a common workaround for this issue: differences (or contrasts) in trait values are computed for each pair of species and each node of the phylogeny; these are statistically independent, and represent the evolutionary divergences in traits at each node (for more detailed information, see Felsenstein, 1985; Garland *et al.*, 1992). Furthermore, the PIC method is used to test for correlated evolution between traits: a significant positive trend (i.e. PICs for trait A are positively correlated with PICs for trait B) means that for each node of the phylogeny a change in the value of trait A is associated with the evolution of trait B. Phylogenetically independent contrasts analyses (PICs; Felsenstein, 1985) were run in R (R Development Core Team, 2008) using the 'ape' package (Paradis *et al.*, 2004). This method requires knowledge of the phylogeny of the studied taxa with branch lengths. To this end, DNA sequences for three generally available genes (chloroplast genes *rbc*L and *mat*K, and nuclear gene *phy*P) were retrieved from GenBank (Benson *et al.*, 2010) and aligned using PHLAWD (PHyLogeny Assembly With Databases; Smith *et al.*, 2009; http://code.google.com/p/phlawd). Alignements were visually checked and trimmed in MEGA 5.0 (Tamura *et al.*, 2011). Maximum Likelihood (ML) phylogenetic analyses were run in RAxML (version 7.0.3; Stamatakis, 2006). A separate GTR+CAT rate model was assigned to each partition, and each search was conducted 100 times and the best maximum likelihood (ML) tree was retained.

Results

Inclusion of phylogenetic information was useful to identify adaptive relationships between anatomical properties and cavitation resistance. Below both cross-species correlations between variables analysed with Pearson or Spearman correlation (r or s) coefficients and phylogenetically independent contrasts (PICs) are presented.

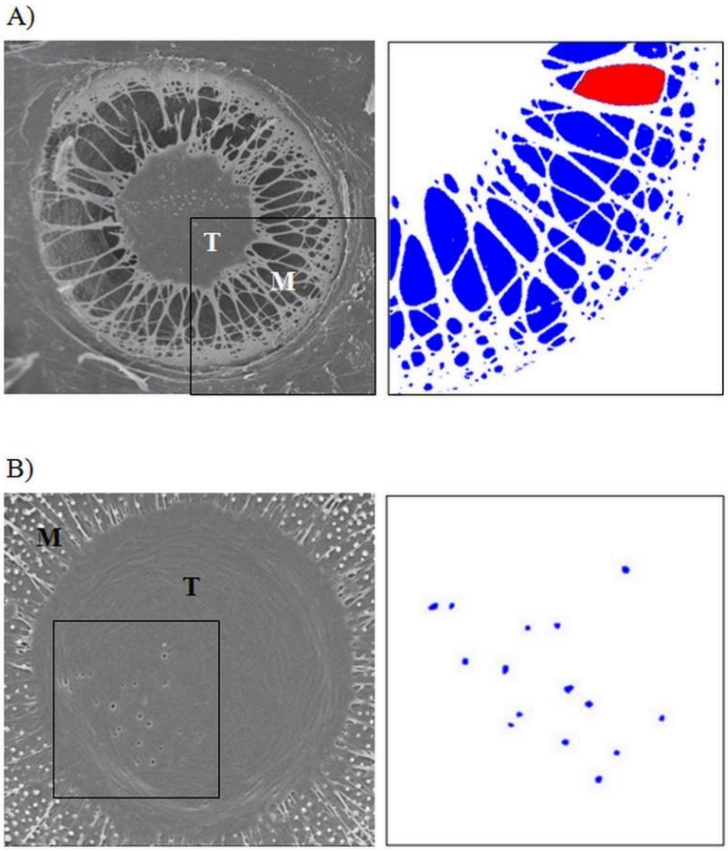

Fig. 2. Pit membrane porosity. T, torus; M, margo. (A) Radial view of a pit membrane with a porous margo. ImageJ software was used to measure the diameter of the largest pore in the margo (D_{MPmax}; red pores) and the average of margo pore diameter (D_{MP}; average of blue and red pores). (B) Radial view of a pit membrane with punctured torus. ImageJ software was used to estimate the average diameter of the pores in a torus (D_{TP}).

Anatomical properties

Across species, cavitation resistance (P_{50}) was negatively correlated with pit aperture diameter (D_{PA}; Table 3) showing that species with narrower pit apertures are more resistant to cavitation. However, these relationships were not supported by correlations using PICs (Table 3). No relationship was found between cavitation resistance and other anatomical traits such as tracheid lumen diameter (D_T), torus diameter (D_{TO}), or pit membrane diameter (D_{PM}). The same results were found for correlations with P_{12}, P_{88}, and the slope of vulnerability curves (Supplementary Table S2 available at *JXB* online).

Pit membrane functional properties

P_{50} was significantly correlated with functional properties of the bordered pit such as torus–aperture overlap (O) and valve effect (V_{EF}; product of torus overlap and margo flexibility) (Table 3, Fig. 3). This relationship was also supported by the PIC analyses, suggesting a correlative evolution between cavitation resistance and pit membrane functional properties. Increasing valve effect (V_{EF}) increased cavitation resistance. Variation in valve effect was mainly due to change in torus–aperture overlap as margo flexibility varied weakly among species. Following cross-species correlations, pit aperture diameter (D_{PA}) contributed more to torus–aperture overlap than to torus diameter (D_{TO}) (Fig. 3). However, the PIC analyses did not confirm this trend (Table 3).

Based on interspecific analyses, rupture stretching pressure (P_{RS}) was highly correlated to P_{50} (Table 3). Margo strength increased with increasing cavitation resistance. However, P_{RS} was always much lower than P_{50} (P_{RS}= –4.67 to –71.31 MPa; P_{50}= –2.23 to –15.79 MPa; Supplementary Fig. S1 available at *JXB* online), suggesting that cavitation took place before mechanical rupture of the margo strands. For all species, torus aspiration occurred at a relatively high xylem pressure (close to 0 MPa, P_{TD}= –0.03 to –0.33 MPa; Supplementary Fig. S1 available at *JXB* online) as compared with the xylem air entry pressure (P_{12}= –0.91 to –12.66 MPa; Supplementary Fig. S1 available at *JXB* online). Moreover, the pressure difference inducing margo capillary rupture (P_{MC}) was lower (more negative) than the pressure difference required to deflect the torus towards the pit aperture (P_{TD}) (P_{MC}= –0.10 to –0.75 MPa; Supplementary Fig. S1 available at *JXB* online). This means that torus deflection occurs before an air–water meniscus breaks through the margo of a pit membrane. Cavitation resistance was positively correlated with total pit resistivity (R_P) and pit aperture resistivity ($R_{PA;}$ Table 3; Fig. 5A, C) but not with margo resistivity (R_M; Table 3; Fig. 5B), suggesting that the margo pores

Table 3. *Pearson (r) and Spearman correlation (s), and phylogenetically independent contrast correlations (PICs) for relationships between anatomical and functional traits with cavitation resistance (P_{50}) in conifers*

The number of species measured is mentioned for each parameter.

	Correlation with P50			PIC		n
	r	**s**	**P-value**	**PIC**	**p-value**	
Pit membrane properties						
D_{MP}	0.21		0.19			38
D_{MPmax}	0.05		0.71			38
D_{PA}		**-0.30**	**0.002**	-0.13	0.23	**97**
D_{PM}	0.12		0.21	0.18	0.07	96
D_{TO}	0.06		0.54			88
F		-0.04	0.7	0.02	0.82	88
N_{MP}	0.22		0.14			42
O		**0.46**	**<0.0001**	**0.24**	**0.03**	**87**
P_{MC}	0.1		0.94			38
P_{RS}	**-0.43**		**0.0002**			**65**
P_{TC}	**0.52**		**0.046**			16
P_{TD}	0.20		0.10			66
V_{EF}		**0.52**	**<0.0001**	**0.30**	**0.006**	**87**
Mechanical features						
D_T	-0.17		0.12			72
D_H		**-0.31**	**0.007**	-0.06	0.59	**72**
T_W		0.15	0.17	0.22	0.007	81
Mechanical properties						
P_{WI}		**-0.51**	**0.0001**	**0.49**	**<0.0001**	**63**
$TW\ DT\text{-}1$		**0.41**	**0.0003**	**0.30**	**0.01**	**73**
Pit membrane resistance						
R_{PA}		**0.30**	**0.01**	**0.23**	**0.05**	**73**
R_{MP}		0.09	0.57	**0.37**	**0.03**	38
R_P		**0.47**	**0.005**	-0.09	0.60	**33**

Bold values indicate significant correlations at $P<0.05$.

are not involved in cavitation resistance in conifers. However, these trends were not confirmed by the PIC analysis (Table 3). Concerning the 70 species tested for the torus capillary-seeding hypothesis, only 16 species were found with punctured tori, mostly belonging to the Pinaceae family. The size of the pores varied from 12 nm to 144 nm. Only a weak but significant correlation was found between cavitation resistance and torus capillary-seeding pressure (P_{TC}, s=0.52, P=0.046; Supplementary Fig. S2 available at *JXB* online). The air-seeding pressure based on the size of plasmodesmatal pores in tori was of the same order of magnitude as the P_{50} values.

Mechanical properties

Spearman correlations and PIC analyses showed a positive correlation between the thickness to span ratio ($T_W\ D_{T\ -1}$) and cavitation resistance (P_{50}; Fig. 4A; Table 3). Variation in $T_W\ D_{T\ -1}$ across conifers was mainly determined by changes in double cell-wall thickness (T_W; s=0.60, PIC=0.57) rather than a change in tracheid lumen diameter (D_T; Fig. 4B). Moreover, tracheid lumen diameter and wall thickness were positively correlated (s=0.65, PIC=0.52; Fig. 4C), meaning that wall thickness and tracheid lumen diameter varied in the same way when total tracheid size changed. Wall implosion pressure (P_{WI}) was also positively correlated with cavitation resistance (Table 3; Fig. 4C). For most of the species, P_{WI} was always more negative than P_{50} (P_{WI}= – 4.69 to – 32.14 MPa), suggesting that conduit implosion does not occur before cavitation. Comparing the data plot in Fig. 4C with the 1:1 line, the difference between P_{WI} and P_{50} decreased from vulnerable species (low absolute P_{50} values) to resistant species (high absolute P_{50} values). The PIC analyses suggest that traits related to cavitation resistance and mechanical strength have evolved jointly.

Species distribution

Significant differences in xylem anatomy and hydraulic properties were found between the four biomes. In general, torus–aperture overlap, valve effect, and thickness to span ratio were significantly higher for the Mediterranean biome than the other biomes (Table 5). Species from Mediterranean regions showed a 2-fold higher cavitation resistance (more negative P_{50}) than in the other biomes (Table. 5).

Discussion

Pit anatomy and cavitation resistance

Across the 115 species studied, bordered pit properties of early wood tracheids (torus–aperture overlap and valve

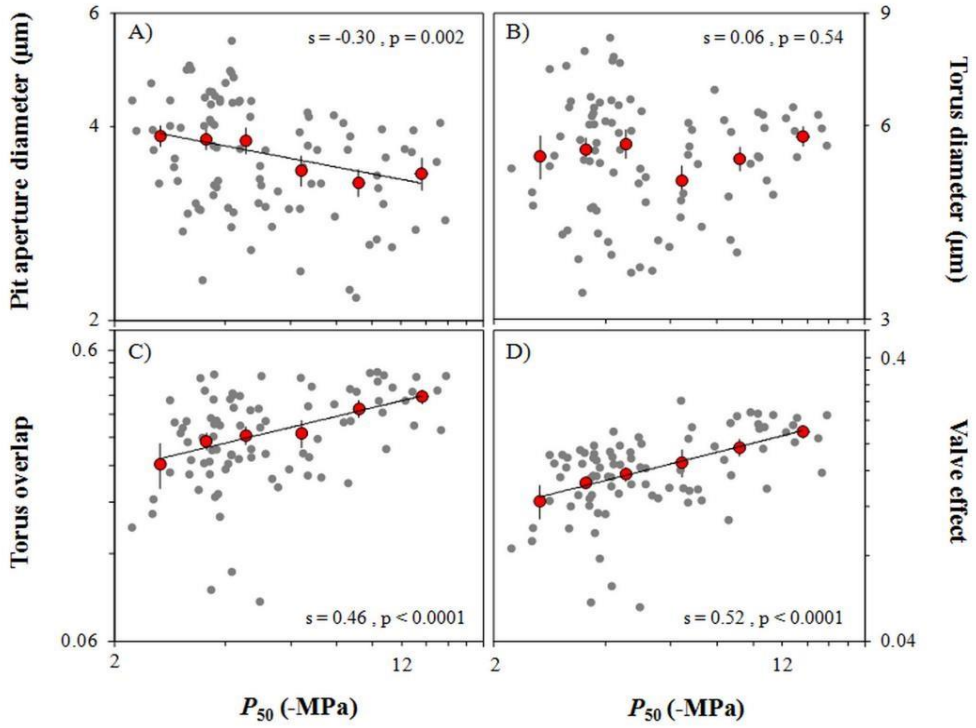

Fig. 3. Relationship between cavitation resistance (P_{50}) and anatomical traits [pit aperture diameter (A), torus diameter (B)] and functional properties [torus overlap (C), valve effect (D)] of pit membrane in conifers. Red circles are binned into ranges of P_{50} and plotted in log scale. Raw data (mean values per species) are shown as small grey points behind binned data. Linear regressions shown are based on raw data and indicate when the correlation is significant.

effect) are the best proxy to explain the variability of cavitation resistance: species resistant to cavitation have a high valve effect (corresponding to both torus–aperture overlap and membrane flexibility). This is consistent with the seal capillary-seeding hypothesis (Delzon *et al.*, 2010). Regarding the flexibility of the margo, previous studies suggested that this feature could play an important role in the process of cavitation. First, Hacke *et al.* (2004) mentioned that margo flexibility could allow the torus to be pulled out through the pit aperture, so that species that are vulnerable to cavitation should have a more flexible margo. In contrast, Delzon *et al.* (2010) reported that a high margo flexibility may facilitate the torus to move toward the pit border and improve the seal between the torus and the pit aperture. The present study showed that most of the valve effect efficiency is due to variation in the torus–aperture overlap, while the flexibility of the margo does not seem to play a substantial role. Furthermore, the results confirm that torus capillary-seeding may provide an additional airseeding mechanism in Pinaceae. While this must be interpreted with caution because SEM observations do not allow pores that completely pass through the torus to be distinguished from those that are limited to the surface of the torus, Jansen *et al.* (2012) showed that at least a few pores in each species with punctured tori completely pass through the torus. Punctured tori are also observed in some members of Cupressaceae and Cephalotaxaceae (see Table 4, and Jansen *et al.*, 2012). Plasmodesmata need to be associated with early developmental stages of the torus in combination with a lack of matrix removal from the torus by autolytic enzymes during cell hydrolysis (Murmanis and Sachs, 1969; Dute, 1994; Dute *et al.*, 2008). Thus, the taxonomic limitation of punctured tori to these families is assumed to reflect developmental differences in torus ontogeny. However, because of the lack of a distinct torus in Araucariaceae (Bauch *et al.*, 1972), no comment can be made on the mechanism of air-seeding for this family. Nevertheless, in terms of cavitation resistance, Araucariaceae are highly vulnerable to air-seeding (P_{50}= –2.02 to –3.3 MPa). Pittermann *et al.* (2010) showed that the more cavitation resistant a species is the more pronounced is the torus–margo difference.

In this study, two additional mechanisms of air-seeding were also investigated, and they were excluded in agreement with Cochard *et al.* (2009). The pressure difference needed to break the margo (P_{RS}) was more negative than P_{50}, regardless of the number of margo strands (Supplementary Fig. S1 available at *JXB* online). Therefore, cavitation was not due to breaking of the margo strands but to capillary rupture of the air–sap meniscus (Cochard *et al.*, 2009). Furthermore, the results demonstrate that cavitation does not occur at the pores in the margo, but when the torus becomes aspirated against the pit border and seals the pit aperture (Petty, 1972; Sperry and Tyree, 1990; Hacke *et al.*, 2004; Domec *et al.*, 2006; Delzon *et al.*, 2010).

Mechanical properties

The present data indicated a strong trade-off between hydraulic and mechanical safety with a significant

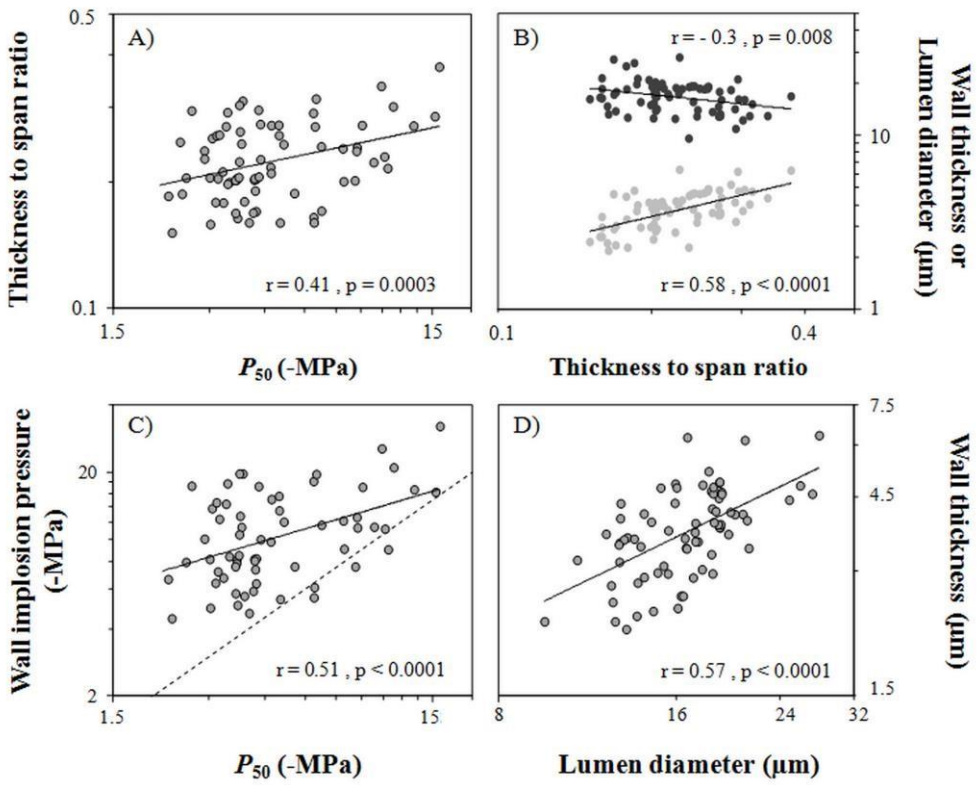

Fig. 4. Relationship between (A) thickness to span ratio and cavitation resistance (P_{50}); (B) wall thickness (grey circles), lumen diameter (black circles), and thickness to span ratio; (C) wall implosion pressure and cavitation resistance (P_{50}); and (D) wall thickness and lumen diameter. Regression lines are indicated when the correlation is significant.

evolutionary association between increasing cavitation resistance and increasing thickness to span ratio of tracheids. As in previous studies (Sperry *et al.*, 2006; Pittermann *et al.*, 2005), the present results show that species resistant to cavitation have thicker tracheid walls relative to lumen area. While Pittermann *et al.* (2006*b*) and Sperry *et al.* (2006) concluded that variation in the thickness to span ratio was determined by lumen diameter rather than cell wall thickness, the present study demonstrated the opposite: the wall thickness but not the lumen diameter appears to be responsible for the trade-off between hydraulic safety and mechanical strength. A mechanical constraint on xylem anatomy could explain this relationship. Higher cavitation resistance is associated with lower negative sap pressure (Maherali *et al.*, 2004; Choat *et al.*, 2012), which requires tracheids with a higher thickness to span ratio to resist mechanical stresses. Cavitation resistance might therefore be indirectly linked to thickness to span ratio. From a functional perspective, thicker walls in relation to lumen area do not improve drought-related cavitation resistance as this phenomenon occurs at the bordered pit level. Taking into account that there is certainly a carbon cost limitation in building up tracheid walls, Sperry *et al.* (2006) suggested that walls are close to their maximum thickness. Thereby, conifer trees can only compete for higher mechanical strength by narrowing their tracheid lumina, while levels of ray and axial parenchyma remain typically low. However, our study showed that as cell diameter increased, cell-wall thickness varied proportionally much more than lumen diameter. This suggests that there could be a minimum lumen diameter threshold that maintains a minimum level of hydraulic conductance.

The results confirm that hydraulic failure by implosion is unlikely in lignified tracheids of conifers. Conduit implosion of xylem has been observed in stems of a few Pinaceae, but only in tracheids with severe reduction of lignification in their secondary walls (Barnett, 1976; Donaldson, 2002). Indeed, some degree of lignification is required to allow normal xylem function and water conduction. The data show that the pressure needed to cause conduit implosion in lignified tracheids is related to cavitation resistance, but is for most species more negative than P_{50}. The minimum water potential measured in conifer species is generally less negative than P_{50}, suggesting that the conduit implosion pressure is unlikely to occur under field conditions (Choat *et al.*, 2012). These results suggest that cavitation always occurs before xylem collapse. According to Domec *et al.* (2009), safety factors for implosion are high compared with air-seeding. One interpretation of such a safety margin is that there has been strong selective pressure to avoid implosion (Pittermann *et al.*, 2006*b*). Even so, evidence of collapse has been observed in needles of Podocarpaceae, but localized in extra-xylary transfusion tracheids (Brodribb and Holbrook, 2005). Dysfunction by collapse seems more likely to occur in these cells than in the xylem because of their parenchymatous origin, irregular shape, large lumen, and high pit density (Aloni *et al.*, 2013).

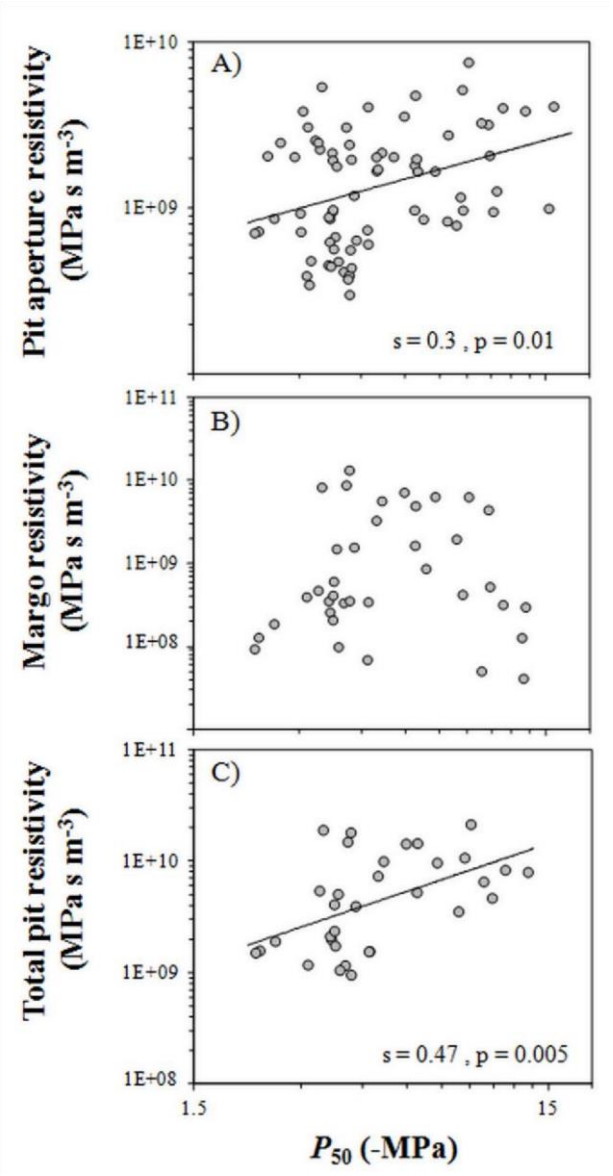

Fig. 5. Relationship between pit aperture resistance (A), margo resistance (B), and total pit resistance (C) and cavitation resistance (P_{50}). The regression line is indicated when the correlation is significant.

Species distribution

Only a few investigations were carried out on the relationship between conifer species distribution and xylem anatomy. Previous studies on hydraulic traits have provided evidence of considerable variations of cavitation resistance between species from contrasting environments, with individuals from xeric regions more resistant than those from mesic regions (Maherali *et al.*, 2004; Choat *et al.*, 2005, 2012; Vinya *et al.*, 2013). Swenson and Enquist (2007) and Slik *et al.* (2008) highlighted the existence of geographic variations in wood density with significantly denser wood in dryer habitats. The present study confirmed these trends and, in addition, it was hypothesized that xylem anatomical and, in particular, bordered pit properties would differ between the different biomes, in agreement with the variability of cavitation resistance. The distribution analyses strengthen the conclusion that species growing in arid environments such as the Mediterranean region present the following combination of distinct anatomical features: wide torus–aperture overlap, high valve effect, and large thickness to span ratio. Results from the variation in cavitation resistance in combination with the distribution of species showed a substantial ability of species from xeric habitats to resist drought induced cavitation and support mechanical strength. However, it does not mean that conifers from Mediterranean habitats are immune to drought stress (Choat *et al.*, 2012).

Table 4. *Ratio of species with punctured tori per total number of species studied with reference to their taxonomic family*

Family	Punctured torus species/total species*
Araucariaceae	-
Cephalotaxaeae	1/3
Cupressaceae	3/32
Pinaceae	15/17
Podocarpaceae	0/15
Sciadopityaceae	0/1
Taxaceae	0/4
Total	19/72

a Species studied for the torus capillary-seeding hypothesis

Conclusion

Based on both cross-species correlations and PIC analyses, the wide taxonomic sample examined here enabled the demonstration that cavitation is most likely to occur by seal capillary-seeding via the overlap of the torus on the pit aperture, while torus capillary-seeding could provide an additional mechanism in Pinaceae. Testing the consequences of increasing cavitation resistance highlighted an indirect tradeoff between hydraulic safety (P_{50}) and mechanical strength (thickness to span ratio) over a broad range of species. This study illustrates that the torus–aperture overlap and the thickness to span ratio represent the two most useful proxies to estimate cavitation resistance. It was also found that dysfunction by conduit implosion in xylem tracheids is unlikely as the theoretical implosion pressure is unrealistic for most species. Secondly, increased cavitation resistance did not come at a cost of decreased tracheid lumen diameter and should therefore have only a minor impact on hydraulic efficiency. Compared with angiosperms, conifers seem to be able to achieve greater cavitation resistance without considerably sacrificing hydraulic efficiency. This growth strategy could allow conifers to colonize seasonally arid habitats that are subject to freezing-induced embolism formation (Hacke *et al.*, 2005). The bordered pit anatomy of the xylem could slightly affect the ability of the species to resist drought induced embolism and consequently conifer distribution. Although it is felt that the approach used here of studying few individuals per species is valid when covering a large number of species, further work on the intraspecific and intra-individual variability of conifers would be required to better understand hydraulic trade-offs and functional adaptations to different environments.

Table 5. *Variation in anatomical and hydraulic traits among biomes*

Mean values of P_{50}, torus–aperture overlap (O), valve effect (V_{EF}), and thickness to span ratio (T_W/D_T) for the four main biomes represented in this study.

	Torus-aperture overlap		Valve effect		Thickness to span ratio		P_{50}	
Mediterranean	0.41 ±0.02	a	0.21 ±0.008	a	0.25 ±0.01	a	7.93 ±0.1	a
Tropical	0.29 ±0.03	b	0.16 ±0.01	b	0.23 ±0.01	ab	4.23 ±0.2	b
Temperate	0.28 ±0.01	b	0.14 ±0.006	b	0.22 ±0.008	ab	3.87 ±0.34	b
Boreal	0.32 ±0.03	b	0.15 ±0.01	b	0.19 ±0.01	b	3.39 ±0.62	b
p-value	<0.0001		<0.0001		0.01		<0.0001	

A *P*-value <0.05 indicates a significant difference between biomes, and the letters (a, b) indicate to what extent the biomes differ from each other.

Supplementary data

Supplementary data are available at *JXB* online.

Figure S1. Relationship between (A) cavitation resistance (P_{50}) and rupture stretching pressure, (B) xylem air entry pressure (P_{12}) and torus deflection pressure, and (C) margo capillary-seeding pressure and torus deflection pressure.

Figure S2. Relationship between torus capillary-seeding pressure and cavitation resistance (P_{50}).

Table S1. List of species studied with reference to their taxonomic family, origin, and average cavitation resistance values (P_{50}).

Table S2. Pearson (*r*) and Spearman correlation (*s*) for relationship between anatomical/functional traits and cavitation traits (P_{50}, P_{12}, P_{88}, and slope) in conifers.

Acknowledgements

We are grateful to the Royal Botanic Gardens, Kew; the Royal Botanic Gardens, Sydney; the the Royal Tasmanian Botanic Garden; and the National Pinetum of Bedgebury for permission to collect samples. We thank the Electron Microscopy Section of Ulm University for assistance with preparation of SEM and TEM samples. This work was supported by an International Joint grant from the Royal Society (UK), the programme 'Investments for the Future' (ANR-10-EQPX-16, XYLOFOREST) from the French National Agency for Research, and mobility grants from the Franco-German University (UFA) and the EU & Australia–New Zealand TRANZFOR programme.

References

Allen CD, Macalady AK, Chenchounic H, *et al.* 2010. A globaloverview of drought and heat-induced tree mortality reveals emerging climate change risks for forests. *Forest Ecology and Management* **259**, 660–684.

Aloni R, Foster A, Mattsson J. 2013. Transfusion tracheids in the conifer leaves of *Thuja plicata* (Cupressaceae) are derived from parenchyma and their differentiation is induced by auxin. *American Journal of Botany* **100**, 1–8.

Arbellay E, Fonti P, Stoffel M. 2012. Duration and extension ofanatomical changes in wood structure after cambial injury. *Journal of Experimental Botany* **63**, 3271–3277.

Baas P, Ewers FW, Davis SD, Wheeler EA. 2004. Evolution of xylem physiology. In: Poole I, Hemsley A, eds. *Evolution of plant physiology. Linnaean Society Symposium Series*. London: Elsevier Academic Press, 273–295.

Bailey IW. 1913. The preservative treatment of wood. II. The structure of the pit membranes in the tracheids of conifers and their relation to the penetration of gases, liquids and finely divided solids into green and seasoned wood. *Forestry Quarterly* **11**, 12– 20.

Barnett JR. 1976. Rings of collapsed cells in *Pinus radiata* stemwood from lysimeter-grown trees subjected to drought. *New Zealand Journal of Forestry Science* **6**, 461–465. **Barigah TS, Bonhomme S, Lopez D**. 2013. Modulation in bud survival in *Populus nigra* sprouts in response to water stressinduced embolism. *Tree Physiology* **33**, 261–274. **Bauch JW, Liese W, Schultze R**. 1972. The morphological variability of the bordered pit membranes in gymnosperms. *Wood Science and Technology* **6**, 165–184.

Benson DA, Karsch-Mizrachi I, Lipman DJ, Ostell J, Sayers EW. 2010. GenBank. *Nucleic Acids Research* **39**, 32–37.

Bigler C, Gavin DG, Gunning C, Veblen TT. 2007. Drought induces lagged tree mortality in a subalpine forest in the Rocky Mountains. *Oikos* **116**, 1983–1994.

Breshears DD, Cobb NS, Rich PM, *et al.* 2005. Regional vegetation die-off in response to global-change-type drought. *Proceedings of the National Academy of Sciences, USA* **102**, 15144–15148.

Brodribb TJ, Bowman DJMS, Nichols S, Delzon S, Burlett R. 2010. Xylem function and growth rate interact to determine recovery rates after exposure to extreme water deficit. *New Phytologist* **188**, 533–542.

Brodribb TJ, Cochard H. 2009. Hydraulic failure defines the recovery and point of death in water-stressed conifers. *Plant Physiology* **149**, 575–584.

Brodribb TJ, Holbrook NM. 2005. Water stress deforms tracheids peripheral to the leaf vein of a tropical conifer. *Plant Physiology* **137**, 1139–1146.

Choat B, Ball M, Luly J, Holtum J. 2003. Pit membrane porosity and water stress-induced cavitation in four co-existing dry rainforest tree species. *Plant Physiology* **131**, 41–48. **Choat B, Ball MC, Luly GJ, Holtum JAM**. 2005. Hydraulic architecture of deciduous and evergreen dry rainforest tree species from north-eastern Australia. *Trees* **19**, 305–311. **Choat B, Jansen S, Brodribb TJ**, *et al*. 2012. Global convergence in the vulnerability of forests to drought. *Nature* **491**, 752–755.

Choat B, Jansen S, Zwieneicki MA, Smets E, Holbrook NM. 2004. Changes in pit membrane porosity due to deflection and stretching: the role of vestured pits. *Journal of Experimental Botany* **55**, 1569–1575.

Choat B, Sack L, Holbrook NM. 2007. Diversity of hydraulic traits in nine *Cordia* species growing in tropical forests with contrasting precipitation. *New Phytologist* **175**, 686–698.

Christman MA, Sperry JS, Adler FR. 2009. Testing the 'rare pit' hypothesis for xylem cavitation resistance in three species of *Acer*. *New Phytologist* **182**, 664–674.

Cochard H. 2006. Cavitation in trees. *Comptes Rendus Physique* **7**, 1018–1026.

Cochard H, Cruizat P, Tyree MT. 1992. Use of positive pressures to establish vulnerability curves. Further support for the air-seeding hypothesis and implications for pressure–volume analysis. *Plant Physiology* **100**, 205–209.

Cochard H, Delzon S. 2013. Hydraulic failure and repair are not routine in trees. *Annals of Forest Science* **70**, 659–661. **Cochard H, Holtta T, Herbette S, Delzon S, Mencuccini M**. 2009. New insights into the mechanisms of water-stress-induced cavitation in conifers. *Plant Physiology* **151**, 949–954. **Cochard H, Tete Barigah S, Kleinhentz M, Eshel A**. 2008. Is xylem cavitation resistance a relevant criterion for screening drought resistance among *Prunus* species? *Journal of Plant Physiology* **165**, 976–982.

Crombie DS, Hipkins MF, Milburn JA. 1985. Gas penetration of pit membranes in the xylem of *Rhododendron* as the cause of acoustically detectable sap cavitation. *Australian Journal of Plant Physiology* **12**, 445–453.

Delzon S, Cochard H. 2014. Recent advances in tree hydraulics highlight the ecological significance of the hydraulic safety margin. *New Phytologist* (in press).

Delzon S, Douthe C, Sala A, Cochard H. 2010. Mechanism of water-stress induced cavitation in conifers: bordered pit structure and function support the hypothesis of seal capillary-seeding. *Plant, Cell and Environment* **33**, 2101–2111.

Domec JC, Gartner BL. 2002. How do water transport and water storage differ in coniferous earlywood and latewood? *Journal of Experimental Botany* **53**, 2369–2379.

Domec JC, Gartner BL. 2001. Cavitation and water storage capacity in bole xylem segments of mature and young Douglas-fir trees. *Trees* **15**, 204–214.

Domec JC, Lachenbruch B, Meinzer FC. 2006. Bordered pit structure and function determine spatial patterns of air-seeding thresholds in xylem of Douglas-fir (*Pseudotsuga menziesii*; *Pinaceae*) trees. *American Journal of Botany* **93**, 1588–1600.

Domec JC, Lachenbruch B, Meinzer FC, Woodruff DR, Warren JM, McCulloh KA. 2008. Maximum height in a conifer is associated with conflicting requirements for xylem design. *Proceedings of the National Academy of Sciences, USA* **105**, 12069–12074.

Domec JC, Warren J, Lachenbruch B, Meinzer FC. 2009. Safety factors from air seeding and cell wall implosion in young and old conifer trees. *International Association of Wood Anatomists* **30**, 100–120.

Donaldson LA. 2002. Abnormal lignin distribution in wood from severely drought stressed *Pinus radiata* trees. *International Association of Wood Anatomists* **23**, 161–178.

Dute RR. 1994. Pit membrane structure and development in *Ginkgo biloba*. *International Association of Wood Anatomists* **15**, 75–90.

Dute R, Hagler L, Black A. 2008. Comparative development of intertracheary pit membranes in *Abies firma* and *Metasequoia glyptostroboides*. *International Association of Wood Anatomists* **29**, 277–289.

Engelbrecht B, Comita L, Condit R, Kursar T, Tyree M, Turner B, Hubbell S. 2007. Drought sensitivity shapes species distribution patterns in tropical forests. *Nature* **447**, 80–82. **Farjon A**. 2008. *A natural history of conifers*. Portland, OR: Timber Press, Inc.

Felsenstein J. 1985. Phylogenies and the comparative methods. *American Naturalist* **125**, 1–15.

Garland T, Harvey PH, Ives AR. 1992. Procedures for the analysis of comparative data using phylogenetically independent contrasts. *Systematic Biology* **41**, 18–32.

Hacke UG, Sperry JS, Pittermann J. 2004. Analysis of circular bordered pit function—II. Gymnosperm tracheids with torus–margo pit membranes. *American Journal of Botany* **91**, 386–400. **Hacke UG, Sperry JS, Pittermann J.** 2005. Efficiency versus safety tradeoffs for water conduction in angiosperm vessels versus gymnosperm tracheids. In: Holbrook NM, Zwieniecki M, eds. *Vascular transport in plants*. Amsterdam: Elsevier, 333–353.

Hacke UG, Sperry JS, Pockman WT, Davis SD, McCulloh KA. 2001. Trends in wood density and structure are linked to prevention of xylem implosion by negative pressure. *Oecologia* **126**, 457–461.

Hartmann H, Ziegler W, Kolle O, Trumbore S. 2013. Thirst beats hunger—declining hydration during drought prevents carbon starvation in Norway spruce saplings. *New Phytologist* **200**, 340–349.

Harvey PH, Pagel MD, eds. 1991. *The comparative method in evolutionary biology*. Oxford: Oxford University Press. **Jansen S, Lamy JB, Burlett R, Cochard H, Gasson P, Delzon S.** 2012. Plasmodesmatal pores in the torus of bordered pit membranes affect cavitation resistance of conifer xylem. *Plant, Cell and Environment* **35**, 1109–1120.

Jansen S, Choat B, Pletsers A. 2009. Morphological variation of intervessel pit membranes and implications to xylem function in angiosperms. *American Journal of Botany* **96**, 409–419. **Jarbeau J, Ewers F, Davis S.** 1995. The mechanism of waterstressed induced embolism in two species of chaparral shrubs. *Plant, Cell and Environment* **18**, 189–196.

Lens F, Sperry JS, Christman M, Choat B, Rabaey D, Jansen S. 2011. Testing hypotheses that link wood anatomy to cavitation resistance and hydraulic conductivity in the genus *Acer*. *New Phytologist* **190**, 709–723.

Liese W, Bauch J. 1967. On the closure of bordered pits in conifers. *Wood Science and Technology* **1**, 1–13. **Maherali H, Pockman WT.** 2004. Adaptive variation in the vulnerability of woody plants to xylem cavitation. *Ecology* **85**, 2184–2199.

Martínez-Vilalta J, Cochard H, Mencuccini M, *et al*. 2009. Hydraulic adjustment of Scots pine across Europe. *New Phytologist* **184**, 353–364.

Matzner SL, Rice KJ, Richards JH. 2001. Intra-specific variation in xylem cavitation in interior live oak (*Quercus wislizenii*). *Journal of Experimental Botany* **52**, 783–789. **Murmanis L, Sachs IB**. 1969. Seasonal development of secondary xylem in *Pinus strobus* L. *Wood Science and Technology* **3**, 177–193.

Pammenter NW, Vander Willigen C. 1998. A mathematical and statistical analysis of the curves illustrating vulnerability to cavitation. *Tree Physiology* **18**, 589–593. **Paradis E, Claude J, Strimmer K.** 2004. APE: analyses of phylogenetics and evolution in R language. *Bioinformatics* **20**, 289– 290.

Peng C, Ma Z, Lei X, Zhu Q, Chen H, Wang E, Liu S, Li W, Fang X, Zhou X. 2011. A drought-induced pervasive increase in tree mortality across Canada's boreal forests. *Nature Climate Change* **1**, 467–471.

Petty JA. 1972. The aspiration of bordered pits in conifer wood. *Proceedings of the Royal Society B: Biological Sciences* **181**, 395–406.

Pittermann J, Choat B, Jansen S, Stuart S, Lynn L, Dawson TE. 2010. The relationships between xylem safety and hydraulic efficiency in the Cupressaceae: the evolution of pit membrane form and function. *Plant Physiology* **153**, 1919–1931. **Pittermann J, Limm E, Rico C, Christman M.** 2011. Structure– function constraints of tracheid-based xylem: a comparison of conifers and ferns. *New Phytologist* **192**, 449–461. **Pittermann J, Sperry JS, Hacke UG, Wheeler JK, Sikkema EH.** 2005. The torus–margo pit valve makes conifers hydraulically competitive with angiosperms. *Science* **310**, 1924. **Pittermann J, Sperry JS, Wheeler JK, Hacke UG, Sikkema E.** 2006a. Mechanical reinforcement against tracheid implosion compromises the hydraulic efficiency of conifer xylem. *Plant, Cell and Environment* **29**, 1618–1628.

Pittermann J, Sperry JS, Wheeler JK, Hacke UG, Sikkema EH. 2006b. Inter-tracheid pitting and the hydraulic efficiency of conifer wood: the role of tracheid allometry and cavitation protection. *American Journal of Botany* **93**, 1265–1273.

R Development Core Team. 2008. *R: a language and environment for statistical computing*. R Foundation for Statistical Computing, Vienna, Austria.

Sanchez-Salguero R, Navarro-Cerrillo RM, Camarero JJ, Fernández-Cancio Á. 2012. Selective drought-induced decline of pine species in southeastern Spain. *Climate Change* **113**, 767– 785.

Schoonmaker AL, Hacke UG, Landhausser SM, Lieffers VJ, Tyree MT. 2010. Hydraulic acclimation to shading in boreal Conifers of varying shade tolerance. *Plant, Cell and Environment* **33**, 382–393.

Slik JW, Bernard CS, Breman FC, Van Beek M, Salim A, Sheil D.2008. Wood density as a conservation tool: quantification of disturbance and identification of conservation-priority areas in tropical forests. *Conservation Biology* **22**, 1299–1308.

Smith SA, Beaulieu JM, Donoghue MJ. 2009. Mega-phylogeny approach for comparative biology: an alternative to supertree and supermatrix approaches. *BMC Evolutionary Biology* **9**, 37. **Sperry H.** 2006. Size and function in conifer tracheids and angiosperm vessels. *American Journal of Botany* **93**, 1490–1500. I. Angiosperm vessels with homogenous pit membranes. *American Journal of Botany* **91**, 369–385.

Sperry JS, Meinzer FC, McCulloh KA. 2008. Safety and efficiency conflicts in hydraulic architecture: scaling from tissues to trees. *Plant, Cell and Environment* **31**, 632–645.

Sperry JS, Tyree MT. 1990. Water-stress-induced xylem embolism in three species of conifers. *Plant, Cell and Environment* **13**, 427–436.

Stamatakis A. 2006. RAxML-VI-HPC: maximum likelihood phylogenetic analyses with thousands of taxa and mixed models. *Bioinformatics* **22**, 2688–2690.

Swenson NG, Enquist BJ. 2007. Ecological and evolutionary determinants of a key plant functional trait: wood density and its community-wide variation across latitude and elevation. *American Journal of Botany* **94**, 451–459.

Tamura K, Peterson D, Peterson N, Stecher G, Nei M, Kumar S. 2011. MEGA5: molecular evolutionary genetics analysis using maximum likelihood, evolutionary distance, and maximum parsimony methods. *Molecular Biology and Evolution* **28**, 2731–2739.

Tyree MT, Zimmermann MH. 2002. *Xylem structure and the ascent of sap*. Berlin: Springer.

Urli M, Porté AJ, Cochard H, Guengant Y, Burlett R, Delzon S. 2013. Xylem embolism threshold for catastrophic hydraulic failure in angiosperm trees. *Tree Physiology* **33**, 672–683.

Van Mantgem PJ, Stephenson NL, Byrne JC, *et al*. 2009. Widespread increase of tree mortality rates in the western United States. *Science* **323**, 521–524.

Vinya R, Malhi Y, Fisher JB, Brown N, Brodribb TJ, Aragoa LE. 2013. Xylem cavitation vulnerability influences tree species' habitat preferences in miombo woodlands. *Oecologia* **113**, 711–720.

Willson CJ, Manos PS, Jackson RB. 2008. Hydraulic traits are influenced by phylogenetic history in the drought-resistant, invasive genus *Juniperus* (Cupressaceae). *American Journal of Botany* **95**, 299–314.

Supporting information

Table S1. *List of species studied with reference to their taxonomic family, origin and average cavitation resistance values (P_{50}).[a] Material studied in this paper; [b] Material studied by Delzon et al. 2010; [c] Material studied by Jansen et al. 2012.*

Family	Species	Authority	Origin and accesion number	P_{50} (MPa) ± SE
Araucariaceae	*Agathis atropurpurea* [a]	Hyland	RBG Sydney, 20100069	-2.89 ± 0.27
Araucariaceae	*Agathis australis* [a]	(D.Don) Lindl.	Bedgeburry National Pinetum, 17-0581	-2.13
Araucariaceae	*Agathis microstachya* [a]	J.F.Bailey & C.T.White	RBG Mount Annan, 865566	-2.55 ± 0.07
Araucariaceae	*Agathis robusta* [a]	(C.Moore ex F.Muell.) F.M.Bailey	RBG Mount Annan	-2.90 ± 0.06
Araucariaceae	*Araucaria araucana* [a]	(Molina) K.Koch	Argentina	-3.06 ± 0.81
Araucariaceae	*Araucaria bidwillii* [a]	Hook.	RBG Sydney, 19074	-3.01 ± 0.08
Araucariaceae	*Araucaria cunninghamii* [a]	Aiton ex D.Don	RBG Sydney, 863087	-2.64 ± 0.08
Araucariaceae	*Araucaria heterophylla* [a]	(Salisb.) Franco	RBG Sydney, 15960	-2.96 ± 0.07
Araucariaceae	*Araucaria hunsteinii* [ab]	K.Schum.	RBG Sydney, 902638	-2.43 ± 0.08
Araucariaceae	*Wollemia nobilis* [a]	W.G.Jones, K.D.Hill & J.M.Allen	RBG Sydney	-3.32 ± 0.15
Cephalotaxaceae	*Cephalotaxus fortunei* [ac]	Hook.	RBG Kew, 1969-16466	-7.26 ± 0.48
Cephalotaxaceae	*Cephalotaxus harringtonia* [ac]	(Knight ex J.Forbes) K.Koch	RBG Kew, 1969-16244	-7.21± 0.47
Cephalotaxaceae	*Cephalotaxus wilsoniana* [a]	Hayata	Bedgeburry National Pinetum, 22-0202	-7.92 ± 0.29
Cupressaceae	*Actinostrobus pyramidalis* [b]	Miq.	Clermont-Ferrand, France	-10.72 ± 0.57
Cupressaceae	*Athrotaxis cupressoides* [a]	D.Don	RBG Kew, 2003-2212	-3.16 ± 0.34
Cupressaceae	*Athrotaxis laxifolia* [a]	Hook.	Bedgeburry National Pinetum, 10-671	-2.47 ± 0.19
Cupressaceae	*Austrocedrus chilensis* [a]	(D.Don) Pic.Serm. & Bizzari	Argentina	-4.96 ± 0.19
Cupressaceae	*Callitris columellaris* [ac]	F.Muell.	University of Tasmania, Hobart	-15.79 ± 0.18
Cupressaceae	*Callitris endlicheri* [a]	(Parl.) F.M.Bailey	RBG Tasmania, Hobart	-12.94 ± 0.70
Cupressaceae	*Callitris glaucophylla* [a]	Joy Thomps. & L.A.S.Johnson	RBG Mount Annan, 873453	-15.30 ± 0.36
Cupressaceae	*Callitris gracilis* [ac]	R.T.Baker	University of Tasmania, Hobart	-12.26 ± 0.59
Cupressaceae	*Callitris intratropica* [a]	R.T.Baker & H.G.Smith	RBG Sydney	-12.81 ± 0.73
Cupressaceae	*Callitris oblonga* [a]	Rich. & A.Rich.	Bedgeburry National Pinetum, 22-0229	-10.88 ± 0.85
Cupressaceae	*Callitris preissii* [ac]	Miq.	University of Tasmania, Hobart	-14.97 ± 0.50
Cupressaceae	*Callitris rhomboidea* [abc]	R.Br. ex Rich & A.Rich.	University of Tasmania, Hobart	-10.32 ± 0.53
Cupressaceae	*Calocedrus formosana* [a]	(Florin) Florin	Bedgeburry National Pinetum, 22-279	-4.92 ± 0.65
Cupressaceae	*Chamaecyparis obtusa* [ac]	(Siebold & Zucc.) Endl.	RBG Kew, 1969-10594	-3.71 ± 0.12
Cupressaceae	*Chamaecyparis pisifera* [ac]	(Siebold & Zucc.) Endl.	RBG Kew, 607-1260702	-3.46 ± 0.21
Cupressaceae	*Cryptomeria japonica* [a]	(Thunb. ex Lf.) D.Don	Japan	-3.66 ± 0.16
Cupressaceae	*Cunninghamia lanceolata* [a]	(Lamb.) Hook.	RBG Kew, 1973-16525	-3.50 ± 0.17
Cupressaceae	*x Cupressocyparis leylandii* [a]	(A.B.Jacks. & Dallim.) Dallim.	RBG Kew	-8.58 ± 0.17

Family	Species	Authority	Origin and accesion number	P_{50} (MPa) ± SE
Cupressaceae	*Cupressus dupreziana* [ac]	A.Camus	RBG Kew, 1970-61193	-10.29 ± 0.06
Cupressaceae	*Cupressus funebris* [a]	Endl.	Bedgeburry National Pinetum, 21-0595	-10.63 ± 0.61
Cupressaceae	*Cupressus glabra* [ab]	Sudw.	France	-11.32 ± 1.03
Cupressaceae	*Cupressus macrocarpa* [a]	Hartw.	Bedgeburry National Pinetum, 29-0407	-6.73 ± 0.38
Cupressaceae	*Cupressus sempervirens* [ab]	L.	France	-10.39 ± 1.10
Cupressaceae	*Cupressus torulosa* [ac]	D.Don	RBG Kew, 1996-1799	-8.35 ± 0.59
Cupressaceae	*Diselma archeri* [a]	Hook.f.	RBG Tasmania, Hobart	-8.72 ± 0.54
Cupressaceae	*Fitzroya cupressoides* [a]	(Molina) I.M.Johnst.	Argentina	-5.00 ± 0.37
Cupressaceae	*Juniperus chinensis* [a]	L.	Bedgeburry National Pinetum , 03-4	-10.88 ± 0.54
Cupressaceae	*Juniperus communis* [ab]	L.	France	-6.37 ± 0.22
Cupressaceae	*Juniperus osteosperma* [ab]	(Torr.) Little	Utah, USA	-8.68 ± 0.35
Cupressaceae	*Juniperus scopulorum* [ab]	Sarg.	Montana, USA	-9.83 ± 0.30
Cupressaceae	*Metasequoia glyptostroboides* [bc]	Hu & W.C.Cheng	RBG Kew, 1980-6256	-2.91 ± 0.13
Cupressaceae	*Papuacedrus papuana* [a]	(F.Muell.) H.L.Li	RBG Sydney, 20114	-4.69 ± 0.23
Cupressaceae	*Platycladus orientalis* [ac]	(L.) Franco	RBG Kew, 1976-3574	-9.04 ± 0.45
Cupressaceae	*Sequoia sempervirens* [abc]	(D.Don) Endl.	University of Bordeaux, Château du Haut-carré	-4.38 ± 0.17
Cupressaceae	*Sequoiadendron giganteum* [abc]	(Lindl.) J.Buchholz	University of Bordeaux, Château du Haut-carré	-3.78 ± 0.06
Cupressaceae	*Taiwania cryptomerioides* [ac]	Hayata	RBG Kew, 1994-900	-3.38 ± 0.29
Cupressaceae	*Taxodium distichum* [ab]	(L.) Rich.	France	-2.29 ± 0.07
Cupressaceae	*Taxodium mucronatum* [a]	Ten.	RBG Sydney, 2005973	-2.23 ± 0.11
Cupressaceae	*Tetraclinis articulata* [a]	(Vahl) Mast.	RBG Sydney, 940902	-13.21 ± 0.75
Cupressaceae	*Thuja plicata* [abc]	Donn ex D.Don	RBG Kew, 1973-18600	-4.20 ± 0.13
Cupressaceae	*Thujopsis dolabrata* [ac]	(L.f.) Siebold & Zucc.	RBG Kew, 1969-16072	-4.15 ± 0.38
Cupressaceae	*Widdringtonia nodiflora* [a]	(L.) E.Powrie	RBG Tasmania, Hobart	-7.87 ± 0.49
Cupressaceae	*Xanthocyparis nootkatensis* [ac]	(D.Don) Farjon & D.K.Harder	RBG Kew, 1969-13806	-5.13 ±0.25
Pinaceae	*Abies alba* [ab]	Mill.	France	-4.00 ± 0.11
Pinaceae	*Abies balsamea* [c]	(L.) Mill.	University of Alberta, Edmonton, Canada	-3.64 ± 0.34
Pinaceae	*Abies forrestii* [a]	Craib	RBG Kew, 1993-1445	-3.42 ± 0.07
Pinaceae	*Abies grandis* [ab]	(Douglas ex D.Don) Lindl.	Idaho, USA	-3.65 ± 0.06
Pinaceae	*Abies lasiocarpa* [ab]	(Hook.) Nutt.	Idaho, USA	-3.62 ± 0.07
Pinaceae	*Abies pinsapo* [ab]	Boiss.	France	-4.15 ± 0.14
Pinaceae	*Abies sachalinensis* [a]	Mast.	Hokkaido, Japan	-3.23 ± 0.07
Pinaceae	*Cedrus atlantica* [abc]	(Endl.) G.Manetti ex Carrière	RBG Kew, 2000-4686	-5.13 ± 0.08
Pinaceae	*Cedrus deodara* [bc]	(Roxb. ex D.Don) G.Don	Clermont-Ferrand, France	-6.69 ± 0.36
Pinaceae	*Larix decidua* [abc]	Mill.	RBG Kew, 1979-6300	-4.11 ± 0.27
Pinaceae	*Larix gmelinii* [a]	(Rupr.) Kuzen.	Bedgeburry National Pinetum, 07-0095	-3.13 ± 0.18
Pinaceae	*Larix occidentalis* [ab]	Nutt.	Idaho, USA	-4.21 ± 0.14
Pinaceae	*Picea abies* [b]	(L.) H.Karst.	France	-3.66 ± 0.09
Pinaceae	*Picea engelmannii* [b]	Parry ex Engelm.	Montana, USA	-4.18 ± 0.09
Pinaceae	*Picea glauca* [c]	(Moench) Voss	University of Alberta, Edmonton, Canada	-4.35 ± 0.26

Family	Species	Authority	Origin and accesion number	P_{50} (MPa) ± SE
Pinaceae	*Picea likiangensis* [a]	(Franch.) E.Pritz.	RBG Kew, 1970-6137	-3.86 ± 0.13
Pinaceae	*Picea mariana* [c]	(Mill.) BSP.	Edson, Canada	-5.21 ± 0.19
Pinaceae	*Pinus albicaulis* [ab]	Engelm.	Montana, USA	-3.19 ± 0.10
Pinaceae	*Pinus cembra* [ab]	L.	Austria, Europe	-3.02 ± 0.17
Pinaceae	*Pinus contorta* [b]	Douglas ex Loudon	Montana, USA	-3.90 ± 0.18
Pinaceae	*Pinus edulis* [b]	Engelm.	Utah, USA	-4.03 ± 0.06
Pinaceae	*Pinus flexilis* [ab]	E.James	Montana, USA	-3.71 ± 0.18
Pinaceae	*Pinus halepensis* [ab]	Mill.	France	-4.67 ± 0.05
Pinaceae	*Pinus hartwegii* [c]	Lindl.	RBG Kew, 1996-1016	-3.42 ± 0.05
Pinaceae	*Pinus mugo* [ab]	Turra	Austria, Europe	-3.74 ± 0.07
Pinaceae	*Pinus nigra* [c]	J.F.Arnold	RBG Kew, 1973-15503	-3.52
Pinaceae	*Pinus pinaster* [abc]	Aiton	Bordeaux, France, 503, 361, 441, 463B	-3.72 ± 0.07
Pinaceae	*Pinus pinea* [ab]	L.	France	-4.34 ± 0.16
Pinaceae	*Pinus ponderosa* [ab]	Douglas ex Loudon	Montana, USA	-3.86 ± 0.05
Pinaceae	*Pinus radiata* [c]	D.Don	University of Tasmania, Hobart	-4.37 ± 0.14
Pinaceae	*Pinus sylvestris* [b]	Frankis ex Businsky	France	-3.20 ± 0.02
Pinaceae	*Pinus uncinata* [ab]	Ramond ex DC.	France	-0.17 ± 0.17
Pinaceae	*Pinus wallichiana* [c]	A.B.Jacks.	RBG Kew, 1979-2373	-2.83 ± 0.11
Pinaceae	*Pseudolarix amabilis* [a]	(J.Nelson) Rehder	RBG Kew, 1960-13101	-4.16 ± 0.15
Pinaceae	*Pseudotsuga menziesii* [ab]	(Mirb.) Franco	Montana, USA	-3.68 ± 0.15
Podocarpus	*Acmopyle pancheri* [a]	(Brongn. & Gris) Pilg.	RBG Tasmania, Hobart	-3.62 ± 0.07
Podocarpus	*Afrocarpus gracilior* [a]	(Pilg.) C.N.Page	RBG Tasmania, Hobart, 10128	-6.36 ± 0.10
Podocarpus	*Dacrycarpus dacrydioides* [b]	(A.Rich.) de Laub.	Australia	-2.51 ± 0.16
Podocarpus	*Dacrydium araucarioides* [a]	Brongn. & Gris	Noumea, New Caledonia	-3.78 ± 0.39
Podocarpus	*Falcatifolium taxoides* [a]	(Brongn. & Gris) de Laub.	RBG Tasmania, Hobart	-5.55 ± 0.53
Podocarpus	*Halocarpus bidwillii* [a]	(Hook.f. ex Kirk) Quinn	Bedgeburry National Pinetum, 14-465	-5.35 ± 0.21
Podocarpus	*Lagarostrobos franklinii* [a]	(Hook.f.) Quinn	RBG Kew, 14-53	-4.35 ± 0.36
Podocarpus	*Manoao colensoi* [a]	(Hook.) Molloy	RBG Tasmania, Hobart, 40838	-2.88 ± 0.21
Podocarpus	*Phyllocladus trichomanoides* [a]	D.Don	Bedgeburry National Pinetum, 17-0386	-7.10 ± 0.25
Podocarpus	*Podocarpus elatus* [a]	R.Br ex Endl.	RBG Sydney, 20040141	-6.74 ± 0.39
Podocarpus	*Podocarpus lawrencei* [a]	Hook.f.	Bedgeburry National Pinetum, 14-464	-3.82 ± 0.21
Podocarpus	*Podocarpus rubens* [a]	de Laub.	RBG Tasmania, Hobart, 10116	-3.73 ± 0.04
Podocarpus	*Podocarpus salignus* [a]	D.Don	Bedgeburry National Pinetum, 1993-1660	-4.28 ± 0.16
Podocarpus	*Podocarpus spinulosus* [a]	(Sm.) R.Br ex Mirb.	RBG Sydney, 990828	-6.84 ± 0.34
Podocarpus	*Podocarpus totara* [a]	G.Benn. ex D.Don	Wakehurst, 2009-2494	-4.95 ± 0.16
Podocarpus	*Prumnopitys ladei* [a]	(F.M.Bailey) de Laub.	RBG Sydney, 822906	-6.68 ± 0.23
Podocarpus	*Retrophyllum comptonii* [a]	(J.Buchholz) C.N.Page	RBG Tasmania, Hobart, 99069	-2.54 ± 0.09
Podocarpus	*Saxegothaea conspicua* [a]	Lindl.	Argentina	-3.39 ± 0.23
Podocarpus	*Sundacarpus amarus* [a]	(Blume) C.N.Page	RBG Tasmania, Hobart, 1331	-2.83 ± 0.14
Sciadopityaceae	*Sciadopitys verticillata* [ac]	Siebold & Zucc.	RBG Kew, 1979-48	-4.07 ± 0.10

Family	Species	Authority	Origin and accesion number	P_{50} (MPa) ± SE
Taxaceae	*Taxus baccata* [ab]	L.	France	-6.49 ± 0.31
Taxaceae	*Taxus brevifolia* [ab]	Nutt.	Montana, USA	-6.44 ± 0.30
Taxaceae	*Torreya californica* [ac]	Torr.	RBG Kew, 1969-14196	-6.39 ± 0.30
Taxaceae	*Torreya grandis (fortune)* [ac]	Fortune ex. Lindl.	RBG Kew, 1973-20815	-4.69 ± 0.25
Taxaceae	*Torreya nucifera* [ac]	(L.) Siebold & Zucc.	RBG Kew, 1969-15523	-5.95 ± 0.30

Table S2. *Pearson (r) and Spearman correlation (s) for relationship between anatomical/ functional traits and cavitation/hydraulic traits ($P_{50,}$ P_{12}, P_{88} and slope) in conifers.*

	Pearson correlations			
	P_{50}	P_{12}	P_{88}	slope
D_{MP}	0.21	0.25	0.18	0.2
D_{MPmax}	0.05	0.03	0.07	0.06
D_{PM}	0.12	0.18	0.08	0.11
D_{T}	-0.17	-0.17	-0.17	0.01
D_{TO}	0.06	0.16	0.0008	0.36***
N_{MP}	0.22	0.19	0.24	-0.23
P_{WI}	-0.51***	-0.46***	-0.51***	0.38**
T_{TW}	0.15	0.14	0.15	-0.19
(T_{TW}/D_{T})	0.41***	0.36**	0.42***	-0.3**

	Spearman correlations			
	P_{50}	P_{12}	P_{88}	slope
D_{PA}	-0.3**	-0.13	-0.39***	0.46***
D_{H}	-0.31**	-0.20	-0.31**	0.26*
F	-0.01	-0.21*	0.12	-0.26*
O	0.46***	0.5***	0.4***	-0.3**
P_{MC}	0.01	0.11	-0.03	0.03
P_{RS}	-0.43***	-0.34**	-0.47***	0.43***
P_{TC}	0.52*	0.55*	0.42	-0.31
P_{TD}	0.12	-0.14	0.3*	-0.41***
R_{MP}	0.09	-0.04	0.15	-0.17
R_{PA}	0.3**	0.1	0.41***	-0.49***
R_{P}	0.47**	0.33	0.58***	-0.54***
V_{EF}	0.52***	0.5***	0.5***	-0.4***

Supplementary figures

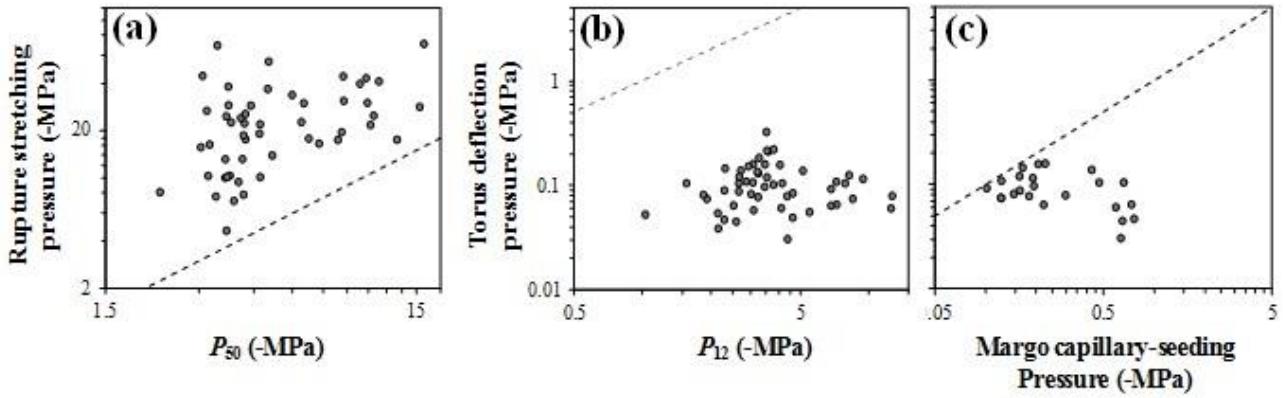

Figure S1. *Relationship between (a) cavitation resistance (P_{50}) and rupture stretching pressure, (b) xylem air entry pressure (P_{12}) and torus deflection pressure and (c) between margo capillary-seeding pressure and torus deflection pressure.*

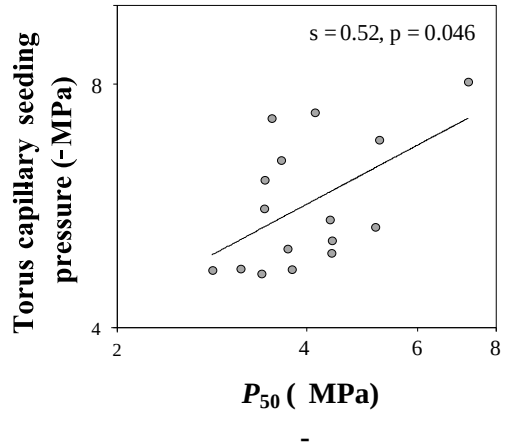

Figure S2. *Relationship between torus capillary-seeding pressure and cavitation resistance (P_{50}).*

Part II: The evolution of embolism-resistance and its role in the diversification of Conifers

Chapter 4: Drought and the evolution of embolism resistance drives Conifer diversification. Maximilian Larter, Sylvain Delzon et al. (in prep.)

Drought and the evolution of embolism resistance drives Conifer diversification

Maximilian Larter[1], Delzon Sylvain[1], et al. (*In preparation)*

[1]BIOGECO, INRA, Univ. Bordeaux, 33615 Pessac, France

Abstract

Conifers are an ancient group of trees that has evolved and adapted to occupy the broad range of habitats available today. Several combined factors are considered to have shaped this group to its current distribution and diversity, notably the emergence of flowering plants during the late Cretaceous. Recent work has shown the remarkable variation that exists in conifers for resistance to drought-induced xylem embolism (P_{50}), a trait that has been linked to survival during extreme drought. Furthermore, embolism resistance displays some interesting macro-evolutionary patterns, with some families seemingly in stasis (Pinaceae, Araucariaceae) while others seem more labile (Cupressaceae, Podocarpaceae). Using a time-calibrated phylogeny and embolism resistance data for over 250 species from the seven extant conifer families, we assessed both cavitation resistance evolution and conifer diversification, and tested the hypothesis that drought is a major driver of conifer diversification. We uncovered multiple evolutionary dynamics, with low background rates of diversification and P_{50} evolution shifting to several faster evolving regimes. By modelling both processes simultaneously we show that diversification rate increases across conifer lineages with increasing cavitation resistance. The rapid dynamics we found in Cupressaceae crown groups composed of genera *Juniperus* and *Cupressus* in the Northern Hemisphere, and *Callitris* in the Southern Hemisphere are paralleled by huge upticks in P_{50} evolution rate. However, the diversification shifts in Pinaceae (around 150 Mya) and Podocarpaceae (~70 Mya) are likely uncoupled from drought and possibly related to the emergence of cold environments and the rise of Angiosperms, respectively. We provide the first conclusive evidence of climate driving the diversification of conifers, with two parallel radiations into dry habitats in both hemispheres through xylem evolution towards increased cavitation resistance.

Introduction

Conifers are an extraordinarily diverse group of trees, occurring in all continents except

Antarctica, with over 600 species in 70 genera and 7 families (Farjon, 2010). With a long evolutionary history detailed by the fossil record, conifers were globally dominant in the early Cretaceous, they have since declined in most parts of the world concomitantly with the rise to dominance of flowering plants (Angiosperms) from around 100 million years ago (Mya) (Augusto et al., 2014). They nonetheless remain a major component of many ecosystems and are present in every eco-region across the world, from wet tropical forests and arid deserts to the boreal and alpine tree-lines. Despite a reputation for being "living fossils", they display remarkable variation in shape, size, morphology and physiology, in keeping with their ecological ubiquity (Eckenwalder, 2009). However, conifer diversity is not uniformly distributed across the globe, notably with low diversity in higher latitudes and several regions of high endemism (e.g. New Caledonia). Similarly, while some genera contain a single species with an extremely limited distribution (e.g. *Sciadopytis*, sole member of its family), some genera with a host of species are distributed widely across the globe, but remain restricted to one hemisphere, for example *Pinus* (113 species), *Podocarpus* (97 species), *Juniperus* (53 species) or *Abies* (47 species). Restricted distributions and lack of diversity of extant conifer taxa are the legacy of a long history of extinction during most of the Cenozoic (65 Mya to present), with high rates inferred from the fossil record especially around 29 and 16 Mya (Crepet and Niklas, 2009). Many competing hypotheses have been proposed to explain both the decline of Gymnosperms and the rise of Angiosperms, including reproduction (entomophily vs. anemophily), seedling establishment and growth, light-harvesting, and water transport (Bond, 1989). However, at such temporal and spatial scales, multiple events and processes are likely involved (Augusto et al., 2014). Of particular interest is the proposed "climate framework" (Augusto et al., 2014), as it could explain both the decline of some lineages due to increased climatic stress during the global drying of the Eocene and the subsequent success of some coniferous lineages due to increased drought tolerance.

Although more research is needed to explain what exactly kills a plant during drought (Sala et al., 2010) hydraulic failure due to embolism is emerging as a leading cause of mortality (Anderegg et al., 2012; Balducci et al., 2014; Anderegg et al., 2016), either alone or in complex species-dependent interactions with other factors like depletion of non-structural carbohydrates or biotic attacks (Mitchell et al., 2013; Dickman et al., 2014; Sevanto et al., 2014). Resistance to drought induced cavitation, or the ability of vascular plants to withstand very negative water-potentials is therefore an adaptive trait which could be implicated in a species' survival during climatic upheavals. A species' cavitation resistance (described by P_{50}) is related to its climate

of origin (annual rainfall, aridity index) across a wide range of tree species (both angiosperms and gymnosperms) and biomes (Brodribb and Hill, 1999; Maherali et al., 2004; Bouche et al., 2014). Furthermore, the remarkable scale of variation in this trait within Conifers – i.e. from -1.6 MPa to -18.8 MPa (Delzon et al., 2010; Larter et al., 2015) - and multiple occurrences of convergent evolution of high resistance to cavitation (Maherali et al., 2004; Choat et al., 2012; Pittermann et al., 2012; Bouche et al., 2014) leave a pattern of evolutionary lability and a strong signal of adaptive evolution.

The combined rise of phylogenetics, large trait databases and the development of new comparative methods has allowed the analysis of diversification and trait evolution in large clades within a statistical framework (for a review see Pennell and Harmon, 2013) - from simple models fitting single speciation and extinction rates across whole phylogenies to more complex models allowing multiple clade-specific evolutionary dynamics (Rabosky et al., 2014). Recent investigations have also focused on the relationship between diversification patterns and trait evolution, i.e. finding evidence for a link between higher rates of speciation in a group that displays a particular trait (or trait value) than a related group that doesn't (Maddison et al., 2007; FitzJohn, 2012).

The aim of this study was to investigate the evolution of drought tolerance in conifers and its importance for the diversification of Conifers. Specifically, we wanted to identify when and in which conifer lineages increasing xylem cavitation-resistance evolved, and whether these clades have diversified more rapidly as a result of increased drought tolerance. To this end, we constructed a dated molecular phylogeny for over 300 species of conifers, and combined this with physiological information for over 250 species from a conifer cavitation resistance database. We find strong evidence for multiple evolutionary dynamics in Conifers, both in diversification patterns and in the evolution of embolism resistance with the highest rates observed in crown groups within Cupressaceae. We also detected trait-dependent diversification, with higher drought-tolerance associated with increased speciation rates in non-Pinaceous conifers.

In the current context of climate change, the predicted increase in frequency and severity of drought events has already led some regions to experience severe die-back of some species, notably conifers (Allen et al., 2010). Rapid climate change likely outpaces the migration capacity of long-lived woody plant species such as conifers, therefore possibly resulting in extirpation or even extinction for species with either i) a severely restricted distribution with

low diversity like many conifer species today (IUCN, 2015), or ii) conservative lineages with low adaptability or evolvability, another characteristic of gymnosperm lineages. On the other hand, physiological (or phenological) adaptation to drought could enable increased survival in dry environments giving some lineages a competitive edge over other tree species, over time even resulting in ecological radiations. Using our knowledge of current conifer ecophysiology, we can look into the past and examine the diversification of conifer lineages with contrasting strategies facing drought.

Methods:

Phylogenetic reconstruction and dating:

We obtained DNA sequences using PHLAWD (PHyLogeny Assembly with Databases, http://phlawd.net/), a pipeline that queries the GenBank database using a specified list of species , and a template sequence as a comparison base to filter-out non-homologous sequences (Smith et al., 2009). The resulting alignments were manually checked and trimmed using Mega 5 (Tamura et al., 2011). We constructed a large dataset of DNA sequences for chloroplast genes RBCL, MATK and nuclear gene PHYP, and the ITS1-5.8S-ITS2 nuclear ribosomal DNA region. Since the ITS region is highly variable at this evolutionary scale, we separately built five different alignments, based on family relationships, i.e. one alignement for each of Pinaceae, Araucariaceae, Podocarpaceae, Cupressaceae and Taxaceae-Cephalotaxaceae (we did not include *Sciadopitys verticillata* in the datasets for this region). We used three cycad species (*Cycas micronesica*, *Zamia furfuracea* and *Encephalartos ferox*) as outgroup, and also included *Nothotsuga longibracteata* to add a fossil calibration point within the Pinaceae family. We also included 58 other conifer species, that haven't been included in the physiological dataset, so they were pruned from the tree prior to comparative analyses, but their sequences were present for the phylogenetic analyses. Then we used Mesquite (Maddison and Maddison, 2015) to concatenate the sequences into a single file for phylogenetic analysis. The final dataset of 314 species contained 11578 sites with a large proportion of missing data (about 65%; accessions used in Suppl. Table 1). We used RAXML (Stamatakis, 2006) to construct a maximum likelihood tree, using a separate GTR+GAMMA model for each data partition. We conducted 1000 bootstrap searches and a full ML search using "-# 1000" and "–f a" options.

To test the impact of tree topology on our analysis, we also ran MrBayes (v3.2, (Ronquist et al., 2012), a Bayesian phylogenetic inference program that uses Monte-Carlo Markov Chains to estimate parameter posterior distributions for two parallel independent runs of 30 million

generations each, and computed maximum clade credibility trees for each run. Convergence was checked by examining runs parameters in Tracer (Rambaut et al., 2014).

We largely followed the fossil calibration points from Leslie et al. (2012), except for the *Picea-Cathaya* divergence, which is based on *Picea burtonii* a fossil spruce from the early Cretaceous (~140-133 Mya), because of some uncertainty in the placement of *Cathaya* (i.e. Lin et al., 2010). To have more age constraints within the Pinaceae family, we added two fossils from Mao et al. (2012), for the age of crown Pinaceae and the split between *Pinus* and *Picea*. We implemented a conservative approach by placing a 40 million year interval on all calibrations that are based on a minimum age only (due to the presence of fossil taxa), and a less conservative approach with a 20 million year interval. We also tested the impact of crown group fossil calibrations with a "deep nodes" analysis that contained only 4 constraints: on the root, and at the base of Pinaceae, the Araucariaceae – Podocarpaceae clade, and the split between Taxaceae – Cupressaceae. The complete information for the fossils used in this study are available in the supplementary text and Suppl. Table 2).

We used the *chronos* function in the R package "*ape*" to transform the RAxML tree and the two MrBayes consensus phylograms into fossil calibrated chronograms. This function implements a penalized-likelihood approach similar to the program r8s (Sanderson, 2002; Kim and Sanderson, 2008; Paradis, 2013). Fossil ages are specified as minimum and maximum age constraints on nodes indicated using the most recent common ancestor (MRCA) of two species (e.g. the root node was specified as the MRCA of *Cycas micronesica* and *Pinus pinaster*, with a minimum age of 275, and a maximum age of 350). We tested values for the smoothing parameter λ from 10^{-6} to 10^{6} by increments of 10, and selected the value with the highest likelihood – in all cases this was 10^{-6}. Low values of λ (close to 0) allow rates to vary more between branches, resulting in a less "clock-like" model. Molecular and time-calibrated phylogenies (with calibrated nodes indicated) are available as Supplementary Fig. S1 (RAxML analysis) and S2 (MrBayes analysis). Similar tree topologies were obtained with RAxML and MrBayes, and most genus-level nodes receive strong support, represented by bipartition frequencies from the 1000 bootstraps in RAxML and Bayesian Posterior Probablities for the Bayesian analysis in MrBayes. Pinaceae are sister to all remaining conifers, Araucariaceae and Podocarpaceae are grouped together, with *Sciadopitys* sister to the Cupressaceae – Taxaceae (sensua lato, i.e. including Cephalotaxaceae) clade. Some deep nodes within early diverging Podocarpaceae have low support, similarly to previous work with the matK and ITS regions

(Biffin et al., 2011). *Phyllocladus-Lepidothamnus* are sister to all remaining Podocarps in the RAxML topology, but are grouped with the Prumnopityoid clade (*Prumnopitys*, *Sundacarpus*, *Halocarpus*, *Lagarostrobos*, *Manoao*) in the MrBayes consensus tree (albeit with low support). Our dating analyses yielded consistent dates across topologies and calibration sets, with dates with the 20 MA interval slightly younger overall (Supplementary Fig. S3). The "deep nodes only" resulted in unrealistically young crown group ages. We present results for all subsequent analyses on the more conservative 40 MA calibration analysis using the "best tree" from the RAxML tree search.

Physiological data:

We used the cavitation resistance database developed at the Caviplace lab (Delzon et al. 2015 - INRA/University of Bordeaux - BIOGECO UMR 1202, Pessac), using 252 species, covering the seven extant conifer families, and over 90% of genera. This dataset also covers the large ecological distribution evident among conifers, from boreal forest, high altitude tree-lines, to wet tropical rainforest species and drought-tolerant desert shrubs. Xylem pressure inducing 50% loss of conductance due to cavitation (P_{50}) varies in this group from around -2 MPa to close to -19 MPa (Delzon et al. 2015, Larter et al. 2015). Cavitation resistance was measured using the Cavitron technique (Cochard et al., 2005), that uses centrifugal force to generate xylem pressure analogous to drought in plants. By measuring water flow as the sample branch is spinning, we can determine loss of conductance as cavitation events occur in the xylem, resulting in a vulnerability curve (representing percent loss of conductance as a function of xylem pressure) from which we derive the P_{50} parameter using the Pammenter sigmoid model (Pammenter and Vander Willigen, 1998).

Diversification and trait evolution using BAMM and *diversitree*.

1) We separately modelled conifer diversification and the evolution of drought tolerance using BAMM (Bayesian Analysis of Macroevolutionary Mixtures (Rabosky, 2014)), that implements complex models with multiple macro-evolutionary dynamics (speciation/extinction and trait evolution) on phylogenetic trees in a Bayesian framework. The program uses reversible-jump MCMC to explore candidate models with any number of shifts to new evolutionary dynamics, each with their own speciation, extinction, or phenotypic evolutionary processes. BAMM evaluates anything from a simple model with a single tree-wide evolutionary dynamic to more complex models where any branch can contain a shift to a new evolutionary regime. Each candidate model is therefore composed of a set of evolutionary

dynamics, with associated shifts (between dynamics) and rates painted onto the phylogeny. The program implements an exponential change model, where evolutionary rates decrease or increase through time (time-varying model), and also allows for time-constant processes. By summarizing across the posterior distribution we can, i) calculate an average evolutionary rate for each branch of the phylogeny (see Fig. 1-A and B), ii) determine the probability that two species belong to the same dynamic (i.e. that there are no shifts on the branches leading to them from their most recent common ancestor – see Fig. 1-C and D), iii) determine the marginal posterior odds that each branch contains a shift (see Fig. 2) and iv) extract which models (i.e. which sets of shifts) seem most likely, based on their frequency in the posterior distribution (see Suppl. Fig. S6 and S7). BAMM is linked to a set of analysis and visualization tools within the R statistical environment ("*Bammtools*"). Convergence of the BAMM runs was checked by visualizing the log-likelihood throughout the run, and making sure effective sample sizes were >1000, using the "*coda*" package in R. Diversification analyses we run for 10 million generations (sampling every 1000) and trait evolution analyses for 40 million generations (sampling every 10'000). In all cases we discarded the first 25% of the chain as burn-in.

2) Trait dependent diversification models were fit using maximum likelihood with the "*diversitree*" package in R, that implements models where different trait values are associated with increased/decreased speciation and extinction rates (Quantitative State Speciation and Extinction (Fitzjohn, 2010; FitzJohn, 2012)). Diversification is modeled according to a birth-death process (with speciation and extinction parameters), and trait evolution is modelled by a diffusion process, that includes both a directional "drift" parameter and a stochastic "noise" parameter. We fit models where speciation was linear, sigmoidal functions of trait values, which were compared to the "trait independent" diversification model (i.e. constant speciation). Extinction was kept constant or as a linear function of trait values. QUASSE also allows the tree to be split to fit separate trait dependent speciation and extinction models in different clades. We used this option to test the hypothesis that diversification in Pinaceae is driven by different factors from the rest of conifers. We therefore specified a split at the corresponding node in the phylogeny, i.e. the most recent common ancestor of all non-Pinaceous conifers. We incorporated incomplete sampling by specifying a global sampling fraction of 0.42, since our dataset contained around 250 species out of the total of around 600 conifers total. We tested models with and without the trait "drift" parameter. Models were compared using Akaike's Information Criterion, which measures the goodness of fit of each model while correcting for the increasing number of parameters, and model improvement was tested using the likelihood

ratio test. We used -P_{50} as positive trait values to facilitate interpretation of the models (i.e. an upward trend indicates a positive effect of increased cavitation resistance on diversification). To ensure proper convergence of the optimizer, we started optimization runs from different starting points, and run each optimization multiple times. Some concerns have been raised recently concerning all SSE methods including QUASSE (Rabosky and Goldberg, 2015; O'Meara and Beaulieu, 2016). Not least, they are susceptible to infer false positives, i.e. find conclusive evidence of trait dependent diversification for neutral simulated traits (Rabosky and Goldberg, 2015). It is hypothesized that some phylogenies fall victim to this bias due to possibly to high heterogeneity in diversification rates. We tested this issue by simulating trait evolution using Brownian motion (using the BM parameter best fit to the P_{50} data) along our phylogeny. For each trait, we then compared a neutral model to a model where speciation is a linear function of trait value. We also ran QUASSE on the MrBayes topology and the 20 MA calibration set to evaluate the impact of topology on our results, and to test whether the RAxML tree (or the inferred dates) was responsible for "false positive" results of trait-dependent diversification.

Results

BAMM analyses:

We found overwhelming evidence for multiple evolutionary dynamics in conifer diversification and cavitation resistance evolution. Accordingly, evolutionary rates varied widely across the phylogeny, with approximately 10-fold increases in net diversification rates (Fig. 1A) and several hundredfold increases in cavitation resistance evolution rates (Fig. 1B). In both analyses, low background rates in Pinaceae, Araucariaceae, Taxaceae, and the early diverging Cupressaceae (old Taxodiaceae) give way to more rapidly evolving dynamics in Podocarpaceae and Cupressaceae. Crown Callitroidae (i.e. genus *Callitris* and associated genera *Neocallitropsis* and *Actinostrobus*) display the highest diversification and trait evolution rates (Fig. 1A and B).

Conifer diversification dynamics:

We found a constant low speciation and extinction dynamic was shared across most basal Pinaceae, Araucariaceae, Taxaceae and the early diverging Cupressaceae, and basal lineages of the Cupressoidae subfamily (respectively letters A, C, F and H in Fig. 1C). Several clades have transitioned to new rapid diversification dynamics: in Pinaceae, *Pinus* and *Picea* (Fig. 1C – "B") and both crown Callitroidae (Fig. 1C – "G") and the *Cupressus*-*Juniperus* clade (Figure 1C – "I") within Cupressaceae. A shift is also recovered at the base of a large Podocarpoid – Dacrydioid clade (Podocarpaceae), with evidence for an additional shift on the branch leading to genus *Podocarpus* (Fig. 1C – "D" and "E").

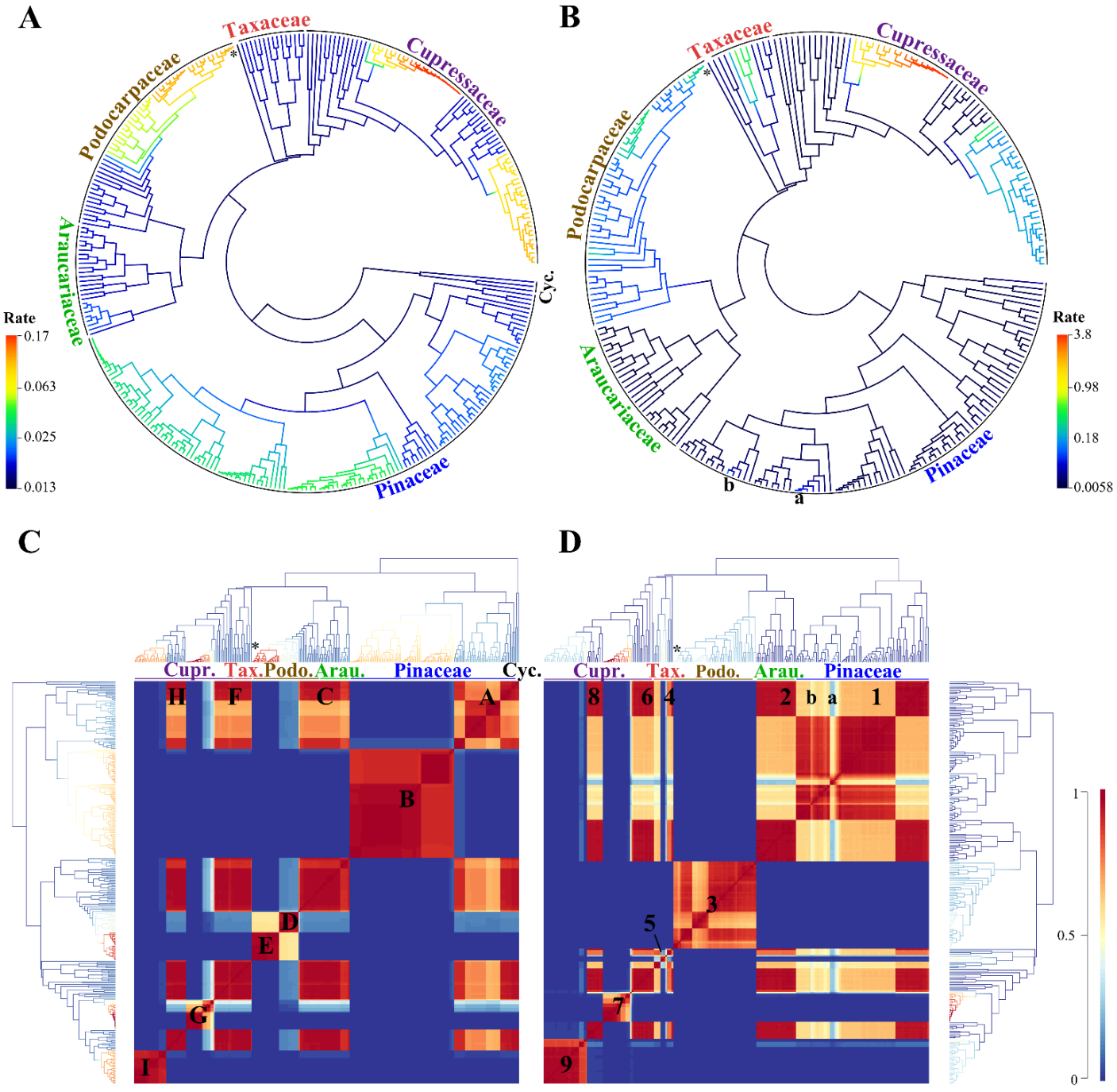

Figure 1. Conifers diversification and cavitation resistance evolution rates and dynamics in Conifers. Average branch rates across all post-burn-in samples for the BAMM diversification (**A**) and P_{50} (**B**) analyses. Conifer diversification (**C**) and P_{50} evolution (**D**) macro-evolutionary cohort analyses representing the probability that two species belong to the same evolutionary dynamic. Family names in C and D are abbreviations of those in A-B. The Cycad outgroup is indicated as "Cyc.". The star represents *Sciadopytis*, and Taxaceae (Tax.) includes Cephalotaxaceae for clarity. Letters "a" and "b" indicates the P_{50} dynamic shifts within *Pinus* (see main text). Block letters (C) and numbers (D) highlight groups of species that share a dynamic.

Drought-resistance evolution dynamics:

Modelling of cavitation resistance evolution follows strikingly similar patterns, with an ancestral low background rate giving way to more rapidly evolving processes in several clades. Rates remain low throughout the history of the Pinaceae family (Fig. 1D – "1"; Fig. 3). There is nonetheless strong support for two recent shifts within genus *Pinus*: i) for a group of Mexican and Western American pines (section Trifoliae, sub-section Ponderosae) that includes *P. ponderosa*, *P. jeffreyi*, *P. coulteri*, *P. devoniana*, and *P. hartwegii* (Fig. 1B, D: "a") and ii) on the branch leading to *P. pinaster* (Fig. 1B, D: "b"), both supported by high marginal odd ratios (Fig. 2B). These shifts are linked to rapid increases in P_{50} to relatively vulnerable species (*P. devoniana* P_{50} = -3 MPa and *P. pinaster* -3.7 respectively), which are nested in more resistant groups (respectively, *P. ponderosa* with P_{50} = -3.9 MPa and P_{50} = -4.7 MPa for *P. brutia* and *P. halepensis*). P_{50} evolution shifts to a faster family level evolutionary dynamic for Podocarpaceae, with further evidence of shifts within genus *Podocarpus* (see Fig. 2B). These dynamics are characterized by much variation in P_{50} with the emergence of very resistant species within very vulnerable clades (e.g. *Pherosphaera* and *Afrocarpus*). Embolism resistant genus *Cephalotaxus* displays higher rates of evolution than the more vulnerable Taxaceae (Fig. 1B). The two largest shifts are placed within Cupressaceae, i) at the base of the crown Cupressoid clade including *Cupressus*, *Juniperus*, *Calocedrus* and *Tetraclinis* (see Fig. 1D - "9") and ii) within crown Callitroidae (Fig. 1D – "7"). In both these clades, large upticks in evolution rate lead to the emergence of extreme embolism resistance crown groups from much more vulnerable basal lineages (i.e. *Papuacedrus*, *Austrocedrus* and *Thuja*, *Chamaecyparis* respectively).

We summarized branch level support for the shifts by computing shift marginal odd ratios, which are the branch-specific probabilities of shifts corrected by their prior probabilities (that depend on branch length) (Shi and Rabosky, 2015). The previously described evolutionary dynamics are overwhelmingly well supported, with both high marginal shift probabilities and odd ratios (Fig. 2). There is however some uncertainty on the exact placement of the shift leading to crown Callitroidae, for both analyses, with successive branches with strong evidence of a shift. In this clade, the basal lineages of *Papuacedrus* and *Austrocedrus* are generally not included in the new dynamics, with strongest support on the branch leading to the remaining Callitroids. Similarly, the shift in P_{50} evolution within Taxaceae-Cephalotaxaceae is not well resolved, and is not well as well supported by marginal odd ratios (Fig. 2B).

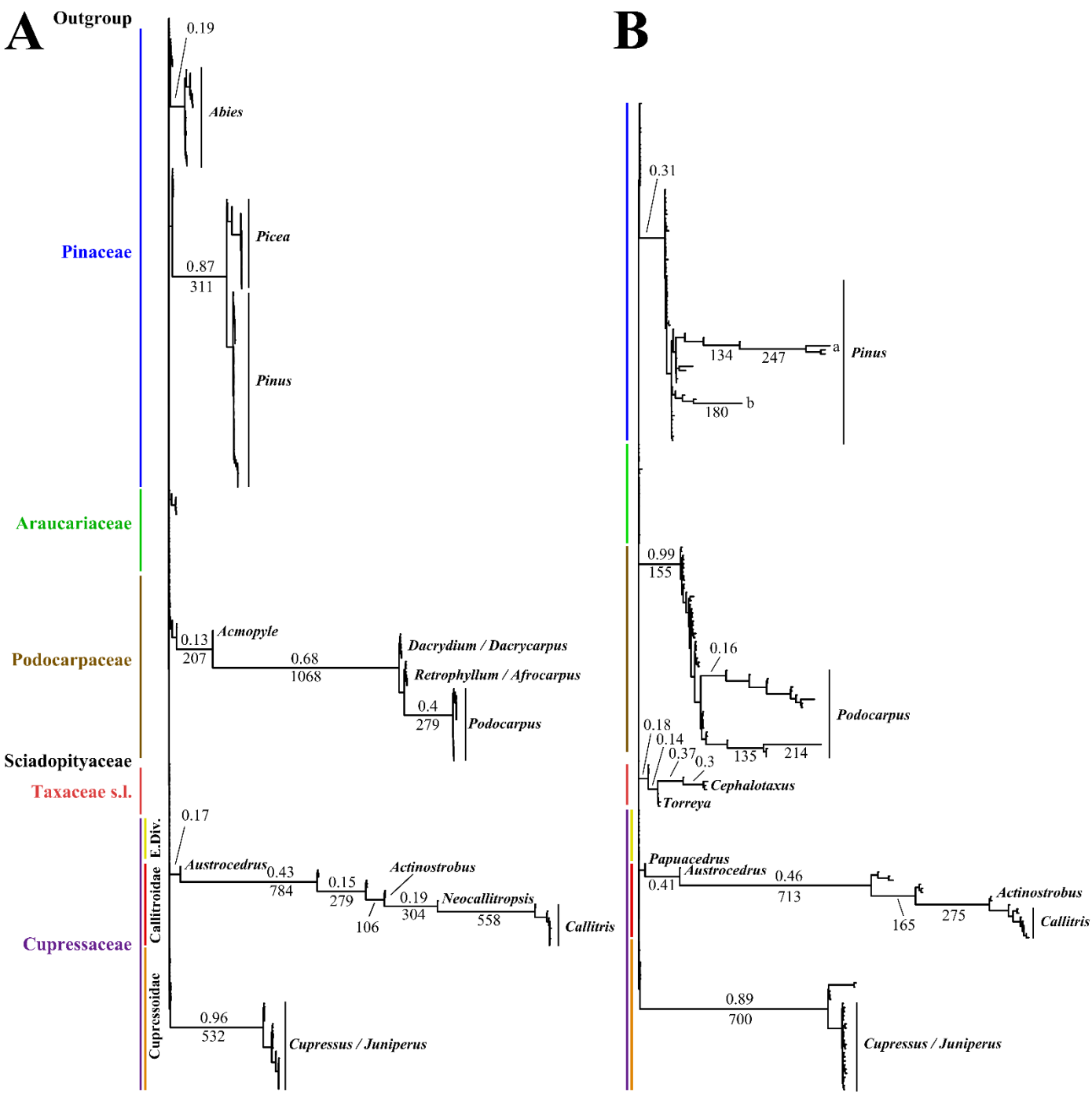

Figure 2. Phylogenetic trees showing locations of BAMM shifts in diversification (**A**) and cavitation resistance (**B**) evolutionary dynamics. Branches lengths are scaled according to marginal odd ratios, which represent the posterior probability of a shift being present on each branch, adjusted by the corresponding prior probability (a longer branch has high probability of a shift based on length alone). Numbers above branches represent the ten highest posterior shift probabilities (their frequency in the BAMM output) and numbers below branches are the 10 highest shift marginal odd ratios. Conifer families and some relevant genera are indicated on in each panel. As in Fig. 1, letters "a" and "b" indicate the two recent shifts within *Pinus*.

To explore the temporal patterns of trait evolution and diversification, we constructed time series of the average rates from both analyses, separating rates from each family across all post-burn-in samples from the BAMM analyses (Fig. 3). The overall diversification rate in conifers has increased gradually through time (Fig. 3A). The increase in rates associated with the shift in Pinaceae is visible at around 150 Mya (Fig. 3A – blue line) whereas the other shifts happened more recently, i.e. about 70 Mya in Podocarpaceae and around 50 Mya in Cupressaceae. When we decompose diversification into speciation and extinction rates (Suppl. Fig. 5), we see that the gradual increase in diversification rate in Pinaceae is in fact a huge uptick in lineage turnover rate with high speciation and extinction rates from before 150 Mya, with speciation only slightly outpacing extinction – overall the Pinaceae family had the highest speciation rates until approximately the start of the Neogene (20 Mya). For cavitation resistance (Fig. 3B), the most ancient shift occurred in Podocarpaceae a little over 150 Mya, followed by the gradual acceleration visible in Taxaceae-Cephalotaxaceae around 110 Mya. In Cupressaceae, a gradual uptick in rates occurred about 75 Mya, followed by a second major shift around 35 Mya. Rates of P_{50} evolution are very low throughout the history of Pinaceae, despite the evidence of slight upward shifts within *Pinus* (Fig.1).

The overwhelming majority of samples from the BAMM output contained at least three and four core shifts for the diversification and trait evolution analyses, respectively (Supplementary Fig. S5). We found similar results across time-tree calibration schemes and phylogeny inference methods (Supplementary Fig. S6 and S7).

Trait-dependent diversification: QUASSE

Our analyses strongly support models where conifer diversification is linked to cavitation resistance (Table 1). For the first analysis, trait dependent models were fit uniformly across the whole phylogeny, and the trait dependent models generally improved on the constant (trait-independent) diversification model. The only exception was the model with constant speciation and trait dependent extinction. The best model was when both speciation and extinction were linear functions of P_{50}. All models produced positive trends, i.e. speciation increased with increasing resistance to cavitation – either as a linear function or by rapidly increasing at a threshold value for the sigmoid function (see Suppl. Table S4 for details). This indicates a strong effect of cavitation resistance on diversification trends in conifers, with vulnerable lineages diversifying more slowly than resistant lineages.

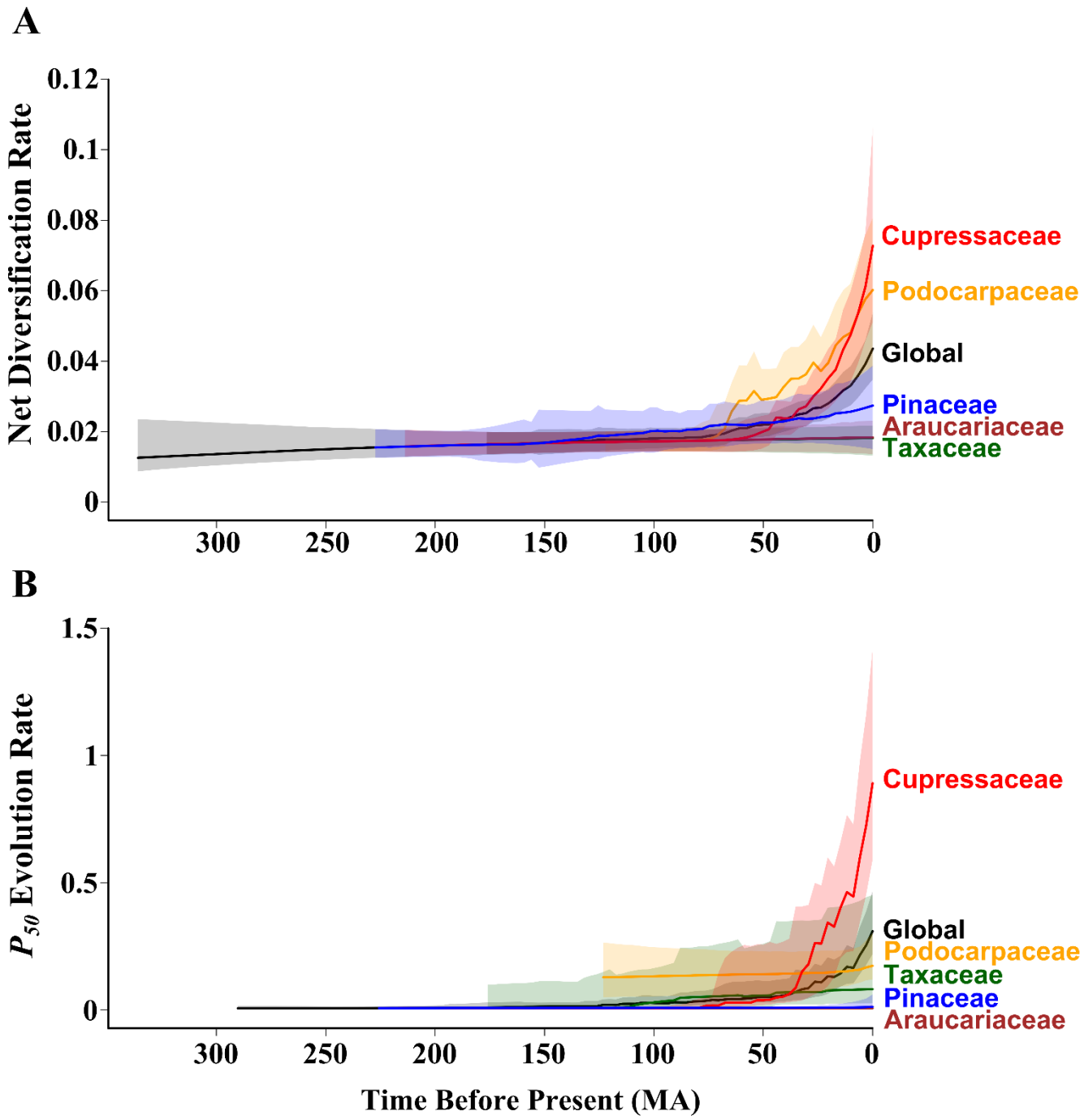

Figure 3. Family evolutionary rates through time from the BAMM analysis. (**A**) Net diversification rate and (**B**) cavitation resistance rate through time for each conifer family, average over all post-burn-in samples from the BAMM analyses. Shaded areas show 95% confidence interval, line represents median value of the rate distribution for each time slice. Different colors represent subdivisions of the conifer phylogeny, split from the rest of the tree at the most recent common ancestor for each family (excluding the stem). As throughout this paper, Taxaceae and Cephalotaxaceae are pooled together. Global rates represent the rates over the whole phylogeny.

Table 1. Trait dependent diversification models fit using QUASSE. Simple models (top half) and split-models (bottom half) were fit and compared using likelihood ratio tests. All models where speciation was a function of P_{50} were a significant improvement on the neutral model (indicated with bold font). The best simple and split models are underlined.

Speciation	Extinction	Df	Log Likelihood	AIC	X^2 test	p
constant	constant	4	-1633.3	3274.6	-	-
linear	constant	5	-1626.1	3262.2	14.426	**0.0001458**
sigmoidal	constant	7	-1629.4	3272.8	7.785	***0.0506678***
constant	linear	5	-1633.2	3276.5	0.163	0.6860005
<u>linear</u>	<u>linear</u>	<u>6</u>	<u>-1625.4</u>	<u>3262.8</u>	<u>15.773</u>	**<u>0.0003758</u>**
sigmoidal	linear	8	-1628.0	3272.0	10.638	**0.0309492**

Background	Foreground						
constant	constant	constant	8	-1546.2	3108.4	174.261	< **2.2e-16**
linear	constant	constant	9	-1547.9	3113.8	170.846	< **2.2e-17**
<u>constant</u>	<u>linear</u>	<u>constant</u>	<u>9</u>	<u>-1531.2</u>	<u>3080.4</u>	<u>204.228</u>	< **2.2e-18**
linear	linear	constant	10	-1535.2	3090.5	196.119	< **2.2e-19**

Splitting the phylogeny improved the model likelihood considerably, with all split models performing better than the global models. The best model is where the speciation rate in Pinaceae is maintained constant, while it is allowed to vary with P_{50} for the rest of the conifers. In this case again, increased cavitation resistance is associated with increasing diversification rates, in all Conifer families except Pinaceae. We found similar results when constraining the BM drift parameter to zero (see Suppl. Table S4 for full model parameters).

Discussion:

For the first time, we analyzed conifer diversification in a phylogenetic framework explicitly

allowing multiple dynamics. The BAMM analysis identified several independent bursts of diversification in Pinaceae, Podocarpaceae, and two within Cupressaceae, implying several underlying driving factors, especially given these clades occur in different hemispheres, and the timing of these shifts ranges from around 150 Mya for Pinaceae to the last 20 Mya in *Callitris*. Meanwhile, P_{50} evolution underwent four major upticks, early in the evolution of the Podocarpaceae family, deep within Cephalotaxaceae, and especially in both crown groups of Cupressaceae.

These two diversification rate upticks in Cupressaceae correspond to well-recognized drought-adapted clades in crown Cupressoidae and Callitroidae. The first is placed confidently on the branch leading to the *Cupressus* – *Juniperus* clade, therefore dated to between 45 and 75 Mya in our phylogeny. This is consistent with dates from the literature, both from phylogenetic dating analyses (Leslie et al., 2012) and fossil information. For example, *Tetraclinis* of early Eocene age (Stockey et al., 2005) indicate a likely pre-Eocene origin for the *Juniperus-Cupressus* clade. Despite some variation in shift placement in the BAMM analysis, the second shift likely occurred after the split between *Austrocedrus* and other Callitroidae, and before the appearance of *Callitris* s.s. which places the time interval for the diversification rate change to anywhere between 36 and 8 Mya. There is however evidence of *Fitzroya* and possibly *Callitris* being present by the early Oligocene (~32-30 Mya; (Paull and Hill, 2010)), which possibly means an older crown age for this group than in our dating analysis. The global trend towards colder and drier climate started after the Eocene climatic maximum around 50 Mya, and culminated in permanent ice at the poles around the end of the Eocene and maintained largely throughout the Oligeocene to about 26 Mya (Zachos et al., 2001). Over this drier period, diverse conifer clades with xeric affinities arose, i.e. *Juniperus* and *Cupressus* in the Northern Hemisphere and their Southern Hemisphere counterparts Callitris, a finding that supports the drought-driven diversification hypothesis. Despite a slight increase in the rate of P_{50} evolution in Cupressaceae before the beginning of the Eocene, the most impressive explosion in rates seems to have unfolded in the second half of the Paleogene, from 40 Mya onwards, which again is consistent with this hypothesis. In the Cupressoidae clade, this trait evolutionary dynamic seems to have appeared before the diversification uptick (since the shift is confidently placed on an older branch). This is consistent with the "ecological innovation" hypothesis that implies that a new, innovative trait triggers an adaptive radiation by opening up new ecological niche space. Unfortunately, the uncertain placement of both diversification and trait evolution shifts in Callitroidae do not allow us to make the same inference. However, there is evidence of a time

lag between i) the shift in diversification rate, with high marginal odds support on branches within the *Callitris* - *Actinostrobus* – *Neocallitropsis* clade, and ii) the shift in cavitation resistance evolution, which most likely occurred happened before this based on marginal probabilities and odds ratios on deep branches within Callitroidae.

The results from the BAMM analyses strongly suggest a link between speciation, extinction and drought tolerance evolutionary dynamics, at least within Cupressaceae. By explicitly modelling both processes, the trait-dependent diversification analysis from QUASSE provides strong evidence of a link between drought and conifer diversification. Splitting the tree to separate processes in Pinaceae from the other families greatly improved the model likelihood, further backing up the hypothesis that this family is driven by different dynamics from other conifer clades. he BAMM results strongly suggest a link between speciation, extinction and drought tolerance evolutionary dynamics, at least within Cupressaceae. By explicitly modelling both processes, the trait-dependent diversification analysis from QUASSE provides strong evidence of a link between drought and conifer diversification. Splitting the tree to separate processes in Pinaceae from the other families greatly improved the model likelihood, further backing up the hypothesis that this family is driven by different dynamics from other conifer clades. A recent study of conifer behavior patterns facing drought discovered two contrasting strategies: the first “ancestral” strategy found in Pinaceae, Podocarpaceae, Araucariaceae and basal Cupressaceae lineages involves high levels of abscisic acid (ABA) to induce stomatal closure, while the second is predominantly found in derived Cupressaceae and Taxaceae that rely on leaf desiccation to clamp shut stomata (Brodribb et al., 2014). This more recent strategy implies exposure to more negative water potentials, and seems to have driven an increase in cavitation resistance in these clades (Brodribb and McAdam, 2013). Our results for cavitation resistance shifts largely confirm this strategic shift in Taxaceae, Cupressoidae and Callitroidae, but we find evidence that the “embolism resistance” evolutionary pathway has also been followed by some other clades (notably within the Podocarpaceae family). This difference is possibly explained by the genera-level approach in Brodribb et al. (2014), which could obscure finer scale transitions the shifts within Podocarpaceae and Pinaceae.

The Pinaceae family is marked by high turn-over rates (high speciation and high extinction) from about 150 million years ago, which is consistent with the appearance of major extant Pinaceous lineages by the early Cretaceous (Gernandt et al., 2008). Since we only found slight evidence for a deep shift in P_{50} evolution in the BAMM analysis, we cannot tie this

diversification shift to increased resistance to drought. These results seem to refute the hypothesis that they were pushed back into cold, nutrient poor environments by the rise to dominance of flowering plants, which is widely thought to have occurred mainly during the late Cretaceous, i.e. from 100 Mya onwards. It is worth noting that around the Jurassic-Cretaceous boundary was a cool and dry period with relatively low atmospheric CO_2, with possible seasonal polar ice (Royer, 2006). This climatic context could have led to the appearance of temperate to cold environments in higher altitudes and latitudes, areas with which both fossil and extant Pinaceae taxa have affinities. This hypothesis is reinforced by the likely appearance of ectomycorrhizal fungi in the early Cretaceous (Smith and Read, 2010), which could have favored early Pinaceae lineages that appeared at this time (LePage, 2003). Pinaceae almost exclusively form ectomycorrhizal symbiotic relationships, which are predominant in cold environments with lower biomass decomposition rates. Other work has also favoured a role of altitude in increased diversification of Pinaceae, and there is evidence for a major shift in genome size evolution in *Pinus* as compared to both other Pinaceae and the rest of Conifers (Burleigh et al., 2012).

The rapid diversification observed in Podocarpaceae from around 75 Mya supports the hypothesis that *Podocarpus* and other "flattened-leaved" podocarps diversified in the shade of the Angiosperm dominated canopy that formed around this time (Biffin et al., 2012). It's worth noting that the Dacrydioid clade is also included in the more rapid dynamic, despite being mostly composed of imbricate-leaved species. Biffin et al. (2012) highlight the tropical origin of these diverse genera, indicating a possible geographical signal, as opposed to the less speciose temperate podocarp lineages.

Both topological uncertainty and divergence time estimation error can affect diversification and trait evolution models. Our phylogenies were largely consistent with previous work (Leslie et al., 2012; Mao et al., 2012). Within Cupressaceae, in both analyses *Actinostrobus* is sister to the *Neocallitropsis*-*Callitris* clade, with Callitris monophyletic contrary to Mao et al., (2012). However, in accordance with the more recent molecular phylogenetics literature, *Cupressus* is paraphyletic with the old-world cypresses (*Cupressus* s.s.) sister to a clade grouping the new-world cypresses (*Hesperocyparis*), *Juniperus*, and *Xanthocyparis*, where relationships are relatively unresolved. In spite of using similar fossil calibrations, our dating analysis does not completely agree with previous studies where dating was implemented in a Bayesian framework i.e. Leslie et al. 2012. Overall, our dating analyses pulled crown group divergences

further back in time, resulting in a more gradual diversification pattern, with a few exceptions, notably genus Callitris. This contrasts with some other studies, for example Leslie et al. (2012) obtained broom-shaped crown clades, with long stems leading to young crown groups. This "stemmy and broomy" pattern is common with the lognormal relaxed clock model in crown groups that are not constrained with fossil information (Crisp et al., 2014). This is also possibly due to less extensive sampling in our phylogeny, as adding species within crown clades will probably lead to a broom-like pattern with more short branches close to the present. In our time-trees, ages for Cupressaceae divergences tend to be slightly younger than in Mao et al. (2012), and in general agreement with ages from Biffin et al. (2012) in Podocarpaceae, which adds confidence to our dating analysis. Furthermore, since all clades are affected in the same way we do not expect an impact of these discrepancies on the overall diversification patterns. Finally, we ran analyses with the different topologies and calibrations, and obtained largely similar results. The "deep node only" calibration set yielded much younger crown ages, therefore impacting results somewhat negatively. Since the topologies were similar between the MrBayes tress and the RAxML tree, we're not surprised that results are consistent across inference methods. The most notable difference in the BAMM diversification analysis is the regular appearance of a rate shift on the branch leading to the clade formed by orders Cupressales and Araucariales.

The SSE methods (state-dependent speciation and extinction models) are vulnerable to some severe pitfalls (Rabosky and Goldberg, 2015; O'Meara and Beaulieu, 2016). We found evidence of false-positives with our phylogeny, with a number of simulated traits (29/100) resulting in significant trait-dependent diversification. This brings us to use caution when drawing conclusions from this analysis, however some elements give us hope that our result is not due to false positives. Firstly, compared to the simulation analyses, our model performs better than all but 5 outliers (as noted from both the likelihood ratio chi-squared statistic and the improvement in AIC scores – Suppl. Fig. S8). Second, by conducting a split model analysis, we remove a large part of the diversification rate heterogeneity (namely, the heterogeneity in rates within the Pinaceae family) which should greatly reduce the risk of type I error (Rabosky and Goldberg, 2015).

Previous work using comparative phylogenetic approaches have struggled to identify traits driving increased lineage accumulation in conifers, with the exception of leaf morphology in Podocarpaceae (Biffin et al., 2012). For example investigations into conifer breeding system

hypothesized an advantage for either monoecious lineages with dry cones or clades with "fleshy" cones and dioecy, but found no influence on diversification of these particular combinations (Leslie et al., 2013). Our results highlight the influence physiological traits can have on speciation and resistance to extinction, providing directions for future investigations.

Conclusion:

Conifer diversification has undergone multiple shifts throughout the long history of this group. Drought has evidently played a major role in the evolutionary history of conifers, with strong evidence of rapid diversification associated with increased cavitation resistance in crown groups of Cupressaceae over the last 50 MA. While we cannot tie the shifts towards increased drought tolerance in Pinaceae, Podocarpaceae and Taxaceae with higher rates of speciation, we nevertheless find a general trend across conifers linking increased diversification and increased resistance to hydraulic failure. Our results show that at a geological timescale, while some conifer lineages may have been severely limited or even driven to extinction, others have managed to cope, and even seem to have benefitted from these harsher conditions to radiate into a wide range of xeric habitats. However, it remains to be seen whether adaptation can keep up the pace with climate change, even in these rapidly evolving clades.

References

Allen CD, Macalady AK, Chenchouni H, Bachelet D, McDowell N, Vennetier M, Kitzberger T, Rigling A, Breshears DD, Hogg EH (Ted), et al (2010) A global overview of drought and heat-induced tree mortality reveals emerging climate change risks for forests. For Ecol Manage **259**: 660–684

Anderegg WRL, Berry J a, Smith DD, Sperry JS, Anderegg LDL, Field CB (2012) The roles of hydraulic and carbon stress in a widespread climate-induced forest die-off. Proc Natl Acad Sci U S A **109**: 233–7

Anderegg WRL, Klein T, Bartlett M, Sack L, Pellegrini AFA, Choat B (2016) Meta-analysis reveals that hydraulic traits explain cross-species patterns of drought-induced tree mortality across the globe. Pnas. doi: 10.1073/pnas.1525678113

Augusto L, Davies TJ, Delzon S, De Schrijver A (2014) The enigma of the rise of angiosperms: can we untie the knot? Ecol Lett **17**: 1326–38

Balducci L, Deslauriers A, Giovannelli A, Beaulieu M, Delzon S, Rossi S, Rathgeber CBK (2014) How do drought and warming influence survival and wood traits of Picea mariana saplings? J Exp Bot. doi: 10.1093/jxb/eru431

Biffin E, Brodribb TJ, Hill RS, Thomas P, Lowe AJ (2012) Leaf evolution in Southern Hemisphere conifers tracks the angiosperm ecological radiation. Proc Biol Sci **279**: 341–8

Biffin E, Conran JG, Lowe AJ (2011) Podocarp Evolution: A Molecular Phylogenetic Perspective. Smithson Contrib to Bot 1–20

Bond WJ (1989) The tortoise and the hare: ecology of angiosperm dominance and gymnosperm persistence. Biol J Linn Soc **36**: 227–249

Bouche PS, Larter M, Domec J-C, Burlett R, Gasson P, Jansen S, Delzon S (2014) A broad survey of hydraulic and mechanical safety in the xylem of conifers. J Exp Bot. doi: 10.1093/jxb/eru218

Brodribb T, Hill RS (1999) The importance of xylem constraints in the distribution of conifer species. New Phytol **143**: 365–372

Brodribb TJ, McAdam S a M (2013) Abscisic acid mediates a divergence in the drought response of two conifers. Plant Physiol **162**: 1370–7

Brodribb TJ, McAdam S a M, Jordan GJ, Martins SC V (2014) Conifer species adapt to low-rainfall climates by following one of two divergent pathways. Proc Natl Acad Sci U S A. doi: 10.1073/pnas.1407930111

Burleigh JG, Barbazuk WB, Davis JM, Morse AM, Soltis PS (2012) Exploring Diversification and Genome Size Evolution in Extant Gymnosperms through Phylogenetic Synthesis. J Bot **2012**: 1–6

Choat B, Jansen S, Brodribb TJ, Cochard H, Delzon S, Bhaskar R, Bucci SJ, Feild TS, Gleason SM, Hacke UG, et al (2012) Global convergence in the vulnerability of forests to drought. Nature **491**: 752–5

Cochard H, Damour G, Bodet C, Tharwat I, Poirier M, Améglio T (2005) Evaluation of a new centrifuge technique for rapid generation of xylem vulnerability curves. Physiol Plant **124**: 410–418

Crepet WL, Niklas KJ (2009) Darwin's second "abominable mystery": Why are there so many angiosperm species? Am J Bot **96**: 366–381

Crisp MD, Hardy NB, Cook LG (2014) Clock model makes a large difference to age estimates of long-stemmed clades with no internal calibration: a test using Australian grasstrees. BMC Evol Biol **14**: 1–17

Delzon S, Douthe C, Sala A, Cochard H (2010) Mechanism of water-stress induced cavitation in conifers: bordered pit structure and function support the hypothesis of seal capillary-seeding. Plant Cell Environ **33**: 2101–11

Dickman LT, McDowell NG, Sevanto S, Pangle RE, Pockman WT (2014) Carbohydrate dynamics and mortality in a piñon-juniper woodland under three future precipitation scenarios. Plant Cell Environ 1–40

Eckenwalder JE (2009) Conifers of the world: the complete reference. Timber Press

Farjon A (2010) A Handbook of the World's Conifers (2 Vols.). BRILL

FitzJohn RG (2012) Diversitree : comparative phylogenetic analyses of diversification in R. Methods Ecol Evol **3**: 1084–1092

Fitzjohn RG (2010) Quantitative traits and diversification. Syst Biol **59**: 619–633

Gernandt DS, Magallón S, Geada López G, Zerón Flores O, Willyard A, Liston A (2008) Use of Simultaneous Analyses to Guide Fossil-Based Calibrations of Pinaceae Phylogeny. Int J Plant Sci **169**: 1086–1099

IUCN (2015) The IUCN Red List of Threatened Species. Version 2015-4. <http://www.iucnredlist.org>

Kim J, Sanderson MJ (2008) Penalized likelihood phylogenetic inference: bridging the parsimony-likelihood gap. Syst Biol **57**: 665–74

Larter M, Brodribb TJ, Pfautsch S, Burlett R, Cochard H, Delzon S (2015) Extreme aridity pushes trees to their physical limits. Plant Physiol **168**: pp.00223.2015

LePage BA (2003) The evolution, biogeography and palaeoecology of the pinaceae based on fossil and extant representatives. Acta Hortic **615**: 29–52

Leslie AB, Beaulieu JM, Crane PR, Donoghue MJ (2013) Explaining the distribution of breeding and dispersal syndromes in conifers. Proc R Soc B-Biological Sci **280**: 20131812

Leslie AB, Beaulieu JM, Rai HS, Crane PR, Donoghue MJ, Mathews S (2012) Hemisphere-scale differences in conifer evolutionary dynamics. Proc Natl Acad Sci U S A **109**: 16217–21

Lin C-P, Huang J-P, Wu C-S, Hsu C-Y, Chaw SM (2010) Comparative chloroplast genomics reveals the evolution of Pinaceae genera and subfamilies. Genome Biol Evol **2**: 504–17

Maddison WP, Maddison DR (2015) Mesquite: a modular system for evolutionary analysis.

Maddison WP, Midford PE, Otto SP (2007) Estimating a binary character's effect on speciation and extinction. Syst Biol **56**: 701–710

Maherali H, Pockman WT, Jackson RB (2004) Adaptive variation in the vulnerability of woody plants to xylem cavitation. Ecology **85**: 2184–2199

Mao K, Milne RI, Zhang L, Peng Y, Liu J, Thomas P, Mill RR, Renner SS (2012) Distribution of living Cupressaceae reflects the breakup of Pangea. Proc Natl Acad Sci U S A **109**: 7793–8

Mitchell PJ, O'Grady AP, Tissue DT, White D a, Ottenschlaeger ML, Pinkard E a (2013) Drought response strategies define the relative contributions of hydraulic dysfunction and carbohydrate depletion during tree mortality. New Phytol **197**: 862–72

O'Meara BC, Beaulieu JM (2016) Past, future, and present of state-dependent models of diversification. Am J Bot **103**: 1–4

Pammenter NW, Vander Willigen C (1998) A mathematical and statistical analysis of the curves illustrating vulnerability of xylem to cavitation. Tree Physiol **18**: 589–593

Paradis E (2013) Molecular dating of phylogenies by likelihood methods: a comparison of models and a new information criterion. Mol Phylogenet Evol **67**: 436–44

Paull R, Hill RS (2010) Early Oligocene Callitris and Fitzroya (Cupressaceae) from Tasmania. Am J Bot **97**: 809–20

Pennell MW, Harmon LJ (2013) An integrative view of phylogenetic comparative methods: connections to population genetics, community ecology, and paleobiology. Ann N Y Acad Sci **1289**: 90–105

Pittermann J, Stuart SA, Dawson TE, Moreau A (2012) Cenozoic climate change shaped the evolutionary ecophysiology of the Cupressaceae conifers. Proc Natl Acad Sci U S A **109**: 9647–52

Rabosky DL (2014) Automatic detection of key innovations, rate shifts, and diversity-dependence on phylogenetic trees. PLoS One **9**: e89543

Rabosky DL, Donnellan SC, Grundler M, Lovette IJ (2014) Analysis and visualization of complex macroevolutionary dynamics: an example from Australian scincid lizards. Syst Biol **63**: 610–27

Rabosky DL, Goldberg EE (2015) Model Inadequacy and Mistaken Inferences of Trait-Dependent Speciation. Syst Biol **64**: 340–355

Rambaut A, Suchard MA, Xie D, Drummond AJ (2014) Tracer v1.6.

Ronquist F, Teslenko M, Van Der Mark P, Ayres DL, Darling A, Höhna S, Larget B, Liu L, Suchard M a., Huelsenbeck JP (2012) Mrbayes 3.2: Efficient bayesian phylogenetic inference and model choice across a large model space. Syst Biol **61**: 539–542

Royer DL (2006) CO2-forced climate thresholds during the Phanerozoic. Geochim Cosmochim Acta **70**: 5665–5675

Sala A, Piper F, Hoch G (2010) Physiological mechanisms of drought-induced tree mortality are far from being resolved. New Phytol **186**: 274–81

Sanderson MJ (2002) Estimating absolute rates of molecular evolution and divergence times: a penalized likelihood approach. Mol Biol Evol **19**: 101–9

Sevanto S, McDowell NG, Dickman LT, Pangle R, Pockman WT (2014) How do trees die? A test of the hydraulic failure and carbon starvation hypotheses. Plant Cell Environ **37**: 153–61

Shi JJ, Rabosky DL (2015) Speciation dynamics during the global radiation of extant bats. Evolution (N Y) **69**: 1528–1545

Smith SA, Beaulieu JM, Donoghue MJ (2009) Mega-phylogeny approach for comparative biology: an alternative to supertree and supermatrix approaches. BMC Evol Biol **9**: 37

Smith SE, Read DJ (2010) Mycorrhizal symbiosis. Academic press

Stamatakis A (2006) RAxML-VI-HPC: maximum likelihood-based phylogenetic analyses with thousands of taxa and mixed models. Bioinformatics **22**: 2688–90

Stockey R a, Kvacek J, Hill RS, Rothwell GW, Kvacek K (2005) The fossil record of Cupressaceae s. lat. A Monogr Cupressaceae Sciadopitys 64–68

Tamura K, Peterson D, Peterson N, Stecher G, Nei M, Kumar S (2011) MEGA5: molecular evolutionary genetics analysis using maximum likelihood, evolutionary distance, and maximum parsimony methods. Mol Biol Evol **28**: 2731–9

Zachos J, Pagani M, Sloan L, Thomas E, Billups K (2001) Trends, rhythms, and aberrations in global climate 65 Ma to present. Science (80-) **292**: 686–693

Supplementary material

Supplementary tables:

Table S1: GenBank accessions for the sequences used in this study.

Table S2: Fossil calibrations used in the dating analyses. For each calibration point, names of the descendant clades, minimum and maximum age constraints, and the resulting inferred age using *chronos* in R. All ages are in Million years ago. "Deep nodes" refers to the calibration set with only the 4 deepest constraints (nodes A through D).

Table S3: Parameters for QUASSE models across pylogenetic inference methods and calibration settings (RAxML and MrBayes 40 MA calibrations, and RAxML 20 MA calibration). We only fit models with speciation as a linear function of trait values. The improvement in likelihood was consistent across analyses.

Table S4: Model comparisons and full parameters for the QUASSE analysis. The bottom half of the table are without the BM drift parameter. Fg. And Bg. are foreground clades specified in the split analysis (i.e. Taxaceae and Cupressaceae) and background (i.e. Pinaceae, Araucariaceae and Podocarpaceae).

Table S1.

Species	ITS1	PHYP	MATK	RBCL
Abies alba	JN177292.1		HQ619823.1	AB029652.1
Abies amabilis	EF057688.1			AB029650.1
Abies balsamea	EF057709.1			JN935605.1
Abies bracteata	EF057713.1		AF456365.1	AB029647.1
Abies cephalonica	EF057697.1			FR831931.1
Abies cilicica	EF057698.1			
Abies concolor	DQ975364.1	JX560070.1		AB029648.1
Abies fabri	DQ975352.1		JF952937.1	AB029638.1
Abies fargesii	JF416974.1		JF952942.1	AB029639.1
Abies forrestii	EU196132.1		JF952950.1	JF940583.1
Abies fraseri	EF057711.1		AB029660.1	AB029644.1
Abies grandis	EF057690.1			AB029646.1
Abies holophylla	AF283015.1		AF143441.1	JQ512510.1
Abies homolepis	EF057703.1	JX560072.1	AB029662.1	JN935610.1
Abies kawakamii	EF063715.1			DQ112531.1
Abies koreana	JF499944.1		JQ512389.1	JQ512513.1
Abies lasiocarpa	EF057710.1	JX560073.1	AB029664.1	AY664855.1
Abies mariesii	EF057689.1		AB029665.1	
Abies nephrolepis	EF057712.1		JQ512392.1	JQ512514.1
Abies nordmanniana	EF057699.1			AB029654.1
Abies numidica	EF057700.1			AB029655.1
Abies pindrow	EU196128.1			
Abies pinsapo	EF057701.1			AB029656.1
Abies procera	EF057696.1			AB029651.1
Abies recurvata			JF952970.1	JN935618.1
Abies sachalinensis	JF499945.1		AB029667.1	JN935619.1
Abies spectabilis	JF416978.1		JF952975.1	JF940608.1
Abies squamata	JF416982.1		JF952980.1	JF940613.1
Abies veitchii	EF063713.1		AB029669.1	JN935621.1
Acmopyle pancheri		JX560001.1	HM593685.1	HM593587.1
Actinostrobus acuminatus	AY178417.1		AF152175.1	
Actinostrobus arenarius		JX559912.1	JF725837.1	JF725937.1
Actinostrobus pyramidalis	AY178415.1	JX559913.1	HQ245874.1	EU161450.1
Afrocarpus falcatus	JF969615.1	JX560003.1	AF457111.1	X58135.1
Afrocarpus gracilior		JX560004.1	HM593688.1	HM593589.1
Afrocarpus mannii		JX560005.1	HM593689.1	HM593590.1
Afrocarpus usambarensis		JX560006.1	KF713553.1	KF714048.1
Agathis atropurpurea			EU025977.1	AF502087.1
Agathis australis	DQ499065.1		JN627305.1	AF362993.1
Agathis lanceolata	KM459933.1	JX559977.1		U96481.1
Agathis microstachya	JN021508.1		EU025978.1	AF508920.1
Agathis moorei	KM459934.1	JX559980.1		U96480.1
Agathis ovata		JX559981.1		U96483.1

Agathis robusta	EU165010.1	JX559982.1	AF456371.1	EF490509.1
Araucaria angustifolia	EU165012.1	JX559984.1	EF451975.1	U96470.1
Araucaria araucana	JF829718.1	JX559985.1	AF456373.1	U96467.1
Araucaria bernieri	KM459941.1	JX559986.1	AM920138.1	U96460.1
Araucaria bidwillii	EU165011.1	JX559987.1	EU025974.1	U96472.1
Araucaria biramulata	KM459947.1	JX559988.1	AM920177.1	U96475.1
Araucaria columnaris		JX559989.1	AM920145.1	U96461.1
Araucaria cunninghamii	EU165013.1	JX559990.1	JQ512394.1	JQ512518.1
Araucaria heterophylla	EU165014.1	JN656092.1	HQ245919.1	U96462.1
Araucaria hunsteinii	DQ499067.1	JX559992.1	AF456375.1	U96468.1
Araucaria laubenfelsii	KM459959.1	JX559993.1	AM920153.1	U96463.1
Araucaria luxurians		JX559994.1	AM920157.1	U96464.1
Araucaria montana	KM459965.1	JX559995.1	AM920159.1	U96457.1
Araucaria muelleri	KM459968.1	JX559996.1	AM920162.1	U96465.1
Araucaria nemorosa	KM459972.1		AM920166.1	U96458.1
Araucaria rulei	KM459973.1	JX559997.1	AM920169.1	U96466.1
Araucaria scopulorum	KM459979.1		AM920175.1	U96459.1
Araucaria subulata	KM459980.1	JX559999.1	AM920178.1	U96474.1
Athrotaxis cupressoides	AF387545.1		AB030131.1	JF725921.1
Athrotaxis laxifolia	AF387543.1		AB030129.1	L25754.2
Athrotaxis selaginoides	AF387537.1	JX559914.1	AB030130.1	JF725938.1
Austrocedrus chilensis		JX559915.1	HQ245876.1	EU161449.1
Callitris canescens	AY178411.1		JF725845.1	JF725945.1
Callitris columellaris	AY178404.1		HQ245877.1	
Callitris drummondii	AY178423.1		JF725839.1	JF725939.1
Callitris endlicheri	AY178425.1		AY988331.1	JF725932.1
Callitris glaucophylla	AY178399.1			
Callitris intratropica	AY178400.1			
Callitris macleayana	HM116954.1	JX559916.1	HQ245878.1	JF725933.1
Callitris muelleri	AY178412.1		JF725824.1	JF725924.1
Callitris preissii			JF725840.1	JF725940.1
Callitris rhomboidea	AY178408.1		HQ245879.1	L12537.2
Callitris sulcata	AY178422.1		JF725841.1	JF725941.1
Callitris tuberculata	AY178426.1			
Callitris verrucosa	HM116955.1		AY988330.1	JF725942.1
Callitropsis funebris	AY988377.1	JX559935.1	HM023991.1	AY988245.1
Callitropsis nootkatensis	AY380858.1	JX559922.1	HM023980.1	HM024268.1
Callitropsis vietnamensis	AY380877.1	JX559923.1	HM024074.1	HM024352.1
Calocedrus decurrens	AY380854.1	JX559924.1	HM023981.1	L12569.2
Calocedrus formosana	HQ435648.1		FJ475237.1	AB715255.1
Calocedrus macrolepis	AY150686.1	JX559925.1	HM023982.1	EF053220.1
Cedrus atlantica			AF143431.1	AF145457.1
Cedrus deodara	DQ975357.1		JQ512397.1	AF456381.1
Cedrus libani		JX560074.1		HG765045.1
Cephalotaxus fortunei	EF660585.1	JX559893.1	JF953499.1	AY450863.1
Cephalotaxus hainanensis	EF660592.1		JX099351.1	EF660729.1

Cephalotaxus harringtonia	EF660581.1	JX559894.1	AB030138.1	AF227461.1
Cephalotaxus koreana	EF660574.1		EF660656.1	EF660726.1
Cephalotaxus sinensis	EF660591.1	JX559896.1	HQ245920.1	JF725946.1
Cephalotaxus wilsoniana	GQ434684.1		EF660648.1	AB027312.1
Chamaecyparis formosensis	AY211258.1		HM023983.1	HM024271.1
Chamaecyparis lawsoniana	AY211254.1	JX559926.1	HM023984.1	HM024272.1
Chamaecyparis obtusa	AY211253.1	JX559927.1	HM023985.1	JQ512527.1
Chamaecyparis pisifera	DQ269982.1	FJ393260.1	HM023986.1	JQ512530.1
Chamaecyparis thyoides	AY283428.1		FJ475236.1	
Cryptomeria japonica	AB023983.1	AB894549.1	AB030116.1	AJ621937.1
Cunninghamia lanceolata	AF387523.1	JX559930.1	AB030125.1	JQ512534.1
Cunninghamia lanceolata var konis		JX559929.1	AB030126.1	JN039274.1
Cupressus atlantica	AY988367.1		HM023987.1	HM024275.1
Cupressus duclouxiana	AY380864.1	JX559933.1	HM023990.1	AY988242.1
Cupressus dupreziana	AY988375.1	JX559934.1	AY988342.1	AY988243.1
Cupressus sempervirens	FJ705221.1	JX559936.1	HM023994.1	HM024278.1
Cupressus torulosa	AY988393.1	JX559937.1	HM023995.1	AY988257.1
Cycas micronesica		JN655925.1	EU016806.1	EU016864.1
Dacrycarpus dacrydioides			HM593702.1	AF249597.1
Dacrycarpus imbricatus		JX560010.1	HM593703.1	HM593603.1
Dacrycarpus vieillardii			HM593705.1	AF249598.1
Dacrydium araucarioides			HM593690.1	HM593591.1
Dacrydium balansae		JX560011.1	HM593691.1	HM593592.1
Dacrydium guillauminii		JX560012.1	HM593694.1	HM593595.1
Diselma archeri		JX559938.1	HQ245889.1	L12572.2
Encephalartos ferox		JN655989.1	JQ046302.1	AY335243.1
Falcatifolium falciforme			HM593706.1	KF714072.1
Falcatifolium taxoides			HM593707.1	AF249637.1
Fitzroya cupressoides	HQ414213.1	JX559939.1	HQ245890.1	JF725916.1
Glyptostrobus pensilis	AF387525.1	JX559941.1	AB030118.1	L25750.2
Halocarpus bidwillii		JX560016.1	KF713609.1	HM593606.1
Halocarpus biformis			HM593708.1	HM593607.1
Hesperocyparis arizonica	U77962.1	JX559931.1	HM023998.1	AF127430.1
Hesperocyparis glabra	U60748.1		HM024001.1	HM024282.1
Hesperocyparis goveniana	AY380865.1	JX559919.1	HM024002.1	AY380888.1
Hesperocyparis lusitanica		JX559920.1	HM024003.1	
Hesperocyparis macrocarpa	AY380868.1	JX559921.1	HM024005.1	HM024284.1
Hesperocyparis sargentii	U60749.1		HM024007.1	AY988254.1
Juniperus chinensis	FJ980279.1		HM024014.1	HM024292.1
Juniperus communis	EU277677.1	JX559944.1	AY988359.1	AY988260.1
Juniperus coxii			HM024050.1	HM024328.1
Juniperus deppeana	EU277684.1		HM024022.1	HM024300.1
Juniperus flaccida	FJ948470.1		HM024026.1	HM024304.1
Juniperus monticola	FJ948467.1		HM024038.1	HM024316.1
Juniperus osteosperma	EU277693.1		HM024040.1	HM024318.1
Juniperus recurva	GQ118647.1			

Juniperus rigida	AY836797.1		AB030136.1	JQ512551.1
Juniperus scopulorum	EF608964.1	JX559949.1	HM024059.1	HM024337.1
Juniperus squamata	GQ118644.1		HM024061.1	HM024339.1
Juniperus virginiana	EU277699.1	JX559951.1	HM024065.1	JQ512556.1
Lagarostrobos franklinii		JX560017.1	HM593710.1	HM593609.1
Larix decidua	AF041343.1	JX560075.1		FN689379.1
Larix gmelinii		JX560076.1	AF143433.1	
Larix kaempferi	AF041344.1	JX560077.1	JQ512436.1	JQ512559.1
Larix laricina	AF041348.1	JX560078.1		AF479878.1
Larix occidentalis	AF041347.1			X63663.1
Larix potaninii var macrocarpa			AY391402.1	AY389137.1
Larix sibirica	AF041345.1	EU441951.1		
Lepidothamnus laxifolius		JX560019.1	AF457114.1	HM593610.1
Libocedrus bidwillii		JX559953.1	HQ245900.1	JF725927.1
Libocedrus yateensis		JX559954.1	HQ245902.1	
Manoao colensoi		JX560020.1	HM593712.1	AF249644.1
Metasequoia glyptostroboides	AF387527.1	JX559955.1	AB030122.1	JQ512563.1
Microbiota decussata	AY380874.1	JX559956.1	HM024066.1	L12575.2
Microcachrys tetragona		JX560021.1	HM593713.1	HM593611.1
Nageia fleuryi	JF829693.1		HM593714.1	HM593612.1
Neocallitropsis pancheri	AY178420.1	JX559957.1	HQ245905.1	AF127426.1
Nothotsuga longibracteata	DQ975351.1		AF143437.1	AF145459.1
Papuacedrus papuana		JX559958.1	HQ245906.1	EU161451.1
Pherosphaera fitzgeraldii		JX560022.1	HM593719.1	HM593617.1
Pherosphaera hookeriana			HM593720.1	HM593618.1
Phyllocladus aspleniifolius	AY442167.1	JX560027.1	AY442147.1	AY442152.1
Phyllocladus trichomanoides	AY442164.1	AJ286650.1	AY442150.1	AF249654.1
Picea abies	AJ243165.1	U60264.1	AB161012.1	JQ512566.1
Picea asperata			AY729946.1	EF440572.1
Picea brachytyla			AY729949.1	EF440573.1
Picea breweriana		JX560079.1	EF440496.1	EF440574.1
Picea chihuahuana			EF440497.1	EU269030.1
Picea crassifolia			AY729951.1	EF440576.1
Picea engelmannii			EF440499.1	EF440577.1
Picea glauca	AF136619.1	JX560080.1	AF133926.1	EF440579.1
Picea glehnii	AY563413.1		EF440502.1	EF440580.1
Picea jezoensis			JQ512444.1	JQ512568.1
Picea koraiensis			AY729942.1	JQ512570.1
Picea koyamae			EF440505.1	EF440583.1
Picea likiangensis			EF440506.1	EF440584.1
Picea mariana	AF136614.1	JX560081.1	AF133922.1	EF440585.1
Picea maximowiczii			EF440509.1	EF440587.1
Picea meyeri	GQ865721.1		EF440511.1	EF440589.1
Picea morrisonicola			EF440513.1	EF440591.1
Picea obovata			EU199800.1	EF440592.1
Picea omorika			AY035200.1	EF440593.1

Picea orientalis	AY563415.1		EF440516.1	EF440594.1
Picea pungens			EF440519.1	X58136.1
Picea purpurea			AY729950.1	EF440598.1
Picea rubens	AF136610.1		AF133918.1	EF440600.1
Picea schrenkiana			EF440523.1	EF440601.1
Picea sitchensis		HM198950.1	EF440525.1	X63660.1
Picea smithiana			AY729947.1	AF145458.1
Picea wilsonii	GQ463500.1		EF440529.1	EF440606.1
Pilgerodendron uviferum		JX559959.1	HQ245907.1	EU161452.1
Pinus albicaulis	AF036983.2		AY497261.1	AY497225.1
Pinus aristata	AF037000.2		AY115795.1	AY115758.1
Pinus arizonica	U88039.1		DQ166031.1	DQ156484.1
Pinus armandii	AF036980.1		AF143428.1	HQ849874.1
Pinus attenuata	AF037020.1		AB080933.1	DQ353724.1
Pinus ayacahuite	AF036981.1		AY497257.1	AY497221.1
Pinus banksiana		FJ415424.1	AF143427.1	EF440595.1
Pinus brutia	EU647194.1			FR831903.1
Pinus bungeana	AF036992.1		AY729953.1	JQ512573.1
Pinus cembra	AF036987.2		AB160985.1	DQ353720.1
Pinus contorta	AF037014.1	FJ415423.1	AB080921.1	AY497230.1
Pinus coulteri	AF037013.1		AB097785.1	AY724759.1
Pinus densata			AB097779.1	AY555713.1
Pinus densiflora	KC583360.1		JQ512453.1	JQ512577.1
Pinus devoniana			AY497277.1	AY497241.1
Pinus durangensis	AF037010.1		AY497276.1	AY497240.1
Pinus edulis	AF343993.1		AY115765.1	X58137.1
Pinus engelmannii			AB080927.1	AY497239.1
Pinus flexilis	AF344001.1		AY497258.1	AY497222.1
Pinus glabra			DQ353712.1	DQ353728.1
Pinus halepensis	AF037007.1		AB081089.1	AJ271897.1
Pinus hartwegii	AF037008.1		AY497267.1	AY497231.1
Pinus heldreichii			AB161006.1	DQ353730.1
Pinus heldreichii var leucodermis				FR831914.1
Pinus jeffreyi	U88040.1		AB080926.1	AY497235.1
Pinus koraiensis	KC583357.1		EF440518.1	JQ512579.1
Pinus leiophylla	AF037017.1		AB081085.1	AY497243.1
Pinus massoniana	JF829705.1	KJ921381.1	AB081088.1	DQ353732.1
Pinus mugo		KC980592.1	AB081087.1	EU269032.1
Pinus mugo subsp uncinata		KC980603.1	AB097778.1	AB097774.1
Pinus muricata			AB080935.1	DQ353725.1
Pinus nigra		FJ415421.1	AB084498.1	JQ512593.1
Pinus palustris	AF305062.1		AB080937.1	JQ512582.1
Pinus parviflora	AF036984.1	KJ195157.1	JQ512462.1	JQ512586.1
Pinus patula	AF037019.1		AB080944.1	AY497248.1
Pinus peuce	AF036989.1	FJ415426.1	AY497254.1	AY497218.1
Pinus pinaster	AF037024.1	JQ970317.1	AB084493.1	FR831913.1

Pinus pinea	X87936.1		AB084496.1	X58133.1
Pinus ponderosa	AF037011.1	FJ415425.1	AB080924.1	AY497234.1
Pinus pseudostrobus			AY497268.1	AY497232.1
Pinus pumila	AF036986.1		AB161013.1	AB161042.1
Pinus radiata		EU301707.1	AB080934.1	X58134.1
Pinus resinosa	AF037002.1	FJ415422.1	AB080945.1	AY497252.1
Pinus rigida	KC583358.1		JQ512465.1	JQ512589.1
Pinus sabiniana			AY497272.1	AY497236.1
Pinus serotina			AB080930.1	AY724761.1
Pinus sibirica	AY430077.1		AB161014.1	AY497228.1
Pinus strobiformis		FJ415427.1	EF546726.1	AB455588.1
Pinus strobus	AF036982.1	JX560082.1	JQ512467.1	JQ512591.1
Pinus sylvestris	AF037003.1	X96738.1	AB097781.1	AB097775.1
Pinus tabuliformis	KJ474644.1		AB161015.1	AY555716.1
Pinus taeda	AF200523.1		JQ512468.1	JQ512592.1
Pinus taiwanensis	JF829712.1		AB161016.1	AB161045.1
Pinus thunbergii	AF037025.1	FJ393244.1	JQ512471.1	JQ512595.1
Pinus virginiana	AF037015.1		AB080923.1	JQ512596.1
Pinus wallichiana	AF036991.1		AY734482.1	X58131.1
Pinus washoensis			DQ353706.1	DQ353721.1
Pinus yunnanensis			AB161017.1	AY555695.1
Platycladus orientalis	AY380875.1	JX559960.1	HM024067.1	JQ512599.1
Podocarpus acutifolius		JX560029.1	HM593725.1	HM593622.1
Podocarpus coriaceus	JF969584.1	JX560036.1	HM593737.1	HM593634.1
Podocarpus cunninghamii	DQ499127.1	JX560038.1	HM593740.1	HM593637.1
Podocarpus elatus			AF457113.1	HM593641.1
Podocarpus elongatus	JF969598.1	JX560041.1	HM593746.1	HM593643.1
Podocarpus grayae			HM593750.1	HM593647.1
Podocarpus henkelii	JF969600.1		HM593751.1	HM593648.1
Podocarpus lambertii	JF969580.1		HM593753.1	HM593650.1
Podocarpus latifolius	JF969601.1	JX560044.1	HM593754.1	AF249612.1
Podocarpus lawrencei		JX560030.1	HM593756.1	HM593651.1
Podocarpus longifoliolatus		JX560045.1	HM593758.1	HM593654.1
Podocarpus lucienii		JX560046.1	HM593759.1	HM593655.1
Podocarpus neriifolius	JF829692.1	JX560049.1	HM593765.1	AF249618.1
Podocarpus nivalis	JF969574.1		HM593757.1	HM593653.1
Podocarpus novae-caledoniae	JF969603.1	JX560050.1	HM593766.1	HM593662.1
Podocarpus nubigenus			HM593767.1	HM593663.1
Podocarpus oleifolius	JF969583.1	JX560051.1	KF713750.1	KF714168.1
Podocarpus polystachyus			HM593771.1	HM593667.1
Podocarpus rubens	JF969608.1	JX560055.1	HM593774.1	HM593670.1
Podocarpus salignus		JX560057.1	HM593776.1	HM593672.1
Podocarpus spinulosus		JX560060.1	HM593780.1	HM593676.1
Podocarpus totara		JX560062.1	JN627357.1	HM593678.1
Prumnopitys andina		JX560063.1	HM593721.1	HM593619.1
Prumnopitys ferruginea			AF457115.1	AF249656.1

Prumnopitys ladei		JX560065.1	HM593723.1	HM593620.1
Prumnopitys taxifolia			HM593724.1	HM593621.1
Pseudolarix amabilis	DQ975355.1	JX560084.1	AF143432.1	X58782.1
Pseudotsuga macrocarpa	AF041354.1	EU866024.1		
Pseudotsuga menziesii	AF041353.1	JX560085.1	AF143439.1	X52937.1
Retrophyllum comptonii		JX560066.1	HM593785.1	HM593681.1
Retrophyllum minus		JX560067.1	KF713811.1	AF249661.1
Retrophyllum rospigliosii	JF969612.1		HM593786.1	HM593682.1
Saxegothaea conspicua		JX560068.1	AF457116.1	HM593684.1
Sciadopitys verticillata	AB023993.1	JX559887.1	AB023994.1	AB645804.1
Sequoia sempervirens	HQ414215.1	JX559961.1	AB030123.1	L25755.2
Sequoiadendron giganteum	AF387520.1	JX559962.1	AB030124.1	JQ512604.1
Sundacarpus amarus		JX560069.1	HM593788.1	AF249663.1
Taiwania cryptomerioides	AY916973.1	KJ195155.1	AB030127.1	L25756.2
Taxodium distichum	AF387531.1	JX559964.1	AF152212.1	AF119185.1
Taxodium mucronatum	JF829707.1	JX559965.1	AB030119.1	JF725913.1
Taxus baccata	AF259294.1	JX559898.1	AB023996.1	AF456388.1
Taxus brevifolia	AF259295.1	JX559899.1	EU078561.1	AF249666.1
Taxus canadensis	AF259298.1	JX560092.1	EF660661.1	EF660724.1
Taxus cuspidata	HM590971.1	JX559901.1	HM591011.1	DQ478793.1
Taxus sumatrana	HM590968.1	JX559905.1	EF660646.1	EF660706.1
Tetraclinis articulata	AY380876.1	JX559966.1	HM024068.1	L12576.2
Thuja koraiensis	EU183427.1		HM024069.1	JQ512617.1
Thuja occidentalis	EU183434.1	JX559967.1	HM024070.1	JQ512620.1
Thuja plicata	HQ414209.1	JX559968.1	HM024071.1	AY237154.1
Thuja standishii	EU183441.1	JX559969.1	HM024072.1	HM024350.1
Thujopsis dolabrata	AY380853.1	JX559971.1	HM024073.1	JQ512621.1
Torreya californica	AB023997.1	JX559907.1	AB023998.1	AY664858.1
Torreya grandis	EF660590.1	JX559908.1		DQ478794.1
Torreya nucifera	EF660595.1	AJ286666.1	AB030137.1	JQ512624.1
Torreya taxifolia	EF660587.1	JX559911.1	AF457110.1	AF456389.1
Tsuga canadensis	EF395467.1	JX560086.1	AF143438.1	AY056581.1
Tsuga caroliniana	EF395474.1	JX560087.1		
Tsuga chinensis	DQ975358.1	JX560088.1		AF145462.1
Tsuga diversifolia	EF395497.1	JX560089.1		
Tsuga dumosa	EF395514.1			AF145460.1
Tsuga heterophylla	EF395533.1	JX560090.1		X63659.1
Tsuga mertensiana	EF395538.1		AF143434.1	AF145463.1
Widdringtonia nodiflora	AY178419.1	JX559973.1	HQ245917.1	JF725930.1
Wollemia nobilis	EU165015.1	JX560000.1	AF456377.1	AF030419.1
Zamia furfuracea		JN656065.1	JQ770303.1	JQ770263.1

Table S2.

		Calibration sets	20 MA interval		40 MA interval		"Deep nodes"	
Node	Calibrated divergence	min age	max age	Inferred	max age	Inferred	Inferred ages	References
A	Cycads - Conifers	275	350*	**336,1**	350	**335,9**	348,6	Leslie et al. 2012
B	*Araucariaceae - Podocarpaceae*	176	230*	177,9	230	198,8	208	Leslie et al. 2012
C	*Taxaceae - Cupressaceae*	197	217	205,7	237	236,9	197,9	Leslie et al. 2012
D	*Pinus - Cedrus*	199	219	204,2	239	228,1	230,2	Mao et al. 2012
E	*Araucaria* - (*Agathis, Wollemia*)	165	185	171	205	178,7	138,7	Leslie et al. 2012
F	*Dacrycarpus - Dacrydium*	51,9	71,9	60,1	91,9	61,2	26	Leslie et al. 2012
G	*Phyllocladus - Lepidothamnus*	48	68	**64,6**	88	**52,2**	69,3	Leslie et al. 2012
H	*Podocarpus - Retrophyllum*	28	60*	53,5	60	56,9	27,7	Leslie et al. 2012
I	*Metasequoia - Sequoia*	55	75	58,8	95	72,8	24,4	Leslie et al. 2012
J	*Taxodium - Glyptostrobus*	65	85	80,5	105	101	7,3	Leslie et al. 2012
K	*Papuacedrus* - (other *Callitroidae*)	51,9	71,9	64,7	91,9	72,9	11	Leslie et al. 2012
L	*Thuja - Thujopsis*	58	78	68,3	98	78,8	7,3	Leslie et al. 2012
M	*Tetraclinis - Platycladus*	28	48	36,1	68	40,8	3,9	Leslie et al. 2012
N	*Juniperus - Cupressus*	33	53	**49,8**	73	**45,6**	5,9	Leslie et al. 2012
O	*Larix - Pseudotsuga*	41	61	52,5	81	66,7	115,1	Leslie et al. 2012
P	*Tsuga - Nothotsuga*	41	90*	56,8	90	88,6	38,4	Leslie et al. 2012
Q	*Pinus - Picea*	118,5	138,5	120,8	158,5	153,3	115,1	Mao et al. 2012

Table S3.

		RAxML tree - 40 MA calibrations				
Speciation	Extinction	Df	Log Likelihood	AIC	X^2 test	p
constant	constant	4	-1633.3	3274.6	-	-
linear	constant	5	-1626.1	3262.2	14.426	**0.0001458**
		RAxML tree - 20 MA calibrations				
		Df	Log Likelihood	AIC	X^2 test	p
constant	constant	4	-1818.5	3645.1		
linear	constant	5	-1810.1	3630.2	16.855	**4.034e-05**
		MrBayes tree - 40 MA calibrations				
		Df	Log Likelihood	AIC	X^2 test	p
constant	constant	4	-1878.5	3765.0		
linear	constant	5	-1870.1	3750.2	16.761	**4.239e-05**

Table S4.

With Drift

Sp.	Ex.	Df	Log-Lik.	AIC	X² test	p	Speciation parameters: Sig. inflection point	Slope (Sig., Lin.)	λ0	λ1	Extinction parameters: Slope (Sig., Lin.)	λ0	λ1	drift	diffusion
Cst.	Cst.	4	-1633.3	3274.6	-	-	-	-	0.069110031	-	-	0.053894277	-	-0.001651303	0.134197475
Lin.	Cst.	5	-1626.1	3262.2	14.426	**0.0001458**	-	0.006597219	0.042157740	-	-	0.029637553	-	0.122451424	0.122889633
Sig.	Cst.	7	-1629.4	3272.8	7.785	***0.0506678***	11.64	3.09758582	0.11083970	0.37371592	-	0.10118003	-	0.08169537	0.12475447
Cst.	Lin.	5	-1633.2	3276.5	0.163	0.6860005	-	-	0.10761058	-	0.01202135	0.07559986	-	0.15197416	0.21111783
Lin.	Lin.	6	-1625.4	3262.8	15.773	**0.0003758**	-	0.008733485	0.073258025	-	0.020740558	0.031983269	-	0.142668060	0.219963279
Sig.	Lin.	8	-1628.0	3272.0	10.638	**0.0309492**	10.85	3.30823872	0.10427240	0.25024867	0.01566547	0.06768928	-	0.15739591	0.20199261

Bg.	Fg.							Bg. speciation		Bg. extinction	Bg. drift	Bg. diffusion	Fg. speciation		Fg. extinction	Fg. drift	Fg. diffusion
Cst.	Cst.	Cst.	8	-1546.2	3108.4	174.261	< **2.2e-16**	0.091	-	0.078540908	0.041317210	0.006173748	0.076592322		0.062984433	0.042508667	0.275660689
Lin.	Cst.	Cst.	9	-1547.9	3113.8	170.846	< **2.2e-17**	0.10	-0.006051724	0.068852404	0.007551018	0.005529328	0.052451547		0.033786277	0.014203964	0.259477048
Cst.	Lin.	Cst.	9	-1531.2	3080.4	204.228	< **2.2e-18**	0.081		0.0691856921	-0.0080698315	0.0059499050	0.0006196373	0.0084972803	0.0186814044	-0.0460775255	0.2318147512
Lin.	Lin.	Cst.	10	-1535.2	3090.5	196.119	< **2.2e-19**	0.080	0.000396673	0.068873192	0.005480166	0.005546520	0.006538050	0.007018859	0.008647325	-0.013051863	0.218535153

Without Drift

Sp.	Ex.	Df	Log-Lik.	AIC	X² test	p	Speciation parameters: Sig. inflection point	Slope (Sig., Lin.)	λ0	λ1	Extinction parameters: Slope (Sig., Lin.)	λ0	λ1	diffusion
Cst.	Cst.	3	-1634.3	3274.6			-	-	0.07343851		-	0.05842523	-	0.12027987
Lin.	Cst.	4	-1631.7	3271.3	5.30	**0.0213245**	-	0.002358631	0.047895923		-	0.037893510	-	0.149207414
Sig.	Cst.	6	-1626.8	3265.6	15.01	**0.0018080**	11.67	3.08480490	0.08473772	0.37700102	-	0.07112815	-	0.13900912
Cst.	Lin.	4	-1634.0	3276.0	0.63	0.4267741	-	-	0.084439272		-0.001791103	0.077217642	-	0.127558622
Lin.	Lin.	5	-1627.5	3265.0	13.64	**0.0010927**	-	-	0.064431217	0.007457949	0.006480985	0.056805429	-	0.129521263
Sig.	Lin.	7	-1815.5	3644.9	-	-	10.76	0.44174003	0.01750238	0.12321196	-0.08115655	0.10629343	-	0.13333927

Bg.	Fg.	-						Bg. speciation		Bg. extinction	Bg. diffusion	Fg. speciation		Fg. extinction	Fg. diffusion
Cst.	Cst.	Cst.	5	-1634.0	3278.0	0.63	0.7288041	0.086	-	0.074858392	0.005635311	0.061111167	-	0.045365849	0.268833311
Lin.	Cst.	Cst.	6	-1631.2	3274.3	6.30	0.0977373	0.114	-0.011557214	0.052148307	0.005790138	0.061311554	-	0.045676811	0.245484945
Cst.	Lin.	Cst.	6	-1621.6	3255.2	25.40	**1.273e-05**	0.076	-	0.063818136	0.005319075	0.047820066	0.003502000	0.043761733	0.243547002
Lin.	Lin.	Cst.	7	-1623.5	3261.1	21.54	**0.0002475**	0.087	-0.001972713	0.066805491	0.005696456	0.059305666	0.002303610	0.053330532	0.212346711

Supplementary Figures:

Figure S1: Maximum likelihood phylogeny from the RAxML analysis. Node support is frequency of bi-partitions over 1000 bootstrap replicate searches. Time-tree using the 40 MA calibration set, with numbers A to Q as in Suppl. Table S2.

Figure S2: Bayesian maximum clade credibility phylogeny from the MrBayes analysis. Node support is indicated as posterior support. Time-tree using the 40 MA calibration set, with numbers A to Q as in Suppl. Table S2.

Figure S3: Overlay of different calibrations schemes for the A) MrBayes and B) RAxML phylogenies. The 40 MA calibrations are in red, the 20 MA calibrations in blue. The "deep node" analysis in black (B only). Overall, the 20 MA calibrations are slightly younger throughout the tree.

Figure S4: BAMM rate through time plots for the diversification analysis, separately coloured by family. Shading represents confidence intervals. A. Net diversification rates. B. Speciation rates. C. Extinction rates. As described in main text, this analysis reveals the uptick in turn-over in Pinaceae around 150 Mya.

Figure S5: Prior and posterior distributions of the number of shifts in the post-burn-in. A, B: RAxML phylogeny with 40 MA calibrations. C, D: RAxML phylogeny with 20 MA calibrations. E, F: MrBayes phylogeny with 40 MA calibrations. Left column: Diversification analyses; right: Trait evolution analyses.

Figure S6: Credible shift sets from the BAMM diversification analyses (top four configurations). From top to bottom, for the RAxML phylogeny (40 and 20 MA calibrations) and the MrBayes phylogeny (40 MA calibrations).

Figure S7: Credible shift sets from the BAMM trait evolution analyses (top four configurations). From top to bottom, for the RAxML phylogeny (40 and 20 MA calibrations) and the MrBayes phylogeny (40 MA calibrations).

Figure S8: Boxplots of QUASSE analysis for 100 simulated "neutral" traits. A. Chi-square statistic of the likelihood ratio tests. Red line indicates significance at α=5% (i.e. $X^2 > 3.841$). Red dotted line shows statistic for the analysis with the P_{50} dataset. B. Difference in AIC scores between linear trait-dependent speciation models and neutral models. Red dotted line shows difference in AIC scores for the analysis with the P_{50} dataset (12.4).

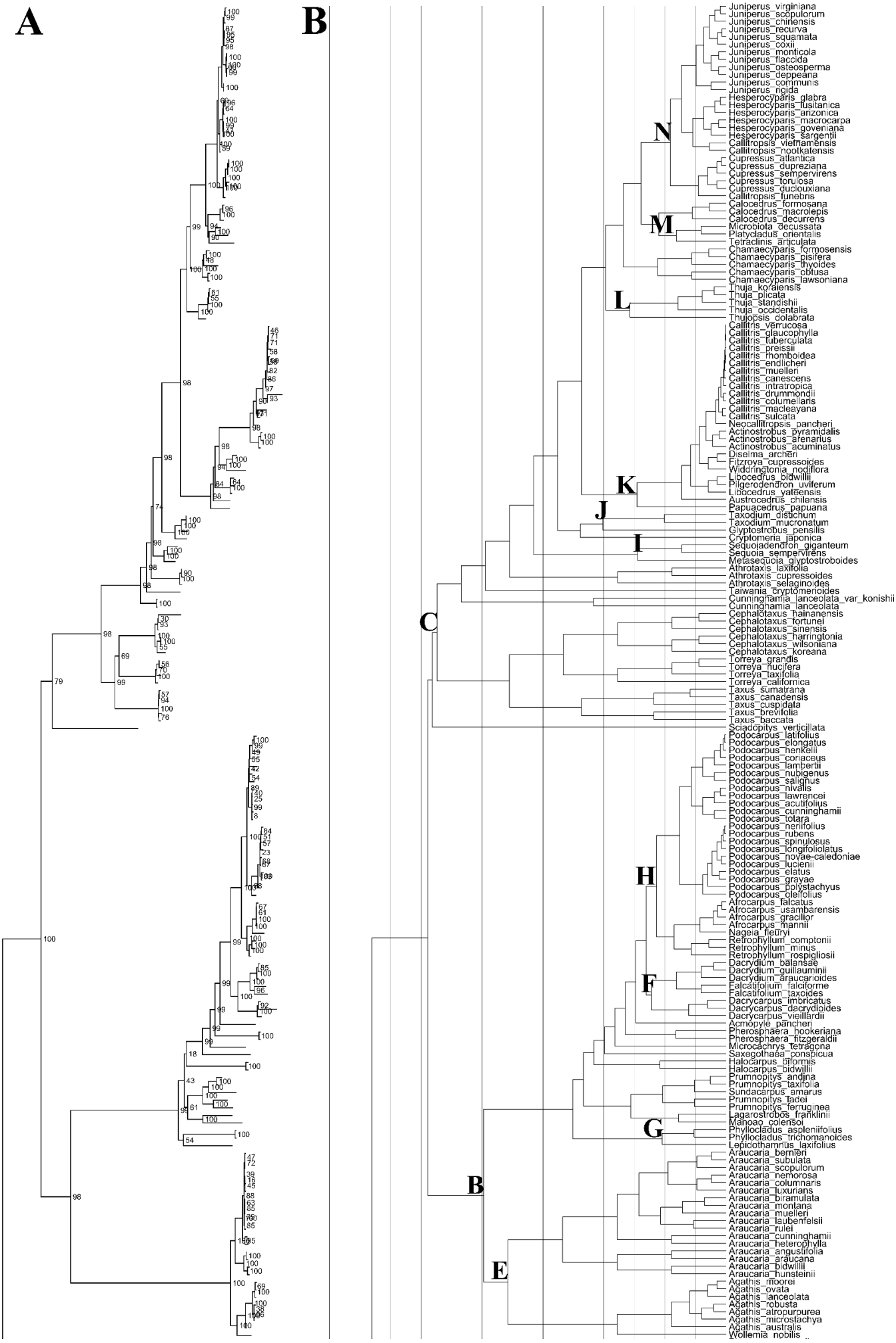
A
B
Juniperus_virginiana
Juniperus_scopulorum
Juniperus_chinensis
Juniperus_recurva
Juniperus_squamata
Juniperus_coxii
Juniperus_monticola
Juniperus_flaccida
Juniperus_osteosperma
Juniperus_deppeana
Juniperus_communis
Juniperus_rigida
Hesperocyparis_glabra
Hesperocyparis_lusitanica
Hesperocyparis_arizonica
Hesperocyparis_macrocarpa
Hesperocyparis_goveniana
Hesperocyparis_sargentii
Callitropsis_vietnamensis
Callitropsis_nootkatensis
Cupressus_atlantica
Cupressus_dupreziana
Cupressus_sempervirens
Cupressus_torulosa
Cupressus_duclouxiana
Callitropsis_funebris
Calocedrus_formosana
Calocedrus_macrolepis
Calocedrus_decurrens
Microbiota_decussata
Platycladus_orientalis
Tetraclinis_articulata
Chamaecyparis_formosensis
Chamaecyparis_pisifera
Chamaecyparis_thyoides
Chamaecyparis_obtusa
Chamaecyparis_lawsoniana
Thuja_koraiensis
Thuja_plicata
Thuja_standishii
Thuja_occidentalis
Thujopsis_dolabrata
Callitris_verrucosa
Callitris_glaucophylla
Callitris_tuberculata
Callitris_preissii
Callitris_rhomboidea
Callitris_endlicheri
Callitris_muelleri
Callitris_canescens
Callitris_intratropica
Callitris_drummondii
Callitris_columellaris
Callitris_macleayana
Callitris_sulcata
Neocallitropsis_pancheri
Actinostrobus_pyramidalis
Actinostrobus_arenarius
Actinostrobus_acuminatus
Diselma_archeri
Fitzroya_cupressoides
Widdringtonia_nodiflora
Libocedrus_bidwillii
Pilgerodendron_uviferum
Libocedrus_yateensis
Austrocedrus_chilensis
Papuacedrus_papuana
Taxodium_distichum
Taxodium_mucronatum
Glyptostrobus_pensilis
Cryptomeria_japonica
Sequoiadendron_giganteum
Sequoia_sempervirens
Metasequoia_glyptostroboides
Athrotaxis_laxifolia
Athrotaxis_cupressoides
Athrotaxis_selaginoides
Taiwania_cryptomerioides
Cunninghamia_lanceolata_var_konishii
Cunninghamia_lanceolata
Cephalotaxus_hainanensis
Cephalotaxus_fortunei
Cephalotaxus_sinensis
Cephalotaxus_harringtonia
Cephalotaxus_wilsoniana
Cephalotaxus_koreana
Torreya_grandis
Torreya_nucifera
Torreya_taxifolia
Torreya_californica
Taxus_sumatrana
Taxus_canadensis
Taxus_cuspidata
Taxus_brevifolia
Taxus_baccata
Sciadopitys_verticillata
Podocarpus_latifolius
Podocarpus_elongatus
Podocarpus_henkelii
Podocarpus_coriaceus
Podocarpus_lambertii
Podocarpus_nubigenus
Podocarpus_salignus
Podocarpus_nivalis
Podocarpus_lawrencei
Podocarpus_acutifolius
Podocarpus_cunninghamii
Podocarpus_totara
Podocarpus_neriifolius
Podocarpus_rubens
Podocarpus_spinulosus
Podocarpus_longifoliolatus
Podocarpus_novae-caledoniae
Podocarpus_lucienii
Podocarpus_elatus
Podocarpus_grayae
Podocarpus_polystachyus
Podocarpus_oleifolius
Afrocarpus_falcatus
Afrocarpus_usambarensis
Afrocarpus_gracilior
Afrocarpus_mannii
Nageia_fleuryi
Retrophyllum_comptonii
Retrophyllum_minus
Retrophyllum_rospigliosii
Dacrydium_balansae
Dacrydium_guillauminii
Dacrydium_araucarioides
Falcatifolium_falciforme
Falcatifolium_taxoides
Dacrycarpus_imbricatus
Dacrycarpus_dacrydioides
Dacrycarpus_vieillardii
Acmopyle_pancheri
Pherosphaera_hookeriana
Pherosphaera_fitzgeraldii
Microcachrys_tetragona
Saxegothaea_conspicua
Halocarpus_biformis
Halocarpus_bidwillii
Prumnopitys_andina
Prumnopitys_taxifolia
Sundacarpus_amarus
Prumnopitys_ladei
Prumnopitys_ferruginea
Lagarostrobos_franklinii
Manoao_colensoi
Phyllocladus_aspleniifolius
Phyllocladus_trichomanoides
Lepidothamnus_laxifolius
Araucaria_bernieri
Araucaria_subulata
Araucaria_scopulorum
Araucaria_nemorosa
Araucaria_columnaris
Araucaria_luxurians
Araucaria_biramulata
Araucaria_montana
Araucaria_muelleri
Araucaria_laubenfelsii
Araucaria_rulei
Araucaria_cunninghamii
Araucaria_heterophylla
Araucaria_angustifolia
Araucaria_araucana
Araucaria_bidwillii
Araucaria_hunsteinii
Agathis_moorei
Agathis_ovata
Agathis_lanceolata
Agathis_robusta
Agathis_atropurpurea
Agathis_microstachya
Agathis_australis
Wollemia_nobilis
N
M
L
K
J
I
C
H
F
G
B
E

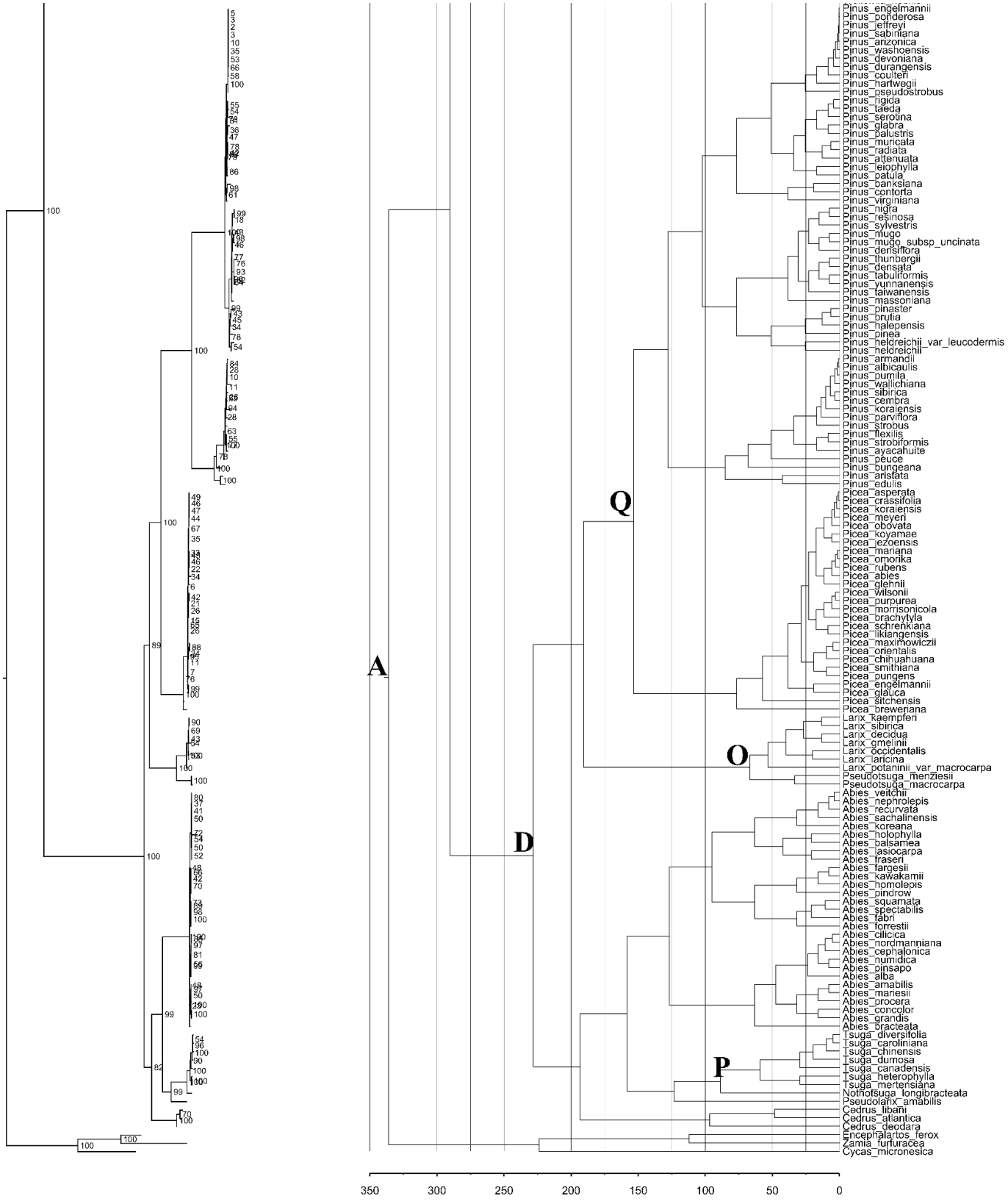

Figure S1: Maximum likelihood phylogeny from the RAxML analysis. Node support is frequency of bi-partitions over 1000 bootstrap replicate searches. Time-tree using the 40 MA calibration set, with numbers A to Q as in Suppl. Table S2.

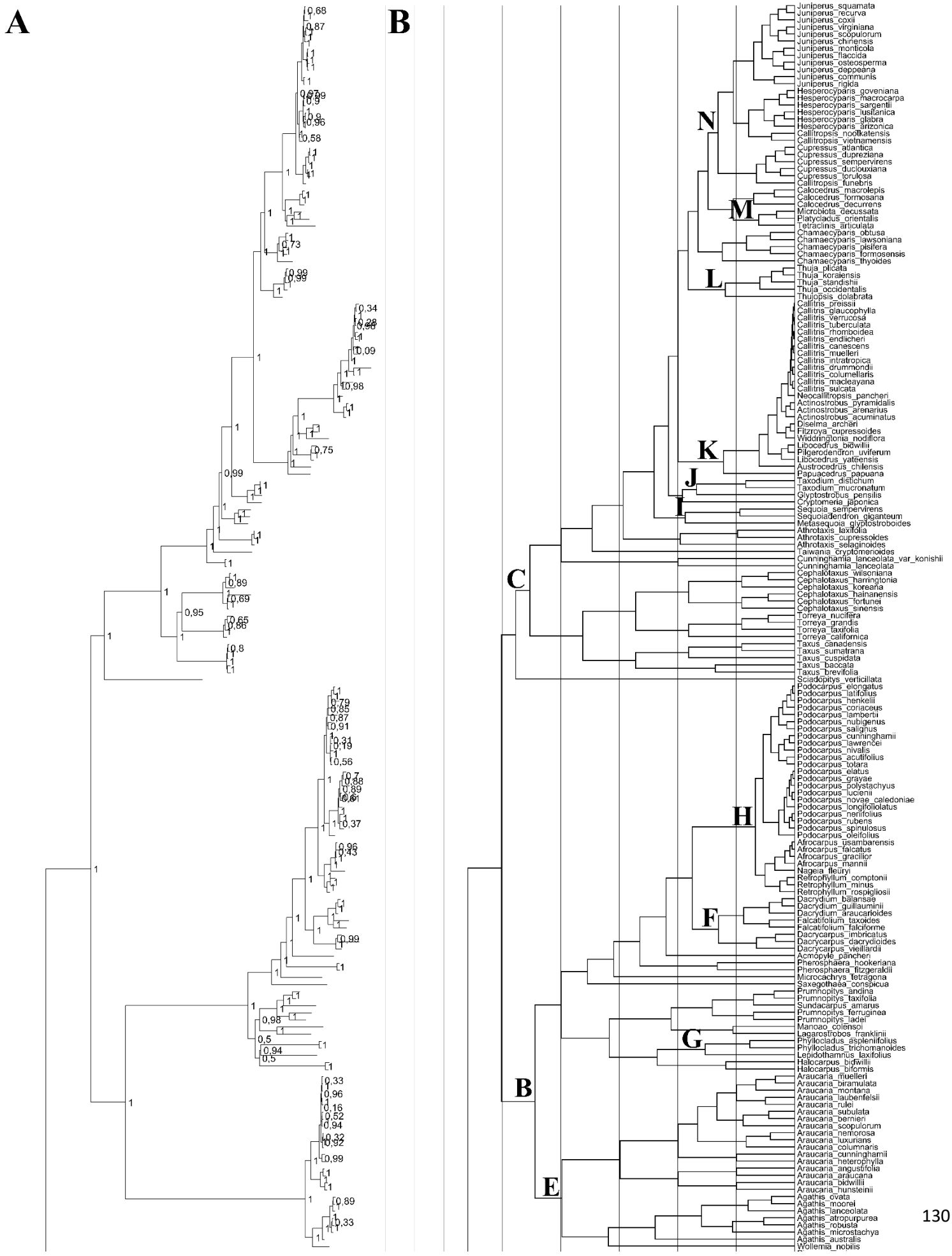
A
B
Juniperus_squamata
Juniperus_recurva
Juniperus_coxii
Juniperus_virginiana
Juniperus_scopulorum
Juniperus_chinensis
Juniperus_monticola
Juniperus_flaccida
Juniperus_osteosperma
Juniperus_deppeana
Juniperus_communis
Juniperus_rigida
Hesperocyparis_goveniana
Hesperocyparis_macrocarpa
Hesperocyparis_sargentii
Hesperocyparis_lusitanica
Hesperocyparis_glabra
Hesperocyparis_arizonica
Callitropsis_nootkatensis
Callitropsis_vietnamensis
Cupressus_atlantica
Cupressus_dupreziana
Cupressus_sempervirens
Cupressus_duclouxiana
Cupressus_torulosa
Callitropsis_funebris
Calocedrus_macrolepis
Calocedrus_formosana
Calocedrus_decurrens
Microbiota_decussata
Platycladus_orientalis
Tetraclinis_articulata
Chamaecyparis_obtusa
Chamaecyparis_lawsoniana
Chamaecyparis_pisifera
Chamaecyparis_formosensis
Chamaecyparis_thyoides
Thuja_plicata
Thuja_koraiensis
Thuja_standishii
Thuja_occidentalis
Thujopsis_dolabrata
Callitris_preissii
Callitris_glaucophylla
Callitris_verrucosa
Callitris_tuberculata
Callitris_rhomboidea
Callitris_endlicheri
Callitris_canescens
Callitris_muelleri
Callitris_intratropica
Callitris_drummondii
Callitris_columellaris
Callitris_macleayana
Callitris_sulcata
Neocallitropsis_pancheri
Actinostrobus_pyramidalis
Actinostrobus_arenarius
Actinostrobus_acuminatus
Diselma_archeri
Fitzroya_cupressoides
Widdringtonia_nodiflora
Libocedrus_bidwillii
Pilgerodendron_uviferum
Libocedrus_yateensis
Austrocedrus_chilensis
Papuacedrus_papuana
Taxodium_distichum
Taxodium_mucronatum
Glyptostrobus_pensilis
Cryptomeria_japonica
Sequoia_sempervirens
Sequoiadendron_giganteum
Metasequoia_glyptostroboides
Athrotaxis_laxifolia
Athrotaxis_cupressoides
Athrotaxis_selaginoides
Taiwania_cryptomerioides
Cunninghamia_lanceolata_var_konishii
Cunninghamia_lanceolata
Cephalotaxus_wilsoniana
Cephalotaxus_harringtonia
Cephalotaxus_koreana
Cephalotaxus_hainanensis
Cephalotaxus_fortunei
Cephalotaxus_sinensis
Torreya_nucifera
Torreya_grandis
Torreya_taxifolia
Torreya_californica
Taxus_canadensis
Taxus_sumatrana
Taxus_cuspidata
Taxus_baccata
Taxus_brevifolia
Sciadopitys_verticillata
Podocarpus_elongatus
Podocarpus_latifolius
Podocarpus_henkelii
Podocarpus_coriaceus
Podocarpus_lamberti
Podocarpus_nubigenus
Podocarpus_salignus
Podocarpus_cunninghamii
Podocarpus_lawrencei
Podocarpus_nivalis
Podocarpus_acutifolius
Podocarpus_totara
Podocarpus_elatus
Podocarpus_grayae
Podocarpus_polystachyus
Podocarpus_lucienii
Podocarpus_novae_caledoniae
Podocarpus_longifoliolatus
Podocarpus_nerifolius
Podocarpus_rubens
Podocarpus_spinulosus
Podocarpus_oleifolius
Afrocarpus_usambarensis
Afrocarpus_falcatus
Afrocarpus_gracilior
Afrocarpus_mannii
Nageia_fleuryi
Retrophyllum_comptonii
Retrophyllum_minus
Retrophyllum_rospigliosii
Dacrydium_balansae
Dacrydium_guillauminii
Dacrydium_araucarioides
Falcatifolium_taxoides
Falcatifolium_falciforme
Dacrycarpus_imbricatus
Dacrycarpus_dacrydioides
Dacrycarpus_vieillardii
Acmopyle_pancheri
Pherosphaera_hookeriana
Pherosphaera_fitzgeraldii
Microcachrys_tetragona
Saxegothaea_conspicua
Prumnopitys_andina
Prumnopitys_taxifolia
Sundacarpus_amarus
Prumnopitys_ferruginea
Prumnopitys_ladei
Manoao_colensoi
Lagarostrobos_franklinii
Phyllocladus_aspleniifolius
Phyllocladus_trichomanoides
Lepidothamnus_laxifolius
Halocarpus_bidwillii
Halocarpus_biformis
Araucaria_muelleri
Araucaria_biramulata
Araucaria_montana
Araucaria_laubenfelsii
Araucaria_rulei
Araucaria_subulata
Araucaria_bernieri
Araucaria_scopulorum
Araucaria_nemorosa
Araucaria_luxurians
Araucaria_columnaris
Araucaria_cunninghamii
Araucaria_heterophylla
Araucaria_angustifolia
Araucaria_araucana
Araucaria_bidwillii
Araucaria_hunsteinii
Agathis_ovata
Agathis_moorei
Agathis_lanceolata
Agathis_atropurpurea
Agathis_robusta
Agathis_microstachya
Agathis_australis
Wollemia_nobilis
N
M
L
K
J
I
C
H
F
G
B
E

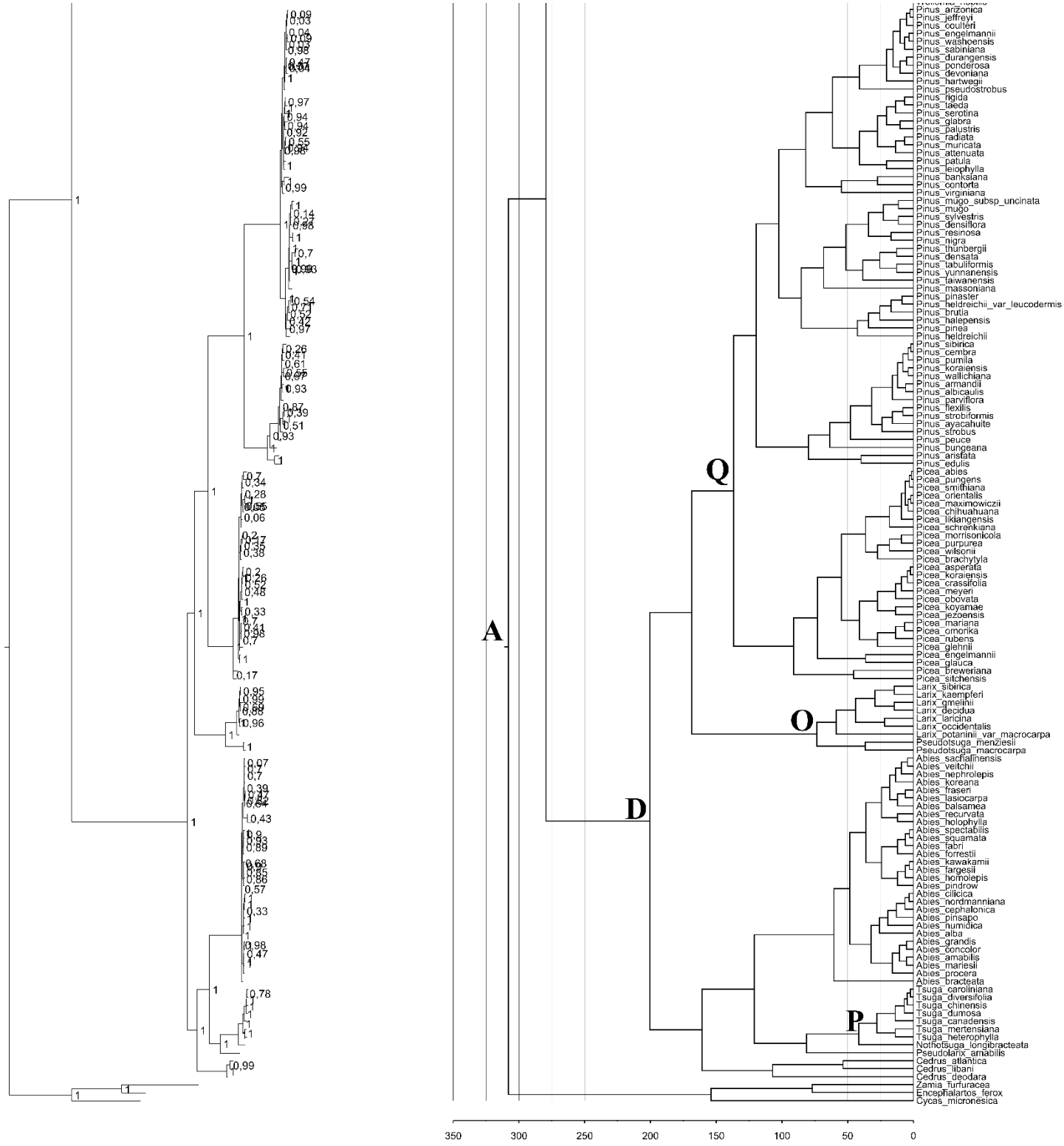

Figure S2: Bayesian maximum clade credibility phylogeny from the MrBayes analysis. Node support is indicated as posterior support. Time-tree using the 40 MA calibration set, with numbers A to Q as in Suppl. Table S2.

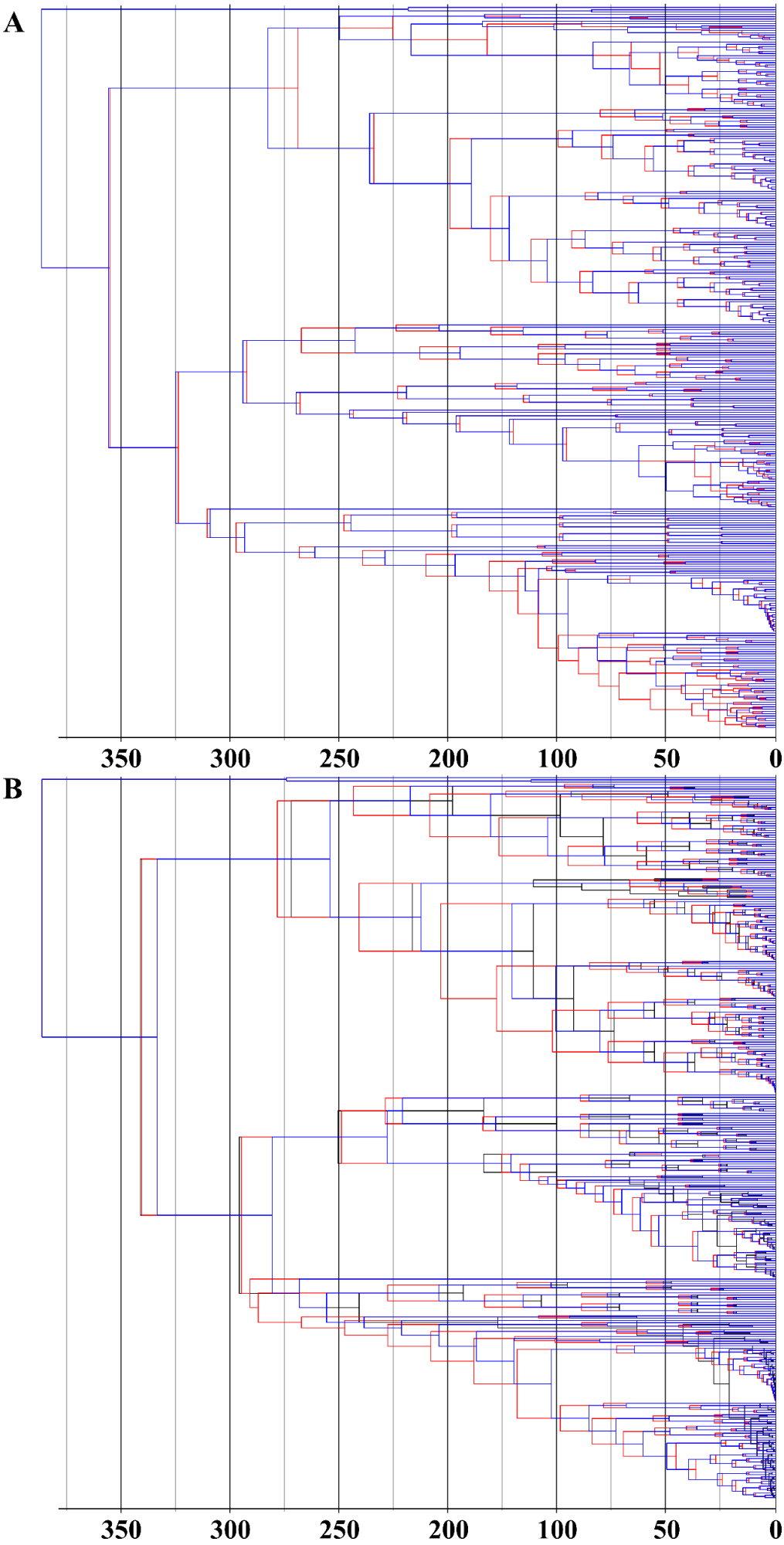

Figure S3. Overlay of different calibrations schemes for the A) MrBayes and B) RAxML phylogenies. The 40 MA calibrations are in red, the 20 MA calibrations in blue. The "deep node" analysis in black (B only). Overall, the 20 MA calibrations are slightly younger throughout the tree.

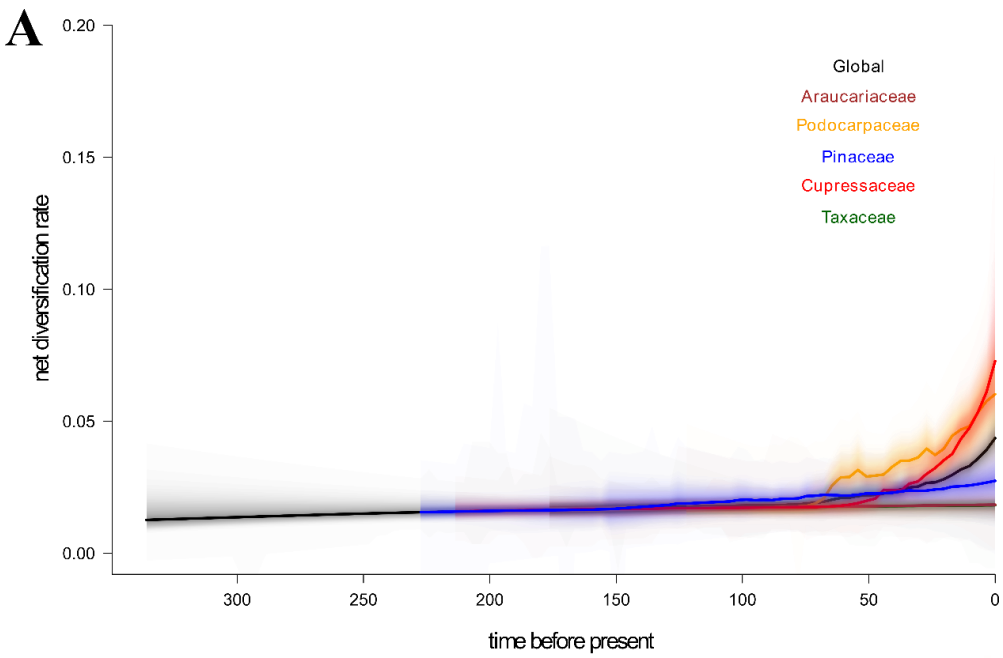

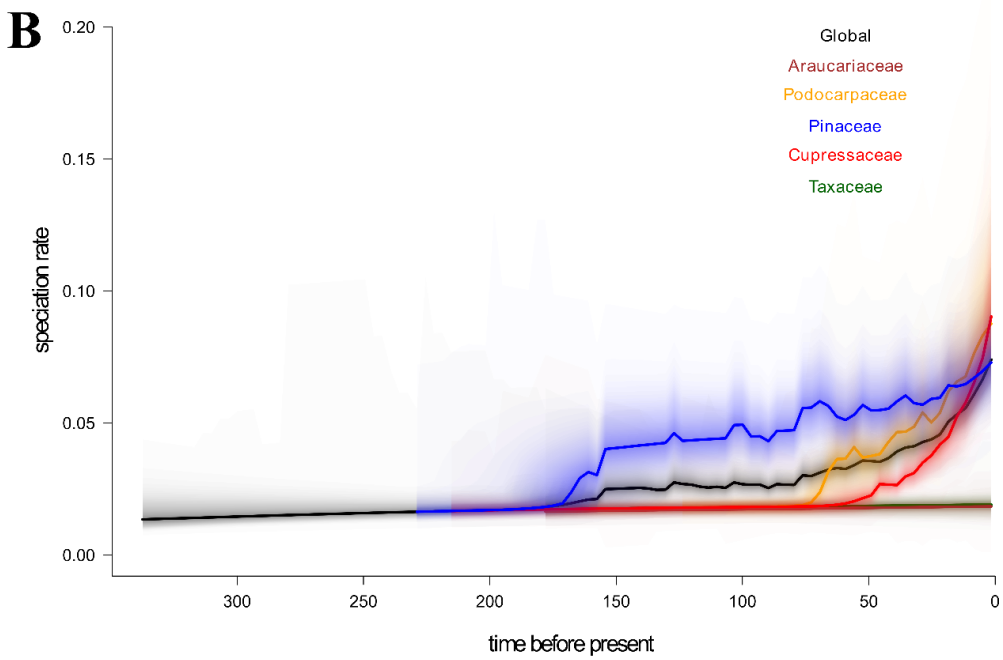

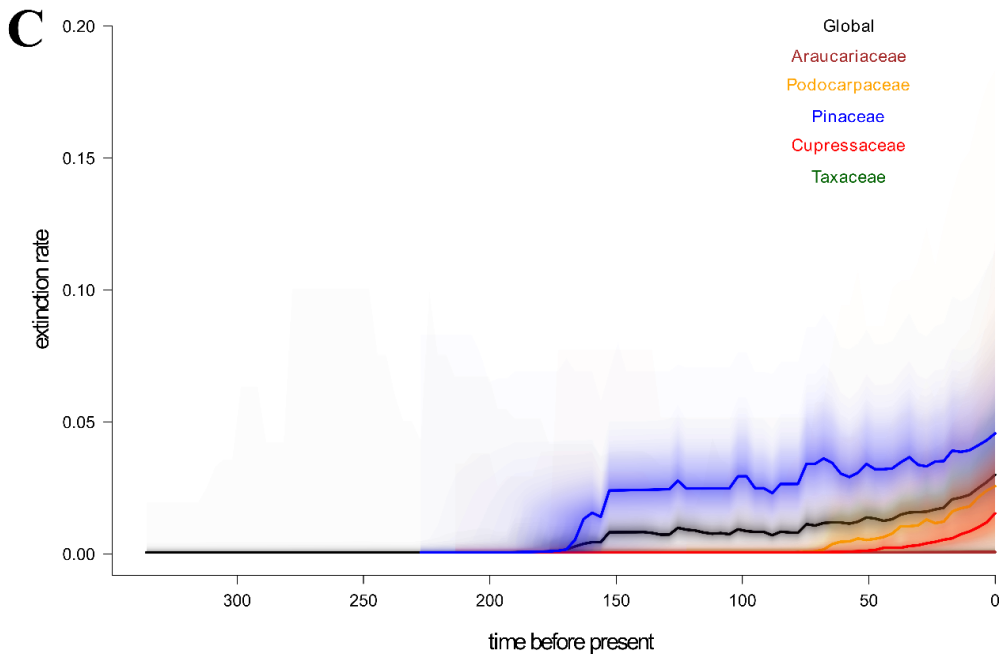

Figure S4: BAMM rate through time plots for the diversification analysis, separately coloured by family. Shading represents confidence intervals. A. Net diversification rates. B. Speciation rates. C. Extinction rates. As described in main text, this analysis reveals the uptick in turn-over in Pinaceae around 150 Mya.

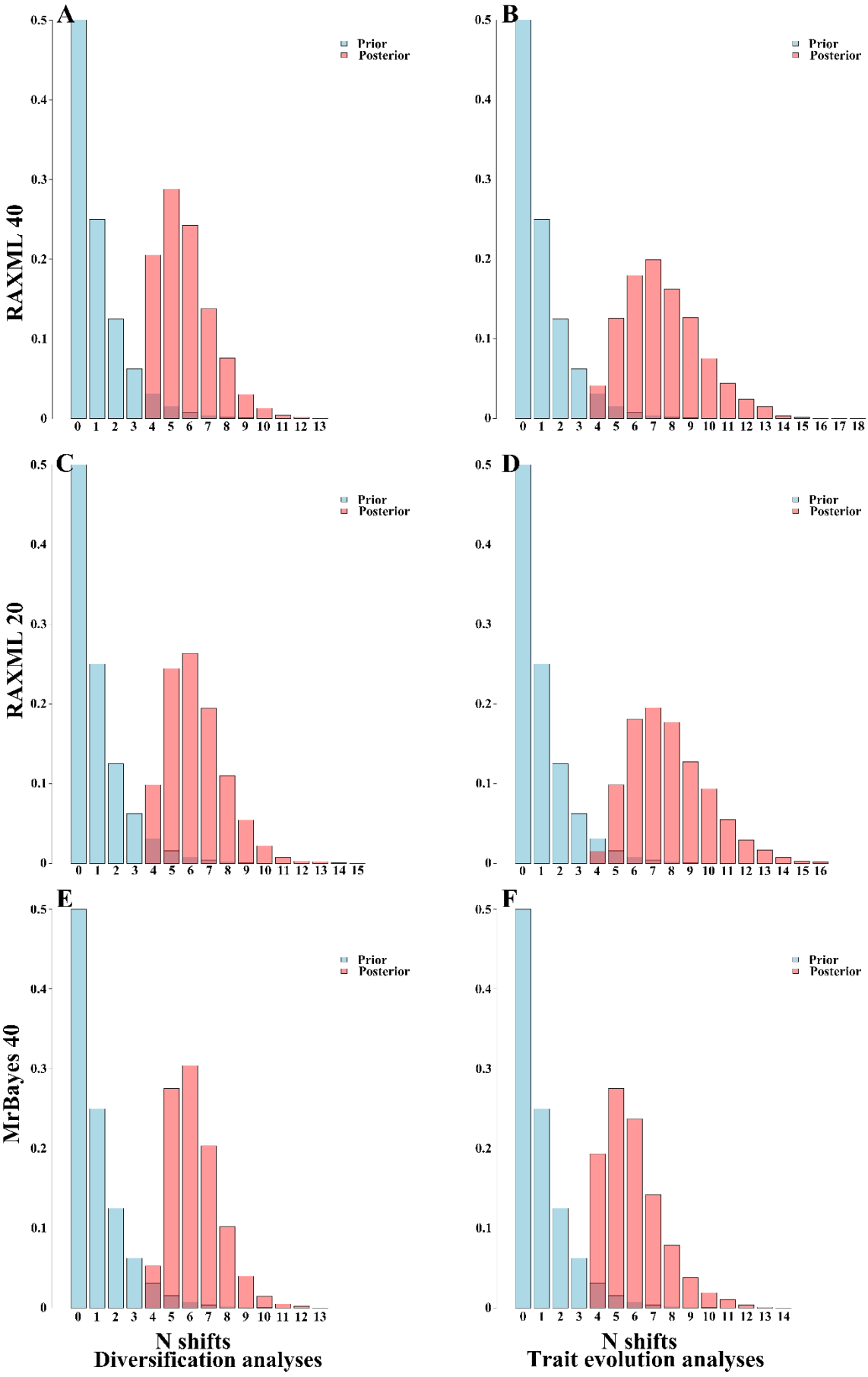

Figure S5: Prior and posterior distributions of the number of shifts in the post-burn-in. A, B: RAxML phylogeny with 40 MA calibrations. C, D: RAxML phylogeny with 20 MA calibrations. E, F: MrBayes phylogeny with 40 MA calibrations. Left column: Diversification analyses; right: Trait evolution analyses.

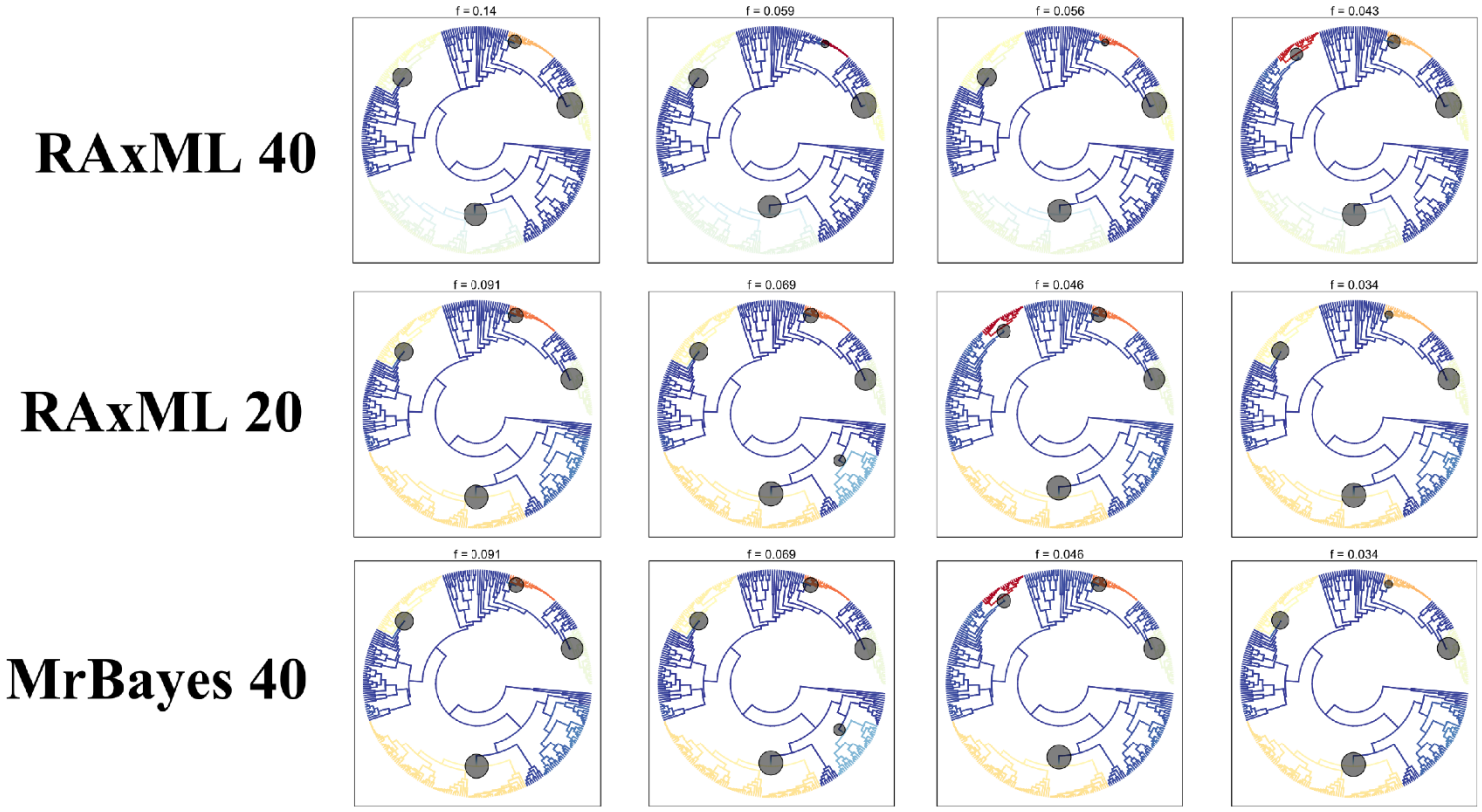

Figure S6: Credible shift sets from the BAMM diversification analyses (top four configurations). From top to bottom, for the RAxML phylogeny (40 and 20 MA calibrations) and the MrBayes phylogeny (40 MA calibrations).

t

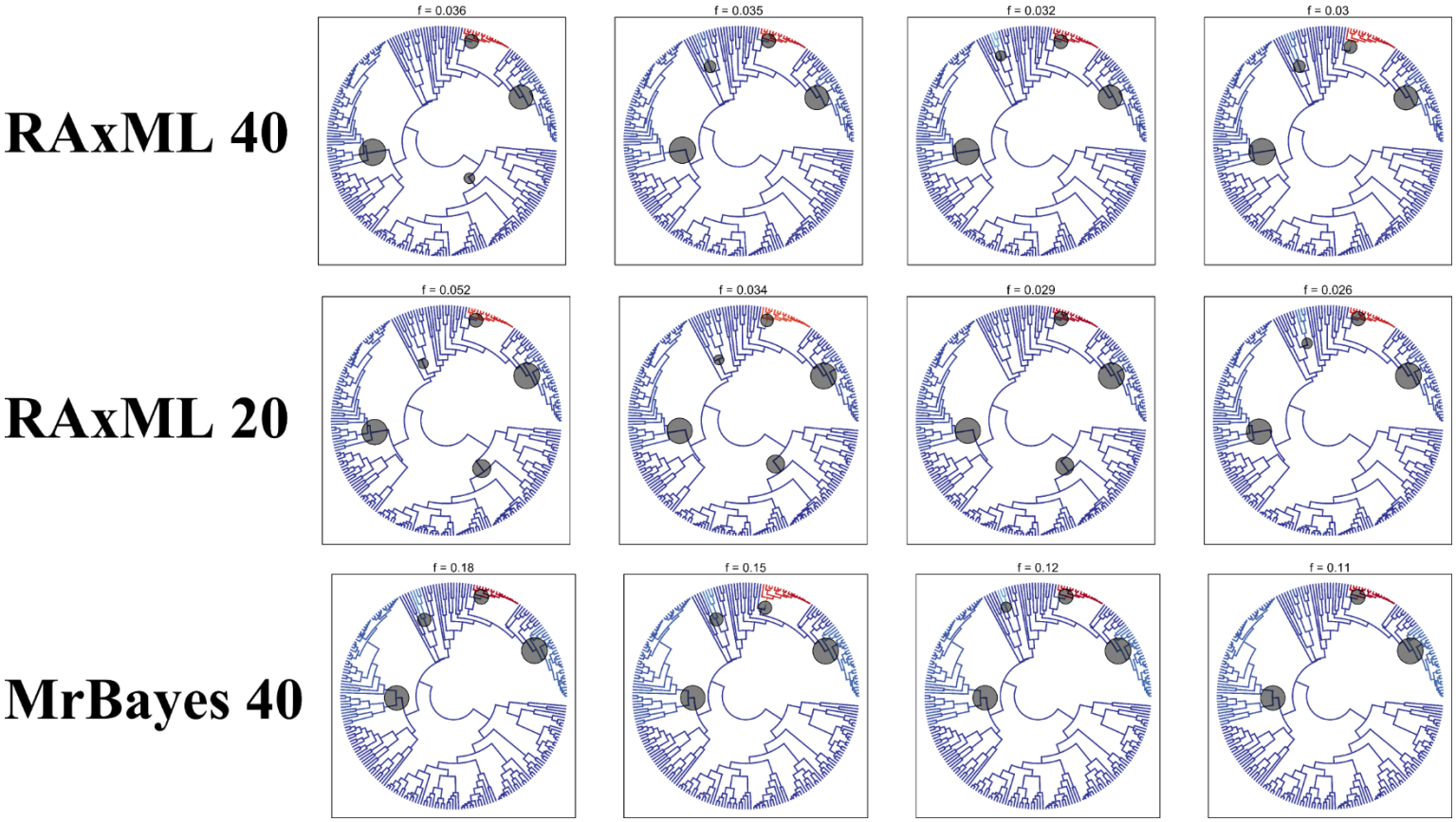

Figure S7: Credible shift sets from the BAMM trait evolution analyses (top four configurations). From top to bottom, for the RAxML phylogeny (40 and 20 MA calibrations) and the MrBayes phylogeny (40 MA calibrations).

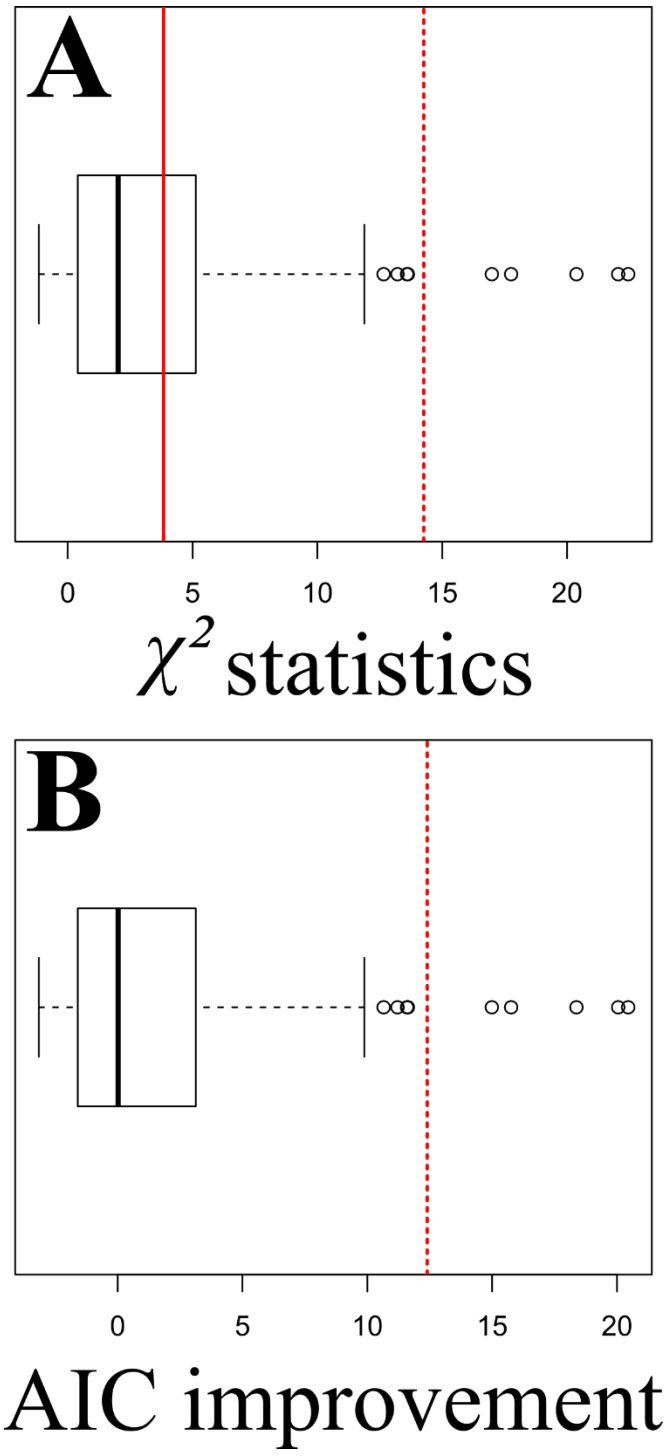

Figure S8: Boxplots of the QUASSE analysis for 100 simulated "neutral" traits. **A**. Chi-square statistic of the likelihood ratio tests. Red line indicates significance at α=5% (i.e. $X^2 > 3.841$). Red dotted line shows statistic for the analysis with the P_{50} dataset. **B**. Difference in AIC scores between linear trait-dependent speciation models and neutral models. Red dotted line shows difference in AIC scores for the analysis with the P_{50} dataset (12.4)

Part III: The Adaptive radiation of Callitris: linking hydraulics, xylem anatomy and climate across the driest continent on Earth

Chapter 5: Evolutionary ecophysiology of the adaptive radiation of *Callitris*, the most drought tolerant genus of trees. Maximilian Larter, Sylvain Delzon et al. (*In preparation)*

Evolutionary ecophysiology of the adaptive radiation of *Callitris*, the most drought tolerant genus of trees

Maximilian Larter[1], Sylvain Delzon[1] et al. (*In preparation)*

[1]BIOGECO, INRA, Univ. Bordeaux, 33610 Pessac, France

Abstract

Understanding how plants adapt and evolve when faced with prolonged drought is becoming urgent with the threat of climate change. The vulnerability of xylem to embolism is emerging as a major factor in drought-related mortality events in forests across the globe. *Callitris* is a group of around 20 conifer species distributed from wet tropical forests in New Caledonia to the edge of Australia's dry deserts with records of xylem embolism resistance. By combining phylogenetics with ecophysiology, we use the adaptive radiation of this group to investigate the evolution of xylem traits with increasing aridity. Firstly, we provide a new insight into the phylogeny of this group, confirming the close relationships between *Callitris*, *Necallitropsis* and *Actinostrobus* and that *Callitris s.s.* is paraphyletic. Our results support the hypothesis that the diversification of the *Callitris* clade is concomitant with the onset of aridity on the Australian continent over two successive periods around 30 Million years ago (Mya) and from 18 Mya to the present. Accordingly, embolism resistance (P_{50}) varies widely across the *Callitris* clade and is strongly related to water-scarcity. Conductive elements (tracheids) become wider with increasing rainfall, but surprisingly neither xylem specific hydraulic conductance (k_s) nor wood density (WD) vary with climate. Although resistant species tend to have many, smaller tracheids, we found no evidence for a safety-efficiency trade-off which is consistent with the general trend in conifers. While studying this group greatly improves our knowledge of how plants evolve to cope with drought, some mystery remains over how some species of *Callitris* manage to maintain high flow through their tracheids while i) reducing tracheid size and ii) increasing resistance to embolism. Further work at the inter-tracheid pit level is needed to clarify these questions.

Introduction

For vascular plants, and trees in particular, providing a continuous stream of water to their photosynthetic aerial shoots is one of their most vital needs and greatest challenges. Water-transport in plants is driven by the passive process of evaporation at the leaf-atmosphere interface that generates a water-potential gradient throughout the plant. Formalized by the

Cohesion-Tension theory, this is possible thanks to the strong bonds between water-molecules (cohesion) that allow liquid water to remain in a meta-stable state, i.e. under negative pressure (tension). The main drawback of this remarkable function is the risk of breakage of the water-column because of cavitation (the formation of air-bubbles), which becomes ever more likely as evaporative demand increases ("dryness" of the air), and as soil water-potential drops during drought ("dryness" of the soil). Resulting emboli restrict water-transport, and high levels of embolism can lead to plant-death (Brodribb and Cochard, 2009; Urli et al., 2013). Various adaptations protect plants from these potentially catastrophic events, such as limiting water-loss by closing stomata, or vascular tissue (xylem) that limits the formation of air-bubbles. Nevertheless, the breakdown of the water-transport system through embolism is thought to be involved in multiple mass mortality events during and after droughts across the globe in recent decades (Anderegg et al., 2012; Anderegg et al., 2016). This trend is worrying given that climate change will increase frequency and severity of droughts and heatwaves (Stocker et al., 2013), prompting much research in this area over the last decades.

Recent advances have highlighted the location of cavitation events that occur at air-sap interfaces in pores (pits) between functional (water-filled) and embolized (air-filled) conduits. In gymnosperms, these structures contain a valve like structure called the torus that is deflected to block the pit aperture, protecting functional cells from air-leakage (Bailey, 1916). While this structure provides conifers with increased protection from embolism compared to Angiosperms (Maherali et al., 2004; Pittermann et al., 2005; Choat et al., 2012), air-leakage still occurs due to imperfect sealing of the pit aperture by the torus (Bouche et al., 2014).

Plants need to balance embolism resistance (xylem safety) with optimizing rates of water transport (xylem efficiency) to their photosynthetic organs (Tyree and Zimmermann, 2002; Hacke et al., 2006). The advantages of xylem safety are evident (i.e. increased survival during drought), and xylem efficiency allows increased carbon allocation to growth relative to sapwood area, for example allowing rapid growth and optimizing photosynthesis in competitive settings (Santiago et al., 2004; Poorter et al., 2010). For example wide conductive elements (with larger lumen) are efficient for water-transport but generally more vulnerable to embolism (i.e. due to drought or frost) and are weak under mechanical stress (i.e. due to drought-induced xylem tension and the effect of gravity or wind) (Sperry et al., 2008). In conifers, higher embolism resistance is associated with increased mechanical strength, as measured by the thickness of xylem cell walls relative to lumen diameter, but is not related to lumen diameter, therefore having only a minor effect on xylem efficiency (Bouche et al., 2014). However,

embolism resistance is mostly linked to pit traits such as torus-aperture overlap in conifers (Bouche et al., 2014), hinting at a potential trade-off with overall tracheid conductance (Domec et al., 2008). Species ecology and phylogeny are major factors in determining these trade-offs and the final compromise reached between safety and efficiency, for example species growing in competitive wet environments are more likely to maximize efficiency over safety (Sperry et al., 2006; Choat et al., 2012). On the other hand, species with drought-adapted ancestors could inherit constraints on the evolution of their xylem, limiting their capacity to compete under higher water availability by adjusting efficiency at the expense of increased safety (Maherali et al., 2004). In any case, there is little evidence of a simple relationship between safety and efficiency at a large ecological and taxonomic scale, the trade-off only suggested by the absence of any resistant and efficient species (Gleason et al., 2015); there are however many "incompetent" species, both vulnerable to embolism and inefficient for water transport. At a more restricted evolutionary scale, xeric *Eucalyptus* species evolved many narrow vessels and denser wood, contrasting with fewer wide vessels and lighter wood in more mesic environments, reflecting this trade-off of hydraulic traits in response to climate across Australia (Pfautsch et al., 2015).

While at broad evolutionary scales there is substantial variation for P_{50} (Maherali et al., 2004; Pittermann et al., 2012; Bouche et al., 2014), at finer infra-generic and intra-specific scales there is generally low variability (Delzon et al., 2010) and little genetic differentiation for embolism resistance (Lamy et al., 2011; Sáenz-Romero et al., 2013; David-Schwartz et al., 2016). However, no studies have examined embolism resistance among closely related species over such a wide climatic gradient.

Callitris is a conifer genus of shrubs and trees that underwent an ecological radiation with the emergence of dry environments in Australia over the last 30 Million years (Pittermann et al., 2012- Chapter 4 of this thesis) making it the most speciose Cupressaceae genus in the Southern Hemisphere (from 15 to 20 species recognized by different authors (Hill and Brodribb, 1999; Farjon, 2005; Eckenwalder, 2009)). This clade displays a marked xeric affinity, despite spanning a huge rainfall gradient across Australia, Tasmania, and New-Caledonia, i.e. from around 200 to over 2000 mm per year. With some of the most drought-tolerant species currently known (Brodribb et al., 2010; Larter et al., 2015), this clade presents a unique opportunity to investigate plant ecophysiology from an evolutionary perspective.

Molecular phylogenetic work has established the affinity of *Callitris* with *Actinostrobus* (three species endemic to Western Australia) and *Neocallitropsis* (one endemic species, New-Caledonia) (Leslie et al., 2012; Mao et al., 2012; Yang et al., 2012), even warranting their grouping as a single genus (Piggin and Bruhl, 2010). While recent studies have tried to disentangle the relationships within this clade (i.e. based on nuclear ITS sequences (Pye et al., 2003) and a morphological database (Piggin and Bruhl, 2010)), more work is required notably including more genetic information (e.g. from other genomic compartments), adding missing species and using dating techniques to provide a time-scale for their evolution.

Our main objective was to investigate the ecophysiological evolution of the most drought-resistant clade of trees in the world. Firstly, we constructed an extensive physiological dataset of embolism resistance, xylem specific hydraulic conductance, and xylem anatomy traits. We hypothesized that in contrast to previous work, due to the large aridity gradient in this clade we should find wide variation in embolism resistance, which should track species climate. We investigated the role of climate in establishing vasculature and in determining any potential xylem level trade-offs. To this end, we used observation data to estimate climatic parameters of each species' distribution, and tested the correlation of species climate with embolism resistance, water-transport efficiency and vascular traits. Given the reduced phylogenetic scale and huge climatic gradient, we expected to establish a trade-off between safety and hydraulic efficiency, due to large selective pressures from competition and climatic stress driving hydraulic traits. We expected the most xeric species to have a resistant, less efficient xylem with many small tracheids, and species from more mesic regions to have wider tracheids favoring xylem efficiency but reduced safety. Finally, we included these results in an evolutionary framework by constructing a fossil-calibrated phylogeny. We hypothesized hydraulic traits in this group evolved rapidly in response to climate, and therefore expected little impact of phylogeny in the investigated traits and trade-offs. We also wanted to investigate the hypothesis that the Callitris clade underwent an ecological radiation in response to increasing aridity in the Australian region since the end of the Eocene.

Methods:

Phylogenetic reconstruction

We build on the increased availability of molecular sequences to produce a new perspective on the phylogeny of the Callitris (and relatives *Neocallitropsis* and *Actinostrobus*. We took a broad view of species delimitations, i.e. treating *C. columellaris*, *C. intratropica*, and *C.*

glaucophylla separately, as well as *C. tuberculata*, *C. preissii*, *C. verrucosa* and *C. gracilis*. Various treatments of these as sub-species and/or synonyms are available in the literature (Hill, 1998; Hill and Brodribb, 1999; Farjon, 2005; Eckenwalder, 2009; Farjon, 2010), prompting the need for further detailed work, hopefully using wide raging sampling and molecular markers. We used the PHLAWD pipeline (Smith et al., 2009) to obtain sequences from Genbank (Benson et al., 2011) in the aim of constructing a large multi-locus dataset. We used a range of loci from both chloroplastic DNA (rbcL, matK, trnL, psbB, petB) and nuclear DNA (ITS, needly, leafy). We didn't use any mitochondrial data due to lack of available species. Alignements were manually trimmed and checked, and we selected the most appropriate DNA substitution models using maximum likelihood implemented in MEGA (Tamura et al., 2011) (see Suppl. Table 1 for details). To check for incongruence between the chloroplastic and nuclear datasets, we first analyzed both matrixes separately using maximum likelihood with RAxML and Bayesian Inference implemented in BEAST (Drummond and Rambaut, 2007) - see Suppl. Figure S1. Finally we combined the data to construct a time-calibrated phylogeny for the sub-family Callitroidae (Cupressaceae). We used the recognized basal position of *Papuacedrus* in this group (Leslie et al., 2012; Mao et al., 2012) to root the tree. We set a minimum constraint on the age of crown Callitroidae (as in (Leslie et al., 2012; Mao et al., 2012)) by using the Patagonian fossil *Papuacedrus prechilensis* (Wilf et al., 2009), based on an ovulate cone from the early to mid-Eocene (51.9 to 47.5 Mya). The maximum age for the appeareance of crown Callitroidae was conservatively set by evidence that crown Cupressaceae (i.e. subfamilies Callitroidae and Cupressoidae) was present by 99.6 Mya, using the fossil *Widdringtonia americana* from the Cenomanian (Mciver, 2001). We used the earliest evidence of *Callitris* (Paull and Hill, 2010) to constrain the crown of the clade containing all *Callitris*, *Neocallitropsis* and *Actinostrobus* species. Since this fossil bears characters of both *Callitris* and *Actinostrobus* and the phylogenetic relationships between the two genera are still ambiguous (Pye et al., 2003; Piggin and Bruhl, 2010). Finally, we used *Fitzroya acutifolia* (Paull and Hill, 2010) to calibrate the split between *Fitzroya* and *Diselma*.

Physiological and anatomical traits

We combined existing physiological data (Delzon et al. 2016 *in prep.*) with new measurements for several species collected in the wild (i.e. *Actinostrobus acuminatus*, *A.arenarius*, *A. pyramidalis*, *Callitris canescens*, *C. drummondii*, *C. endlicheri*, *C. glaucophylla*, *C. gracilis*, *C. muelleri*, *C. roei*, *C. tuberculata* and *C. verrucosa*) or in botanical gardens (*C. baileyi*, *C endlicheri*, *C. macleayana*, *C. monticola* - see Suppl. Table S2). All

hydraulic measurements were conducted using the standard protocol at the University of Bordeaux (for details, see methods section in Delzon et al. 2016 *in prep.*). Sample resistance to embolism was assessed with the "Cavitron" technique (Cochard et al., 2005), which allowed us to construct vulnerability curves and simultaneously estimate xylem specific hydraulic conductance k_s ($m^2.MPa^{-1}.s^{-1}$). A sigmoid model was fit to each individual vulnerability curve (Pammenter and Vander Willigen, 1998), from which we obtained the P_{50} parameter (MPa), the xylem pressure inducing 50% loss of conductance. Values were then averaged across all samples for each species.

Following embolism resistance measurements, small segments of the samples were used to conduct xylem anatomy measurements. Several transverse sections per individual were cut using a hand sliding microtome, colored using safranine at 1%, and examined using a light microscope (DM2500M, Leica Microsystems, Germany). We selected three individuals per species and took five digital images per individual, which were then analyzed using ImageJ (NIH, Bethesda, MD). Magnification was x400 for all samples except for *Neocallitropsis pancheri*, *Callitris sulcata* and *C. neocaledonica*, for which we used x200 magnification to increase the total number of tracheids visible on each image. Sample preparation and photography was either conducted at the University of Bordeaux or at Western Sydney University (Hawkesbury Institute for the Environment), using the same protocol. Images were manually edited to remove debris or staining obscuring tracheid lumens, prior to automatic image analysis. Tracheids on the edges of images were excluded from the analysis. Overall, 80 individual samples and a total of 400 images were analyzed resulting in data for 33652 tracheids. We extracted from each image the area of each tracheid lumen, total image area and number of analyzed tracheids, and pooled the data by individual for analysis. From the total analyzed area, total tracheid number, and area of each tracheid we derived for each individual mean, minimum and maximum tracheid diameter, the average number of tracheid per unit area (TF; cm^{-2}), the ratio of tracheid lumen area divided by total image area (void to wood ratio; %). In addition, we measured tracheid length (µm) and counted bordered pits (hereafter pitting) for 50 tracheids in a subset of 14 species.

According to the Hagen-Poiseuille law, hydraulic conductivity of a conduit varies according to the fourth power of its radius, which means that larger tracheids contribute disproportionately to the overall hydraulic conductance (Tyree and Zimmermann, 2002). To use a hydraulically meaningful measure of tracheid diameter, we calculated the hydraulically weighted hydraulic diameter (D_h; Tyree and Zimmermann, 2002), defined as:

$$D_h = [\frac{\sum D^4}{N}]^{1/4} \quad \textit{Equation 1}$$

where N is the total number of tracheids. D_h is the mean diameter required to achieve the same overall conductance with the same number of conductive elements. We then calculated the theoretical conductance (K_{th}; $m^3.m^{-1}.MPa^{-1}.s^{-1}$) which is the theoretical rate of flow through a cylindrical pipe according to the Hagen-Poiseuille law:

$$K_{th} = \frac{D_h^4 \pi}{128 * \eta} * TF \quad \textit{Equation 2}$$

where η is the viscosity of water at 20°C (1.002 x 10^{-9} MPa.s). For appropriate units, we transformed D_h to meters (x 10^{-6}) and TF to m^{-2} (x 10^5).

Xylem water-flow efficiency depends on conductivity of both tracheid lumens (i.e. K_{th}) and bordered-pits (Hacke et al., 2005). We calculated pit conductivity K_{pit} as follows:

$$K_{pit} = (\frac{1}{Kmax} - \frac{1}{K_{th}})^{-1} \quad \textit{Equation 3}$$

Wood density was estimated using x-ray imagery (Polge, 1966) for 3 individuals per species on transversal sections of approximately 1 mm thickness. Images were analysed using Windendro (Guay et al., 1992) to obtain two radial density profiles per section, from which we estimated mean wood density ($g.cm^3$).

Species climate

We downloaded species occurrence points from the Global Biodiversity Information Facility (GBIF; Booth, 2014). After excluding data with obvious identification or GPS coordinate errors, we extracted climate information for each point using climate data from the WorldClim database (Hijmans et al., 2005) using QGIS software (Quantum, 2011), and potential evapotranspiration (P-ET) and aridity index (AI) from the CGIAR-CSI database (Trabucco and Zomer, 2009). We then extracted the mean and median values of the distributions of each climatic variable for each species.

Statistical analyses

All data manipulation and analysis was conducted in R (R Core Team, 2015) and SAS (SAS Institute Inc., Cary, USA). We performed linear regressions on raw data and log-transformed data with nearly identical results so we present only untransformed correlations to simplify interpretation. Phylogenetic Generalized Least Squares were conducted using caper::pgls (Orme, 2013). PGLS accounts for the statistical non-independence in cross-species trait

correlations by adjusting the residual error structure using a variance/covariance matrix derived from the phylogeny (Garamszegi, 2014). It explicitly allows for varying amounts of phylogenetic signal in the data by using Pagel's lambda (Pagel, 1999), thus removing the risk of over-correcting for phylogeny when shared evolutionary history doesn't affect trait relationships. We mapped the evolution of P_{50} onto the phylogeny using phytools::contMap (Revell, 2013).

Results and discussion

Phylogeny:

Our phylogenetic analyses recover the well-recognized relationships within sub-family Callitroidae, with successive divergences of the *Pilgerodendron-Libocedrus* clade and then *Diselma-Fitzroya* clade, together with their sister lineage *Widdringtonia* (Figure 1). Within the crown *Callitris* clade, early divergences that are dated to between 25 and 30 Mya are not well resolved (Figure 1). This issue is consistent across maximum likelihood and Bayesian methods used, and is also present when we partition the molecular dataset into nuclear and chloroplastic regions. We found five separate sub-clades formed from these early divergences (see letters in Figure 1): a Western Australian clade composed of *Callitris drummondii* (A) and the *Actinostrobus* genus (B), a tropical North Eastern clade composed of *Callitris macleayana* (C) and the New-caledonian species (*Neocallitropsis pancheri* and *C. sulcata* - B), and a well-supported core Callitris clade with the remaining species (E). In this last group, *C. canescens* seems to occupy a solitary basal position, with the remainder consistently separated into i) an eastern group with C. *muelleri*, *C. oblonga*, C. *rhomboidea* and *C. endlicheri* and ii) a "*preissii-glaucophylla*" clade, that groups together the species (or sub-species) *C. gracilis*, C. *preissii*, *C. verrucosa*, *C. tuberculata*, C. *intratropica* and C. *columellaris*. While some divergences in this last clade are not very well supported, it's worth noting that our analyses recover *C. preissii* in the most basal position. Although *C. columellaris* and *C. intratropica* are always grouped together, their supposedly closely allied species *C. glaucophylla* is always closer to *C. gracilis*, *C. verrucosa* and C. *tuberculata*.

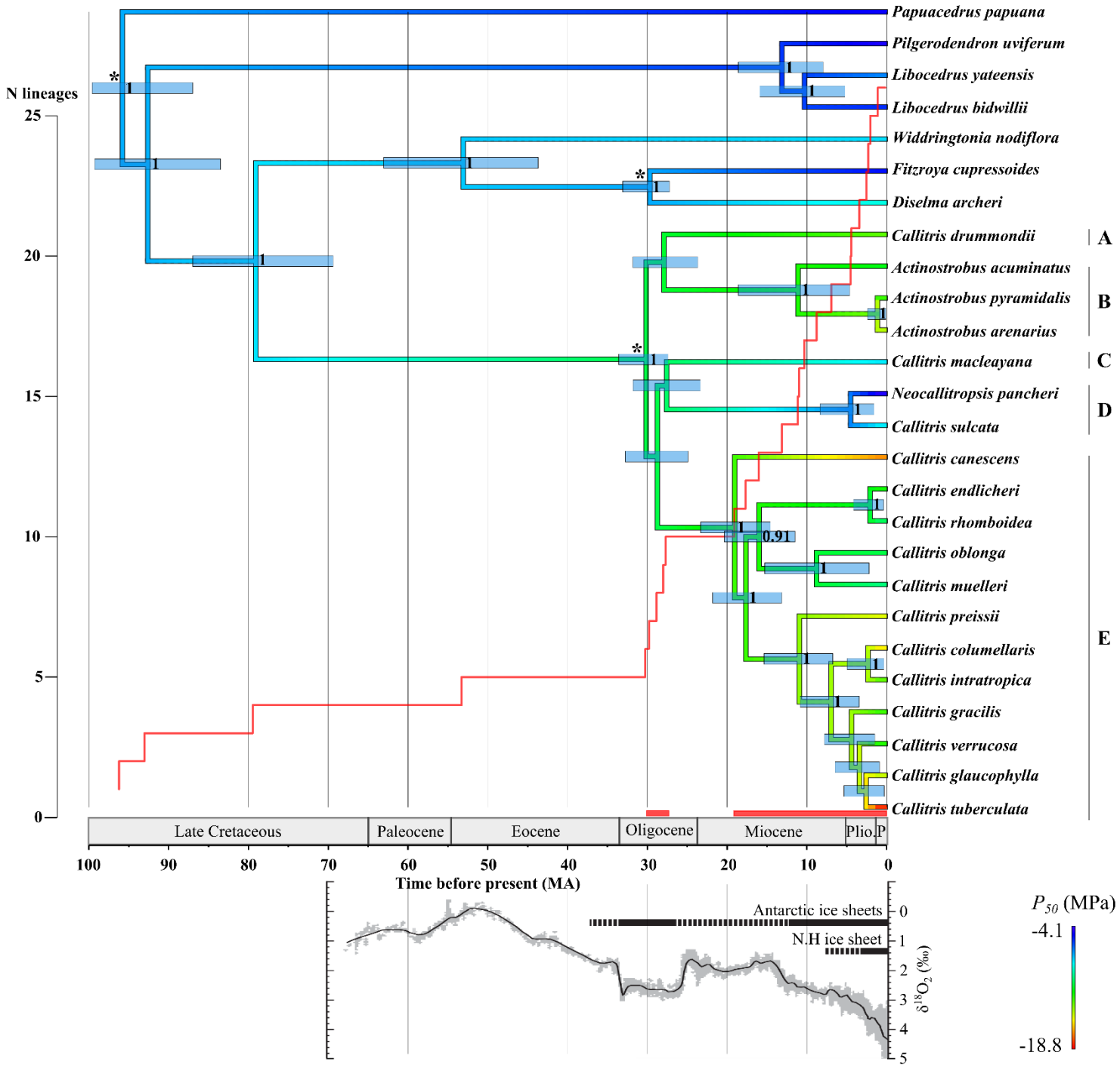

Figure 1: Time-tree of Callitroidae and the evolution of P_{50} in the *Callitris* clade. Branches of the phylogeny are coloured according to reconstructed P_{50} (scale bottom-right). Blue bars at node on the tree represent 95% HPD from the BEAST analysis, number represent posterior Bayesian support values (not shown if <0.9). Stars mark fossil-calibrated nodes. Letters A to E indicate the 5 sub-clades within crown *Callitris*. Red line shows the lineage-through-time plot (scale on left-hand side), with periods of diversification indicated by red bars next to time-axis. Bottom insert shows variation of sea-temperature based on oxygen isotopic composition (Zachos et al., 2001) and periods of glaciation at the poles, modified from (Fujioka and Chappell, 2010).

Our topology largely agrees with previous work (Pye et al., 2003; Piggin and Bruhl, 2010). Although our work is lacking some species, we believe that adding them would not change the results greatly. Given the close relationships between i) *C. roei* and *C. drummondii*, ii) *C. neocaledonica* and *C*. sulcata and iii) C. *monticola* and *C. muelleri*, the topology would likely remain the same, maybe even providing extra support to some nodes. However, the position of *C. baileyi* in the clade is more uncertain, probably occupying a basal position (Piggin and Bruhl, 2010), its inclusion could be informative for the unresolved "deep" divergences in our analyses.

The dating analysis shows a burst of speciation around 30 Mya (Figure 1; LTT plot), which corresponds to the first major shift away from the year-round wet climate of the end of the Eocene to a more seasonal-monsoonal climate, with the emergence of open woodland suggesting dry seasons (Martin, 2006; Fujioka and Chappell, 2010). This could have led some lineages to remain in the year-round wet tropical forests along Eastern Australia to the North, while others adapted to the appearance of more temperate and seasonal climates in South-Eastern and Western Australia (Byrne et al., 2008). The second acceleration in rates of diversification corresponds to the early divergences in the core *Callitris* clade, from around 18 Mya. This is synchronous with the onset of more severe aridity in mainland Australia by the mid-Miocene (Martin, 2006; Fujioka and Chappell, 2010). The extreme aridity over much of central Australia today is relatively young (c. 1-4 Mya), with formation of temporarily dry lakes ("playas") and stony or sand-dune deserts, oscillating between very arid and more mesic periods during the glaciations of the Pleistocene (Byrne et al., 2008). This probably drove the extreme xylem adaptation visible in extant species such as *Callitris tuberculata*, *C. columellaris*, *C. canescens*, and *Actinostrobus arenarius* with P_{50} values more negative than -15 MPa.

Physiology and climate

Embolism resistance in the *Callitris* clade varies widely from -3.8 MPa in *Callitris neocaledonica* to -18.8 MPa in *C. tuberculata* (Figure 1; Suppl. Table S2). This variation is remarkable as it is comparable to the variation across all conifers (Delzon et al 2016 *in prep*), and it dwarfs previous estimates of intra-generic variation (e.g. in pines (Delzon et al., 2010). Recent work has brought to light a deep divergence in conifer water-management strategy, with some species using high levels of ABA to close stomata tightly shut. Other species, mostly from the Cupressaceae family use leaf desiccation to close their stomata, allowing them to recover faster at re-watering (Brodribb and McAdam, 2013; Brodribb et al., 2014). However stomata in these species continue to leak water long after full stomatal closure, exposing their xylem to more negative water potential after stomatal closure during prolonged drought - hence the need

for more negative P_{50}. (Delzon et al. 2016 *in prep*), and therefore likely follow this strategy. Xylem specific hydraulic conductance was similar to that of other conifers, and varied approximately six-fold from 1.88 x 10^{-5} $m^2.MPA^{-1}.s^{-1}$ in *C. oblonga* to 1.25 x 10^{-4} $m^2.MPA^{-1}.s^{-1}$ in *C. intratropica*.

Our analysis of xylem anatomical traits uncovered huge variation across Callitris species. Some species had many small tracheids (e.g. *C. tuberculata*: mean diameter = 9.04 µm, tracheid frequency = 324952 cm^{-2}) and or fewer wide tracheids (e.g. *C. sulcata*: 14.14 µm and 160662 cm^{-2}). Accordingly, theoretical hydraulic conductance also displayed a wide range of values, with *C. sulcata*'s xylem theoretically ten times more efficient than *C. gracilis*'s (0.0132 and 0.00115 $m^3.m^{-1}.MPa^{-1}.s^{-1}$ respectively). Wood density was high in all species, with the lowest density measured in *C. oblonga* (0.57 $g.cm^3$), already above the average for conifers (i.e. 0.54 $g.cm^3$; Delzon et al. 2016), and the maximum reaching 0.74 $g.cm^3$ in *N. pancheri*.

Across the geographical range of the *Callitris* clade, annual rainfall varies from around 300 $mm.y^{-1}$ for *C. tuberculata* in Western Australia to over 2100 $mm.y^{-1}$ for *N. pancheri* in New Caledonia (median values of the species distribution range). Similar variation was found for the aridity index (from 0.21 to 1.78). Driest quarter precipitations vary from 7 mm for the tropical monsoonal *C. intratropica* to 315 mm for *N. pancheri*.

We tested the role of water-availability in determining species' resistance to embolism, xylem conductivity, tracheid dimensions and wood density. Increasingly xeric environments were associated with more negative P_{50} values (Figure 2 – a, b and c), a trend confirmed using PGLS, proving the adaptive role of embolism resistance in *Callitris*. In contrast, we found no evidence for a role of aridity in determining maximum xylem conductivity (Figure 1, d, e and f), which goes against the expectation of reduced xylem conductivity in the face of drought under the safety-efficiency trade-off hypothesis. However, tracheid diameter increased with diminishing aridity (Figure 1, g, h and i). All these relationships (or lack thereof) remained unchanged when using log-transformed data and when taking phylogeny into account using PGLS, indicating a strong influence of climate on embolism resistance and tracheid dimensions, but no effect on overall xylem conductivity or wood density (Suppl. Table 3).

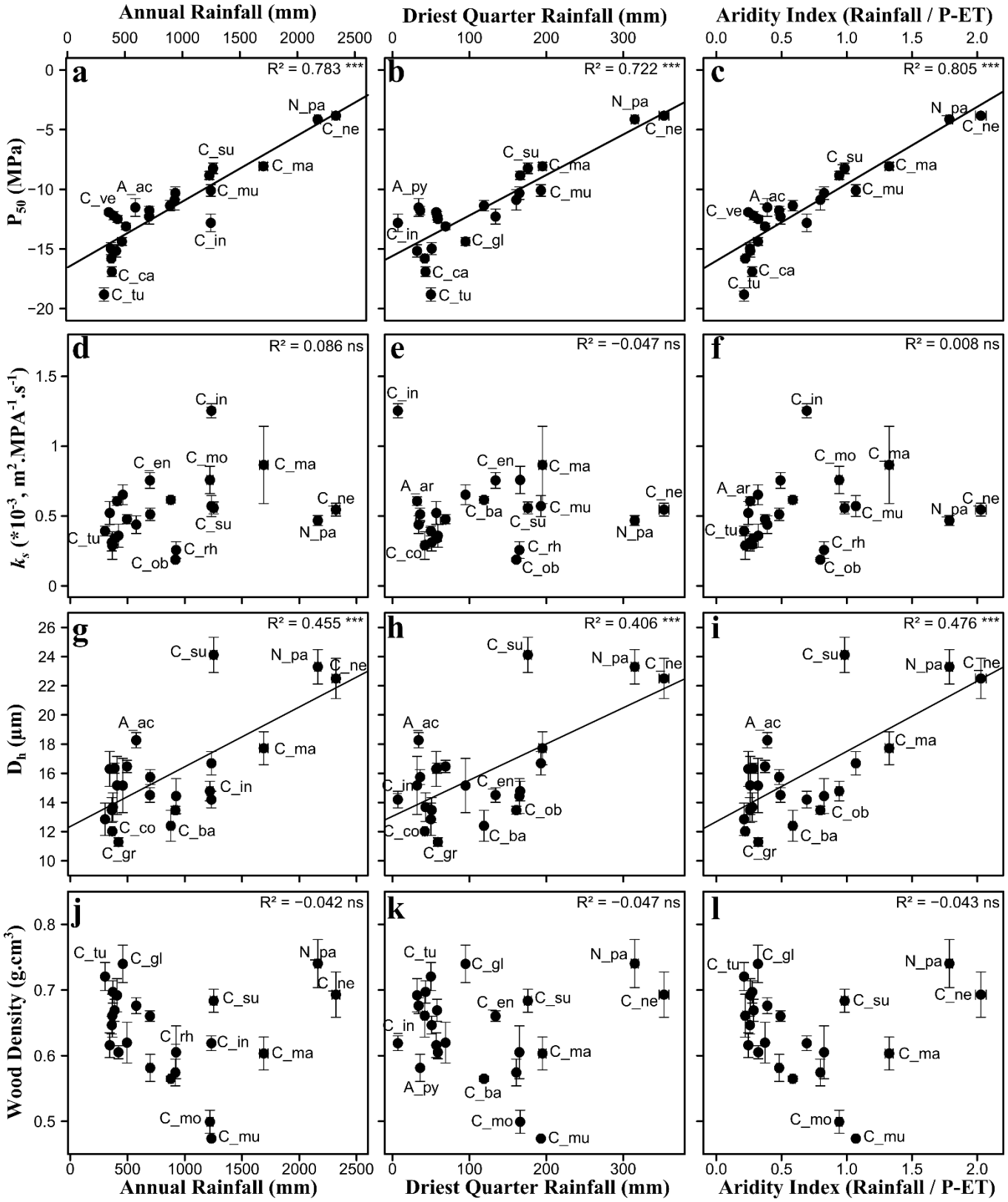

Figure 2: Relationships between xylem hydraulic traits and climate in *Callitris*. Embolism resistance (first row), xylem specific hydraulic conductance (second row), hydraulically weighted tracheid diameter (third row) and wood density (bottom row) in relation to water availability, as measured by annual rainfall (left), driest quarter precipitations (center) and the aridity index (right). Linear regression lines are shown, with the adjusted R^2. "***" indicates p-values < 0.001, and "ns" indicates non-significance at α=0.05. Labels: C= *Callitris*, A=*Actinostrobus*, N=*Neocallitropsis*, followed by first two letters of species name. Error bars represent standard error.

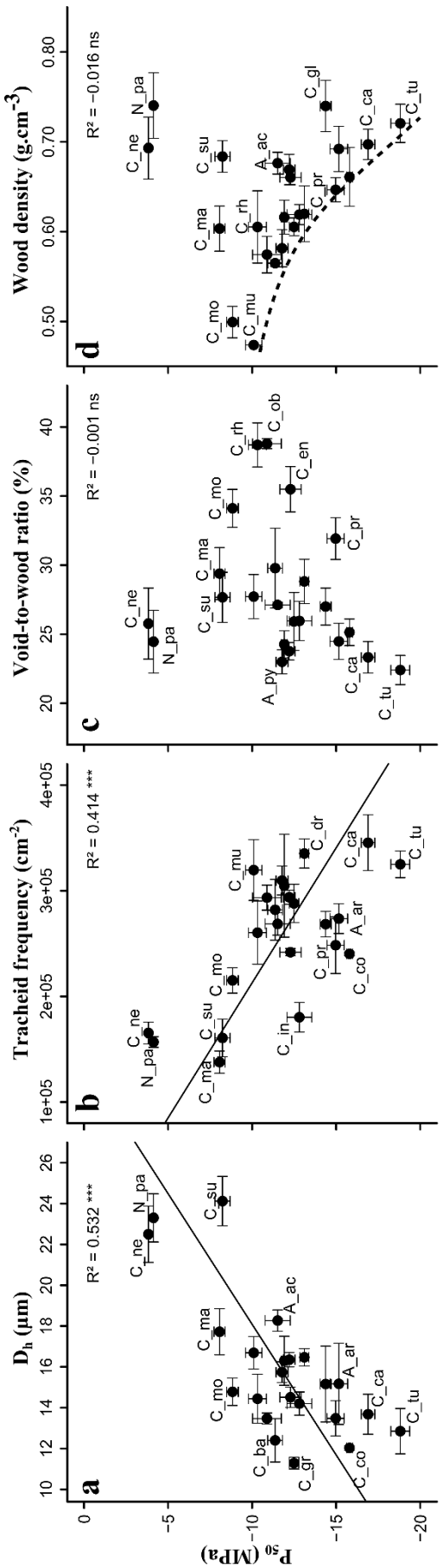

Figure 3. Relations between wood construction traits and hydraulic safety and efficiency and in *Callitris*. Correlations between P_{50} (top four panels) and k_S (bottom four panels) and four wood traits – a and e, tracheid hydraulically weighted diameter; b and f, tracheid frequency; c and g, void-to-wood ratio; d and h, wood density - were tested using linear regressions (adjusted R^2 and significance to α=0.05 are shown in each panel as in Figure 2). Error bars represent ± standard error. The dotted line (**d**) represents the hypothetical limit of wood implosion due to xylem pressure.

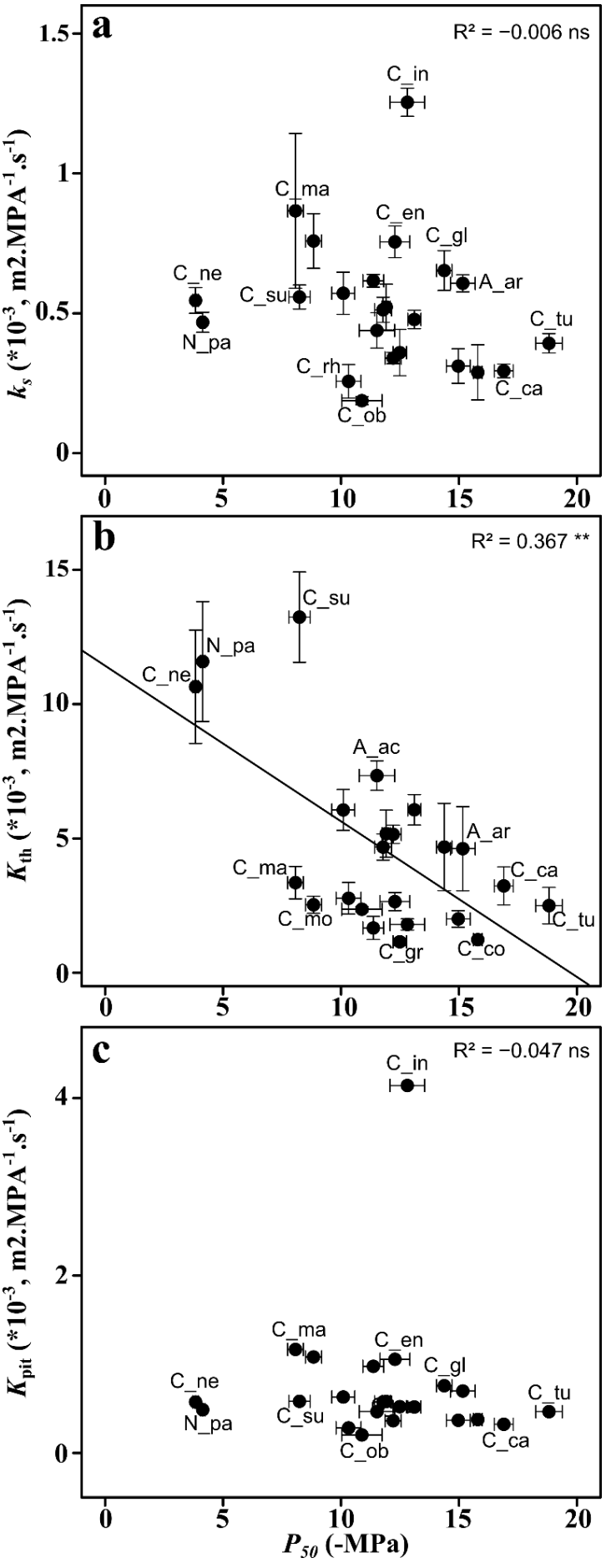

Figure 4 : Xylem safety vs. efficiency relationship in *Callitris*. Embolism resistance in relation to xylem specific hydraulic conductance (k_s; a), theoretical conductance (K_{th}; b), and the derived total pit conductivity (K_{pit}; c). Linear regressions were conducted, with R^2 and significance reported in each panel. Note that P_{50} is positive in this figure, with higher values representing increased embolism resistance.

Because increased embolism resistance allows for more negative xylem pressure under drought conditions, an evolutionary corollary should be increased mechanical strength, for example with thicker tracheid walls in proportion to tracheid lumen diameter. In turn, this increased proportion of wood should lead to reduced xylem conductance because of a reduction in total conductive area. In our dataset, we found a strong correlation between P50 and tracheid diameter, and tracheid frequency, with resistant species having many more, smaller tracheids than vulnerable species (Figure 3, a and b). However, void-to-wood ratio and wood density were not related to P_{50} (Figure 3, c and d). In turn, k_s seems disconnected to some extent from tracheid and wood level traits, with the only significant relationship with tracheid frequency: having fewer conducting elements is linked to a more efficient xylem (Figure 1, f). It's worth noting here the

remarkable conductance measured for *C. intratropica*, which is surprisingly combined with relatively small tracheid diameter but not a large frequency of tracheids, high void-to-wood ratio or low wood density. Overall, safety and efficiency are not tightly linked to wood traits, yet resistant species develop smaller, more densely packed tracheids. These results confirm previous studies involving multiple conifer species (Pittermann et al., 2006b). Conversely, conducting efficiency seems to be linked to a reduction in tracheid frequency, but not lower wood density, which goes against the trend evidenced for all conifer taxa (Delzon et al. 2016, *in prep.*). We hypothesize that this could be a by-product of increased growth rates in species from higher rainfall areas. Developmental constraints restrict evolution of tracheid wall thickness (the main driver of resistance to implosion) while climatic conditions allow for more rapid growth, leading to an increase in tracheid lumen diameter (Vaganov et al., 2006). We also measured tracheid length and average pitting (number of pits per tracheid) on a subset of species.

By increasing transport area and offering more possible locations for air-seeding, longer tracheids and more numerous pits should reduce overall end-wall resistance to water-flow and increase vulnerability to embolism (Sperry et al., 2006). Both parameters were weakly correlated to embolism resistance, i.e. more resistant species had shorter tracheids with fewer pits, however higher pitting was not associated with an increase in overall conductance (Suppl. Figure S2).

Finally, we investigated the safety-efficiency trade-off hypothesis, but we found no significant relationship between P_{50} and k_s (Figure 4). The theoretical maximum hydraulic conductance K_{th} is negatively correlated to embolism resistance: resistant species have a theoretically less efficient xylem when only considering tracheid lumen conductivity (Fig. 4; b), which is consistent with the trend for smaller tracheids with increasing resistance. In contrast, bordered-pit conductivity was unrelated to P_{50} (Fig. 4; c). The overall pit-resistance to water-flow is mainly linked to the size and distribution of pores in the pit-membrane (margo) and the depth/width of the pit aperture tunnel (Hacke et al., 2004; Bouche et al. in prep.). Embolism resistance is linked to the sealing of the pit aperture by the torus (torus-overlap) in conifers (Bouche et al., 2014). Increasing torus size relative to pit-aperture (i.e. increasing torus-overlap) has been shown to be related to more negative P_{50}, but does not reduce overall pit conductivity, which is mostly related to the size of pores in the margo and the pit aperture dimensions (Hacke et al., 2004; Pittermann et al., 2010; Bouche et al. *in prep*). Our results demonstrate that in the *Callitris* clade, water-flow through vascular tissue is mostly limited by

pit resistivity (K_{pit} << K_{th}), which is consistent with previous work (Pittermann et al., 2006a). Additionally, bordered-pits can be both efficient for water-transport (i.e. high values of K_{pit}) and limit air-seeding under high xylem tension (low P_{50}) (Pittermann, 2005). A prime example is *C. intratropica*, with average tracheid diameters but by far the highest xylem conductivity in *Callitris* (k_s), coupled with resistant xylem (P_{50} = -12.8 MPa).

These results bring to light a path for further investigations into the evolution of drought tolerance in this group, by examining pit structures such as torus/pit aperture overlap and margo pore size. Other ongoing investigations concern the ornamentations on the inside of tracheids that are prominent in the *Callitris* clade, namely i) reinforcements surrounding the pit called "callitroid thickenings" (Heady and Evans, 2000) and ii) warts that cover the entire inner surface of tracheids (Heady et al., 1994). These structures are thought to be related to ecology and physiology by limiting the risk of tracheid implosion under large xylem pressures, and increasing the wettability of the tracheid walls somehow limiting inception of cavitation during drought.

Conclusion:

We provide new insights into the phylogeny and diversification of the Callitris clade, although more work is needed to untangle early divergences. Our results confirm the evolutionary lability of xylem resistance to embolism, with a transition towards extreme resistance of several species within the *Callitris* clade. Combined with the onset of severe aridity in Australia, our results detail the remarkable adaptive radiation of this group. Despite overwhelming evidence for the role of decreasing water-availability in shaping some xylem traits, we found no evidence of its effect on xylem water-transport efficiency and wood density. Species from more xeric areas develop smaller tracheids, but both wood traits and embolism resistance are totally disconnected from overall xylem conductivity, suggesting a lack of trade-offs between construction costs and safety on the one hand and efficiency on the other. We also highlight a likely evolutionary role of pit-level traits in this clade, regarding safety and efficiency. One area of interest for future research is the coordination of this remarkable evolutionary of the xylem with the evolution of structures and functions at the leaf-level. Finally, it would be intriguing to test how much of this evolutionary lability is transferred to the species level, especially given the widespread ranges of some *Callitris* species.

References

Anderegg WRL, Berry J a, Smith DD, Sperry JS, Anderegg LDL, Field CB (2012) The roles of hydraulic and carbon stress in a widespread climate-induced forest die-off. Proc Natl Acad Sci U S A **109**: 233–7

Anderegg WRL, Klein T, Bartlett M, Sack L, Pellegrini AFA, Choat B (2016) Meta-analysis reveals that hydraulic traits explain cross-species patterns of drought-induced tree mortality across the globe. Pnas. doi: 10.1073/pnas.1525678113

Bailey IW (1916) The Structure of the Bordered Pits of Conifers and Its Bearing Upon the Tension Hypothesis of the Ascent of Sap in Plants. Bot Gaz **62**: 133

Benson DA, Karsch-Mizrachi I, Lipman DJ, Ostell J, Sayers EW (2011) GenBank. Nucleic Acids Res **39**: D32–7

Booth TH (2014) Using biodiversity databases to verify and improve descriptions of tree species climatic requirements. For Ecol Manage **315**: 95–102

Bouche PS, Larter M, Domec J-C, Burlett R, Gasson P, Jansen S, Delzon S (2014) A broad survey of hydraulic and mechanical safety in the xylem of conifers. J Exp Bot. doi: 10.1093/jxb/eru218

Brodribb TJ, Bowman DJMS, Nichols S, Delzon S, Burlett R (2010) Xylem function and growth rate interact to determine recovery rates after exposure to extreme water deficit. New Phytol **188**: 533–42

Brodribb TJ, Cochard H (2009) Hydraulic failure defines the recovery and point of death in water-stressed conifers. Plant Physiol **149**: 575–84

Brodribb TJ, McAdam S a M (2013) Abscisic acid mediates a divergence in the drought response of two conifers. Plant Physiol **162**: 1370–7

Brodribb TJ, McAdam S a M, Jordan GJ, Martins SC V (2014) Conifer species adapt to low-rainfall climates by following one of two divergent pathways. Proc Natl Acad Sci U S A. doi: 10.1073/pnas.1407930111

Byrne M, Yeates DK, Joseph L, Kearney M, Bowler J, Williams M a J, Cooper S, Donnellan SC, Keogh JS, Leys R, et al (2008) Birth of a biome: Insights into the assembly and maintenance of the Australian arid zone biota. Mol Ecol **17**: 4398–4417

Choat B, Jansen S, Brodribb TJ, Cochard H, Delzon S, Bhaskar R, Bucci SJ, Feild TS, Gleason SM, Hacke UG, et al (2012) Global convergence in the vulnerability of forests to drought. Nature **491**: 752–5

Cochard H, Damour G, Bodet C, Tharwat I, Poirier M, Améglio T (2005) Evaluation of a new centrifuge technique for rapid generation of xylem vulnerability curves. Physiol Plant **124**: 410–418

David-Schwartz R, Paudel I, Mizrachi M, Shklar G, Delzon S, Cochard H, Lukyanov V, Badel E, Capdeville G, Cohen S (2016) Evidence for genetic differentiation in vulnerability to embolism in Pinus halepensis. Front. Plant Sci.

Delzon S, Douthe C, Sala A, Cochard H (2010) Mechanism of water-stress induced cavitation in conifers: bordered pit structure and function support the hypothesis of seal capillary-seeding. Plant Cell Environ **33**: 2101–11

Domec J-C, Lachenbruch B, Meinzer FC, Woodruff DR, Warren JM, McCulloh K a (2008) Maximum height in a conifer is associated with conflicting requirements for xylem design. Proc Natl Acad Sci U S A **105**: 12069–74

Drummond AJ, Rambaut A (2007) BEAST: Bayesian evolutionary analysis by sampling trees. BMC Evol Biol **7**: 214

Eckenwalder JE (2009) Conifers of the world: the complete reference. Timber Press

Farjon A (2005) A monograph of Cupressaceae and Sciadopitys. Kew: Royal Botanic Gardens, Kew 643p.. ISBN

Farjon A (2010) A Handbook of the World's Conifers (2 Vols.). BRILL

Fujioka T, Chappell J (2010) History of Australian aridity: Chronology in the evolution of arid landscapes. Geol Soc Spec Publ **346**: 121–139

Garamszegi Z (2014) Modern Phylogenetic Comparative Methods and Their Application in Evolutionary Biology. doi: 10.1007/978-3-662-43550-2

Gleason SM, Westoby M, Jansen S, Choat B, Hacke UG, Pratt RB, Bhaskar R, Brodribb TJ, Bucci SJ, Mayr S, et al (2015) Weak tradeoff between xylem safety and xylem-specific hydraulic efficiency across the world's woody plant species. New Phytol 123–136

Guay R, Gagnon R, Morin H (1992) A new automatic and interactive tree ring measurement

system based on a line scan camera. For Chron **68**: 138–141

Hacke UG, Sperry JS, Pittermann J (2005) Efficiency Versus Safety Tradeoffs for Water Conduction in Angiosperm Vessels Versus Gymnosperm Tracheids. Vasc Transp plants 333–353

Hacke UG, Sperry JS, Pittermann J (2004) Analysis of circular bordered pit function II. Gymnosperm tracheids with torus-margo pit membranes. Am J Bot **91**: 386–400

Hacke UG, Sperry JS, Wheeler JK, Castro L (2006) Scaling of angiosperm xylem structure with safety and efficiency. Tree Physiol **26**: 689–701

Heady RD, Evans PD (2000) Callitroid (callitrisoid) thickening in Callitris. IAWA J **21**: 293–319

Heady RD, R.B. C, Donnelly CF, Evans PD (1994) Morphology of warts in the tracheids of cypress pine (Callitris Vent.). IAWA J **15**: 265–281

Hijmans RJ, Cameron SE, Parra JL, Jones PG, Jarvis A (2005) Very high resolution interpolated climate surfaces for global land areas. Int J Climatol **25**: 1965–1978

Hill KD (1998) Introduction to the Gymnosperms; Coniferophyta; Cycadophyta; Pinophyta. Flora Aust. vol. 48, Ferns, Gymnosperms, Allied Groups

Hill RS, Brodribb TJ (1999) Southern conifers in time and space. Aust J Bot **47**: 639–696

Lamy J-B, Bouffier L, Burlett R, Plomion C, Cochard H, Delzon S (2011) Uniform Selection as a Primary Force Reducing Population Genetic Differentiation of Cavitation Resistance across a Species Range. PLoS One **6**: e23476

Larter M, Brodribb TJ, Pfautsch S, Burlett R, Cochard H, Delzon S (2015) Extreme aridity pushes trees to their physical limits. Plant Physiol **168**: pp.00223.2015

Leslie AB, Beaulieu JM, Rai HS, Crane PR, Donoghue MJ, Mathews S (2012) Hemisphere-scale differences in conifer evolutionary dynamics. Proc Natl Acad Sci U S A **109**: 16217–21

Maherali H, Pockman WT, Jackson RB (2004) Adaptive variation in the vulnerability of woody plants to xylem cavitation. Ecology **85**: 2184–2199

Mao K, Milne RI, Zhang L, Peng Y, Liu J, Thomas P, Mill RR, Renner SS (2012) Distribution of living Cupressaceae reflects the breakup of Pangea. Proc Natl Acad Sci U

S A **109**: 7793–8

Martin HA (2006) Cenozoic climatic change and the development of the arid vegetation in Australia. J Arid Environ **66**: 533–563

Mciver AEE (2001) Cretaceous Widdringtonia Endl. (Cupressaceae) from North America. Int J Plant Sci **162**: 937–961

Orme D (2013) The caper package : comparative analysis of phylogenetics and evolution in R. R Packag version 05, 2 1–36

Pagel M (1999) Inferring the historical patterns of biological evolution. Nature **401**: 877–84

Pammenter NW, Vander Willigen C (1998) A mathematical and statistical analysis of the curves illustrating vulnerability of xylem to cavitation. Tree Physiol **18**: 589–593

Paull R, Hill RS (2010) Early Oligocene Callitris and Fitzroya (Cupressaceae) from Tasmania. Am J Bot **97**: 809–20

Pfautsch S, Harbusch M, Wesolowski A, Smith R, Macfarlane C, Tjoelker MG, Reich PB, Adams MA (2015) Climate determines vascular traits in the ecologically diverse genus *Eucalyptus*. Ecol Lett n/a–n/a

Piggin J, Bruhl JJ (2010) Phylogeny reconstruction of Callitris Vent. (Cupressaceae) and its allies leads to inclusion of Actinostrobus within Callitris. Aust Syst Bot **23**: 69–93

Pittermann J (2005) Torus-Margo Pits Help Conifers Compete with Angiosperms. Science (80-) **310**: 1924–1924

Pittermann J, Choat B, Jansen S, Stuart SA, Lynn L, Dawson TE (2010) The relationships between xylem safety and hydraulic efficiency in the Cupressaceae: the evolution of pit membrane form and function. Plant Physiol **153**: 1919–31

Pittermann J, Sperry JS, Hacke UG, Wheeler JK, Sikkema EH (2005) Torus-Margo Pits Help Conifers Compete with Angiosperms. Science (80-) **310**: 1924–1924

Pittermann J, Sperry JS, Hacke UG, Wheeler JK, Sikkema EH (2006a) Inter-tracheid pitting and the hydraulic efficiency of conifer wood: The role of tracheid allometry and cavitation protection. Am J Bot **93**: 1265–1273

Pittermann J, Sperry JS, Wheeler JK, Hacke UG, Sikkema EH (2006b) Mechanical reinforcement of tracheids compromises the hydraulic efficiency of conifer xylem. Plant,

Cell Environ **29**: 1618–1628

Pittermann J, Stuart SA, Dawson TE, Moreau A (2012) Cenozoic climate change shaped the evolutionary ecophysiology of the Cupressaceae conifers. Proc Natl Acad Sci U S A **109**: 9647–52

Polge H (1966) Établissement des courbes de variation de la densité du bois par exploration densitométrique de radiographies d ' échantillons prélevés à la tarière sur des arbres vivants Applications dans les domaines Technologique et Physiologique. Ann des Sci For **23**: 215

Poorter L, McDonald I, Alarcón A, Fichtler E, Licona JC, Peña-Claros M, Sterck F, Villegas Z, Sass-Klaassen U (2010) The importance of wood traits and hydraulic conductance for the performance and life history strategies of 42 rainforest tree species. New Phytol **185**: 481–492

Pye MG, Gadek P a., Edwards KJ (2003) Divergence, diversity and species of the Australasian Callitris (Cupressaceae) and allied genera: Evidence from ITS sequence data. Aust Syst Bot **16**: 505–514

Quantum G (2011) Development Team, 2012. Quantum GIS Geographic Information System. Open Source Geospatial Foundation Project. [http://qgis.osgeo.org]

R Core Team (2015) R: A language and environment for statistical computing 3.12.

Revell LJ (2013) Two new graphical methods for mapping trait evolution on phylogenies. Methods Ecol Evol **4**: 754–759

Sáenz-Romero C, Lamy J-B, Loya-Rebollar E, Plaza-Aguilar A, Burlett R, Lobit P, Delzon S (2013) Genetic variation of drought-induced cavitation resistance among Pinus hartwegii populations from an altitudinal gradient. Acta Physiol Plant **35**: 2905–2913

Santiago LS, Goldstein G, Meinzer FC, Fisher JB, Machado K, Woodruff D, Jones T (2004) Leaf photosynthetic traits scale with hydraulic conductivity and wood density in Panamanian forest canopy trees. Oecologia **140**: 543–50

Smith SA, Beaulieu JM, Donoghue MJ (2009) Mega-phylogeny approach for comparative biology: an alternative to supertree and supermatrix approaches. BMC Evol Biol **9**: 37

Sperry JS, Hacke UG, Pittermann J (2006) Size and function in conifer tracheids and

angiosperm vessels. Am J Bot **93**: 1490–1500

Sperry JS, Meinzer FC, McCulloh KA (2008) Safety and efficiency conflicts in hydraulic architecture: scaling from tissues to trees. Plant Cell Environ **31**: 632–645

Stocker TF, Qin D, Plattner G-K, Tignor MM, Allen SK, Boschung J, Nauels A, Xia Y, Bex V, Midgley PM (2013) IPCC, 2013: Climate Change 2013: The Physical Science Basis. Contribution of Working Group I to the Fifth Assessment Report of the Intergovernmental Panel on Climate Change. Cambridge University Press, Cambridge, United Kingdom and New York, NY, USA

Tamura K, Peterson D, Peterson N, Stecher G, Nei M, Kumar S (2011) MEGA5: molecular evolutionary genetics analysis using maximum likelihood, evolutionary distance, and maximum parsimony methods. Mol Biol Evol **28**: 2731–9

Trabucco A, Zomer RJ (2009) Global Aridity Index (Global-Aridity) and Global Potential Evapo-Transpiration (Global-PET) Geospatial Database. CGIAR Consort. Spat. Information.

Tyree MT, Zimmermann MH (2002) Xylem Structure and the Ascent of Sap. Springer Science & Business Media

Urli M, Porté AJ, Cochard H, Guengant Y, Burlett R, Delzon S (2013) Xylem embolism threshold for catastrophic hydraulic failure in angiosperm trees. Tree Physiol **33**: 672–83

Vaganov EA, Hughes MK, Shashkin A V (2006) Growth Dynamics of Conifer Tree Rings: Images of Past and Future Environments. Springer

Wilf P, Little SA, Iglesias A, Del Carmen Zamaloa M, Gandolfo MA, Cúneo NR, Johnson KR (2009) Papuacedrus (Cupressaceae) in Eocene Patagonia: A new fossil link to Australasian rainforests. Am J Bot **96**: 2031–47

Yang ZY, Ran JH, Wang XQ (2012) Three genome-based phylogeny of Cupressaceae s.l.: Further evidence for the evolution of gymnosperms and Southern Hemisphere biogeography. Mol Phylogenet Evol **64**: 452–470

Zachos J, Pagani M, Sloan L, Thomas E, Billups K (2001) Trends, rhythms, and aberrations in global climate 65 Ma to present. Science (80-) **292**: 686–693

Supplementary information

Supplementary tables:

Table S1: GenBank accessions for the sequences used in this study, and model parameters specified for the BEAST analysis.

Table S2: Trait data for the 23 species studied in this paper. Abbreviations as follows: N = number of individuals measured for hydraulic traits; P50 = xylem pressure inducing 50% loss of hydraulic conductance; slope = slope of the vulnerability curve; Kmax = xylem specific hydraulic conductance; WD = wood density; MeanD, MinD, MaxD = mean, minimum and maximum tracheid diameters respectively; Ds = hydraulically weighted tracheid diameter calculated as D^5/D^4; Dh = hydraulically weighted diameter as (Tyree and Zimmermann, 2002): $D_h = [\frac{\sum D^4}{N}]^{1/4}$; Vwr = void to wood ratio (%); TF = tracheid frequency (cm^{-2}); Kth = theoretical hydraulic conductance (calculated using the Hagen-Poiseuille law; N_tracheids = total number of tracheids measured for each species. PCT = frequency of callitroid thickening; CTT = callitroid thickening type; WT = wart type; WD = wart density; WN = wart nodularity (these parameters derived from Heady et al. (1994) and Heady & Evans (2000), taken from Piggin & Bruhl (2010); Median values over each species distribution for AI = Aridity index, Med_bio12 = annual precipitations and Med_bio17 = driest quarter rainfall. Variables starting with SE or ending with e are standard error.

Table S3. Correlation between climate variables and P_{50}, tracheid diameter, and wood density. We tested means and medians of species climates, and log transformed data (on the medians), and correcting for phylogenetic relatedness using PGLS.

Table S1

Species	RBCL	MATK	TRNL	ITS1	PSBB	PETB	NEEDLY	LEAFY
Actinostrobus acuminatus		AF152175.1		AY178417.1				
Actinostrobus arenarius	JF725937.1	JF725837.1	JF725897.1		JF725977.1	JF725790.1		
Actinostrobus pyramidalis	JF725931.1	JF725831.1	JF725891.1	AY178415.1	JF725970.1	JF725783.1	HQ245712.1	HQ245806.1
Callitris canescens	JF725945.1	JF725845.1	JF725905.1	AY178411.1	JF725985.1	JF725798.1		
Callitris columellaris			AB723688.1	AY178404.1			HQ245715.1	HQ245809.1
Callitris drummondii	JF725939.1	JF725839.1	JF725899.1	AY178423.1	JF725979.1	JF725792.1		
Callitris endlicheri	JF725932.1	JF725832.1	AY988417.1	AY178425.1	JF725971.1	JF725784.1		
Callitris glaucophylla	KM895763.1		AB723697.1					
Callitris gracilis			AB723693.1					
Callitris intratropica			AB723690.1	AY178400.1				
Callitris macleayana	JF725933.1	JF725833.1	JF725893.1	AY178421.1	JF725972.1	JF725785.1	HQ245716.1	HQ245810.1
Callitris muelleri	JF725924.1	JF725824.1	JF725884.1	AY178412.1	JF725963.1	JF725776.1		
Callitris oblonga				AY178429.1				
Callitris preissii	JF725940.1	JF725840.1	JF725900.1		JF725980.1	JF725793.1		
Callitris rhomboidea	JF725925.1	JF725825.1	JF725885.1	AY178406.1	JF725964.1	JF725777.1	HQ245717.1	HQ245811.1
Callitris sulcata	JF725941.1	JF725841.1	JF725901.1	AY178422.1	JF725981.1	JF725794.1		
Callitris tuberculata				AY178426.1				
Callitris verrucosa	JF725942.1	JF725842.1	AB723695.1	HM116955.1	JF725982.1	JF725795.1		
Diselma archeri	JF725926.1	JF725826.1	JF725886.1		JF725965.1	JF725778.1	HQ245730.1	HQ245823.1
Fitzroya cupressoides	JF725916.1	JF725816.1	JF725876.1		JF725955.1	JF725768.1	HQ245732.1	HQ245825.1
Libocedrus bidwillii	JF725927.1	JF725827.1	JF725887.1		JF725966.1	JF725779.1	HQ245746.1	HQ245838.1
Libocedrus yateensis		HQ245902.1					HQ245748.1	HQ245840.1
Neocallitropsis pancheri	JF725934.1	JF725834.1	JF725894.1	AY178420.1	JF725974.1	JF725787.1	HQ245751.1	HQ245843.1
Papuacedrus papuana	JF725935.1	JF725835.1	JF725895.1		JF725975.1	JF725788.1	HQ245752.1	HQ245844.1
Pilgerodendron uviferum	JF725929.1	HQ245907.1	JF725889.1		JF725968.1	JF725781.1	HQ245753.1	HQ245845.1
Widdringtonia nodiflora	JF725930.1	JF725830.1	AY988418.1		JF725969.1	JF725782.1	HQ245766.1	HQ245856.1
Alignment length (nucleotides)	1278	1551	395	1051	1344	1289	3705	2942
Substitution model (BEAST)	HKY+G	HKY+G	HKY	HKY+G	HKY+G	HKY+G	HKY+I	TN93+G

Table S2

Species	N	P50	slope	Kmax	WD	WDe	P50e	slopee	Kmaxe	MeanD	Ds	MinD	Max_D	Dh
Actinostrobus_acuminatus	10	-11.52	15.11	0.00044	0.68	0.012	0.75	0.66	0.000063	10.86	14.30	3.41	20.78	18.27
Actinostrobus_arenarius	11	-15.16	11.13	0.00061	0.69	0.025	0.52	0.87	0.000030	10.26	13.37	3.09	18.86	15.17
Actinostrobus_pyramidalis	12	-11.78	17.83	0.00051	0.58	0.021	0.36	1.29	0.000045	9.26	12.30	2.85	17.19	15.74
Callitris_baileyi	3	-11.37	20.35	0.00062	0.56	0.004	0.44	0.58	0.000023	11.31	13.99	3.56	19.92	12.40
Callitris_canescens	21	-16.90	9.87	0.00029	0.70	0.017	0.40	0.62	0.000024	9.08	11.39	2.93	15.89	13.68
Callitris_columellaris	3	-15.80	15.23	0.00029	0.66	0.033	0.18	2.62	0.000099	11.27	13.16	4.46	18.34	12.03
Callitris_drummondii	13	-13.11	18.16	0.00048	0.62	0.031	0.28	0.99	0.000033	10.15	12.30	3.24	17.17	16.47
Callitris_endlicheri	9	-12.28	17.58	0.00076	0.66	0.008	0.63	2.01	0.000057	13.18	16.37	4.43	23.21	14.51
Callitris_glaucophylla	13	-14.37	19.81	0.00065	0.74	0.029	0.33	1.30	0.000071	11.02	13.37	3.93	18.99	15.16
Callitris_gracilis	8	-12.49	19.54	0.00036	0.61	0.010	0.28	1.27	0.000083	10.37	12.68	3.93	18.07	11.29
Callitris_intratropica	5	-12.81	14.24	0.00125	0.62	0.011	0.73	1.75	0.000050	13.22	15.60	4.87	21.86	14.20
Callitris_macleayana	3	-8.07	27.22	0.00087	0.60	0.025	0.33	3.58	0.000277	15.91	20.31	5.01	28.54	17.72
Callitris_monticola	7	-8.84	18.52	0.00076	0.50	0.018	0.34	1.62	0.000098	13.96	16.03	6.38	22.11	14.78
Callitris_muelleri	8	10.10	20.46	0.00057	0.47	0.001	0.49	1.45	0.000075	10.22	12.54	3.00	18.67	16.69
Callitris_neocaledonica	11	-3.83	50.67	0.00055	0.69	0.035	0.12	7.80	0.000046	13.57	17.31	2.97	26.03	22.50
Callitris_oblonga	4	10.88	17.09	0.00019	0.57	0.020	0.85	2.13	0.000014	12.71	14.58	5.08	19.83	13.47
Callitris_preissii	3	14.97	15.56	0.00031	0.65	0.013	0.50	2.02	0.000062	12.56	14.78	4.65	20.44	13.48
Callitris_rhomboidea	8	-10.32	27.46	0.00026	0.61	0.040	0.53	5.64	0.000060	13.66	15.57	5.57	21.50	14.44
Callitris_roei	9	-12.21	12.37	0.00034	0.67	0.017	0.34	0.90	0.000020	9.73	12.90	3.39	19.96	16.35
Callitris_sulcata	9	-8.24	17.91	0.00056	0.68	0.018	0.45	1.75	0.000043	14.14	18.82	3.82	26.61	24.12
Callitris_tuberculata	11	-18.82	13.99	0.00039	0.72	0.021	0.56	1.16	0.000035	9.04	11.27	3.28	15.42	12.85
Callitris_verrucosa	9	-11.92	18.30	0.00052	0.62	0.019	0.17	2.22	0.000082	9.87	12.45	3.32	17.60	16.30
Neocallitropsis_pancheri	18	-4.14	46.58	0.00047	0.74	0.037	0.10	4.84	0.000036	13.16	18.92	3.47	26.23	23.30

Table S2 (continued)

Species	Vwr	TF	Kth	meanD_SE	Ds_SE	MinD_SE	Max_D_SE	Dh_SE	Vwr_SE	TF_SE	Kth_SE	N_tracheids
Actinostrobus_acuminatus	27.12	268577.40	0.0073	0.17	0.78	0.57	2.59	0.52	0.20	10605.75	0.0005	798.00
Actinostrobus_arenarius	24.48	273552.97	0.0046	0.52	0.61	0.21	0.67	1.99	1.31	14040.35	0.0016	1782.00
Actinostrobus_pyramidalis	23.00	309638.11	0.0047	0.26	0.54	0.41	0.87	0.51	0.87	13700.23	0.0005	920.00
Callitris_baileyi	29.78	281954.98	0.0017	1.13	0.94	0.15	1.09	1.06	2.88	28767.34	0.0004	1447.00
Callitris_canescens	23.33	345407.86	0.0032	0.53	0.54	0.28	0.57	0.98	1.14	26381.42	0.0007	3210.00
Callitris_columellaris	25.14	240256.04	0.0012	0.20	0.11	0.42	0.92	0.11	0.96	1753.69	0.0001	822.00
Callitris_drummondii	28.82	335216.91	0.0061	0.35	0.22	0.40	0.36	0.42	1.60	13745.63	0.0006	996.00
Callitris_endlicheri	35.49	241814.88	0.0027	0.35	0.73	0.38	1.62	0.50	1.64	3447.33	0.0003	1241.00
Callitris_glaucophylla	27.00	268331.28	0.0047	0.44	0.53	0.14	0.57	1.86	1.34	12087.07	0.0016	2224.00
Callitris_gracilis	25.92	287995.48	0.0012	0.26	0.38	0.04	0.83	0.29	2.10	18056.43	0.0001	1478.00
Callitris_intratropica	25.96	180240.74	0.0018	0.50	0.67	0.07	1.93	0.57	1.42	14051.18	0.0002	925.00
Callitris_macleayana	29.39	137762.38	0.0034	1.16	0.95	0.64	0.58	1.13	1.88	10464.27	0.0006	707.00
Callitris_monticola	34.11	215119.76	0.0025	0.62	0.71	0.43	1.29	0.67	1.37	12041.65	0.0003	1104.00
Callitris_muelleri	27.72	319561.97	0.0061	0.62	0.42	0.45	0.62	0.80	1.60	28719.78	0.0008	1640.00
Callitris_neocaledonica	25.77	165387.38	0.0106	0.87	0.99	1.26	1.76	1.38	2.57	10357.61	0.0021	1960.00
Callitris_oblonga	38.79	293451.41	0.0024	0.22	0.37	0.18	0.64	0.27	0.36	11812.45	0.0001	1506.00
Callitris_preissii	31.92	248439.94	0.0020	0.82	1.03	0.70	1.39	0.86	1.51	26790.24	0.0003	1275.00
Callitris_rhomboidea	38.70	260326.09	0.0028	1.13	1.27	0.55	1.33	1.20	1.59	29906.89	0.0006	1336.00
Callitris_roei	23.77	293819.64	0.0052	0.23	0.23	0.22	0.88	0.35	0.63	6620.98	0.0003	873.00
Callitris_sulcata	27.67	160662.03	0.0132	0.77	0.86	0.17	1.14	1.21	1.81	17763.62	0.0017	1904.00
Callitris_tuberculata	22.41	324951.65	0.0025	0.23	0.38	0.32	0.73	1.11	1.06	12606.13	0.0007	2082.00
Callitris_verrucosa	24.27	304753.00	0.0052	0.75	0.91	0.91	1.27	1.20	0.98	48740.60	0.0009	1564.00
Neocallitropsis_pancheri	24.46	156780.49	0.0116	0.70	0.95	0.14	1.65	1.18	2.27	5025.47	0.0022	1858.00

Table S2 (continued)

Species	PCT	CTT	WT	WD	WN	Med_AI	Med_bio12	Med_bio17	SE_AI	SE_bio12	SE_bio17
Actinostrobus_acuminatus	c	b	b	NA	NA	0.39	576.00	34.00	0.01	13.42	0.54
Actinostrobus_arenarius	c	b	b	NA	NA	0.26	408.50	32.00	0.01	10.65	0.87
Actinostrobus_pyramidalis	c	b	b	NA	NA	0.48	698.00	36.00	0.02	22.49	1.47
Callitris_baileyi	b	a	b	b	b	0.59	878.00	119.00	0.02	20.95	2.51
Callitris_canescens	c	b	b	b	c	0.28	372.00	43.00	0.00	3.87	0.40
Callitris_columellaris	b	a	b	b	b	0.22	367.00	42.00	0.02	22.92	3.23
Callitris_drummondii	c	b	b	b	b	0.37	495.00	69.00	0.01	8.14	0.71
Callitris_endlicheri	c	b	b	b	b	0.49	696.00	134.00	0.00	4.22	0.77
Callitris_glaucophylla	c	b	b	b	b	0.32	459.00	95.00	0.00	2.53	0.55
Callitris_gracilis	c	b	b	b	b	0.32	421.00	59.00	0.00	3.74	0.43
Callitris_intratropica	b	a	a	a	a	0.69	1232.50	7.00	0.00	6.78	0.41
Callitris_macleayana	a	a	a	a	a	1.32	1690.00	195.00	0.03	37.04	4.77
Callitris_monticola	b	a	b	c	b	0.94	1220.00	166.00	0.02	27.14	1.83
Callitris_muelleri	b	a	b	c	b	1.07	1233.00	193.00	0.02	14.70	2.25
Callitris_neocaledonica	a	a	a	a	a	2.03	2320.00	353.00	0.04	34.39	6.38
Callitris_oblonga	a	a	b	c	c	0.80	918.00	161.00	0.01	18.65	1.87
Callitris_preissii	c	b	b	b	b	0.26	363.00	51.00	0.01	9.41	0.80
Callitris_rhomboidea	b	a	b	b	c	0.83	924.00	165.00	0.01	15.00	2.24
Callitris_roei	c	b	b	b	b	0.29	387.00	58.00	0.00	5.24	0.71
Callitris_sulcata	a	a	a	b	a	0.98	1252.00	176.00	0.03	29.23	4.68
Callitris_tuberculata	c	b	b	b	b	0.21	304.00	50.00	0.01	6.99	0.75
Callitris_verrucosa	c	b	b	b	b	0.25	345.00	57.00	0.00	1.92	0.44
Neocallitropsis_pancheri	NA	NA	NA	NA	NA	1.79	2162.00	315.00	0.02	27.00	4.58

Table S3.

		Median			Mean			Log transformed			PGLS			
		R^2	p	sig	R^2	p	sig	R^2	p	sig	lambda	R^2	p	sig
P50	Mean Annual Rainfall	**0.7833**	**0.000**	***	**0.761**	**0.000**	***	**0.732**	**0.000**	***	**0.000**	**0.806**	**0.001**	***
	Driest Quarter Rainfall	**0.7216**	**0.000**	***	**0.711**	**0.000**	***	**0.462**	**0.000**	***	**0.000**	**0.790**	**0.001**	***
	Aridity Index	**0.8055**	**0.000**	***	**0.788**	**0.000**	***	**0.769**	**0.000**	***	**0.000**	**0.929**	**0.000**	***
Kmax	Mean Annual Rainfall	0.0863	0.094	ns	0.065	0.127	ns	0.119	0.060	ns	0.000	-0.082	0.551	ns
	Driest Quarter Rainfall	-0.0469	0.906	ns	-0.047	0.940	ns	-0.037	0.648	ns	0.000	-0.036	0.423	ns
	Aridity Index	0.0075	0.292	ns	-0.009	0.378	ns	0.047	0.163	ns	0.000	-0.142	0.958	ns
Dh	Mean Annual Rainfall	**0.4553**	**0.000**	***	**0.429**	**0.000**	***	**0.344**	**0.002**	**	**0.000**	**0.739**	**0.002**	**
	Driest Quarter Rainfall	**0.4056**	**0.001**	***	**0.404**	**0.001**	***	**0.180**	**0.025**	*	**0.000**	**0.650**	**0.005**	**
	Aridity Index	**0.4761**	**0.000**	***	**0.451**	**0.000**	***	**0.360**	**0.001**	**	**0.000**	**0.766**	**0.001**	**
WD	Mean Annual Rainfall	-0.0418	0.7362	ns	-0.0430	0.7637	ns	0.022	0.234	ns	0.000	0.140	0.114	ns
	Driest Quarter Rainfall	-0.0469	0.9081	ns	-0.0471	0.9167	ns	-0.026	0.516	ns	0.000	0.060	0.211	ns
	Aridity Index	-0.0426	0.7547	ns	-0.0428	0.7580	ns	0.032	0.204	ns	0.000	0.197	0.072	ns

Supplementary Figures:

Figure S1: Timetree from the BEAST analysis using (A) only cpDNA and (B) only nuclear sequences.

Figure S2: Tracheid length and number of pits per tracheid against P_{50} and k_s. Partial datasets only. Linear models fit through the data are shown. Linear regression lines are shown, with the adjusted R^2. "***" indicates p-values < 0.001, and "ns" indicates non-significance at α=0.05.

Figure S1

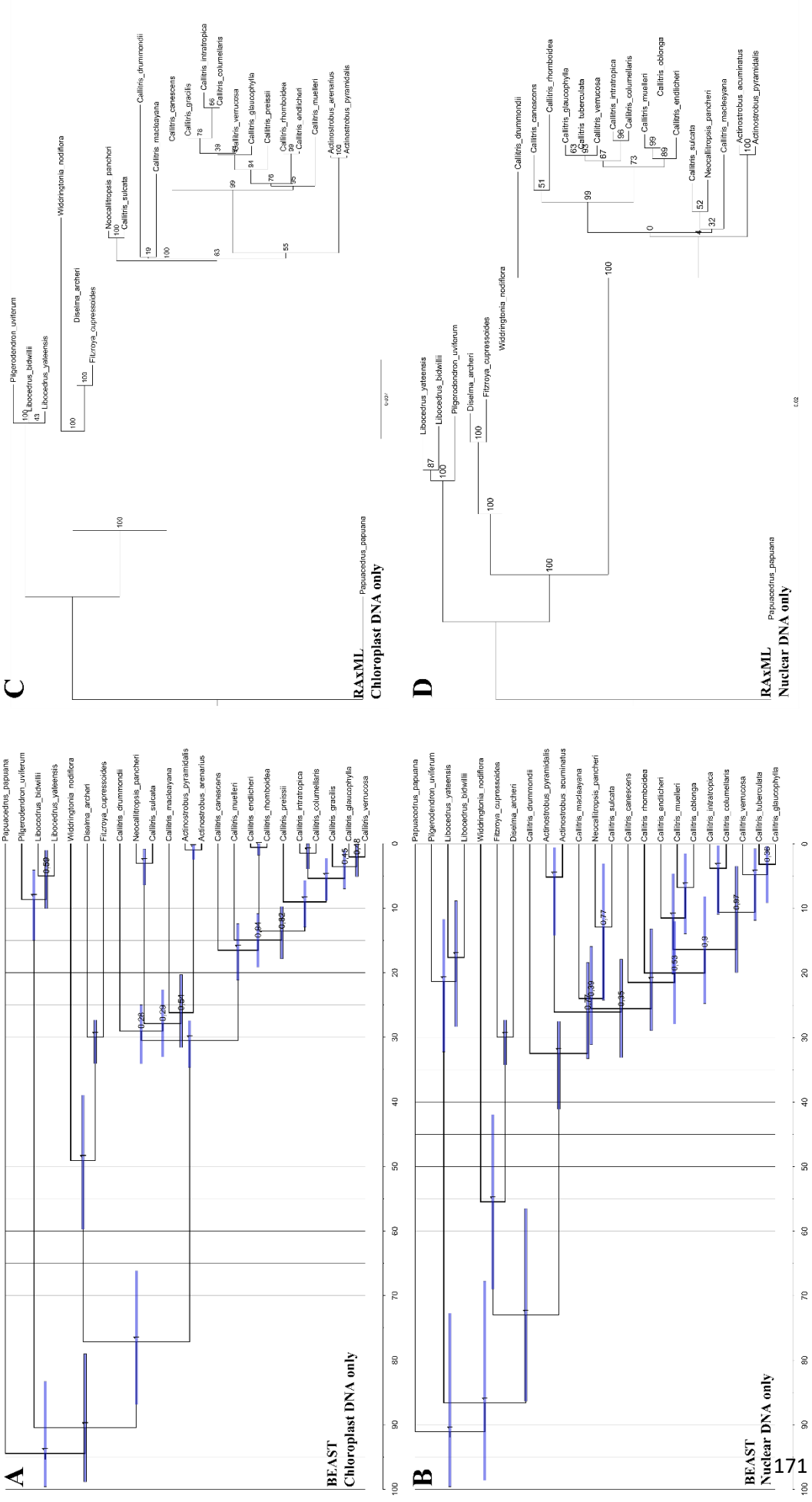
A
BEAST
Chloroplast DNA only
B
BEAST
Nuclear DNA only
C
RAxML
Chloroplast DNA only
D
RAxML
Nuclear DNA only

Figure S2.

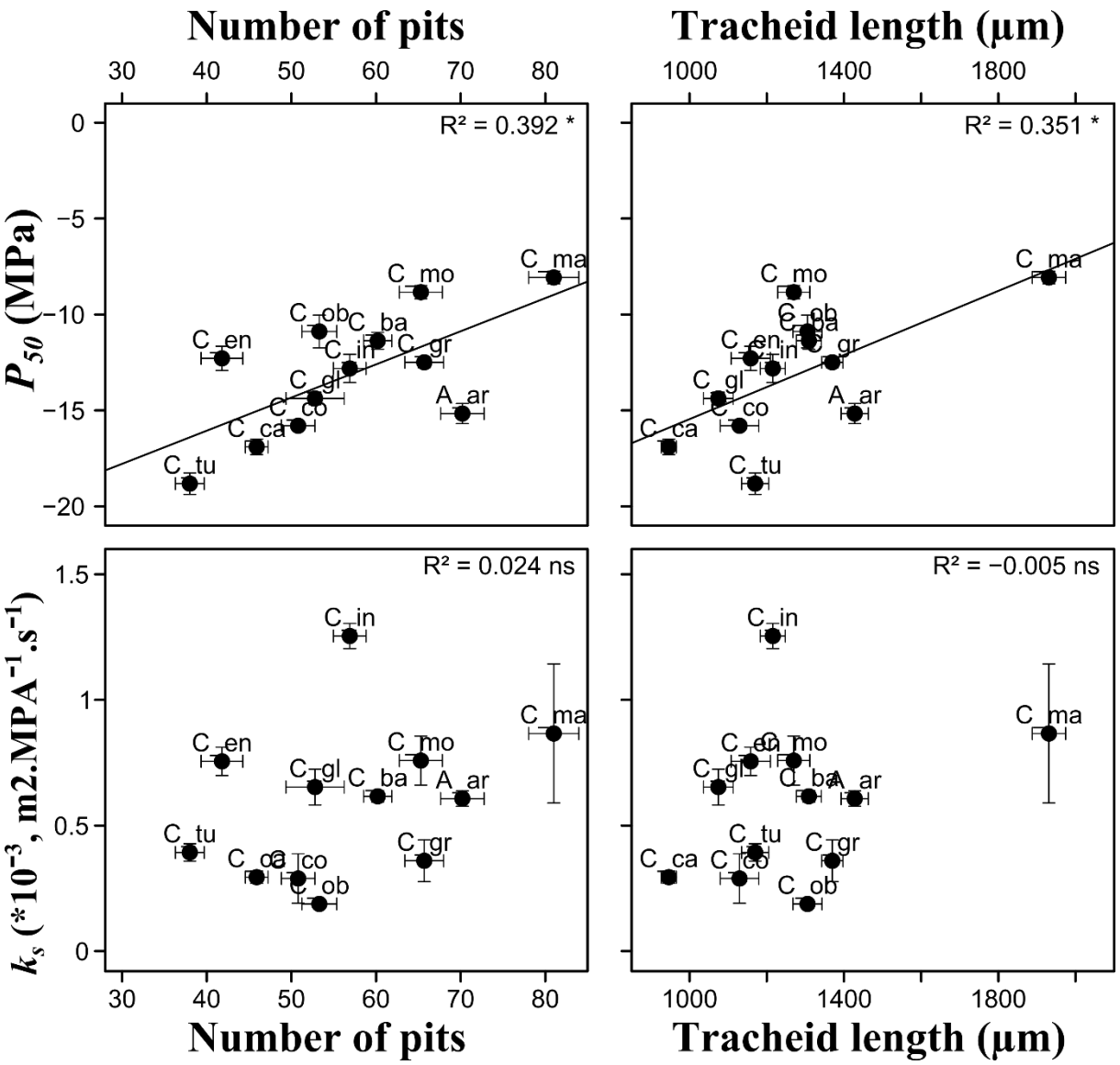

References

Heady RD, Evans PD (2000) Callitroid (callitrisoid) thickening in Callitris. IAWA Journal **21**: 293–319

Heady RD, R.B. C, Donnelly CF, Evans PD (1994) Morphology of warts in the tracheids of cypress pine (Callitris Vent.). IAWA Journal **15**: 265–281

Piggin J, Bruhl JJ (2010) Phylogeny reconstruction of Callitris Vent. (Cupressaceae) and its allies leads to inclusion of Actinostrobus within Callitris. Australian Systematic Botany **23**: 69–93

Tyree MT, Zimmermann MH (2002) Xylem Structure and the Ascent of Sap. Springer Science & Business Media

Discussion

1. Summary of main results:

The aim of this project was to investigate conifer physiology and ecology from an evolutionary point of view.

In Part I, we presented an unprecedented physiological database, spanning the whole range of conifer diversity and ecology. We uncovered huge variation in embolism resistance, especially within Cupressaceae, Taxaceae and Podocarpaceae, but generally little variation below the genus level (i.e. species from the same genera have similar trait values - but there are exceptions, see Part III). We highlight the adaptive nature of embolism resistance, with a meaningful link between species climate and P_{50}, except for the Pinaceae family, where there is little variation in P50 despite broad climatic species preferences (Chapter 1). By focusing on extremely resistant species we have extended the range of known embolism-resistance up to the theoretical limit of liquid-water transport. It appears that plants' xylem has been driven to this physical boundary by natural selection in some of the most xeric environments on the planet (Chapter 2). Finally, across over a hundred species of conifers, we found an evolutionary relationship between air-seeding pressure (P_{50}) and the diameter of the torus relative to the pit aperture (Chapter 3). While the air-seeding mechanism leading to embolism was well-established for angiosperms, i.e. breakage of an air-sap meniscus within the pit-membrane (Tyree and Zimmermann, 2002), several possible locations were hypothesized in torus-bearing gymnosperms (Delzon et al., 2010; Jansen et al., 2012).

In Part II, we combined this physiological data with phylogenetics and various evolutionary modelling approaches. First, we constructed a time-calibrated phylogeny for over three hundred species of conifers, which we combined with the embolism resistance database in an evolutionary framework (Chapter 4). We detected multiple evolutionary dynamics, with several major upticks in the rate of evolution of P_{50}, together with jumps to higher diversification rates. We further found a significant association between higher diversification rates and increased embolism resistance, making water-availability a major driver of conifer diversification.

Finally, in Part III of this thesis, we examined in detail the evolution of the most embolism-resistant genus, *Callitris* and its close relatives *Actinostrobus* and *Neocallitropsis* (Chapter 5). We described the remarkable adaptive radiation into dry environments of this clade, which occurred during a trend of increasing aridity across Australia and New Caledonia over the last 30 million years. Additionally, we show the role of climate in determining traits pertaining to

resistance to embolism, but when examining other xylem traits, we found no evidence of trade-offs between xylem safety and efficiency in this group.

2. Conifer physiology – global variation

a. Hydraulic traits and strategies in Conifers

Embolism resistance is an adaptive trait directly linked to survival, and therefore it is somewhat evident that it should vary widely in an ancient and wide-ranging clade such as conifers. However, an extensive and systematic approach to sampling and employing the same standard procedure across species has allowed us to unearth some surprising patterns, notably the remarkable scale and distribution of this variation. Firstly, P_{50} varies approximately 10-fold across all conifers, yet very different patterns are observed at the family level, with very little variation in Pinaceae but the whole range of variability in Cupressaceae. For the most part, the genus to which a species belongs is a good predictor of embolism resistance, responsible for 62% of variation of P_{50}, yet some ecologically diverse genera offer a wide range of P_{50} (e.g. *Callitris* – P_{50} from -3.8 to -18.8 MPa). Other genera of even wider ecology and diversity have not attained this level of variation, e.g. *Pinus* with P_{50} varying only from -2.7 to -5 MPa. Some clades seem to be restricted to a narrow range of embolism resistance, while others display remarkable evolutionary lability. Zooming in even further to the species level, our knowledge so far indicates low levels of variation for this trait. For example, a comparison of populations spanning the broad range of *Pinus pinaster* planted in a common garden showed they are more similar for embolism resistance than expected under genetic drift (Lamy et al., 2012). This is interpreted as a sign of uniform selection (Lamy et al., 2011), with all populations selected towards an optimum value, which is not therefore climate-dependent. Similar results were found in common garden experiments for other pine species, i.e. *Pinus hartwegii* (Sáenz-Romero et al., 2013), *Pinus halepensis* (David-Schwartz et al., 2016, N. Martin-StPaul, pers. comm.), and in beech (*Fagus sylvatica*; Wortemann et al., 2011; Hajek et al., 2016). We have also investigated intra-species variation in several Mexican conifers (Saenz-Romero et al., accepted; see Annex 1). We show that there are no significant differences in P_{50} between natural populations and individuals grown in a common garden in spite of marked climatic differences. It's worth noting that some species show phenotypic plasticity for this trait, with a slight trend of increasing embolism resistance with increasing aridity in natural populations of *P. canariensis* (López et al., 2013) and in *Fagus sylvatica* (Aranda et al., 2014; Schuldt et al., 2015).

So why is embolism resistance constrained in some groups, and labile in others? These different patterns reflect differences in water management strategies. Water-loss is monitored by opening and closure of stomata, which is governed by the turgor of the guard-cells. By regulating overall stomatal conductance, plants can limit water-loss during drought, at the cost of reduced photosynthesis. If plants kept stomata fully open during drought, leaf and xylem water potentials (φ_L and φ_x respectively) would rapidly decrease, to a point where permanent damage through embolism can occur. Plants avoid this area of dangerous water-potential by closing stomata, thereby both stopping water-flow to the leaves, with the consequence of drastically reducing photosynthesis by restricting carbon entry.

Traditionally, we separate species into two groups, i) those strongly regulating water-potential variation by limiting stomatal conductance relatively early in drought, and maintaining minimum daily (or midday) φ_L above -2 MPa, implementing a water-management strategy called isohydric. On the other hand, ii) anisohydric species follow a more reckless strategy, taking more time to close their stomata during drought and thereby allowing more variation in minimum water-potential. In fact, a broad spectrum of strategies exists between these two extremes with most species being anisohydric or slightly isohydric (moderate decline in minimum φ_L compared to pre-dawn φ_L; Martinez-Vilalta et al., 2014), and most species have stomata completely closed well before φ_L reaches -4 MPa. In conifers, the lowest φ_L reported in (Choat et al., 2012) were around -5 MPa in *Cupressus sempervirens*, *Tetraclinis articulata* and *Actinostrobus acuminatus* – which are all embolism-resistant species with P_{50} < -8.5 MPa. It seems there is convergence across species for complete stomatal closure before xylem cavitation starts to occur (i.e. the inflexion point of the vulnerability curves P_{12}) (Brodribb et al., 2003; Domec et al., 2008). Species across all environments have similar hydraulic safety margins, which means that trees' vascular system is primed to close stomata before embolism starts to affect their capacity to transport water (Choat et al., 2012). Based on recent work, we hypothesize that the driving factor behind the magnitude of the pressure drop in the xylem (i.e. the difference between minimum of midday φ_L and pre-dawn φ_L) and the risk that embolisms can form (i.e. mortality unless P_{50} is adapted) is the degree of "leakiness" of fully closed stomata in the case of prolonged drought. The important parameter is not when stomata close (since they are always completely closed when drought reaches potentially dangerous levels) but how "leaky" they are, and to which extent species limit the pressure drop *once all meaningful gas exchange has ceased*.

Two divergent pathways for stomatal closure have been brought to light in line with this dichotomy regarding water-management (Brodribb and McAdam, 2013; Brodribb et al., 2014). Some plants reduce guard-cell turgor with hormonal signals (using abscisic acid), while others use leaf desiccation to passively reduce stomatal conductance under prolonged drought conditions (Brodribb et al., 2014). The first strategy (called Rising or R-type) offers the advantage of rapid reaction to changing soil water-content by closing stomata, avoiding continued water-loss. However, high ABA levels make re-opening of stomata a lengthy process, slowing down recovery of photosynthesis with the return of well hydrated soils. For the anisohydric strategy (termed Peaking or P-type), since ABA levels drop as drought intensifies, if re-watered these species rapidly recover guard-cell turgor and normal functioning. While both strategies exist in low rainfall environments (Brodribb et al., 2014), conifer species with embolism-resistant xylem and the more "risky" strategy seem to stretch further into regions with regular prolonged drought (such as Callitris species in Australia).

Since proponents of both strategies close stomata early on in drought, transpiration and photosynthesis always stop before damage can be done to the xylem. So when does embolism occur during drought? Recent work points to prolonged water-loss in some species despite stomata being completely closed (Brodribb et al., 2014). ABA-induced closure seems to seal stomata more effectively, since the R-type species reach minimum g_s much more rapidly from 90% stomatal closure (3 days vs. 20 days for P-type). Furthermore, minimum g_s is higher in P-type species, meaning leaves continue to "leak" water-vapor after full stomatal closure. This leakage is overwhelmingly due to the stomatal surface, pointing to inefficient sealing by the guard-cells (Brodribb et al., 2014).

Both strategies have advantages, for example isohydry allows species to protect themselves from drops xylem tension during most mild droughts, while anisohydry allows species to recover leaf function more rapidly upon re-watering. Although the taxonomic resolution in (Brodribb et al., 2014) is insufficient to draw definite conclusions as to when and how these strategies evolved, it seems the ABA driven strategy is ancestral and the passive leaf-desiccation strategy derived in Taxaceae, and crown Cupressaceae groups. These clades correspond to the clades having evolved increased embolism resistance we identified in Chapter 4 of this thesis. The need for extremely resistant xylem has been at least partially explained by this "leaky stomata" hypothesis – although more extensive work involving both experimental drought and field work is needed for many species. It would be interesting for example to monitor trees in the field during extreme drought to examine when complete stomatal closure

happens in the most resistant species, to test the hypothesis that these species (P-type, anisohydric) can function for longer periods at the onset of drought, and how long it takes for them to reach minimum g_s. More generally, additional research focus is needed on the stage of drought after complete stomatal closure, since this is when embolism starts, carbon stocks are depleted and ultimately plant death can occur (see (Blackman et al., 2016).

b. Hydraulic trait interactions

It's worth reiterating here the remarkable coordination that exists between leaf and xylem hydraulics, highlighted here by these water-management strategies (Meinzer, 2002; Sperry et al., 2002; Mencuccini, 2003). Indeed, plant water-usage is the result of the combination of efficient uptake of water by the roots, safe and efficient water-transport through the xylem (in the roots, trunk, branches and leaves), and gas exchange in the leaves (photosynthesis, evaporation).

At both short (daily) and longer term (seasonal) time scales, regulation of g_s through a multitude of environmental cues and plant feedback signals are in part responsible for limiting water-loss (Nardini and Salleo, 2000; Schroeder et al., 2001; Cochard et al., 2002; Buckley, 2005). Roots detect water-stress and signal to the leaves through ABA synthesis. VPD (Vapor Pressure Deficit or "dryness" of the air) induces production of ABA in the leaves across land plants (McAdam and Brodribb, 2016). A reduction in xylem transport efficiency (due to embolism) can also induce a reduction of stomatal conductance, maintaining φ_L and therefore avoiding runaway embolism (Salleo et al., 2000). At a longer time-scale, acclimation of the whole plant hydraulic system to drought likely results in changes of carbon allocation through a reduction of leaf area relative to conducting tissue (Mencuccini, 2003), either by increased production of conductive tissue, roots, or a reduction in leaf area per stem area. As a consequence of these strong functional links at shorter time scales, physiological traits both of the leaf and the xylem interact to define the plants overall strategy regarding drought at wider adaptive and evolutionary timescales (Westoby and Wright, 2006; Pivovaroff et al., 2014). For example, seasonal minimum φ_L is related to lower leaf area:sapwood area, smaller conduit diameters, and increased wood density across a number of species (Ackerly, 2004). Wood density is negatively correlated with leaf size and leaf area:shoot dry mass across species and climates (Wright et al., 2006). It is clear that changes in any hydraulic trait will necessarily dictate changes in other related physiological traits or at least limit their range of variation.

In this thesis, our viewpoint from species level (and above) allows us to integrate over a variety of selection pressures (i.e. environmental conditions) and physiological strategies, yet limited to a group of species with comparable structures both in the xylem (i.e. tracheids, bordered-pits) and leaves (i.e. limited venation) allowing meaningful comparisons across species. One of the goals of our work was to increase our understanding of this network of xylem hydraulic traits in conifers. As discussed previously, theory predicts that xylem traits are determined at the species level by several trade-offs. 1) Embolism-resistant species expose their xylem to large tensions, so their tracheids are at increased risk of implosion. Therefore, more negative P_{50} should be related to an increase in tracheid-wall width relative to lumen diameter. Wood density is also a measure of this increased xylem construction cost, as it measures the cell wall:cell lumen ratio. 2) Increased embolism-resistance could reduce hydraulic conductance because of this reduction in tracheid diameter and changes of the inter-tracheid pit structure, for example reductions in pit-aperture.

We found some support for a relationship between xylem safety and mechanical strength across all conifer taxa. Although high wood density exists in both resistant and vulnerable species, there are no highly resistant species with soft wood and a general positive trend towards resistant, dense xylem. This is reinforced by the positive correlation between the thickness:span ratio, with a significant reduction in lumen size with increasing embolism resistance, but especially a strong increase in wall thickness. Previous studies found that the thickness:span ratio depended mostly on a decrease in tracheid diameter (Pittermann et al., 2006; Sperry et al., 2006). While we found a similar trend of smaller tracheids in resistant *Callitris* species, we did not evidence any trend for wood density. This is simply because *Callitris* wood is exceptionally dense in all species, notably the New Caledonian, more vulnerable species, which could obscure any tendency related to embolism resistance.

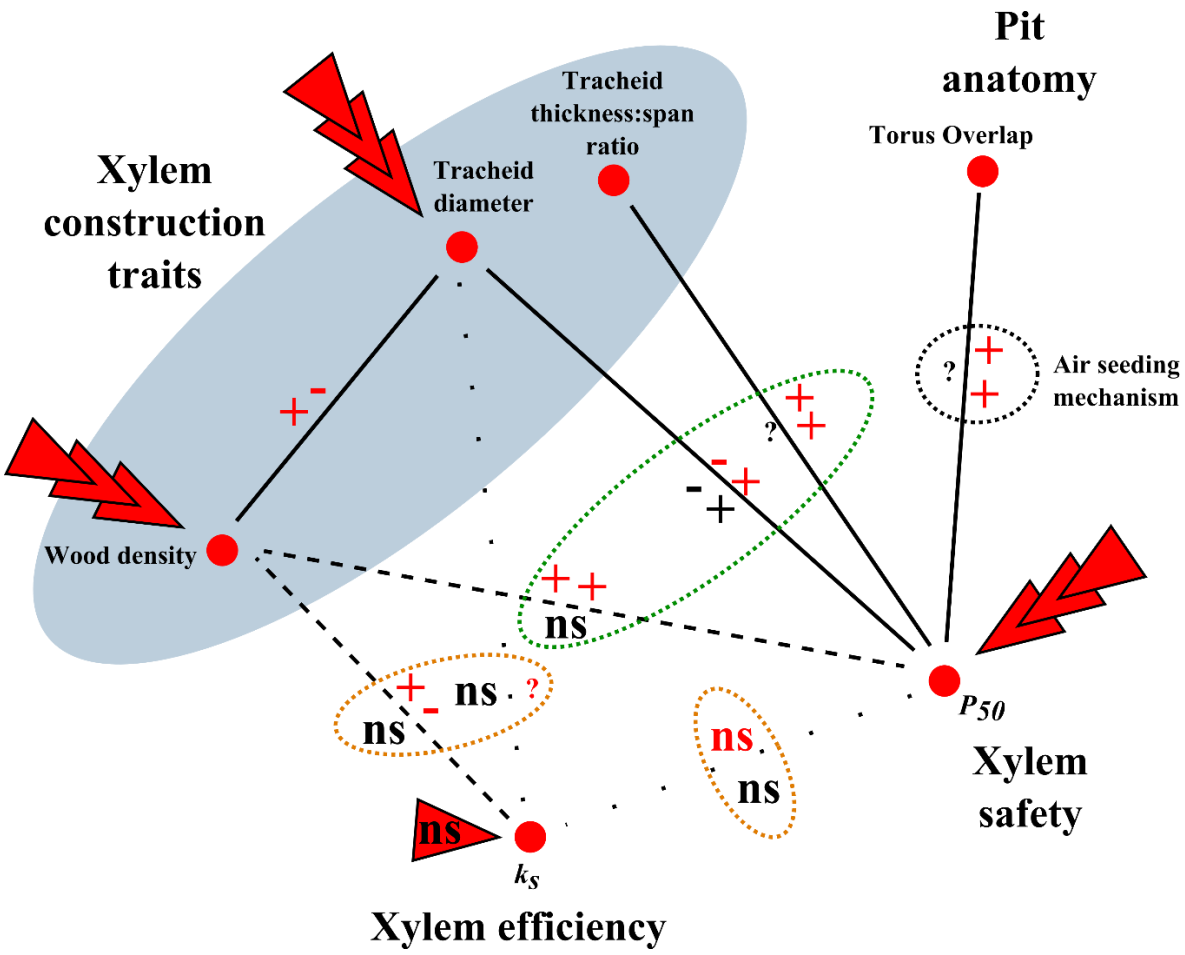

Figure 1. Interaction network of the hydraulic traits studied in this thesis. Lines indicate significant relationships, dashes weakly supported ones, and dotted lines non-significant or not explored (indicated by "**?**"). + and – indicate relationship directions, i.e. increase in one trait is linked to increase/decrease in the other. Red symbols show results from the whole conifer database, black ones from the *Callitris* clade. P_{50} is treated as positive to facilitate interpretation (increase in P_{50} = increase in embolism resistance). Trade-offs are highlighted in green and orange dotted ellipses, when supported and not-supported by our data, respectively. Significant link to climate aridity (or lack thereof) is shown in huge red arrows.

Over all conifers, we found that xylem conductivity scales with wood density, illustrating the efficiency/safety from implosion trade-off. Once more, this relation is mostly a slight trend of decreasing density with increasing efficiency with seemingly a barrier limiting efficiency in species with denser wood. However, we found no link between xylem construction traits (wood density or tracheid diameter) and a decrease in conductivity in the *Callitris* clade.

Across all conifers and at the smaller scale of the *Callitris* clade, we found no evidence of a safety-efficiency trade-off, i.e. no relation between P_{50} and k_s. At the pit level, it seems increased embolism resistance comes at the price of reduced pit-conductivity (through reduce pit aperture), but this does not scale to total xylem conductivity. Within *Callitris*, there is no

relation between P_{50} and pit-conductivity. This is consistent with previous work (Maherali et al., 2004). Although it has been mentioned that no species attain both high safety and high efficiency (Gleason et al., 2015), we provide evidence to the contrary, with *Callitris intratropica* reaching P_{50} = -13 MPa and the fifth highest conductivity within our conifer dataset. Since this species does not have extremely wide tracheids, we conclude that it somehow manages much higher pit-level conductivity. This holds true for other species as well, with diminishing tracheid lumen size reducing theoretical conductivity yet they manage to maintain k_s, e.g. *Callitris glaucophylla*, *Actinostrobus arenarius*. These two species are also extremely embolism resistant (P_{50} = -15 MPa and -16.5 MPa respectively), so pit modifications to increase end-wall conductivity is not detrimental to P_{50}. This disconnect between embolism resistance and conductivity is consistent with data showing that P_{50} in conifers is linked to torus-pit aperture overlap, whereas conductivity is driven only by margo pore size (Bouche, 2015 - Chapter 2).

Overall our results confirm previous results of a somewhat increased construction cost of embolism-resistant wood (Figure 1 – green ellipse), but not at the cost of reduced transport efficiency (Figure 1 – orange ellipses). Furthermore, our results in the *Callitris* clade support strong climate determinism of xylem traits, but not hydraulic efficiency (Figure 1). Hydraulic safety is also related to species climate over all conifer species, either based on biomes (our dataset) or on annual rainfall (Maherali et al., 2004; Choat et al., 2012; Reich, 2014). Preliminary results on our data suggest the same relation across all species, but it's worth noting that at a family level, Pinaceae embolism resistance shows no relation to climate aridity in contrast to other families (N. Gonzalez Muñoz, *pers. comm.*). Previous work has shown that conifer xylem conductivity does not scale with rainfall, in opposition to deciduous Angiosperms (Maherali et al., 2004). The interesting thing to note is that in spite of this disconnect between the need for efficiency and rainfall, *Callitris* species in wet climates have wider tracheids, and fewer tracheids per unit xylem area than species in dry environments. This once more highlights the lack of a safety-efficiency trade-off in Conifers, allowing wider variation in tracheid size to compensate for higher risk of implosion in xeric species, without affecting hydraulic efficiency.

3. The relevance of stem P_{50}

Why focus on xylem traits, and hydraulic failure in particular? The driver behind much of our work is understanding how drought affects trees, and how it potentially leads to plant death. While necessarily limiting our view of whole plant function, focusing on xylem hydraulic traits

is a pertinent approach. While the jury is still out as to what exactly kills a plant during drought, hydraulic dysfunction is likely the leading culprit, since it has been linked directly to plant death (Brodribb and Cochard, 2009; Brodribb et al., 2010; Urli et al., 2013). Furthermore, the alternative suspect, death by carbon starvation (Sala et al., 2010) is strongly related to dysfunction of the water-transport pathway (Hartmann, 2015), since lack of carbon assimilation is directly caused by stomatal closure induced by whole plant responses to lack of water (including reductions in hydraulic conductance (Plaut et al., 2012)). Finally, recent meta-analysis has placed P_{50} and the hydraulic safety margin at the forefront of plant traits predicting mortality (Anderegg et al., 2016a). In other words, species operating at water-potentials close to their embolism threshold are more vulnerable to climate-change drought induced mortality events. While we lack precise measurements of daily/seasonal minimum water-potentials for many species, others have estimated the hydraulic safety margin to be relatively constant across species (Choat et al., 2012). We have therefore strong confidence that our P_{50} database is vital for predicting species specific vulnerability to drought. There are no known methodological issues with our estimations of embolism resistance in conifers using the CAVITRON technique, which has been shown to be reliable in tracheid bearing species (Cochard et al., 2013; Pivovaroff et al., 2016).

Furthermore, P_{50} appears to be relatively constant across organs within a tree (Bouche et al., 2016) at least within Pinaceae species, reducing the risk of high measurement error through sampling among different branch cohorts, heights or exposition in different trees and/or species. It has been suggested that more vulnerable leaves could act as fuses for the vascular system (Tyree and Ewers, 1991; Tyree and Zimmermann, 2002). Since they are exposed to more negative water-potentials, they could "cavitate" first, thereby avoiding dangerous pressure drops in more long-lived and carbon-costly organs (branches, trunks, roots). This so-called "segmentation hypothesis" has been investigated recently, and it seems there are no huge differences between leaf and stem xylem P_{50} (Bouche et al., 2015). There are methodological issues with measuring whole leaf hydraulic conductance during drought, because of the difficulty to separate xylem conductance from the flow through extra-xylary pathways.

Although no methodological innovations were necessary for this thesis, we can mention the special rotor that was needed to measure the more resistant species (especially in *Callitris*), which is reinforced to allow increased maximum rotor speed to 15000 rpm (up from 12000 rpm on the standard rotor). This has considerably stretched the range of xylem pressures at which we can measure water-flow down to around -21 MPa.

4. The evolutionary perspective

We have shown the capacity of conifers to follow a wide variety of ecological strategies and evolutionary pathways. In spite of their reputation as ancient declining lineages, the physiology of some groups of conifers has been remarkably adaptable to climate change at geological time-scales. We explained their current diversity and distribution by recent radiations into habitats where they can compete with broadleaved trees, notably in arid areas via xylem adaptations to low water potentials. Previous work on the evolution of conifer drought resistance combined graphical representations of species phylogeny with observed trait values at the tips (Maherali et al., 2004; Pittermann et al., 2012). While necessarily limited to descriptions of trait distributions across taxa, these studies highlighted the remarkable lability of embolism resistance, with evolutionary convergence of some conifer clades toward very negative P_{50}. By placing these results in an informed timeframe, these parallel evolutionary trends were hypothesized i) to be linked to climate change during the Cenozoic, and ii) to correspond to adaptive radiations with increased speciation or reduced extinction rates in xeric clades. Building on our physiological database we were able to explicitly model lineage diversification and trait evolution, and we found strong evidence backing up these hypotheses. With four times more Cupressaceae species, our more extensive dataset and modelling approach allows us to separate trait evolution from diversification. We also found two parallel upshifts in the rate of evolution of drought-resistance in Cupressaceae (in crown Callitroids and Cupressoids), echoing the shift to drier and colder climate towards the end of the Eocene (Chapter 4). These shifts in trait evolution dynamics were followed by shifts in diversification rates. However, there are some differences between our results and previous work (i.e. Pittermann et al. 2012).

In the Cupressoid clade, the accelerated dynamic we recover includes drought resistant clades such as *Tetraclinis* and *Platycladus* (P_{50} approximately of -13 and -9 MPa respectively) as well as *Juniperus* and *Cupressus*. This means we locate the transition to more resistant xylem slightly earlier in this clade. Additionally, Pittermann et al. (2012) report *Austrocedrus* with P_{50} = -10 MPa, whereas we found more moderate values of around -5 MPa. Combined with the younger ages for this group in our phylogeny, this places the shift in this group closer to the present, at around 30 Mya, in our analysis. Whereas the previous study only hypothesized that speciose extant genera underwent more rapid diversification, we implemented specific modelling of speciation and extinction dynamics while accounting for missing species. The shift we recover for diversification corresponds well with that inferred by Pittermann et al. for the *Cupressus*/*Juniperus* clade, but not so much for the Callitroids, where the comparison is

once more rendered difficult by incongruence between phylogenies and lack of resolution in our analysis. In Part III of this thesis, further investigations into the diversification of *Callitris* strongly links it to increasing aridity in Australia and the related emergence of extreme xylem resistance to embolism. In that work, we place the start of the shift in both diversification and embolism resistance evolution at around 30 MA, with a subsequent shift closer to the present. Overall, our results don't conflict with the conclusions of the previous study, but we find that the Callitroid radiation is probably more recent than in the Northern Hemisphere Cupressoids, and we present the hypothesis that a strategy involving increased embolism resistance started emerging before the shifts in diversification. A more detailed investigation into the dynamics in the *Cupressus*/*Juniperus* clade is warranted, as relationships within this group are not well resolved (see (Terry et al., 2012; Terry and Adams, 2015; Terry et al., 2016), and we lack physiological information for around 80% of *Juniperus* species, notably from North-America.

a. Conifer phylogenetics.

Literature on the phylogeny of conifers has been building up recently, with much efforts aimed at disentangling the few controversies that remain resulting in confidence in deeper relationships between families and genera. From early molecular studies with few species and low resolution in the early 2000s, recent years have produces well supported large phylogenies with hundreds of species and sequence data thousands of nucleotides long, and using fossil data to implement complex molecular clocks (Leslie et al., 2012).

Arguably the greatest challenge of this thesis was constructing reliable, accurate, dated molecular phylogenies tailor made for our physiological datasets. Rather than building on previous work and adding species to existing trees, we chose to build new phylogenies using existing sequence data. Firstly, even in the case of the most extensive phylogenies there were many missing species, and including these species as polytomies to their closest relatives (at the genera level, for example) would have introduced too much uncertainty into the phylogeny. Secondly, these existing trees are built on slowly evolving gene sequences, which provide strong support for deep nodes, but low differentiation between closely related genera. By incorporating sequences for faster-evolving regions (such as the intergenic spacers ITS1), we provided better resolution within genera – although aligning these sequences across the whole Order was challenging, a problem we overcame by creating family specific matrixes. As outlined in the introduction (Box 1), several methods exist to both construct molecular phylogenies and time-calibrate branch lengths using independent dating information. Perhaps the most commonly used, Bayesian software BEAST allows these estimation simultaneously,

and presents the advantages of providing probabilistic estimations of node support and age intervals, while implementing different relaxed-clock methods. However, given the number of species and alignment length in the conifer study, computation times were long prohibiting extensive testing of different parameters, calibration schemes and sequence sets. We chose the more time-efficient RAxML, which still needed several days to complete the final estimation of the molecular phylogeny (with 1000 bootstrap iterations). The other argument in favor of this method is the separation of time-calibration and molecular tree building, allowing us to compare different dating methods, and various set of fossil calibrations. Overall, we are satisfied that our dating analysis yields accurate ages (but see discussion in Chapter 4). The phylogeny of the *Callitris* clade was constructed using BEAST, because the smaller size of the sequence matrix allowed us to test various configurations. Also, there were fewer fossils available for calibration points. As stated in the discussion in Chapter 5, our phylogeny agrees with previous work (Pye et al., 2003; Piggin and Bruhl, 2010).

The phylogeny created for the purpose of studying the evolution of embolism resistance in Conifers (Chapter 4) was also used to represent the variation of P_{50} across families in Chapter 1, as well as account for phylogenetic proximity in the PGLS analyses. Additionally, the phylogeny was used to investigate how phylogenetic relatedness between pine species influenced herbivory by the pine processionary moth (see Annex 2). Finally, we have used this phylogeny to investigate genome size evolution in conifers using the genome size database from Kew Gardens (http://data.kew.org/cvalues), and the relationship between genome size and physiological traits. It is known that some members of genus *Pinus* have extremely large genomes (e.g. subgenus *strobus*), and it has been hypothesized that their physiology could be linked to genome size because for example larger genomes tend to produce larger cells which tend to be more conductive. So far, it seems there is no strong relationship between embolism resistance, hydraulic conductance or wood density and genome size (see Annex 3).

b. Modelling evolution

From accounting for phylogenetic proximity in cross-species trait relationships to simple evolutionary models such as Brownian motion (BM), comparative methods have had large success in ecology in recent years driving a growing field of research. Nowadays, multiple evolutionary models can be implemented both for reconstructing trait evolution, lineage diversification, or both at the same time. Most applications build on quantifying the probability of observing the data (i.e. the tree and/or the species trait values) given the evolutionary model chosen (for example the speciation, extinction, and rate of trait evolution) (Maddison et al.,

2007; Fitzjohn, 2010). For example, given our phylogeny for conifers and our P_{50} database, we can fit a simple BM model, to estimate the optimal BM rate parameter. As described in the Introduction, BM is appropriate for situations where trait evolve under genetic drift (random changes), selection when there are fluctuations in the trait optimum or long periods of stasis interrupted by rapid trait evolution (punctuate change) (Hansen and Martins, 1996; O'Meara et al., 2006). Traits varying under directional selection towards an optimum, or traits with natural bounds restricting their evolution in one direction (for example, P_{50} is bounded by 0) are not well modelled by BM.

In our case, BM can seem appropriate, because i) it seems unlikely that selection occurred over 300 MA in all conifer lineages towards the same optimum P_{50} value (e.g. obvious stasis or uniform selection in Pinaceae, and fluctuation of the climate driving selection), and ii) although P_{50} is limited to negative values, no conifer species likely evolved sufficiently close to the limit for it to pose problems (O'Meara et al., 2006). However, since different families have hugely different patterns regarding embolism-resistance, we investigated primarily models that aim to fit multiple processes across the tree. Although several implementations are available, the broad idea remains the same: at some point in the evolution of a clade, the ancestral evolutionary rates (i.e. speciation, extinction (or both) or trait rate of change) shift towards new dynamics. Either an increase in the speciation (or trait evolution) rate leads to rapid diversification (or wider trait variation), or a slowdown occurs, leading to lower diversity (or trait evolutionary stasis). The challenge lies in identifying, locating, and quantifying these rate shifts and these new evolutionary dynamics.

Briefly, these methods can be grouped into 2 families:

1. Stepwise likelihood comparison methods: the algorithm recursively moves through the tree, adding shifts in evolutionary dynamics (new speciation/extinction or trait evolutionary rates) for a sub-tree, recalculating the likelihood of the model, and comparing it to previous models, and keeping the "best" one : these are "MEDUSA" type models, i.e. for diversification analsyes : MEDUSA (Alfaro et al., 2009); trait evolution using BM, MOTMOT (Thomas and Freckleton, 2012) and implementing Ornstein-Ulhenbeck, OUwie (Beaulieu et al., 2012) and Surface (Ingram and Mahler, 2013).
2. Bayesian methods that implement reversible-jump Markov Chain Monte Carlo algorithms to explore model space, providing us with a large sets of models, sampled according to their posterior probabilities that can then be summarized to extract the most probable set(s) of shifts between differing evolutionary dynamics. Implementing BM models of trait evolution, the

"auteur" method (Eastman et al., 2011) and for both diversification and trait evolution using exponential change, BAMM (Rabosky et al., 2013; Rabosky et al., 2014; Rabosky, 2014; Shi and Rabosky, 2015).

Both types have their advantages and drawbacks, however a preference for the probabilistic Bayesian implementations is emerging, principally because they are not restricted to a single "optimum" model solution, in opposition to the "MEDUSA" type models. When multiple sets of rate shifts are more or less equally likely (e.g. an upward shift in one clade or a slowdown in the related sister-clade), the output from BAMM or "auteur" will present this uncertainty, whereas the likelihood models will ignore one some good models, selecting the single "best" one. After some testing, we opted for the BAMM method, which provides both extensive analysis and graphical tools in R, and strong confidence that meaningful evolutionary dynamics and shifts can be accurately recovered. Furthermore, the specific model for evolution implemented in BAMM is highly flexible, because it is based on exponential rate change through time, allowing for accelerations or slow-downs of rates within a dynamic. We also ran auteur on our data (see Annex 4), and found nearly identical patterns with this method, i.e. 4 well supported shift to higher evolutionary rates at the base of Podocarpaceae, within the Taxaceae-Cephalotaxaceae clade, and in crown Callitroidae and Cupressoidae. This result reinforces our results from the BAMM analysis.

Finally, because we wanted to test the hypothesis that increased drought resistance is implicated in higher diversification rates in conifers, we used the QUASSE method (Fitzjohn, 2010) for trait dependent speciation and extinction models. As discussed previously (see Discussion, Chapter 4) these methods are known to have some substantial pitfalls (O'Meara and Beaulieu, 2016), mainly the risk of inferring spurious statistical dependence between trait values and speciation. Firstly, because correlation does not imply causation, there was always a risk that heterogeneous speciation/extinction could be associated statistically to trait with some degree of overlapping variation, with no need for "real" correlation (Rabosky and Goldberg, 2015). The authors in this paper found increased diversification in small cetaceans (i.e. the dolphin clade). However, they simulated trait evolution (under BM) on the whale phylogeny, and recovered association between rate of speciation and simulated character state. This indicates the possibility of false-positives, i.e. identifying trait-dependent diversification when there is no such dependence. Although there are no certainties as to what causes this level of error in the model, some hypotheses have been advanced. For example, if distributions of trait values differ between a derived clade with higher diversification rates and a background

clade with lower "ancestral" diversification rates, the model will likely recover a link between the considered trait and diversification, whether a significant relationship exists or not. Furthermore, one assumption of the SSE models is that diversification rate heterogeneity can only be assigned to the characters included in the model (Rabosky and Goldberg, 2015). Differences in diversification could be due to an unrelated "hidden" character not included in the study, which could for example show some level of co-distribution with the trait of interest (Maddison and FitzJohn, 2015). Other potential issues are related to the "shape" of the phylogeny, i.e. methods used for phylogeny construction and dating analysis, and sampling bias.

We tried to account for these issues at several levels, described in the discussion of Chapter 4. 1) Firstly, given the diversification rate heterogeneity in our data based on the BAMM analysis, we partitioned the QUASSE model to exclude families where diversification was probably related to other "hidden" factors, i.e. specifying a background clade of Pinaceae, Podocarpaceae and Araucariaceae, and a foreground group with Taxaceae, Cephalotaxaceae and Cupressaceae. Using this split model, we found strong evidence of that trait-dependent diversification was only significant in the foreground group. 2) We conducted QUASSE analyses on simulated traits to verify if our phylogeny was liable to "false-positive" trait-diversification relationships. 3) We conducted analyses using the different phylogenies we generated, with MrBayes and different calibration schemes. We recognize a potential sampling bias, with differences in sampling frequency between clades. For example, we included many more species from the *Araucaria* genus (~90%) that the *Juniperus* genus (~20%), but overall there is no strong tendency for oversampling of embolism-resistant genera.

Overall, our data is not immune to common pitfalls of these model-based inferences. However, our data strongly supports the idea that drought-resistant clades have been diversifying more rapidly than other conifers. Although it's difficult to unequivocally prove a link between increased embolism resistance and speciation/extinction, it seems highly likely that the evolutionary success that drought-tolerant clades in Cupressaceae have enjoyed over the last 50 to 30 million years is related to their ability to develop highly resistant xylem.

c. Conifer diversification

Our work is not the first to investigate the diversification dynamics of conifers. Here we briefly review other work on this topic. Firstly, a strong hemisphere-scale signal in

diversification dynamics has been found (Leslie et al., 2012), with more recent diversification in the Northern Hemisphere (NH) clades, and especially more species turn-over, possibly linked to glacial cycles in the NH. Other work has challenged the long held notion that Gymnosperms are ancient relicts (Crisp and Cook, 2011; Nagalingum et al., 2011), showing that crown groups in Conifers are of young age, and that strong extinction (mostly during the Oligocene and Miocene) explains their slower diversification closer to the present compared to Angiosperms.

Attempts to point to diversification drivers have shown that Podocarps diversified under the spreading Angiosperm canopy by evolving flattened leaves (Biffin et al., 2012). A role of high altitude in driving increased speciation has been advanced for NH clades (Cardoso et al., 2015), and in more general "ecological dissimilarity" from their Angiosperm competitors. This highlights the likely strong role of the Angiosperms' rise to dominance globally in the decline of Gymnosperms in most environments (Bond, 1989; Augusto et al., 2014). Finally, it seems there is no effect of breeding and dispersal syndromes (i.e. monecy vs. dioecy and dry vs. fleshy cones) on diversification (Leslie et al., 2013). This is the only other attempt to find an effect of species level traits on diversification rates in Conifers using large phylogeny and extensive trait sampling in a modelling framework.

Our study on conifer diversification and drought-resistance evolution is of high significance, since it is the first to explicitly model multiple diversification dynamics across conifers, and to link them to a fitness related trait. Furthermore, we put drought on the map as a major driver of conifer diversification, although this role was already hypothesized (Pittermann et al., 2012; Augusto et al., 2014).

5. Implications and perspectives

The results presented in this thesis greatly further our understanding of conifer physiology. By knowing in advance which areas and species are most vulnerable to drought-induced mortality, we can prevent major impacts of future droughts and heatwaves. Since many conifers are planted or ecologically dominant notably in the Northern Hemisphere, this knowledge is vital for managing forest and ecosystems in the context of climate change. A need for physiological data has been highlighted in order to improve species distributions modelling beyond occurrence-environment correlative models (Kearney and Porter, 2009). The predictive power of climate models that include land-cover is also dependent on accurate prediction of vegetation changes with the risk of widespread mortality following drought. These large-scale catastrophic events can affect the carbon and water cycles (Anderegg et al., 2015), with

complex feed-back effects on the world's climate (Bonan, 2008; Kurz et al., 2008; Zhao and Running, 2010) – but see (Anderegg et al., 2016b).

We have highlighted the evolutionary role of inter-tracheid pit anatomy in determining species embolism-resistance. Beyond the theoretical implications, these results could provide tools for breeding and selection programs, as drought-tolerance become a desirable trait under climate change. Embolism-resistance (measured by P_{50}) is a pertinent trait regarding drought-tolerance but requires individuals of a certain age (ideally several years old) to be accurately estimated. Using good proxies at the cellular level could improve efficiency in selecting good breeders or clones by examining their xylem at a young age.

The interior surface of the tracheids of some species are not regular and smooth, but can be covered with small globular warts and other ornamentations – see Annex 5 (Heady et al., 1994). While the precise role of these structures is not completely understood, it is believed that thickenings of the cell wall surrounding the pits, i.e. in "vestured pits" and so-called callitroid-thickening (CT) provide additional support against implosion at high xylem tensions. Warts on the inside of the tracheid lumen could increase the contact surface between the cell wall and the sap, reducing the possibility of air-bubbles appearing. Finally, smaller air-bubbles (i.e. too small to kickstart the process of cavitation) could be trapped by warts with more complex shapes, limiting accretion into larger, more dangerous bubbles, protecting against embolism. In any case, both "wartiness" (Heady et al., 1994) and CT shape and frequency (Heady and Evans, 2000) supposedly vary with species ecology in *Callitris*. We initially wanted to produce our own data for these parameters, but for lack of time, we used data from these publications, as summarized and coded in Piggin et al. (2010). We found that the more pronounced CT type was associated with increasing P_{50}. Additionally, embolism resistance seems to be linked to the shape of the warts, i.e. higher frequency of complex warts with nodular branching patterns. The link between these structures and climate is much more evident however, with aridity and to a lesser extent more extreme cold correlated to more marked CTs and larger more protuberant warts. These preliminary results can be found in Annex 5, however since the original study focused only on *Callitris* we have no data for *Neocallitropsis* and *Actinostrobus* – adding more extensive sampling and maybe more precise measurements could reveal stronger roles of these structures, since already they are strongly related to species climate.

We have shown the ability of conifers to respond to past episodes of climatic upheavals, notably by increasing their capacity to survive drought by withstanding extremely negative

xylem pressure. Some remarkably resistant species even seem to have reached an absolute physical boundary to liquid water transport in vascular tissue in plants. While this knowledge can provide us with some hope for the future of conifers as a whole in the long term, it's worth noting several worrying facts. Firstly, driven by human activity, current climate change is occurring at an unprecedented rate (Stocker et al., 2013). While climate change has happened in the past, it is likely that current rates are several orders of magnitude faster than historical events (Zachos et al., 2001; Diffenbaugh and Field, 2013). For example, climatic shifts described in Chapter 5 as driving the early diversification and P_{50} evolution in *Callitris* happened over millions of years. Species will therefore need to adapt at unprecedented rates or be displaced, although migration rates for long-lived plants such as conifers is also probably too slow to keep up with temperature shifts in many parts of the world (Delzon et al., 2013). Given the already vulnerable or critical status for many conifer species (IUCN, 2015), it seems the future does not bode well for many members of this emblematic and historic group of plants.

In spite of all our efforts over several years, we only have estimates of embolism resistance for under half of all species of conifers. The "Cavitating the Conifers of the World" project still has some way to go before completion. Our sampling strategy however has managed to cover in our opinion much of the existing diversity and physiological variation that exists in Conifers. Two main axes of progress come to mind however. First, the ecological equivalent to *Callitris* in the Northern Hemisphere, *Juniperus* is arguably the most under-sampled genus in our dataset, with only around 20% of species sampled. With some remarkable ecological variation in this genus, from the highest reaches of the Himalaya to the dry deserts of North America it would be worth investigating in a more systematic manner. Second, there is desperate need for more work on intra-specific variability of embolism resistance (and other hydraulic traits). The current premise that there is low intra-specific variability is built on restricted results from a handful of un-informative genera (i.e. *Pinus*). A valuable addition to the existing literature on the subject would be to include multiple species from across different evolutionary regimes identified here and in other work (e.g. within *Podocarpus*, *Cephalotaxus*, *Callitris*, *Juniperus*). These groups are more likely to reveal some level of genetic differentiation between climatically contrasted populations, since P_{50} is an integral part of their ecophysiological strategy toward water-management. We are currently working on examining the link between species climate and P_{50}, notably trends at the family level.

Finally, limited from the outset to tracheid-bearing conifers by methodological constraints and the regional bias towards conifers (pines in particular) that exists in Bordeaux, it seems

logical to expand this type of work to include Angiosperms. While differences in wood and leaf structure make direct comparisons with gymnosperms challenging, woody flowering plants offer an even wider scope of strategies, evolutionary innovations and potential adaptive radiations worth investigating. For example, some of the most extreme environments in Australia are populated by drought-adapted Angiosperms trees and shrubs from genera such as *Eucalyptus*, *Acacia*, *Banksia*, *Cassuarina* and more. Recent work has shown great adaptation to climate of *Eucalyptus* xylem (Pfautsch et al., 2015), and further investigations including direct estimations of embolism vulnerability and hydraulic conductivity in these species would be a highly intriguing path for future investigations. In a similar vein, wet tropical forests, crucial both in terms of biodiversity and carbon storage, are being recognized as equally vulnerable to climate-change induced drought despite relatively high historic rainfall (Corlett, 2016). Newly developed equipment (i.e. the "cavi1000") capable of accurately measuring species with long vessels is enabling projects aiming at characterizing angiosperm trees' resistance to embolism, and opens up new avenues for evolutionary ecophysiology research.

References

Ackerly DD (2004) Functional strategies of chaparral shrubs in relation to seasonal water deficit and disturbance. Ecol Monogr **74**: 25–44

Aitken SN, Yeaman S, Holliday J a., Wang T, Curtis-McLane S (2008) Adaptation, migration or extirpation: climate change outcomes for tree populations. Evol Appl **1**: 95–111

Alfaro ME, Santini F, Brock C, Alamillo H, Dornburg A, Rabosky DL, Carnevale G, Harmon LJ (2009) Nine exceptional radiations plus high turnover explain species diversity in jawed vertebrates. Proc Natl Acad Sci **106**: 13410–13414

Allen CD, Macalady AK, Chenchouni H, Bachelet D, McDowell N, Vennetier M, Kitzberger T, Rigling A, Breshears DD, Hogg EH (Ted), et al (2010) A global overview of drought and heat-induced tree mortality reveals emerging climate change risks for forests. For Ecol Manage **259**: 660–684

Anderegg WRL (2015) Spatial and temporal variation in plant hydraulic traits and their relevance for climate change impacts on vegetation. New Phytol **205**: 1008–1014

Anderegg WRL, Anderegg LDL (2013) Hydraulic and carbohydrate changes in experimental drought-induced mortality of saplings in two conifer species. Tree Physiol **33**: 252–60

Anderegg WRL, Berry J a, Smith DD, Sperry JS, Anderegg LDL, Field CB (2012) The roles of hydraulic and carbon stress in a widespread climate-induced forest die-off. Proc Natl Acad Sci U S A **109**: 233–7

Anderegg WRL, Flint A, Huang C, Flint L, Berry J a., Davis FW, Sperry JS, Field CB (2015a) Tree mortality predicted from drought-induced vascular damage. Nat Geosci 1–5

Anderegg WRL, Hicke JA, Fisher RA, Allen CD, Aukema J, Bentz B, Hood S, Lichstein JW, Macalady AK, Mcdowell N, et al (2015b) Tree mortality from drought, insects, and their interactions in a changing climate. New Phytol **208**: 674–683

Anderegg WRL, Klein T, Bartlett M, Sack L, Pellegrini AFA, Choat B (2016a) Meta-analysis reveals that hydraulic traits explain cross-species patterns of drought-induced tree mortality across the globe. Pnas. doi: 10.1073/pnas.1525678113

Anderegg WRL, Martinez-Vilalta J, Cailleret M, Camarero JJ, Ewers BE, Galbraith D, Gessler A, Grote R, Huang C, Levick SR, et al (2016b) When a Tree Dies in the Forest: Scaling Climate-Driven Tree Mortality to Ecosystem Water and Carbon Fluxes. Ecosystems. doi: 10.1007/s10021-016-9982-1

Anderegg WRL, Schwalm C, Biondi F, Camarero JJ, Koch G, Litvak M, Ogle K, Shaw JD, Shevliakova E, Williams AP, et al (2015c) Pervasive drought legacies in forest ecosystems and their implications for carbon cycle models. Science (80-) **349**: 528–532

Anderson CL (2007) Dating divergence times in phylogenies. Compr Summ Uppsala Disserations from Fac Sci Technol. doi: ISBN 978-91-554-6937-5

Angeles G, Bond B, Boyer JS, Brodribb TJ, Brooks JR, Burns MJ, Cavender-Bares J, Clearwater M, Cochard H, Comstock J, et al (2004) The Cohesion-Tension Theory. New Phytol **163**: 451–452

Aranda I, Cano FJ, Gasco A, Cochard H, Nardini A, Mancha JA, Lopez R, Sanchez-Gomez D (2014) Variation in photosynthetic performance and hydraulic architecture across European beech (Fagus sylvatica L.) populations supports the case for local adaptation to water stress. Tree Physiol **35**: 34–46

Augusto L, Davies TJ, Delzon S, De Schrijver A (2014) The enigma of the rise of angiosperms: can we untie the knot? Ecol Lett **17**: 1326–38

Bailey IW (1916) The Structure of the Bordered Pits of Conifers and Its Bearing Upon the Tension Hypothesis of the Ascent of Sap in Plants. Bot Gaz **62**: 133

Balducci L, Deslauriers A, Giovannelli A, Beaulieu M, Delzon S, Rossi S, Rathgeber CBK (2014) How do drought and warming influence survival and wood traits of Picea mariana saplings? J Exp Bot. doi: 10.1093/jxb/eru431

Beaulieu JM, Jhwueng D-C, Boettiger C, O'Meara BC (2012) Modeling stabilizing selection: expanding the Ornstein-Uhlenbeck model of adaptive evolution. Evolution **66**: 2369–83

Bennett AC, McDowell NG, Allen CD, Anderson-Teixeira KJ (2015) Larger trees suffer most during drought in forests worldwide. Nat Plants **1**: 15139

Benson DA, Karsch-Mizrachi I, Lipman DJ, Ostell J, Sayers EW (2011) GenBank. Nucleic Acids Res **39**: D32–7

Biffin E, Brodribb TJ, Hill RS, Thomas P, Lowe AJ (2012) Leaf evolution in Southern Hemisphere conifers tracks the angiosperm ecological radiation. Proc Biol Sci **279**: 341–8

Bigler C, Gavin DG, Gunning C, Veblen TT (2007) Drought induces lagged tree mortality in a subalpine forest in the Rocky Mountains. Oikos **116**: 1983–1994

Blackman CJ, Brodribb TJ, Jordan GJ (2009) Leaf hydraulics and drought stress: response, recovery and survivorship in four woody temperate plant species. Plant Cell Environ **32**: 1584–95

Blackman CJ, Pfautsch S, Choat B, Delzon S, Gleason SM, Duursma RA (2016) Toward an index of desiccation time to tree mortality under drought. Plant Cell Environ. doi: 10.1111/pce.12758

Bonan GB (2008) Forests and climate change: forcings, feedbacks, and the climate benefits of forests. Science (80-) **320**: 1444–1449

Bond WJ (1989) The tortoise and the hare: ecology of angiosperm dominance and gymnosperm persistence. Biol J Linn Soc **36**: 227–249

Bouche PS (2015) Cavitation resistance and the functional role of bordered pits in xylem of conifers - from inter-specific to within tree variability. Ulm University

Bouche PS, Delzon S, Choat B, Badel E, Brodribb TJ, Burlett R, Cochard H, Charra-Vaskou K, Lavigne B, Li S, et al (2015) Are needles of *Pinus pinaster* more vulnerable to xylem embolism than branches? New insights from X-ray computed tomography. Plant Cell Environ n/a–n/a

Bouche PS, Jansen S, Sabalera JC, Cochard H, Burlett R, Delzon S (2016) Low intra-tree variability in resistance to embolism in four Pinaceae species. Ann For Sci. doi: 10.1007/s13595-016-0553-6

Breshears DD, Myers OB, Meyer CW, Barnes FJ, Zou CB, Allen CD, McDowell NG, Pockman WT (2009) Tree die-off in response to global change-type drought: mortality insights from a decade of plant water potential measurements. Front Ecol Environ **7**: 185–189

Brodersen CR, McElrone AJ, Choat B, Matthews M a, Shackel K a (2010) The dynamics of embolism repair in xylem: in vivo visualizations using high-resolution computed tomography. Plant Physiol **154**: 1088–95

Brodribb T, Hill RS (1999) The importance of xylem constraints in the distribution of conifer species. New Phytol **143**: 365–372

Brodribb TJ, Bowman DJMS, Nichols S, Delzon S, Burlett R (2010) Xylem function and growth rate interact to determine recovery rates after exposure to extreme water deficit. New Phytol **188**: 533–42

Brodribb TJ, Cochard H (2009) Hydraulic failure defines the recovery and point of death in water-stressed conifers. Plant Physiol **149**: 575–84

Brodribb TJ, Holbrook NM, Edwards EJ, Gutiérrez M V. (2003) Relations between stomatal closure, leaf turgor and xylem vulnerability in eight tropical dry forest trees. Plant, Cell Environ **26**: 443–450

Brodribb TJ, McAdam S a M (2013) Abscisic acid mediates a divergence in the drought response of two conifers. Plant Physiol **162**: 1370–7

Brodribb TJ, McAdam S a M, Jordan GJ, Martins SC V (2014) Conifer species adapt to low-rainfall climates by following one of two divergent pathways. Proc Natl Acad Sci U S A. doi: 10.1073/pnas.1407930111

Brodribb TJ, Skelton RP, Mcadam SAM, Lucani CJ, Marmottant P (2016) Visual quantification of embolism reveals leaf vulnerability to hydraulic failure. New Phytol.

Buckley TN (2005) The control of stomata by water balance. New Phytol **168**: 275–292

Cardoso GC, Cortesão M, García C (2015) Ecological Marginalization Facilitated Diversification in Conifers. Evol Biol. doi: 10.1007/s11692-015-9306-y

Choat B, Badel E, Burlett R, Delzon S, Cochard H, Jansen S (2016) Noninvasive Measurement of Vulnerability to Drought-Induced Embolism by X-Ray Microtomography. Plant Physiol **170**: 273–282

Choat B, Jansen S, Brodribb TJ, Cochard H, Delzon S, Bhaskar R, Bucci SJ, Feild TS, Gleason SM, Hacke UG, et al (2012) Global convergence in the vulnerability of forests to drought. Nature **491**: 752–5

Cochard H, Badel E, Herbette S, Delzon S, Choat B, Jansen S (2013) Methods for measuring plant vulnerability to cavitation: a critical review. J Exp Bot **64**: 4779–91

Cochard H, Coll L, Le Roux X, Améglio T (2002) Unraveling the Effects of Plant Hydraulics on Stomatal Closure during Water Stress in Walnut. Plant Physiol **128**: 282–290

Cochard H, Delzon S, Badel E (2015) X-ray microtomography (micro-CT): a reference technology for high-resolution quantification of xylem embolism in trees. Plant Cell Environ **38**: 201–206

Cochard H, Herbette S, Barigah T, Badel E, Ennajeh M, Vilagrosa A (2010) Does sample length influence the shape of xylem embolism vulnerability curves? A test with the Cavitron spinning technique. Plant Cell Environ **33**: 1543–1552

Cochard H, Hölttä T, Herbette S, Delzon S, Mencuccini M (2009) New insights into the mechanisms of water-stress-induced cavitation in conifers. Plant Physiol **151**: 949–54

Corlett RT (2016) The Impacts of Droughts in Tropical Forests. Trends Plant Sci **xx**: 1–10

Crisp MD, Cook LG (2011) Cenozoic extinctions account for the low diversity of extant gymnosperms compared with angiosperms. New Phytol **192**: 997–1009

Darwin C (1859) On the origin of species. John Murray

David-Schwartz R, Paudel I, Mizrachi M, Shklar G, Delzon S, Cochard H, Lukyanov V, Badel E, Capdeville G, Cohen S (2016) Evidence for genetic differentiation in vulnerability to embolism in Pinus halepensis. Front. Plant Sci.

Delzon S, Cochard H (2014) Recent advances in tree hydraulics highlight the ecological significance of the hydraulic safety margin. New Phytol **203**: 355–358

Delzon S, Douthe C, Sala A, Cochard H (2010) Mechanism of water-stress induced cavitation in conifers: bordered pit structure and function support the hypothesis of seal capillary-seeding. Plant Cell Environ **33**: 2101–11

Delzon S, Urli M, Samalens J-C, Lamy J-B, Lischke H, Sin F, Zimmermann NE, Porté AJ (2013) Field Evidence of Colonisation by Holm Oak, at the Northern Margin of Its Distribution Range, during the Anthropocene Period. PLoS One **8**: e80443

Dickman LT, McDowell NG, Sevanto S, Pangle RE, Pockman WT (2014) Carbohydrate dynamics and mortality in a piñon-juniper woodland under three future precipitation scenarios. Plant Cell Environ 1–40

Diffenbaugh NS, Field CB (2013) Changes in ecologically critical terrestrial climate conditions. Science (80-) **341**: 486–92

Dixon HH (1914) Transpiration and the Ascent of Sap in Plants. Macmillan's Sci Monogr. doi: 10.1038/094558a0

Dixon HH, Joly J (1895) On the Ascent of Sap. Philos Trans R Soc B Biol Sci **186**: 563–576

Domec J-C, Lachenbruch B, Meinzer FC, Woodruff DR, Warren JM, McCulloh K a (2008) Maximum height in a conifer is associated with conflicting requirements for xylem design. Proc Natl Acad Sci U S A **105**: 12069–74

Drummond AJ, Rambaut A (2007) BEAST: Bayesian evolutionary analysis by sampling trees. BMC Evol Biol **7**: 214

Eastman JM, Alfaro ME, Joyce P, Hipp AL, Harmon LJ (2011) A novel comparative method for identifying shifts in the rate of character evolution on trees. Evolution **65**: 3578–89

Eckenwalder JE (2009) Conifers of the world: the complete reference. Timber Press

Enright NJ, Hill RS (1995) Ecology of the southern conifers. Smithsonian Institution Press, Washington, D.C.

Fang Y, Xiong L (2015) General mechanisms of drought response and their application in

drought resistance improvement in plants. Cell Mol Life Sci **72**: 673–689

Farjon A (2010) A Handbook of the World's Conifers (2 Vols.). BRILL

Felsenstein J (1985) Phylogenies and the comparative method. Am Nat 1–15

Fitzjohn RG (2010) Quantitative traits and diversification. Syst Biol **59**: 619–633

FitzJohn RG (2012) Diversitree : comparative phylogenetic analyses of diversification in R. Methods Ecol Evol **3**: 1084–1092

Fitzjohn RG, Maddison WP, Otto SP (2009) Estimating trait-dependent speciation and extinction rates from incompletely resolved phylogenies. Syst Biol **58**: 595–611

Gaylord ML, Kolb TE, McDowell NG (2015) Mechanisms of pinon pine mortality after severe drought: a retrospective study of mature trees. Tree Physiol 1–11

Gleason SM, Westoby M, Jansen S, Choat B, Hacke UG, Pratt RB, Bhaskar R, Brodribb TJ, Bucci SJ, Mayr S, et al (2015) Weak tradeoff between xylem safety and xylem-specific hydraulic efficiency across the world's woody plant species. New Phytol 123–136

Hacke UG, Sperry JS (2001) Functional and ecological xylem anatomy. Perspect Plant Ecol Evol Syst **4**: 97–115

Hacke UG, Sperry JS, Wheeler JK, Castro L (2006) Scaling of angiosperm xylem structure with safety and efficiency. Tree Physiol **26**: 689–701

Hajek P, Kurjak D, von Wühlish G, Delzon S, Schuldt B (2016) Intraspecific variation in wood anatomical, hydraulic and foliar traits in ten European beech provenances differing in growth yield. Front. Plant Sci. Accepted:

Hansen TF, Martins EP (1996) Translating between microevolutionary process and macroevolutionary patterns: the correlation structure of interspecific data. Evolution (N Y) **50**: 1404–1417

Hartmann H (2015) Carbon starvation during drought - induced tree mortality – are we chasing a myth ? J. Plant Hydraul. 2:

Hartmann H, Adams HD, Anderegg WRL, Jansen S, Zeppel MJB (2015) Research frontiers in drought- induced tree mortality: crossing scales and disciplines. New Phytol **205**: 965–969

Hartmann H, Ziegler W, Kolle O, Trumbore S (2013) Thirst beats hunger - declining hydration during drought prevents carbon starvation in Norway spruce saplings. New Phytol **200**: 340–349

Ho SYW, Duchêne S (2014) Molecular-clock methods for estimating evolutionary rates and timescales. Mol Ecol **23**: 5947–5965

Hoegh-Guldberg O, Mumby PJ, Hooten AJ, Steneck RS, Greenfield P, Gomez E, Harvell CD, Sale PF, Edwards AJ, Caldeira K, et al (2007) Coral Reefs Under Rapid Climate Change and Ocean Acidification. Science (80-) **318**: 1737–1742

Ingram T, Mahler DL (2013) SURFACE: detecting convergent evolution from comparative data by fitting Ornstein-Uhlenbeck models with stepwise Akaike Information Criterion. Methods Ecol Evol **4**: 416–425

IUCN (2015) The IUCN Red List of Threatened Species. Version 2015-4. <http://www.iucnredlist.org>

Jacobsen AL, Pratt RB (2012) No evidence for an open vessel effect in centrifuge-based vulnerability curves of a long-vesselled liana (Vitis vinifera). New Phytol **194**: 982–90

Jansen S, Lamy J-B, Burlett R, Cochard H, Gasson P, Delzon S (2012) Plasmodesmatal pores in the torus of bordered pit membranes affect cavitation resistance of conifer xylem. Plant Cell Environ. doi: 10.1111/j.1365-3040.2011.02476.x

Kearney M, Porter W (2009) Mechanistic niche modelling: Combining physiological and spatial data to predict species' ranges. Ecol Lett **12**: 334–350

Kim J, Sanderson MJ (2008) Penalized likelihood phylogenetic inference: bridging the parsimony-likelihood gap. Syst Biol **57**: 665–74

Knipfer T, Cuneo I, Brodersen C, McElrone AJ (2016) In-situ visualization of the dynamics in xylem embolism formation and removal in the absence of root pressure: A study on excised grapevine stems. Plant Physiol pp.00136.2016

Kumar S (2005) Molecular clocks: four decades of evolution. Nat Rev Genet **6**: 654–662

Kurz WA, Dymond CC, Stinson G, Rampley GJ, Neilson ET, Carroll AL, Ebata T, Safranyik L (2008) Mountain pine beetle and forest carbon feedback to climate change. Nature **452**: 987–990

Lamy J (2012) Résistance à la cavitation : Des mécanismes physiologiques à la génétique évolutive. Université de Bordeaux

Lamy J-B, Bouffier L, Burlett R, Plomion C, Cochard H, Delzon S (2011) Uniform Selection as a Primary Force Reducing Population Genetic Differentiation of Cavitation Resistance across a Species Range. PLoS One **6**: e23476

Lamy J-B, Plomion C, Kremer A, Delzon S (2012) QST is less than FST As a signature of canalization. Mol Ecol **21**: 5646–5655

Lens F, Tixier A, Cochard H, Sperry JS, Jansen S, Herbette S (2013) Embolism resistance as a key mechanism to understand adaptive plant strategies. Curr Opin Plant Biol **16**: 287–92

Leslie AB, Beaulieu JM, Crane PR, Donoghue MJ (2013a) Explaining the distribution of breeding and dispersal syndromes in conifers Explaining the distribution of breeding and dispersal syndromes in conifers. Proc R Soc B-Biological Sci **280**: 20131812

Leslie AB, Beaulieu JM, Crane PR, Donoghue MJ (2013b) Explaining the distribution of breeding and dispersal syndromes in conifers. Proc R Soc B-Biological Sci **280**: 20131812

Leslie AB, Beaulieu JM, Rai HS, Crane PR, Donoghue MJ, Mathews S (2012) Hemisphere-scale differences in conifer evolutionary dynamics. Proc Natl Acad Sci U S A **109**: 16217–21

Levitt J (1980) Responses of plants to environmental stresses. Volume II. Water, radiation, salt, and other stresses.

López R, López de Heredia U, Collada C, Cano FJ, Emerson BC, Cochard H, Gil L (2013) Vulnerability to cavitation, hydraulic efficiency, growth and survival in an insular

pine (Pinus canariensis). Ann Bot **111**: 1167–79

Losos JB (2011) Seeing the forest for the trees: the limitations of phylogenies in comparative biology. (American Society of Naturalists Address). Am Nat **177**: 709–27

Maddison WP, FitzJohn RG (2015) The Unsolved Challenge to Phylogenetic Correlation Tests for Categorical Characters. Syst Biol **64**: 127–136

Maddison WP, Midford PE, Otto SP (2007) Estimating a binary character's effect on speciation and extinction. Syst Biol **56**: 701–710

Maherali H, Pockman WT, Jackson RB (2004) Adaptive variation in the vulnerability of woody plants to xylem cavitation. Ecology **85**: 2184–2199

van Mantgem PJ, Stephenson NL, Byrne JC, Daniels LD, Franklin JF, Fulé PZ, Harmon ME, Larson AJ, Smith JM, Taylor AH, et al (2009) Widespread increase of tree mortality rates in the western United States. Science **323**: 521–4

Martínez-Vilalta J, Cochard H, Mencuccini M, Sterck F, Herrero a., Korhonen JFJ, Llorens P, Nikinmaa E, Nolè a., Poyatos R, et al (2009) Hydraulic adjustment of Scots pine across Europe. New Phytol **184**: 353–364

Martínez-Vilalta J, Piñol J (2002) Drought-induced mortality and hydraulic architecture in pine populations of the NE Iberian Peninsula. For Ecol Manage **161**: 247–256

Martinez-Vilalta J, Poyatos R, Aguadé D, Retana J, Mencuccini M (2014) A new look at water transport regulation in plants. New Phytol **204**: 105–115

McAdam SAM, Brodribb TJ (2016) Linking turgor with ABA biosynthesis: implications for stomatal responses to vapour pressure deficit across land plants. Plant Physiol pp.00380.2016

McDowell N, Pockman WT, Allen CD, Breshears DD, Cobb N, Kolb T, Plaut J, Sperry J, West A, Williams DG, et al (2008) Mechanisms of plant survival and mortality during drought: why do some plants survive while others succumb to drought? New Phytol **178**: 719–39

McDowell NG, Williams a P, Xu C, Pockman WT, Dickman LT, Sevanto S, Pangle RE, Limousin J-M, Plaut J a., Mackay DS, et al (2015) Multi-scale predictions of massive conifer mortality due to chronic temperature rise. Nat Clim Chang In press

Meinzer FC (2002) Co-ordination of vapour and liquid phase water transport properties in plants. Plant, Cell Environ **25**: 265–274

Mencuccini M (2003) The ecological significance of long-distance water transport: Short-term regulation, long-term acclimation and the hydraulic costs of stature across plant life forms. Plant, Cell Environ **26**: 163–182

Miehe G, Miehe S, Vogel J, Co S, La D (2007) Highest Treeline in the Northern Hemisphere Found in Southern Tibet. Mt Res Dev **27**: 169–173

Milburn JA, Johnson RPC (1966) The conduction of sap. 2. Detection of vibrations produced by sap cavitation in Ricinus xylem. Planta **69**: 43–52

Mitchell PJ, O'Grady AP, Tissue DT, White D a, Ottenschlaeger ML, Pinkard E a (2013) Drought response strategies define the relative contributions of hydraulic dysfunction and carbohydrate depletion during tree mortality. New Phytol **197**: 862–72

Nagalingum NS, Marshall CR, Quental TB, Rai HS, Little DP, Mathews S (2011) Recent synchronous radiation of a living fossil. Science **334**: 796–9

Nardini A, Salleo S (2000) Limitation of stomatal conductance by hydraulic traits: Sensing or preventing xylem cavitation? Trees - Struct Funct **15**: 14–24

Nee S, Holmes EC, May RM, Harvey PH (1994) Extinction rates can be estimated from molecular phylogenies. Philos Trans R Soc Lond B Biol Sci **344**: 77–82

Nee S, Mooers a O, Harvey PH (1992) Tempo and mode of evolution revealed from molecular phylogenies. Proc Natl Acad Sci U S A **89**: 8322–6

O'Meara BC, Ané C, Sanderson MJ, Wainwright PC (2006) Testing for different rates of continuous trait evolution using likelihood. Evolution **60**: 922–33

O'Meara BC, Beaulieu JM (2016) Past, future, and present of state-dependent models of diversification. Am J Bot **103**: 1–4

Paradis E (2013) Molecular dating of phylogenies by likelihood methods: a comparison of models and a new information criterion. Mol Phylogenet Evol **67**: 436–44

Patz JA, Campbell-Lendrum D, Holloway T, Foley JA (2005) Impact of regional climate change on human health. Nature **438**: 310–317

Pearson RG (2006) Climate change and the migration capacity of species. Trends Ecol Evol (Personal Ed **21**: 111–3

Peng C, Ma Z, Lei X, Zhu Q, Chen H, Wang W, Liu S, Li W, Fang X, Zhou X (2011) A drought-induced pervasive increase in tree mortality across Canada's boreal forests. Nat Clim Chang **1**: 467–471

Pfautsch S, Harbusch M, Wesolowski A, Smith R, Macfarlane C, Tjoelker MG, Reich PB, Adams MA (2015) Climate determines vascular traits in the ecologically diverse genus *Eucalyptus*. Ecol Lett n/a–n/a

Piggin J, Bruhl JJ (2010) Phylogeny reconstruction of Callitris Vent. (Cupressaceae) and its allies leads to inclusion of Actinostrobus within Callitris. Aust Syst Bot **23**: 69–93

Pittermann J, Choat B, Jansen S, Stuart SA, Lynn L, Dawson TE (2010) The relationships between xylem safety and hydraulic efficiency in the Cupressaceae: the evolution of pit membrane form and function. Plant Physiol **153**: 1919–31

Pittermann J, Sperry JS, Hacke UG, Wheeler JK, Sikkema EH (2006a) Inter-tracheid pitting and the hydraulic efficiency of conifer wood: The role of tracheid allometry and cavitation protection. Am J Bot **93**: 1265–1273

Pittermann J, Sperry JS, Hacke UG, Wheeler JK, Sikkema EH (2005) Torus-Margo Pits Help Conifers Compete with Angiosperms. Science (80-) **310**: 1924–1924

Pittermann J, Sperry JS, Wheeler JK, Hacke UG, Sikkema EH (2006b) Mechanical reinforcement of tracheids compromises the hydraulic efficiency of conifer xylem. Plant, Cell Environ **29**: 1618–1628

Pittermann J, Stuart SA, Dawson TE, Moreau A (2012) Cenozoic climate change shaped the evolutionary ecophysiology of the Cupressaceae conifers. Proc Natl Acad Sci U S A **109**: 9647–52

Pivovaroff AL, Burlett R, Lavigne B, Cochard H, Santiago LS, Delzon S (2016) Testing the ' microbubble effect ' using the Cavitron technique to measure xylem water extraction curves. AoB Plants 1–10

Pivovaroff AL, Sack L, Santiago LS (2014) Coordination of stem and leaf hydraulic conductance in southern California shrubs: A test of the hydraulic segmentation hypothesis. New Phytol **203**: 842–850

Plaut JA, Yepez EA, Hill J, Pangle R, Sperry JS, Pockman WT, McDowell NG (2012) Hydraulic limits preceding mortality in a piñon-juniper woodland under experimental drought. Plant Cell Environ **35**: 1601–17

Pye MG, Gadek P a., Edwards KJ (2003) Divergence, diversity and species of the Australasian Callitris (Cupressaceae) and allied genera: Evidence from ITS sequence data. Aust Syst Bot **16**: 505–514

Pyron RA, Wiens JJ (2013) Large-scale phylogenetic analyses reveal the causes of high tropical amphibian diversity. Proc Biol Sci **280**: 20131622

Quentin AG, Pinkard EA, Ryan MG, Tissue DT, Baggett LS, Adams HD, Maillard P, Marchand J, Landhäusser SM, Lacointe A, et al (2015) Non-structural carbohydrates in woody plants compared among laboratories. Tree Physiol tpv073

Rabosky DL (2014) Automatic detection of key innovations, rate shifts, and diversity-dependence on phylogenetic trees. PLoS One **9**: e89543

Rabosky DL, Donnellan SC, Grundler M, Lovette IJ (2014) Analysis and visualization of complex macroevolutionary dynamics: an example from Australian scincid lizards. Syst Biol **63**: 610–27

Rabosky DL, Goldberg EE (2015) Model Inadequacy and Mistaken Inferences of Trait-Dependent Speciation. Syst Biol **64**: 340–355

Rabosky DL, Santini F, Eastman J, Smith SA, Sidlauskas B, Chang J, Alfaro ME (2013) Rates of speciation and morphological evolution are correlated across the largest vertebrate radiation. Nat Commun **4**: 1958

Reich PB (2014) The world-wide "fast-slow" plant economics spectrum: A traits manifesto. J Ecol **102**: 275–301

Revell LJ (2010) Phylogenetic signal and linear regression on species data. Methods Ecol Evol **1**: 319–329

Rockwell FE, Wheeler JK, Holbrook NM (2014) Cavitation and Its Discontents: Opportunities for Resolving Current Controversies. Plant Physiol **164**: 1649–1660

Rolland J, Condamine FL, Jiguet F, Morlon H (2014) Faster speciation and reduced extinction in the tropics contribute to the Mammalian latitudinal diversity gradient. PLoS Biol **12**: e1001775

Ronquist F, Teslenko M, Van Der Mark P, Ayres DL, Darling A, Höhna S, Larget B, Liu L, Suchard M a., Huelsenbeck JP (2012) Mrbayes 3.2: Efficient bayesian phylogenetic inference and model choice across a large model space. Syst Biol **61**: 539–542

Rowland L, da Costa ACL, Galbraith DR, Oliveira RS, Binks OJ, Oliveira AAR, Pullen AM, Doughty CE, Metcalfe DB, Vasconcelos SS, et al (2015) Death from drought in

tropical forests is triggered by hydraulics not carbon starvation. Nature **528**: 119–122

Sáenz-Romero C, Lamy J-B, Loya-Rebollar E, Plaza-Aguilar A, Burlett R, Lobit P, Delzon S (2013) Genetic variation of drought-induced cavitation resistance among Pinus hartwegii populations from an altitudinal gradient. Acta Physiol Plant **35**: 2905–2913

Sala A, Piper F, Hoch G (2010) Physiological mechanisms of drought-induced tree mortality are far from being resolved. New Phytol **186**: 274–81

Salleo S, Nardini A, Pitt F, Lo Gullo MA (2000) Xylem cavitation and hydraulic control of stomatal conductance in Laurel (Laurus nobiris L.). Plant, Cell Environ **23**: 71–79

Sanderson MJ (2002) Estimating absolute rates of molecular evolution and divergence times: a penalized likelihood approach. Mol Biol Evol **19**: 101–9

Scholander PF, Hammel HT, Hemmingsen E a., Bradstreet ED (1964) Hydrostatic Pressure and Osmotic Potential in Leaves of Mangroves and Some Other Plants*. Proc Natl Acad Sci U S A **52**: 119–125

Schroeder JI, Kwak JM, Allen GJ (2001) Guard cell abscisic acid signalling and engineering drought hardiness in plants. Nature **410**: 327–330

Schuldt B, Knutzen F, Delzon S, Jansen S, Müller-Haubold H, Burlett R, Clough Y, Leuschner C (2015) How adaptable is the hydraulic system of European beech in the face of climate change-related precipitation reduction? New Phytol. doi: 10.1111/nph.13798

Settele J, Scholes R, Brando P, Chini LP, Zealand N, France FC (2014) Terrestrial and Inland Water Systems. *In* CB Field, VR Barros, D D.J., KJ Mach, MD Mastrandrea, TE Bilir, M Chatterjee, KL Ebi, YO Estrada, RC Genova, et al., eds, Clim. Chang. 2014 Impacts, Adapt. Vulnerability. Part A Glob. Sect. Asp. Contrib. Work. Gr. II to Fifth Assess. Rep. Intergov. Panel Clim. Chang. Cambridge University Press, Cambridge, United Kingdom and New York, NY, USA, pp 271–359

Sevanto S, McDowell NG, Dickman LT, Pangle R, Pockman WT (2014) How do trees die? A test of the hydraulic failure and carbon starvation hypotheses. Plant Cell Environ **37**: 153–61

Shi JJ, Rabosky DL (2015) Speciation dynamics during the global radiation of extant bats. Evolution (N Y) **69**: 1528–1545

Sperry JS (2003) Evolution of water transport and xylem structure. Int J Plant Sci **164**: S115–S127

Sperry JS, Christman MA, Torres-Ruiz JM, Taneda H, Smith DD (2012) Vulnerability curves by centrifugation: is there an open vessel artefact, and are "r" shaped curves necessarily invalid? Plant, Cell Environ **35**: 601–610

Sperry JS, Hacke UG, Oren R, Comstock J (2002) Water deficits and hydraulic limits to leaf water supply. Plant Cell Environ **25**: 251–263

Sperry JS, Hacke UG, Pittermann J (2006) Size and function in conifer tracheids and angiosperm vessels. Am J Bot **93**: 1490–1500

Sperry JS, Meinzer FC, McCulloh KA (2008) Safety and efficiency conflicts in hydraulic architecture: scaling from tissues to trees. Plant Cell Environ **31**: 632–645

Sperry JS, Sullivan JE (1992) Xylem embolism in response to freeze-thaw cycles and water stress in ring-porous, diffuse-porous, and conifer species. Plant Physiol **100**: 605–613

Sperry JS, Tyree MT (1988) Mechanism of water stress-induced xylem embolism. Plant Physiol **88**: 581–7

Stadler T (2013) Recovering speciation and extinction dynamics based on phylogenies. J Evol Biol **26**: 1203–1219

Stamatakis a, Ludwig T, Meier H (2005) RAxML-III: a fast program for maximum likelihood-based inference of large phylogenetic trees. Bioinformatics **21**: 456–63

Stocker TF, Qin D, Plattner G-K, Tignor MM, Allen SK, Boschung J, Nauels A, Xia Y, Bex V, Midgley PM (2013) IPCC, 2013: Climate Change 2013: The Physical Science Basis. Contribution of Working Group I to the Fifth Assessment Report of the Intergovernmental Panel on Climate Change. Cambridge University Press, Cambridge, United Kingdom and New York, NY, USA

Tamura K, Peterson D, Peterson N, Stecher G, Nei M, Kumar S (2011) MEGA5: molecular evolutionary genetics analysis using maximum likelihood, evolutionary distance, and maximum parsimony methods. Mol Biol Evol **28**: 2731–9

Terry RG, Adams RP (2015) A molecular re-examination of phylogenetic relationships among Juniperus, Cupressus, and the Hesperocyparis-Callitropsis-Xanthocyparis clades of Cupressaceae. Phytologia **97**: 67–75

Terry RG, Bartel JA, Adams RP (2012) Phylogenetic relationships among the New World cypresses (Hesperocyparis; Cupressaceae): evidence from noncoding chloroplast DNA sequences. Plant Syst Evol **298**: 1987–2000

Terry RG, Pyne MI, Bartel JA, Adams RP (2016) A molecular biogeography of the New World cypresses (Callitropsis, Hesperocyparis; Cupressaceae). Plant Syst Evol. doi: 10.1007/s00606-016-1308-4

Thomas GH, Freckleton RP (2012) MOTMOT: models of trait macroevolution on trees. Methods Ecol Evol **3**: 145–151

Tixier A, Cochard H, Badel E, Dusotoit-Coucaud A, Jansen S, Herbette S (2013) Arabidopsis thaliana as a model species for xylem hydraulics: Does size matter? J Exp Bot **64**: 2295–2305

Torres-Ruiz JM, Cochard H, Mayr S, Beikircher B, Diaz-Espejo A, Rodriguez-Dominguez CM, Badel E, Fernández JE (2014) Vulnerability to cavitation in *Olea europaea* current-year shoots: further evidence of an open-vessel artifact associated with centrifuge and air-injection techniques. Physiol Plant **152**: 465–474

Torres-Ruiz JM, Jansen S, Choat B, McElrone AJ, Cochard H, Brodribb TJ, Badel E, Burlett R, Bouche PS, Brodersen CR, et al (2015) Direct X-Ray Microtomography Observation Confirms the Induction of Embolism upon Xylem Cutting under Tension. Plant Physiol **167**: 40–43

Tyree MT (1972) The Measurement of the Turgor Pressure and the Water Relations of Plants by the Pressure-bomb Technique. J Exp Bot **23**: 267–282

Tyree MT (1997) The Cohesion-Tension theory of sap ascent : current controversies. J Exp Bot **48**: 1753–1765

Tyree MT (2003) The ascent of water. **1205**: 2003

Tyree MT, Cochard H, Cruiziat P, Sinclair P, Ameglio T (1993) Drought-Induced Leaf Shedding in Walnut: Evidence for Vulnerability segmentation. Plant Cell Environ **16**: 879–882

Tyree MT, Davis SD, Cochard H (1994) Biophysical perspectives of xylem evolution: is there a tradeoff of hydraulic efficiency for vulnerability to dysfunction? Iawa J. **15**: 335–360

Tyree MT, Ewers FW (1991) The hydraulic architecture of trees and other woody plants. New Phytol 345–360

Tyree MT, Sperry JS (1989) Vulnerability of xylem to cavitation and embolism. Annu Rev Plant Biol **40**: 19–36

Tyree MT, Zimmermann MH (2013) Xylem Structure and the Ascent of Sap. Springer Science & Business Media

Tyree MT, Zimmermann MH (2002) Xylem Structure and the Ascent of Sap. Springer Science & Business Media

Urli M, Porté AJ, Cochard H, Guengant Y, Burlett R, Delzon S (2013) Xylem embolism threshold for catastrophic hydraulic failure in angiosperm trees. Tree Physiol **33**: 672–83

Walther G-R, Post E, Convey P, Menzel A, Parmesan C, Beebee TJ, Fromentin J-M, HoeghGuldberg O, Bairlein F (2002) Ecological responses to recent climate change. Nature **416**: 389–395

Wang R, Zhang L, Zhang S, Cai J, Tyree MT (2014) Water relations of Robinia pseudoacacia L.: do vessels cavitate and refill diurnally or are R-shaped curves invalid in Robinia? Plant Cell Environ. doi: 10.1111/pce.12315

Westoby M, Wright IJ (2006) Land-plant ecology on the basis of functional traits. Trends Ecol Evol **21**: 261–268

Wheeler JK, Huggett B a, Tofte AN, Rockwell FE, Holbrook NM (2013) Cutting xylem under tension or supersaturated with gas can generate PLC and the appearance of rapid recovery from embolism. Plant Cell Environ **36**: 1938–49

Willson CJ, Manos PS, Jackson RB (2008) Hydraulic traits are influenced by phylogenetic history in the drought-resistant, invasive genus Juniperus (Cupressaceae). Am J Bot **95**: 299–314

Wortemann R, Herbette S, Barigah TS, Fumanal B, Alia R, Ducousso A, Gomory D, Roekel-Drevet P, Cochard H (2011) Genotypic variability and phenotypic plasticity of cavitation resistance in Fagus sylvatica L. across Europe. Tree Physiol **31**: 1175–1182

Wright IJ, Falster DS, Pickup M, Westoby M (2006) Cross-species patterns in the coordination between leaf and stem traits, and their implications for plant hydraulics. Physiol Plant **127**: 445–456

Zachos J, Pagani M, Sloan L, Thomas E, Billups K (2001) Trends, rhythms, and aberrations in global climate 65 Ma to present. Science (80-) **292**: 686–693

Zhao M, Running SW (2010) Drought-Induced Reduction in Global Terrestrial Net Primary Production from 2000 Through 2009. Science (80-) **329**: 940–943

Zufferey V, Cochard H, Ameglio T, Spring JL, Viret O (2011) Diurnal cycles of embolism formation and repair in petioles of grapevine (Vitis vinifera cv. Chasselas). J Exp Bot **62**: 3885–3894

Zwieniecki MA, Holbrook NM (2009) Confronting Maxwell's demon: biophysics of xylem embolism repair. Trends Plant Sci **14**: 530–534

Annexes

Annexes.

ANNEX 1. Sáenz-Romero et al. (accepted, major revisions, Journal of Plant Hydraulics): Mexican conifers are not all equal in their ability to face ongoing climate change

ANNEX 2. Castagnerol et al. (accepted – major revisions, Oecologia): Host range expansion is density dependent

ANNEX 3. Analysis of genome size evolution and its relationship with hydraulic traits in conifers.

ANNEX 4. Analysis of cavitation resistance using the auteur method (Eastman et al., 2011).

ANNEX 5. Examination of the relationship between warts and callitroid thickenings and both climate and cavitation resistance in the Callitris clade, based on data from Heady et al. (1994).

ANNEX 6. Les conifères, une famille à évolution complexe. Maximilien Larter et Pauline Bouche (Jardins de France 2013 – Hors-série Les conifères font de la résistance)

ANNEX 7. Le Pinetum de Bedgebury : « la plus belle collection de conifères du monde ». Maximilien Larter (Jardins de France 2012 – Hors-série Les conifères font de la résistance)

Annex 1. Sáenz-Romero et al. (accepted – major revisions, Journal of Plant Hydraulics): Mexican conifers are not all equal in their ability to face ongoing climate change

Mexican conifers are not all equal in their ability to face ongoing climate change

C. Sáenz-Romero[1,2], M. Larter[2], N. González-Muñoz[2], C. Wehenkel[3], A. Blanco-Garcia[4], D. Castellanos-Acuña[1,5], R. Burlett[2] and S. Delzon[2]

[1]Universidad Michoacana de San Nicolás de Hidalgo, Instituto de Investigaciones Agropecuarias y Forestales (UMSNH-IIAF). Km 9.5 Carretera Morelia-Zinapécuaro, Tarímbaro Michoacán 58880, 5 México; [2]Institut National de la Recherche Agronomique (INRA), Unité Mixte de Recherche 1202 Biodiversité Gènes & Communautés (UMR 1202 BIOGECO), F-33610 Cestas, France & Université 7 de Bordeaux, F-33615 Pessac, France; [3]Instituto de Silvicultura e Industria de la Madera, Universidad 8 Juárez del Estado de Durango, Aptdo. Postal 741 Zona Centro, Dgo., C.P. 34000, México; [4] Facultad 9 de Biología, Universidad Michoacana de San Nicolás de Hidalgo, Av. Francisco J. Mújica s/n, Col. 10 Felícitas del Río, Morelia Michoacán 58040, México; [5] Department of Renewable Resources, Faculty 11 of Agricultural, Life, and Environmental Sciences, University of Alberta, 733 General Services 12 Building Edmonton, AB, T6G 2H1, Canada.

Corresponding author: Cuauhtémoc Sáenz-Romero, csaenzromero@gmail.com

Date of submission:

Date of publication:

Abstract

Recent massive die-back of forest trees due to drought stress makes more urgent to assess the variability of physiological traits that might be critical to predict forest response and adaptation to climate change. We investigated xylem vulnerability to cavitation and xylem specific hydraulic conductivity for three principal conifer genera (*Juniperus monticola*, *Juniperus deppeana*, *Juniperus flaccida*, *Pinus pseudostrobus*, *Pinus leiophylla, Pinus devoniana*; endangered *Picea chihuahuana*) of Mexican mountains, in order to identify the more vulnerable species to future warmer and dryer climates. Hydraulic traits have been examined using the *in situ*flow centrifuge technique (Cavitron) on branches collected both on adult trees from natural populations and seedlings growing in common garden. We found evidence for significant differences in xylem safety between genera (P_{50}: pressure inducing 50% loss of hydraulic conductance): the three juniper species exhibited low P_{50} values (ranging from -9.9 to -10.4 MPa), in comparison to much more vulnerable pine and spruce species (P_{50} ranging between - 2.9 to - 3.3 MPa). Hydraulic traits showed also no plasticity: there were no significant differences in P_{50} values between trees assessed *in situ* and seedlings growing in common garden. We hypothesize that if climate change makes their natural habitats much warmer and dryer, as projected, the populations of Mexican pines and spruces will likely severely decline due to drought-stress induced cavitation, meanwhile juniper species will survive.

Introduction

Concerns are increasing due to the mounting evidence of forest decline related to drought stress apparently linked to ongoing climatic change (Breshears et al. 2005; Peñuelas et al. 2007; Mátyás 2010; Allen et al. 2010). Hotter drought periods are inducing massive tree mortality (Allen et al. 2015), and by year 2050, there likely will be a substantial vegetation reorganization (McDowell and Allen 2015), with a plant community composition unfamiliar to modern civilization (Williams et al. 2013). In such context, the study of variation among and within forest species for cavitation resistance is very relevant to predict the potential of adaptation to climatic change (Choat et al. 2012). Resistance to cavitation has been shown as a good estimator of species tolerance to drought in vascular plants (Brodribb and Cochard 2009; Brodribb et al. 2010). Previous studies have reported a high variability of P_{50} (a proxy of cavitation resistance, corresponding to the xylem pressure inducing 50% loss of hydraulic conductance) among conifer species, ranging from -3 to -19 MPa (Delzon et al. 2010, Pittermann et al. 2010; Larter et al. 2015).

There are indications that many forest tree species have a very narrow hydraulic safety margin (< 1 MPa) and therefore they potentially will face long-term reductions in productivity and survival in a drier world (Choat et al. 2012). However, large differences of hydraulic safety margin have been observed between species growing in the same habitat and can therefore favor one species over another (Breshears et al. 2005; Urli et al. 2015). Conifers of genera *Juniperus*, *Picea* and *Pinus* frequently co-occur in the highly biodiverse Mexican mountains (Quiñones-Perez et al. 2014; Figure 1), as they share similar climatic habitat conditions (although they can also occur separately).

Indeed, previous studies of cavitation resistance in conifer forest communities of southern USA (Arizona, New Mexico, Utah and Colorado states, Breshears et al. 2005) have shown large differences in hydraulic safety (P_{50} values), leading to different safety margin between *Pinus edulis* and *Juniperus monosperma*.

Differences among conifer genera sharing similar climatic habitats has not been explored for Mexico in more detail, despite the very large biodiversity for conifers in Mexico (Styles 1993). A previous study focused on differences within *Pinus hartwegii* along an altitudinal gradient, which showed no population-level genetic differentiation for cavitation resistance (Saenz-Romero et al. 2013), a trend that is consistent with much broader studies that indicate remarkably low variation among populations within conifer species (i.e. *Pinus pinaster*, Lamy et al. 2011). At the genus level, pines and spruces seem to be moderately resistant to cavitation (P50: -3 to -4.7 MPa and -3.7 to -5.2 MPa, respectively; Bouche et al. 2014). This pattern contrasts strongly with the more cavitation-resistant genus *Juniperus* (*Cupressaceae*), that also shows much more variation across species, with P_{50}"s ranging from around 6 to -14 MPa (Bouche et al. 2014, Willson et al. 2008).

In the present study, we aim to assess differences in hydraulic safety (drought-induced cavitation resistance) and conductivity (water-transport efficiency) among seven species of Mexican conifer species belonging to three conifer genera: *Juniperus*, *Pinus* and *Picea*. Conifers of genera *Juniperus*, *Pinus* and *Picea* frequently co-occur in the highly biodiverse Mexican mountains (Quiñones-Perez et al. 2014; Figure 1), as they share similar climatic habitat conditions (although they can also occur separately). Mountain conifer forests of Mexico are expected to experience a drier climate with more frequent droughts, which may lead to a 92 % reduction of their suitable climatic habitat along the Trans-Mexican Volcanic Belt by the end of this century (Rehfeldt et al. 2012). Under this scenario, we hypothesize

highly species-specific responses, with a high risk of mortality for species with a high vulnerability to cavitation as a response to drought events and a competitive advantage for highly resistant species to cavitation.

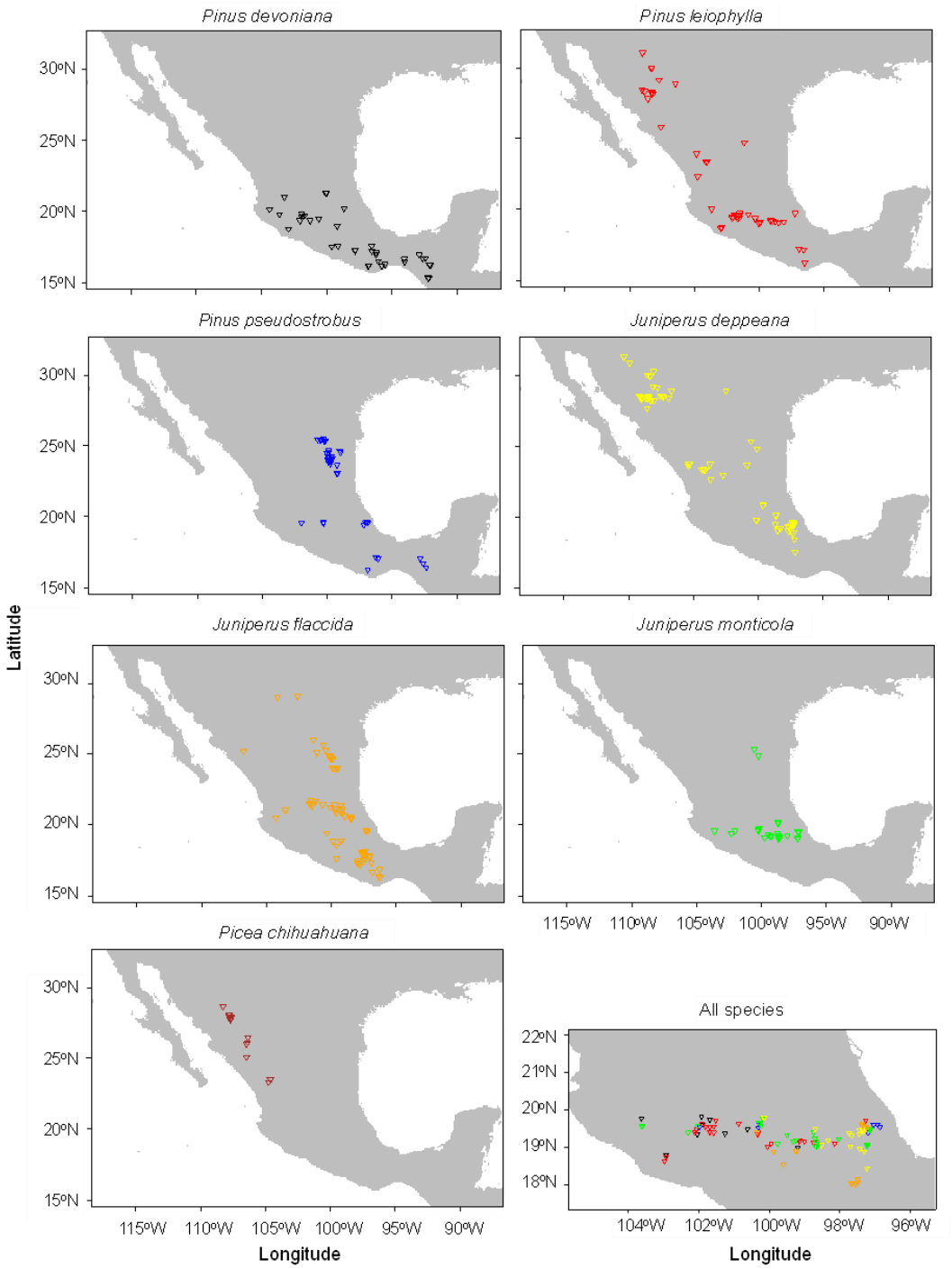

Figure 1. Distribution of the seven studied conifers in México. Sites correspond to plots recorded by the Mexican National Forest Inventory, for which there are climatic and aridity index data available, downloaded from http://www.worldclim.org/bioclim and http://www.cgiar-csi.org/data/global-aridity-and-pet-database, respectively. Last insert zooms on Trans-Mexican Volcanic Belt.

Materials and Methods

Study area and study species

We focused on seven conifer species, six of them occurring along a wide altitudinal gradient along the central Mexican mountains (Trans-Mexican Volcanic Belt, TMVB) and one of them only at the Sierra Madre Occidental (Figure 1). The species were:

(a) Three juniper species along an altitudinal gradient: *Juniperus monticola* (high elevation, cold and humid environments, including sites inside the Monarch Butterfly Biosphere Reserve overwintering sanctuaries), *J. deppeana* (intermediate elevations between 2200-2900 m a.s.l., temperate climate, occurring at the pine-oak forest, wide distribution in Mexico) and *J. flaccida* (lower elevation, representing the lowest altitudinal distribution of the genus in the studied region, marked drought/rainy seasonality and savanna-like vegetation with frequent natural or induced fires, overlapping with the upper altitudinal limits of the tropical dry forest) (Carranza and Zamudio 1994).

(b) Three pine species among the most abundant pine species of the pine-oak forest at the TMVB at the Michoacán state, with partially altitudinal overlapping distributions: *Pinus pseudostrobus* (intermediate to high elevations, the most abundant and economically important specie), *P. leiophylla* (intermediate altitudes, appearing on poorer sites than *P. pseudostrobus*) and *P. devoniana* (low altitudinal limit of the pine-oak forest, close to the upper altitudinal limit of the tropical dry forest). The three pine species overlaps at the middle altitudinal range of the pine-oak forest, approximately at 2.200 to 2.300 m of altitude (Castellanos-Acuña et al. 2015; Table 1)

(c) A very rare, endangered, endemic spruce, *Picea chihuahuana*, with fragmented endogamic populations, at high elevations cold and humid sites on Sierra Madre Occidental, in northwestern Mexico. *Picea chihuahuana* is the most abundant spruce among the only three of that genus existing in México (the others are *Picea martinezii* and *P. mexicana*), where spruces are postglacial relicts (Ledig et al. 2010; Wehenkel and Saenz-Romero et al. 2012; IUCN 2015).

Table 1. Population origin of branch samples analyzed for cavitation, either from collection of field samples, or from populations represented in a common garden test. Except *Picea chihuahuana*, collected in Durango State (Dgo.), northwestern México, all others come from Michoacán state (Mich.), center-western México. Sample size indicate number of trees were samples were collected.

Locality and State	Elevation (m a.s.l.)	Lat (N)	Lon (W)	Species	Sample size (individuals)	
					Field	Common garden
Santa Bárbara, Dgo.	2.725	23.66	105.44	*Picea chihuahuana*	15	-
Sierra Chincua, Mich.	3.142	19.65	100.25	*Juniperus monticola*	8	-
Tlalpuhahua, Mich.	2.575	19.80	100.17	*Juniperus deppeana*	8	-
Tuxpan, Mich.	1.870	19.60	100.48	*Juniperus flaccida*	7	-
Cerro Pario (High), Mich.	2.746	19.47	102.18	*Pinus pseudostrobus*	6	-
Cerro Pario (Int.), Mich.	2.600	19.47	102.19	*Pinus pseudostrobus*	7	-
Cerro Pario (Low), Mich.	2.520	19.46	102.20	*Pinus pseudostrobus*	-	3
La Pila (High), Mich.	2.422	19.45	102.18	*Pinus pseudostrobus*	7	-
				Pinus leiophylla	7	-
La Pila (High), Mich.	2.310	19.44	102.17	*Pinus pseudostrobus*	-	3
				Pinus leiophylla	6	2
				Pinus devoniana	-	5
El Rosario (High), Mich.	2.217	19.43	102.17	*Pinus pseudostrobus*	-	- 2
				Pinus leiophylla	-	-
				Pinus devoniana	6	
El Rosario (Int.), Mich.	2.110	19.43	102.16	*Pinus leiophylla*	-	2
				Pinus devoniana	6	1
El Rosario (Low), Mich.	2.034	19.42	102.15	*Pinus devoniana*	7	-
Jicalán, Mich.	1.650	19.38	102.08	*Pinus devoniana*	6	-

Sampling procedures

Drought-induced resistance to cavitation and hydraulic efficiency were evaluated from branches collected from natural populations of those seven conifer species. For each juniper species, we collected branches of seven to eight trees belonging to one population representative of the distribution range of the species, in zones with high conifer diversity. (Table 1). For each pine species, six to seven trees from two to four populations were collected, aiming to at least partially represent the altitudinal distribution range of each species (Table 1). Fifteen individuals were sampled from *Picea chihuahuana* Santa Barbara population (also known as Arroyo El Infierno; Ledig et al. 2000), at a high elevation (2.725 m) site of Sierra Madre Occidental, Durango State, northwestern México.

As a complementary sampling, we collected branches from the three pine species on individuals growing in a common garden test at Morelia, Michoacán (Lat. 19.69 N, Lon. 101.25 W, altitude 1.900 m a.s.l.). These trees were grown from seeds obtained from some of the natural populations that we 127 sampled, and also from additional populations of the same species and region. However, due to the 128 minimum branch size requirement for xylem cavitation analyses (see details below), only a reduced 129 number of individuals was sampled: two to five seedlings (exceptionally one seedling in one case), 130 from two populations of each pine species (Table 1). This additional common garden sampling was not possible for the rest of the species studied here, as provenance tests were unavailable. The site of the common garden tests has a climate much warmer and dryer (mean annual temperature 17.0 133 ºC, mean annual precipitation 871 mm) than the sites from the studied natural populations (although watering was provided as needed to ensure seedling survival).

Sample processing

Branches were collected in the early morning to avoid high temperatures and all needles were immediately removed to prevent desiccation. The samples were then wrapped in wet paper towels, placed in black bags, and immediately posted to France for their analyses. Vulnerability to drought induced cavitation was determined at the high-throughput phenotyping platform for hydraulic traits (CavitPlace, University of Bordeaux, Talence, France; http://sylvain-delzon.com/caviplace). The samples were kept wet and cool (3°C) until cavitation resistance was measured within three weeks after collection. Prior to measurement, all branches were cut with a razor blade under water to a standard length of 27 cm, and the bark was removed.

Measurement of resistance to cavitation

Xylem cavitation was assessed with the CAVITRON, a flow centrifuge technique following the procedure described in Cochard (2002) and Cochard et al. (2005). In the CAVITRON, a centrifugal force establishes a negative xylem pressure, inducing a loss of conductance by cavitation. Samples are inserted into a custom-built rotor (Precis 2000, Bordeaux, France) mounted on a high-speed centrifuge (Sorvall RC5, USA). Xylem pressure (P_i) is first set to a reference pressure (-0.5 MPa) and hydraulic conductivity (*ki*) is determined by measuring the

flux through the sample. The centrifugation speed is then set to a higher value for 3 minutes to expose the sample to more negative pressure.

The conductance was measured three to four times, and the average was used to compute the percent loss of xylem conductance (PLC in %) at that pressure (see Delzon et al. 2010 for details). This procedure was repeated for at least eight pressure steps with a -0.5 MPa step increment until PLC reached at least 90%. Rotor velocity was monitored with a 10 rpm resolution electronic tachymeter 160 and xylem pressure was adjusted to about -0.02 MPa. Conductance measurements were done with the 161 Cavisoft software (version 2.0, BIOGECO, University of Bordeaux).

The percent loss of xylem conductance as a function of xylem pressure (MPa) represents the sample's vulnerability curve (VC). A sigmoid function (Pammenter and Vander Willigen 1998) was fitted to the VC from each sample using the following equation:

$$PLC = \frac{100}{\left[1 + \exp\left(\frac{S}{25} * \left(P - P_{50}\right)\right)\right]}$$

where P_{50} (MPa) is the xylem pressure inducing 50% loss of conductance and S (% MPa^{-1}) is the slope of the vulnerability curve at the inflexion point. The xylem specific hydraulic conductivity (k_s, m^2 $MPa^{-1}s^{-1}$) was calculated by dividing the maximum hydraulic conductivity measured at low speed by the sapwood area of the sample. More negative P_{50} (xylem pressure inducing 50% loss of conductance) values indicate higher resistance to cavitation, while the slope of the vulnerability curve (S) indicates how fast cavitation progresses at P_{50}.

Statistical analysis

Differences among species were tested for xylem pressure inducing 50% loss of conductance (P_{50}), slope of the vulnerability curve at the inflexion point (S) and xylem specific hydraulic conductivity (k_s), by conducting an analysis of variance (ANOVA), using the Procedure GLM of SAS (SAS Institute, 2004), followed by a multiple mean Tukey tests (α = 0.05).

Because we had field samples from all the species but only for the three pine species also samples from a common garden provenance tests, and in all cases, a relatively reduced

number of samples, we conducted a nested ANOVA to test differences among genus and among species within for the xylem pressure inducing 50% loss of conductance (P_{50}), the slope of the vulnerability curve at the inflexion point (*S*) and the xylem specific hydraulic conductivity (k_s). We used the Procedure GLM of SAS (SAS Institute, 2004).

For the specific case of the genus *Pinus*, we also explored the plasticity of mentioned variables. To do so, we compared the P_{50}, *S* and k_s of field versus common garden samples by a factorial ANOVA. Variance components were estimated using the Procedure VARCOMP with the method of restricted maximum likelihood (REML) of SAS (SAS Institute, 2004).

In order to represent the hydraulic values in the context of the entire climatic range of the species, we conducted a regression analysis between the means of the hydraulic traits of each species (all species, only field data) against the median of three climate variables aiming to represent the overall species climate niche: Mean Annual Temperature (MAT), Mean Annual Precipitation (MAP), Annual Aridity Index (AAI: Mean Annual Precipitation/ Mean Annual Potential EvapoTranspiration). We also regressed the hydraulic traits of each species against extreme values of those three climatic variables, calculated as the median of the 5% of highest MAT (MAT_max), lowest MAP (MAP_min) and more arid AAI (AAI_max) values. These climatic variables have been demonstrated to be in important association with means per species of P_{50} (Choat et al. 2012, Maherali et al. 2005). Climatic and aridity index values averaged per species were estimated from presence points covering the full distribution range of the species (illustrated on Figure 1 for Mexico) and obtained from http://www.worldclim.org/bioclim and http://www.cgiar-csi.org/data/global-aridity-and-pet-database, respectively.

Results

Differences among genera and species

Hydraulic traits varied widely across studied species, with P_{50} ranging from -2.94 MPa (*Pinus pseudostrobus*) to -10.37 MPa (*Juniperus monticola*). Slope of the vulnerability curve varied from extremely steep (87.78 % MPa^{-1} for *Pinus leiophylla*) to very flat (i.e. less than 20 % MPa^{-1} for each juniper species).

Most of this variation is at the genus level, as for example, juniper P_{50} was on average about 7 MPa more negative than for pines and spruce (see Figure 2). Similarly, we found large differences in the slope of the vulnerability curve at the inflexion point (*S*) between the juniper species in comparison to the pines and the spruce. The three *Pinus* species had *S* values well above 50, *Picea chihuahuana* close to it (47), whereas *Juniperus* species had *S* values between 16 and 20. We evidenced significant differences among genera in P_{50} (xylem pressure inducing 50% loss of conductance, $P < 0.0001$) and *S* (slope of the vulnerability curve at the inflexion point, $P = 0.0013$). Differences among genera explained 98 % and 67 % of the total variation for P_{50} and *S*, respectively (Table 2). In contrast, differences between species within genera account for a marginal 0.2%, and 1.9% for P_{50}, and *S*, respectively (Table 2).

Xylem transport efficiency, k_s, varied from 0.0003 m^2 MPa^{-1} s^{-1} for *Picea chihuahuana* to 0.0021 m^2 $MPa^{-1}s^{-1}$ for *Pinus leiophylla* (17 % of the total variation is explained by the species) but no significant difference between genera have been found for this trait ($P = 0.066$).

There is a complete lack of association between P_{50}, *S* and k_s with the six climatic variables (regression: $r^2 < 0.03$; $P > 0.20$). Notice on Figure 2 that *Juniperus monticola*, despite growing in sites much less arid (more cold and humid) than all of the pines and the spruce, its P_{50} is similar to that of *Juniperus deppeana* and *J. flaccida*, that both grow in the warmest and driest sites in this study.

Similar distributions are found when plotting P_{50} against the other five climatic variables: MAT, MAP, MAT_max, MAP_min and AAI_max (plots not shown).

Differences between field and common garden test

There were not statistical differences between the values of the hydraulic traits obtained from field and common garden trees, denoting a lack of plasticity of the measured traits across environments (Table 2). Differences among studies account for a meaningless 0.0 %, 0.9 % and 0.0 % of the total variation for P_{50}, *S* and k_s, respectively (no significant; $P > 0.45$; Table 2). Figure 3 shows how much similar are the P_{50} values between studies and also among pine species.

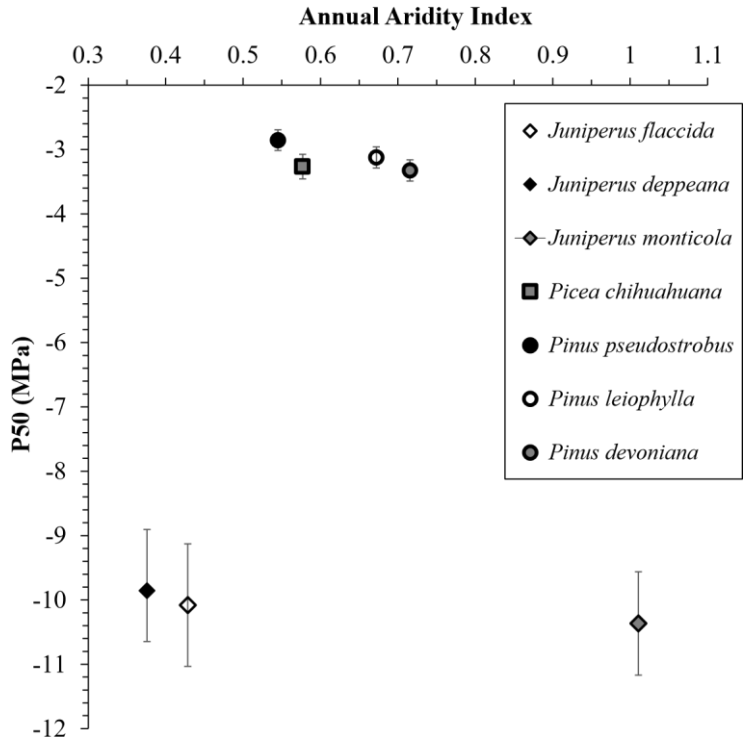

Figure 2. Xylem pressure inducing 50% loss of hydraulic conductance (P_{50}) in MPa, against Annual Aridity Index median per species (larger values indicate colder and moister; smaller values indicate warmer and dryer environments). Vertical bars represent 95 % confidence intervals

Discussion

Large differences among genera

We evidenced here that the three juniper species studied are much more resistant to cavitation than the three co-occurring pines species and the Chihuahua spruce examined: P_{50} values of *Juniperus monticola*, *J. deppeana*, and *J. flaccida* were three time more negative than those of *Picea chihuahuana*, *Pinus devoniana*, *P. leiophylla* and *P. pseudostrobus*. Similar differences have been reported between other juniper and pine species growing in same or similar environments (Linton et al. 1998) and, more generally, for what has been previously reported for species of these two genera (Delzon et al. 2010; Bouche et al. 2014). Regarding the slope of the cavitation curve, Delzon et al. (2010) suggested that slopes > 50 % Mpa^{-1} indicate a very fast rate of embolism. In our results, the three pines and *Picea chihuahuana* had *S* mean values much larger than the *Juniperus* species, confirming the larger vulnerability to cavitation of the pine and spruce species in comparison to the juniper species. These

differences can be linked to an evolutionary divergence in hydraulic strategies within conifers when faced with drought (Brodribb et al. 2014).

Table 2. Analysis of variance (% of contribution to total variance and P, significance) of xylem cavitation resistance traits (P_{50}, xylem pressure inducing 50% loss of conductance and *S*, slope of the vulnerability curve at the inflexion point) and xylem transport efficiency (k_s, xylem specific hydraulic conductivity). Analysis were conducted: (a) comparing among genera from branches collected at natural populations (three species of *Juniperus monticola*, three *Pinus* and one *Picea*), and (b) comparing among studies (field vs. common garden) only for *Pinus* species. Origin of samples as in Table 1.

	df	P50		*S*		*ks*	
		%	P	%	P	%	P
a) All species, only field samples							
Genus	2	97.9	<0.0001	67.3	0.0013	45.6	0.0661
Species(Genus)	4	0.2	0.0483	1.9	0.1516	16.9	<0.0001
Residual	88	1.9		30.8		37.6	
Total	94	100.0		100.0		100.0	
b) Only *Pinus* species, field vs. common garden							
Study	1	0.0	0.7475	0.9	0.5457	0.0	0.4524
Species	2	0.0	0.7957	0.0	0.9145	17.0	0.2763
Study* Species	2	21.5	0.0044	8.5	0.0207	9.2	0.1484
Residual	70	78.5		90.5		73.8	
Total	75	100.0		100.0		100.0	

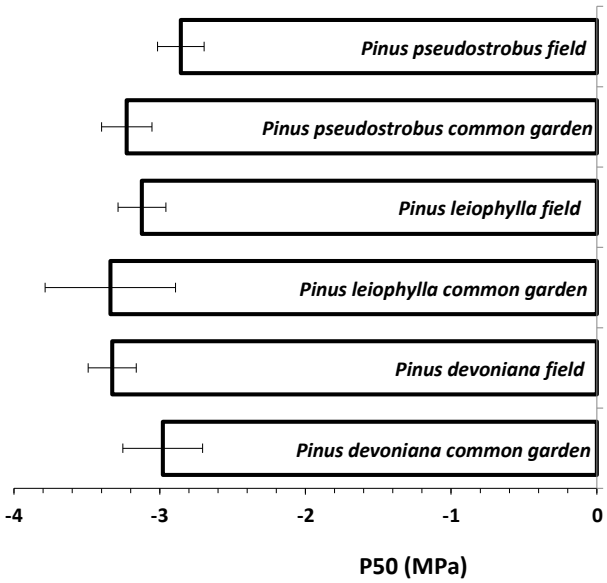

Figure 3. Xylem pressure inducing 50% loss of hydraulic conductance (P_{50}) in MPa, averaged per pine species for each of two studies: samples collected at natural populations (field) and collected from a common garden test. Horizontal bars represent 95 % confidence intervals.

Lack of correlation with climate and conservatism within genera

While several studies reported correlations between P_{50} and MAP or MAT (Maherali et al. 2005; Choat et al. 2012) with species from low precipitation habitats having the lowest P_{50} values, suggesting that the evolutionary associations between increasing cavitation resistance and increasing aridity occurred across functional groups of conifers, no correlations were found here between hydraulic safety (P_{50}, *S*), efficiency traits (k_s) and MAT or MAP across all species studied. For example, *J. monticola* grows at the wettest environment, and yet has similar P_{50} values thank *J. flaccida*, which grows at the driest one, indicating a trait conservatism within genera.

Lack of plasticity

For the *Pinus* genus, we found no difference between cavitation resistance traits between populations growing *in situ* and in common garden, even when the common garden site is much more warmer (1.2 ºC to 3.4 ºC of mean annual temperature difference, depending of which provenance is compared to the common garden test site). This limited plasticity found here suggests that it is unlikely that pines will be able to hydraulically acclimate to accelerated climate change.

The fact that juniper species might be more dominant relative to pine species in future climates than are today, highlight the need of studying variability among juniper populations for cavitation resistant traits, which so far has being studied mostly for pine species.

Implications for climate change adaptation

These results (high vulnerability to cavitation and lack of plasticity for pines) suggest that likely there will be a higher drought-induced mortality of pine species with respect to that of *Juniperus*, if climatic change scenarios turn the current climatic habitats into warmer and dryer environments (Allen et al. 2015), as it is projected for Mexican regions where pine-oak and conifer forest occur (Sáenz-Romero et al. 2010; Rehfeldt et al. 2012). If such process happens in the extremely high biodiverse Mexican forest (Nixon 1993; Styles 1993), it will lead to a serious impoverishment of the forest community, where pines and spruce will suffer higher mortality rates than junipers, as a process at least in part controlled by the resistance to cavitation margins of each species. This has unfolded already in the semiarid woodland communities of Utah, Colorado, Arizona and New Mexico, USA, where two consecutive dry and warm years (2000 to 2003) induced a massive forest decline of *Pinus edulis*, while *Juniperus monosperma* survived (Breshears et al. 2005).

In the particular case of *Picea chihuahuana*, our results indicate that at least regarding resistance to cavitation, it is as vulnerable to drought stress as the three pines studied. Under climate change, this fact will add an additional pressure on *Picea chihuahuana*, an already endangered species due to its narrow and fragmented distribution (Ledig et al. 2010) with some populations displaying signs of genetic erosion (Wehenkel and Sáenz-Romero 2012). Thus, severe drought-stress events due to climatic change may cause massive mortality, as it has already happened in some spruce-dominated forest at Rocky Mountains, USA (Bigler et al. 2007) and Norway (Solberg 2004). However, in our case, that *Picea chihuahuana* as a whole is already endangered, a climatic change-linked massive mortality eventually might cause simply the species extinction.

Conclusions

Our results confirm the larger vulnerability of Mexican pines and spruces to cavitation in comparison to species of the genus *Juniperus*. This is particularly worrisome in the case of *Picea chihuahuana*, an endemic and endangered species, showing a narrow and fragmented distribution. Our results suggest that, if predicted climatic change makes the natural habitats of this species much more warmer and dryer, likely populations of Mexican pines and spruces will severely decline, whereas juniper species might survive. The high biodiversity of the Mexican pine-oak and conifer forest might then be endangered by a process that would look like “savannization” (vegetation recomposition to a sparser tree coverage where pines species might die, meanwhile juniper, more resistant to drought, will remain).

Acknowledgements

Funding was provided to CSR by the joint research funds between the Mexican Council of Science and Technology (CONACyT), and the State of Michoacán (CONACyT-Michoacán, grant 2009127128), a sabbatical year (at INRA-Cestas, France) fellowship from CONACyT (grant 232838) and the Coordinación de la Investigación Científica of the Universidad Michoacana de San Nicolás de Hidalgo (UMSNH), México; to CW funding were from CONACyT and the Ministry of Education (SEP; Project CB-2010-01-158054). This study was also supported by the program „Investments for the Future“ (ANR-10-EQPX-16, XYLOFOREST) from the French National Agency for Research to SD. NGM was supported by the Agreenskills fellowship program, which has received funding from the EU's Seventh Framework Program, under grant agreement FP7-26719 (Agreenskills contract). We thanks Roberto Lindig-Cisneros, IIES-UNAM, Morelia and Miriam Garza-López, DiCiFo, Universidad Autónoma Chapingo, for their help on field collection, and to Felipe López and Manuel Echevarria, Forestry Office of the Native Indian Community of Nuevo San Juan Parangaricutiro, Michoacán, for their help on seed and branch collection in their community forest.

References

Allen CD, Macalady AK, Chenchouni H, Bachelet D, McDowell N, Vennetier M, Kizberger T, Rigling A, Breshears DD, Hogg EH, Gonzalez P, Fensham R, Zhang Z, Castro J, Demidova N, Lim JH, Allard G, Running SW, Semerci A, Cobb N. 2010. A global overview of drought and heat-induced tree mortality reveals emerging climate change risks for forests. *Forest Ecology and Management* 259:660-684

Allen CD, Breshears DD, McDowell NG. 2010. On underestimation of global vulnerability to tree mortality and forest die-off from hotter drought in the Anthropocene. *Ecosphere* 6(8) Article 129:1-55

Bigler C, Gavin DG, Gunning C, Veblen TT (2007) Drought induces lagged tree mortality in a subalpine forest in the Rocky Mountains. *Oikos* 116(12): 1983-1994

Bouche PS, Larter M, Domec JC, Burlett R, Gasson P, Jansen S, Delzon S. 2014. A broad survey of hydraulic and mechanical safety in the xylem of conifers. *Journal of Experimental Botany* 65 (15): 4419-4431

Breshears DD, Cobb NS, Rich PM, Price KP, Allen CD, Balice RG, Romme WH, Kastens JH, Floyd ML, Belnap J, Anderson JJ, Myers OB, Meyer CW. 2005. Regional vegetation die-off in response to global change-type drought. *Proceedings of National Academy of Sciences* 102:15144-15148

Brodribb TJ, Cochard H. 2009. Hydraulic failure defines the recovery and point of death in water-stressed conifers. *Plant Physiology* 149:575-584

Brodribb TJ, Bowman DJMS, Nichols S, Delzon S, Burlett R. 2010. Xylem function and growth rate interact to determine recovery rates after exposure to extreme water deficit. *New Phytologist* 188: 533-542

Brodribb TJ, McAdam SAM, Jordana GJ, Martins SCV. 2014. Conifer species adapt to low-rainfall climates by following one of two divergent pathways. *PNAS* 111(40):14489-14493

Carranza-González E, Zamudio S. 1994. Familia *Cupressaceae*. Flora del Bajío y de Regiones adyacentes, Fascículo 29.

Castellanos-Acuña D, Lindig-Cisneros RA, Sáenz-Romero C. 2015. Altitudinal assisted migration of Mexican pines as an adaptation to climate change. *Ecosphere* 6(1) Article 2:1-16

Choat B, Jansen S, Brodribb TJ, Cochard H, Delzon S, Bhaskar R, Bucci SJ, Feild TS, Gleason SM, Hacke UG, Jacobsen AL, Lens F, Maherali H, Martínez-Vilalta J, Mayr S, Mencuccini M, Mitchell PJ, Nardini A, Pittermann J, Pratt RB, Sperry JS, Westoby M, Wright IJ, Zanne AE. 2012. Global convergence in the vulnerability of forests to drought. *Nature* 491:752-756

Cochard H (2002) A technique for measuring xylem hydraulic conductance under high negative pressures. *Plant Cell and Environment* 25:815-819

Cochard H, Damour G, Bodet C, Tharwat I, Poirier M, Ameglio T. 2005. Evaluation of a new centrifuge technique for rapid generation of xylem vulnerability curves. *Physiologia Plantarum* 124:410-418

Delzon S, Douthe C, Sala A, Cochard H. 2010. Mechanism of water-stress induced cavitation in conifers: bordered pit structure and function support the hypothesis of seal capillary-seeding. *Plant, Cell and Environment* 33(12):2101-2111

Development Core Team R. 2014. A language and environment for statistical computing. R Foundation for Statistical Computing, Vienna, Austria. Available: URL http://www.R-project.org/.

IUCN Red List of Threatened Species. 2015. Version 2015-3. <www.iucnredlist.org>. Accessed 23 September 2015.

Lamy J-B, Bouffier L, Burlett R, Plomion C, Cochard H, Delzon S. 2011. Uniform selection as a primary force reducing population genetic differentiation of cavitation resistance across a species range. *PloS ONE* 6(8):e23476

Larter M, Brodribb TJ, Pfautsch S, Burlett R, Cochard H and Delzon S. 2015. Extreme aridity pushes trees to their physical limits. *Plant Physiology* 168(3):804-807

Ledig FT, Mápula-Larreta M, Bermejo-Velázquez B, Reyes-Hernández V, Flores-López C, Capó-Arteaga MA. 2000. Locations of endangered spruce populations in México and the demography of *Picea chihuahuana*. *Madroño* 47:71-88

Ledig FT, Rehfeldt GE, Sáenz-Romero C, Flores-López C. 2010. Projections of suitable habitat for rare species under global warming scenarios. *American Journal Botany* 97(6): 970-987

Linton MJ, Sperry JS, Williams DG. 1998. Limits to water transport in *Juniperus osteosperma* and *Pinus edulis*: implications for drought tolerance and regulation of transpiration. *Functional Ecology* 12:906-911

Nixon KC. 1993. The genus *Quercus* in México. In: Ramamoorthy TP, Bye R, Lot A, Fa J (eds) Biological diversity of México: origins and distribution. Oxford Univ. Press, New York, pp 447-458

Maherali H, Pockman WT, Jackson RB. 2004. Adaptive variation in the vulnerability of woody plants to xylem cavitation. *Ecology* 85(8):2184-2199

Mátyás C. 2010. Forecasts needed for retreating forests. *Nature* 464:1271

McDowell NG, Allen CD. 2015. Darcy‟s law predicts widespread forest mortality under climate warming. *Nature Climate Change* 5:669-672

Pammenter NW, Van der Willigen C. 1998. A mathematical and statistical analysis of the curves illustrating 406 vulnerability of xylem to cavitation. *Tree Physiology* 18:589-593

Peñuelas J, Oyaga R, Boada M, Jump AS. 2007. Migration, invasion and decline: changes in recruitment and forest structure in a warming-linked shift of European beech forest in Catalonia (NE Spain). *Ecography* 30:830-838

Pittermann J, Choat B, Jansen S, Stuart SA, Lynn L, Dawson TE. 2010. The relationships between xylem safety and hydraulic efficiency in the *Cupressaceae*: the evolution of pit membrane form and function. *Plant* 412 *Physiology* 153:1919-1931

Quiñones-Perez CZ, Simental-Rodriguez SL, Saenz-Romero C, Jaramillo-Correa JP, Wehenkel C. 2014. Spatial genetic structure in the very rare and species-rich *Picea chihuahuana* tree community (Mexico). *Silvae Genetica* 63(4):149-159

Rehfeldt GE, Crookston NL, Warwell MV, Evans JS. 2006. Empirical analyses of plant-climate relationships for 417 the western United States. *International Journal Plant Science* 167:1123-1150

Rehfeldt GE, Crookston NL, Sáenz-Romero C, Campbell E. 2012. North American vegetation model for land use planning in a changing climate: a solution to large classification problems. *Ecological Applications* 22:119-141

Sáenz-Romero C, Rehfeldt GE, Crookston NL, Pierre D, St-Amant R, Bealieau J, Richardson B. 2010. Spline models of contemporary, 2030, 2060, and 2090 climates for Mexico and their use in understanding climate423 change impacts on the vegetation. *Climatic Change* 102:595-623

Sáenz-Romero C, Lamy JP, Loya-Rebollar E, Plaza-Aguilar A, Burlett R, Lobit P and Delzon S. 2013. Genetic 425 variation of drought-induced cavitation resistance among *Pinus hartwegii* populations from an altitudinal gradient. *Acta Physiologiae Plantarum* 35:2905-2913

SAS Institute Inc. 2004. SAS/ STAT 9.1 User's Guide. SAS Institute Inc., Cary, North Carolina.

Solberg S. 2004. Summer drought: a driver for crown condition and mortality of Norway spruce in Norway. 429 *Forest Pathology* 34(2):93-104

Styles BT. 1993. The genus *Pinus*: a México purview. In: Ramamoorthy TP, Bye R, Lot A, Fa J (eds) 431 Biological diversity of México: origins and distribution. Oxford Univ. Press, New York, pp 397-420

Urli M, Lamy J-B, Sin F, Burlett R, Delzon S, Porté AJ. 2015. The high vulnerability of *Quercus robur* to 433 drought at its southern margin paves the way for *Quercus ilex*. *Plant Ecology* 216:177-187

Wehenkel C, Sáenz-Romero C. 2012. Estimating genetic erosion using the example of *Picea chihuahuana* Martínez. *Tree Genetics and Genomes* 8(5):1085-1094

Williams AP, Allen CD, Macalady AK, Griffin D, Woodhouse CA, Meko DM, Swetnam TW, Rauscher SA, 437 Seager R, Grissino-Mayer HD, Dean JS, Cook ER, Gangodagamage C, Cai, M McDowell NG. 2013. Temperature as a potent driver of regional forest drought stress and tree mortality. *Nature Climate Change* 3:292-297

Willson CJ, Jackson RB. 2006. Xylem cavitation caused by drought and freezing stress in four co-occurring *Juniperus* species. *Physiologia Plantarum* 127:374-382

Annex 2. Castagnerol et al. (accepted – major revisions Oecologia): Host range expansion is density dependent

Running headline: Host range is density dependent

Authors: Bastien Castagneyrol1*, Herve Jactel1, Eckehard Brockerhoff2, Nicolas Perrette3,

Maximilien Larter1, Sylvain Delzon1, Dominique Piou4

Affiliations:

1 BIOGECO, INRA, Univ. Bordeaux, 33610 Cestas, France

2 Scion (New Zealand Forest Research Institute), PO Box 29237, Christchurch 8540, New Zealand

3 ONF (Office National des Forets), Arboretum national des Barres, F-45290 Nogent sur Vernisson, France

4 Ministere de l'Agriculture, de l'Agroalimentaire et de la Foret, DGAL-SDQPV, Departement de la Sante des Forets, 252 rue de Vaugirard, F-75732 Paris, France

* **Corresponding author**: Bastien Castagneyrol

INRA UMR BIOGECO
69 route d'Arcachon
33612 Cestas Cedex – France
bastien.c astagneyrol@pierroton.inra.fr
Phone: + 335 57 12 27 30
Fax: + 335 57 12 28 80

Author contributions: DP, EB and HJ developed the original idea. SD and ML provided the phylogenetic tree. DP and NP collected data. BC analysed the data and drafted the first version of the MS. All authors provided comments and contributed to the final version.

ABSTRACT

The realised host range of herbivores is expected to increase with herbivore population density. Theory also predicts that trait similarity and phylogenetic relatedness between native and exotic plants is expected to increase the susceptibility of introduced plants to feeding by native herbivores. Whether the ability of native herbivores to extend their host range to introduced species is density-dependent is still unknown. We addressed this question by monitoring pine processionary moth (PPM, *Thaumetopoea pityocampa*) attacks during nine consecutive years on 41 pine species (8 native and 33 introduced) planted in an arboretum.

The survey encompassed latent and outbreak periods. A total of 28 pine species were attacked by PPM. There was no difference in the probability of attack between native and introduced pine species. Host range increased and was more phylogenetically clustered during outbreak than latent periods. When population density increased, PPM expanded its diet breadth by attacking introduced pine species that were closely related to native hosts. This study demonstrates the density-dependence of host range expansion in a common pine herbivore. Importantly, it supports the idea that the degree of phylogenetic proximity between host species can be a better predictor of attacks than the introduction status, which may help to predict the outcomes of new plant-herbivore interactions.

Keywords: Arboretum, Density dependence, Exotic species, Forestry, Host range, Pine processionary moth

INTRODUCTION

Non-native plants are increasingly introduced outside of their natural range. Yet, their success of establishment may be hindered by damage from herbivores native to the area of introduction (Cappuccino and Carpenter 2005; Parker et al. 2012). For instance, a recent survey showed that 590 European insect herbivore species successfully colonised exotic tree species introduced in Europe (Branco et al. 2015). Predicting the outcomes of novel plant-herbivore interactions is therefore of great theoretical and applied interest (Pearse et al. 2013a; Branco et al. 2014). However, exactly what determines the likelihood of herbivores to incorporate new hosts in their diet remains controversial (Harvey et al. 2010; Forister and Wilson 2013).

Theory predicts that host range may be density dependent, increasing with consumer abundance (Svanback and Bolnick 2007; Araujo et al. 2011; Carrasco et al. 2015). Herbivores may be more likely to exploit new host plants when population densities are high, as a result of a simple sampling effect: intraspecific variability in host use may increase with population density

(Bolnick et al. 2011). Alternatively, increased population density may induce changes in the quality of host plants through induced resistance (Underwood 2010) making them less suitable to herbivores, or intra-specific competition may force herbivores to feed on less preferred or less suitable, but 'competitor free', hosts (White and Whitham 2000; Plath et al. 2011; Nakladal and Uhlikova 2015). Such density-dependent effects on host use may have profound consequences on population dynamics of herbivores by alleviating intra-specific competition, but exposing them to new inter-specific competitors (reviewed in Bolnick et al. 2011).

Phylogenetic relationships among plants can also explain patterns of utilization by a given herbivore (Nakadai and Murakami 2015). Closely related plant species are more likely to share herbivores (Parker et al. 2012; Gilbert et al. 2015). Pearse and Hipp (2009) showed that insect damage on oaks introduced to the US decreased with their phylogenetic distance to native American oaks. This is consistent with phylogenetic niche conservatism for traits involved in plant-herbivore interactions (Srivastava et al. 2012; Nakadai et al. 2014).

However, not all traits show a phylogenetic imprint (Whitfeld et al. 2012) and even closely related plant species may diverge in traits relevant to defence against herbivores (Desurmont et al. 2011). Although biologically meaningful and of practical interest, phylogenetic distance among host plants may not be the best predictor of novel plant-insect interactions (Bezemer et al. 2014).

For a new plant to be incorporated in the diet of a given insect, its traits (*e.g*. phenology, palatability, defences) have to match those that are involved in the insect's host plant colonisation and exploitation behaviour, with no need for previous coevolutionary processes, that is ecological fitting (Agosta 2006). Only those exotic plants that display such traits permitting both recognition and sustained feeding by native herbivore may be used as novel hosts (Pearse et al. 2013b). By contrast, non-native plants may act as ecological traps (Schlaepfer et al. 2002) if they are more or equally attractive to native herbivore adults but are less palatable or more effectively defended, resulting in poorer performance of the offspring (e.g., D'Costa et al. 2014). In particular, the fitness cost experienced by herbivores shifting from one host plant to another was shown to increase with phylogenetic distance between the two hosts (Bertheau et al. 2010).

So far, the consequences of biotic introduction on plant-insect interactions on the one hand and the effect of increased population density on insect host range expansion on the other hand have been studied separately (Araujo et al. 2011; Forister and Wilson 2013; Pearse et al. 2013a; Bezemer et al. 2014; but see Branco et al. 2014). Bridging these two frameworks can provide

important insights into our understanding of the ecological consequences of intentional plant introductions, and, more generally, plant invasions.

Here, we explored the relationships between the population dynamics of the pine processionary moth (*Thaumetopoea pityocampa*, hereafter referred to as PPM) and change in its host range. PPM feeds on several species within the genus *Pinus*, and, occasionally on larch (*Larix* sp.), cedar (*Cedrus* sp.) or Douglas fir (*Pseudotsuga* sp.) (Jactel et al. 2015). Within the genus *Pinus*, PPM can show preferences for some species (Hodar et al. 2002; Stastny et al. 2006; Perez-Contreras et al. 2014). However, there is no general agreement on rank order for host use, probably because of local adaptation of PPM populations (Zovi et al. 2008; Jactel et al. 2015) or because host quality may change during outbreaks (Li et al. 2015). Several tree traits have been suggested to drive host selection and use by PPM, including tree height, needle morphology or volatile organic compounds (Paiva et al. 2011; Jactel et al. 2015).

We monitored PPM infestation on 41 pine species planted in an arboretum during nine consecutive years including an outbreak, i.e., covering periods with very high or very low population densities. We tested whether there were significant changes in host use by PPM as a result of population density and whether host range expansion was density dependent.

Specifically, we tested the three following hypotheses: (i) host range increases with PPM population density; (ii) novel hosts are not chosen at random but preferably among species closely related to natives and/or exhibiting similar traits relevant to host selection or exploitation and (iii) native pines are more likely to be attacked than exotic pines.

MATERIALS AND METHODS

Monitoring PPM densities at *Arboretum National des Barres*

PPM caterpillars feed at night during winter and spend the daytime in silky nests in tree crowns. These so-called winter nests shelter 50-100 larvae and are commonly used to monitor PPM infestation on trees as caterpillars are very conspicuous in tree crowns. The presence of a nest indicates that early instar larvae fed on and survived on the pine tree on which one female moth oviposited.

PPM abundance in the *Arboretum National des Barres* (N. 47.838, E. 2.7596, Paris Basin, France) was monitored in the arboretum (N. 47.838, E. 2.7596, Paris Basin, France) between 1999 and 2007, by counting the number of winter nests on all individual pine trees planted at the arboretum. Hereafter we refer to the total number of nests per year on all sampled trees as ‘PPM population density’.

At the time of the survey, 2556 trees were present in the arboretum, of which 219 belonged to one of 46 *Pinus* species. Pines from hybrid species, or which died or were newly planted before the end of the survey were discarded from the analyses. Likewise, we did not distinguish between subspecies. The final dataset therefore contained 192 individual pines from 41 species of which eight were native to Europe, 11 introduced from Asia and 22 from North America (see Table S1, Supplementary Material). Although arboreta are usually not primarily designed for ecology studies, there were enough tree replicates of European, Asian and American pine species in the *Arboretum National des Barres* to allow testing our hypotheses.

Tree and needle characteristics

The height of all individual pines was measured in 2002. Tree height data were used to assess the effect of height on PPM attacks (Castagneyrol et al. 2014; Regolini et al. 2014). Although it may have changed over the time of the survey, we assumed that the rank order in tree height among individuals and species was maintained throughout the study, an assumption that should hold over a relatively short period.

Although there is no consensus on needle traits correlated with PPM abundance on different pine species (Jactel et al. 2015), pine needles with a shape that allows female moths clasping their tarsi around and holding on to them are expected to be more suitable for oviposition (Demolin 1969). Mean needle length and width per pine species were retrieved from the literature (Richardson 2000). For the three species for which this information was missing (*Pinus cembra, P. arizonica, P. ayacahuite*), 30 needles were collected from five trees of the arboretum, and needle length and width values were averaged at the species level.

Pine phylogeny

A phylogenetic tree for the 41 pine species eventually included in this study was obtained from the conifer phylogeny developed by Delzon et al. (2016, *in prep*). This reconstruction used sequences for chloroplast genes rbcL and matK, nuclear gene phyP, and the ITS1 5.8SITS2 region of ribosomal DNA, downloaded from the online database GenBank (Benson et al. 2011) and aligned using the pipeline PHLAWD (Smith et al. 2009). The complete dataset included over 300 species of conifers, and used three cycad species as outgroup. Following the so-called supermatrix approach (Dequeiroz and Gatesy 2007), a full likelihood search with 1000 bootstrap replicates was conducted on the whole dataset in RAxML (Stamatakis 2006), with each region treated as a separate partition with a distinct GTR+CAT substitution model.

A chronogram was then constructed on the best tree from the likelihood search, using a relaxed-clock model and the *chronos* function from the *ape* package in R (Paradis et al. 2015), with a set of fifteen calibration points (derived from the fossil record) from Leslie et al. (2012).

Analyses

Test of phylogenetic signal in tree height and needle traits

We tested whether there was a phylogenetic signal in pine trait values expected to drive PPM preference. Among the wide array of indices developed to test for the presence of phylogenetic signals in traits, Pagel's λ performs well when it is used to compare different traits within a single phylogeny (Munkemuller et al. 2012). Pagel's λ can theoretically be greater than one (traits of related species are more similar than expected under Brownian motion) but usually varies between zero (no phylogenetic signal) to one (strong phylogenetic signal). Although we did not expect any phylogenetic signal in tree height, given differences in tree age among species, we used Pagel's λ to test for phylogenetic signals in needle traits (needle length and needle width), but also in tree height for sake of completeness.

Testing factors controlling for pine species use by the PPM

We first tested if patterns of PPM attacks differed between pine trees of different introduction status (native *vs.* introduced) or from different origins (Europe, North America, Asia) using Generalized Linear Mixed-effect Model (GLMM) with a binomial error family. The response variable was presence/absence of attack (winter nest) on a given tree using tree status or origin as predictors. GLMM allowed accounting for repeated measurements on the same individuals. Random factors were calendar year, pine species identity and individual tree identity nested within species. Because every tree was surveyed every year, tree and year were crossed random factors. Variance explained by fixed effects (status or origin) and random factors were estimated by calculating marginal R2 values (R2m, for fixed effects) and conditional R2 values (R2c, for fixed *plus* random effects) (Nakagawa and Schielzeth 2013).

Using GLMM with species as a random factor only partially accounts for phylogenetic non independence among residuals. Therefore we then used Phylogenetic Generalized Least Squares (PGLS) models which are extensions of ordinary least square regressions that account for phylogenetic non independence among individual observations (Paradis 2012). PGLS uses a theoretical variance-covariance matrix among species that quantifies how much species resemble each other (covariance), and how much they diverged from their common ancestor (variance). The variance-covariance matrix was estimated with Pagel's λ (Pagel 1999) which improves the performances of phylogenetic regression when there is a phylogenetic signal in the independent variable (Revell 2010). For trait analysis, PGLS were used with data aggregated at the species level, using the mean number of PPM nests per year and per species as response variable and species introduction status, tree height, needle length and needle width as predictors.

Separate models were run for each year of the survey. Predictors were scaled and centred to make coefficients comparable within and between years (Schielzeth 2010). In order to confirm outcomes of year-specific models, we finally used a GLMM to model the probability of an individual tree being attacked, taking height and needle characteristics into account while accounting for repeated measurements (see above for model structure).

Modelling diet breadth

Under the null hypothesis (H0) that female PPM select pines at random for oviposition, the number of pine species with one or more PPM nests should increase with both PPM population and pine densities, simply as a result of a sampling effect: i) the more females, the more nests and the greater the probability of any tree being attacked and ii) the more pine individuals per species, the greater the probability of a particular pine species being infested.

Taking these densities into account, we used null models adapted from Jorge *et al. (2014)* to test H0.

We defined two potential host pools (PHP). In the first one, (PHP1) all pine species were considered potential hosts for PPM. In the second one (PHP2), only those species that were attacked at least once during the seven-year survey were included. Null models were built by randomly drawing *N* trees from the PHP, where *N* was the number of PPM nests observed in a given year. This procedure thus accounted for the unbalanced abundance of the different pine species in the arboretum. Trees were drawn with replacement to make it possible that the same tree holds several nests. Based on this random sample, we calculated the number of host species used by PPM under H0 (*Srandom*). This procedure was repeated 1000 times. We eventually compared observed (*Sobserved*) and simulated (*Srandom*) numbers of host species using a standardized coefficient (see below, Eqn 1).

In order to test the hypothesis that the number of novel hosts increased with PPM population density under a non-random process according to species relatedness (*i.e.*, phylogenetic clustering), we used the same null model but this time added phylogenetic information (Jorge et al. 2014; Parker et al. 2015). We calculated the mean phylogenetic distance between pine species used as hosts in a given year (MPDobserved) and compared this value to the 1000 MPDrandom calculated from random samples generated by the null model. In order to calculate MPD, we first pruned the phylogenetic tree of pines to keep only species with PPM nests (for MPDobserved) or randomly drew from the potential host pool (MPDrandom). We then calculated the mean of all pairwise distances among species (Parker et al. 2015).

Observed and simulated values were compared using a standardized coefficient *k* (*kS* for richness and *kMPD* for phylogenetic clustering) that is equivalent to a z-score (Eqn 1):

$k = (xobserved - mrandom)/srandom$ (Eqn 1)

Where *xobserved*, is either *Sobserved* or *MPDobserved* and *mrandom* and *srandom* are the mean and standard deviation of the 1000 random simulations of either *Srandom* or *MPDrandom*. For host species richness, negative and positive *k* values indicate that the number of pine species on which PPM nests were observed were lower and greater, respectively, than expected by chance. For MPD, *k* was multiplied by –1 so that positive *k* values indicate a greater phylogenetic clustering than expected by chance, while negative values are indicative of phylogenetic overdispersion. If $|k| < 2$, the observed value is approximately within the range expected by chance. Conversely, if $|k| > 2$, then the observed value is approximately in the 5% tail of a normal distribution. We finally tested the effect of PPM population density on *k* for the two potential host pools using linear regressions.

Although the maximal distance between pines was 952m (Appendix 1, Supplementary Material), pines were distributed among two areas within the arboretum. We checked for independence between phylogenetic and geographic (Euclidean) distances between trees of the arboretum (Appendix 1). We finally re-ran previous models for each garden separately to confirm the robustness of the main results (Appendix 1).

All analyses were done in *R* using *markdown* for RStudio (R Core Team 2014) (Allaire et al. 2014, R Core Team 2014). We used the functions *gls, glmer, r.squaredGLMM* from packages *nlme, lme4,* and *MuMIn,* respectively (Bates et al. 2013; Pinheiro et al. 2014; Bartoń 2015). For phylogenetic analyses we used the *phytools* package (Revell 2012).

RESULTS

A total of 2,309 winter nests were counted on pine trees between 1999 and 2007. Among the 41 pine species planted at the National Arboretum des Barres, 28 were attacked by PPM at least once during the survey period (*i.e.*, 68%, Figure 1). PPM population density varied between years but was independent of tree age: it was maximal in 2002, in the middle of the survey, and minimal in 2004 (Figure 2).

PPM attacks were concentrated on *P. nigra*, *P. sylvestris* and *P. ponderosa*. Despite the fact that, together, they represented only 39% of planted trees, they concentrated between 82 and 85% of attacks between years of low and high PPM density (% attacks on *P. nigra* / *P. ponderosa* / *P. sylvestris*, low PPM density: 67 / 15 / 0; high PPM density: 56 / 24 / 5).

Although *P. ponderosa* is non-native to the study area, there was no overall effect of the introduction status (native to Europe vs. introduced, GLMM: $\chi2 = 0.3$, $P = 0.582$, $R^2m < 0.01$, $R^2c = 0.67$) or origin (Europe vs. Asia vs. America, GLMM: $\chi2 = 2.64$, $P = 0.267$, $R^2m = 0.03$,

R^2c = 0.67) of pine species on PPM attack probability (Figure 1). Random factors explained more than 66% of the variance in PPM attack probability.

Closely related species tended to be more similar in terms of needle traits as shown by the significant, though rather weak, phylogenetic signal in needle length ($\lambda = 0.26$, $P = 0.013$) and needle width ($\lambda = 0.29$, $P = 0.015$). As expected, pine height was independent of pine phylogeny ($\lambda = 0.00$, $P = 1.000$, Figure 1).

Overall, needle width had a significant effect on PPM attack probability: the wider the needles, the greater the chance a pine species being attacked (GLMM: $\chi 2 = 11.97$, $P < 0.0001$, R^2m = 0.18, R^2c = 0.67, Figure 3). This pattern remained after phylogenetic non-independence was accounted for (PGLS, Table S2). The strength of the needle width effect increased with PPM population density (Figure 3). Needle length had no effect on PPM attacks (except in 2007, Table S2). There was a tendency for taller trees being attacked more than smaller ones, but this effect was significant only when PPM population density was low (Figure 3). Needle length had no effect on PPM attacks (but in 2007, Table S2).

The number of pine trees and pine species attacked by the PPM increased with PPM population density (Pearson's correlation: *rindividuals* = 0.96, *rspecies* = 0.93, Figure 2).

Regardless of the potential host pool (*i.e.*, all pine species, PHP1, or only species attacked at least once, PHP2), PPM attacked significantly fewer species than expected by chance (all $kS < 2$, Figure 4A). The realized host range departed more from randomness as PPM population density increased (PHP1: $F1,7 = 632$, $P < 0.0001$, $R^2 = 0.99$, PHP2: $F1,7 = 179$, $P < 0.0001$, $R^2 = 0.96$, Figure 4A).

The observed phylogenetic clustering of host trees increased with PPM population density (Pearson's correlation: $r = 0.66$). PPM's host range was more clustered than under the null hypothesis (all $kMPD > 2$, Figure 4B) and phylogenetic clustering increased with PPM population density (PHP1: $F1,7 = 11$, $P < 0.013$, $R^2 = 0.55$, PHP2: $F1,7 = 21$, $P < 0.003$, $R^2 = 0.71$, Figure 4B). When PPM population density increased, the species newly added to the regular host range were more closely related to regular hosts than expected by chance.

DISCUSSION

Our results clearly show that PPM's host range expansion depended more on PPM population density and phylogenetic relationships among pine species than on introduction status of pines. We hypothesized that PPM's host range should increase during outbreaks, by incorporating pine species closely related to hosts normally used during latent periods. Our results are consistent with this hypothesis and with the literature. Closely related host species are more

likely to share common traits and defenses against herbivores (Agrawal and Fishbein 2006; Rasmann and Agrawal 2011; Nakadai and Murakami 2015). It is therefore not surprising that the new hosts were chosen from among the close relatives of regular hosts. This result suggests that in years of low PPM abundance, PPM nests were found on a small set of highly suitable hosts compared to years of high PPM abundance. Increased intraspecific competition during outbreaks may have increased divergence in host use and forced PPM to exploit less preferred, but still suitable hosts (Araujo et al. 2011). Why these optional hosts are only used during outbreaks may be explained by the fitness loss of herbivores feeding on suboptimal plants (Bertheau et al. 2010; Rasmann and Agrawal 2011; Nakadai and Murakami 2015).

During outbreaks, this cost may be a better option than the risk of facing starvation, due to either induced resistance or intra-specific competition (Svanback and Bolnick 2007; Plath et al. 2011; Branco et al. 2014). Alternatively, as PPM abundance increased, the increase in host range at the population level may have simply resulted from a greater number of individuals being able to exploit new hosts, due to larger intra-specific variability in individual insect preferences (Bolnick et al. 2011).

Contrary to our expectations, the marked preferences for some particular species did not result from the avoidance of introduced species: both native and introduced species were equally attacked by PPM. Even if they escape natural enemies from their native range ("the enemy release hypothesis", Keane and Crawley 2002), non-native plant species can face novel herbivores in the area of introduction (Parker et al. 2012), particularly when species from the same genus are present in the introduction area (Branco et al. 2015). The likelihood for introduced plants to recruit new herbivore species was shown to increase with phylogenetic or trait similarity with native plant species (Ness et al. 2011), even within the same genus (Ros et al. 1993; Pearse et al. 2013a). Phylogenetic relatedness among pine species was therefore a stronger driver of host use pattern than tree origin.

We found that needle width was a key predictor of PPM attack probability on a particular pine species. Demolin (1969) observed that the ability of female moth to firmly 'hook' pine needles for oviposition was greatest for needles between 1.6 and 2 mm wide, which corresponded to the length of PPM's tarsi. Accordingly, we showed that the probability of attack was greatest for needles with a width approaching 2 mm, irrespective of species' introduction status. Yet, this trait displayed a phylogenetic signal in pines. Therefore, PPM may have been ecologically fitted to lay eggs on non-native pines having a particular combination of needle traits (Forister and Wilson 2013). This confirms that phylogenetic signals can be detected when considering plant-insect interactions, but this needs not be the result of coevolution (Agosta 2006).

We showed that PPM attacked significantly fewer pine species than it would be expected by chance. This is consistent with previous studies reporting PPM female preferences for alternative host species (Stastny et al. 2006; Paiva et al. 2011), but it conflicts with the view that PPM females are rather unselective regarding oviposition sites (Hodar et al. 2002). In the present study, we counted the number of nests, and not actual oviposition events. It is common that offspring survive or perform better on plants that their mother preferred, and that females prefer plants (for oviposition) that are more suitable to the offspring (i.e., "mother knows best"; Gripenberg et al. 2010). Whether or not this is the case in PPM remains to be tested properly, using behavioral experiments. Although we interpreted host preference in terms of female choice, it cannot be excluded that the observed distribution of PPM nests resulted (in part or entirely) from differential survival of eggs or young larvae. For instance, Hodar *et al*. (2002) found that females were unselective regarding oviposition, while the survival of early instar larvae varied among pine species. By contrast Stastny et al. (2006) reported that host preference based on number of nests in the field was consistent with oviposition preference in controlled experiments. Such discrepancies may result from local adaptations of PPM populations (Zovi et al. 2008), which makes it difficult to generalize findings about host preference in PPM. However, the fact that a certain host trait particularly relevant to female moth behavior (correspondence between needle width and moth tarsi length) was found to explain host preference should provide confidence in our interpretation of host range expansion driven by female's choice.

Our study was conducted in an arboretum at the northern edge of PPM's geographic range (Battisti et al. 2005). It is possible that the hierarchy in host use by herbivores in marginal populations may not reflect preferences in more central populations. For instance, choice ehavior may be less conservative if normally preferred hosts are scarce or missing (Carrasco et al. 2015), which was not the case in the arboretum. However, PPM was shown to act conservatively regarding host preferences (Stastny et al. 2006) and despite the unbalanced design, no less than 41 pine species were available in the arboretum. PPM was therefore given the choice between different potential host species so that we can reject the possibility that the location of the present study biased PPM's choice towards non-native species. In addition, the location of the arboretum at the front edge of PPM geographical range expansion provided further reassurance that no coevolution processes were behind host range expansion.

CONCLUSION

PPM showed clear preference for particular pine species, those which have wider needles.

This choice was independent of pine introduction status indicating that non-native species were neither more nor less likely to be attacked by the PPM than native species. Importantly, the host range increased with PPM population density in a non-random way. Host range expansion occurred on pines closely related to regular hosts, the latter being 'ecologically fitted' to be attacked by the PPM as a result of needle traits that displayed a phylogenetic signal. Regardless of the mechanisms underlying the observed patterns, the density dependence of host use may have profound implications for the population dynamics not only of PPM, but also of other, co-occurring pests on the same host trees (Bolnick et al. 2011).

From an applied point of view, our results allow the identification of pine species that would be at higher risk of PPM attack, should it be accidentally introduced outside its natural geographic range or should exotic pines be planted in the native range of PPM (Lombardero et al. 2012).

ACKNOWLEDGEMENTS

We thank Manuela Branco for providing important ideas and must read papers. Original analyses were done by Colleen Carlson and EB. All authors provided comments and contributed to the final version. Contributions by EB were supported by MBIE core funding to Scion (contract C04X1104).

DATA ACCESSIBILITY

Data used in the present study are uploaded as supplementary material (SM2 and SM3). SM2 corresponds to raw data. SM3 is the phylogenetic tree (Newick format) of pine species planted in *Arboretum National des Barres*.

REFERENCES

Agosta SJ (2006) On ecological fitting, plant–insect associations, herbivore host shifts, and host plant selection. Oikos 114:556–565. doi: 10.1111/j.2006.0030-1299.15025.x Agrawal AA, Fishbein M (2006) Plant defense syndromes. Ecology 87:S132–149.

Araujo MS, Bolnick DI, Layman CA (2011) The ecological causes of individual specialisation. Ecol Lett 14:948–958. doi: 10.1111/j.1461-0248.2011.01662.x

Bartoń K (2015) MuMIn: Multi-Model Inference.

Bates D, Maechler M, Bolker B (2013) lme4: Linear mixed-effects models using S4 classes.

Battisti A, Stastny M, Netheer S, et al (2005) Expansion of Geographic Range in the Pine Processionary Moth Caused by Increased Winter Temperatures. Ecol Appl 15:2084–2096.

Benson DA, Karsch-Mizrachi I, Lipman DJ, et al (2011) GenBank. Nucleic Acids Res 39:D32–D37. doi: 10.1093/nar/gkq1079

Bertheau C, Brockerhoff EG, Roux-Morabito G, et al (2010) Novel insect-tree associations resulting from accidental and intentional biological "invasions": a meta-analysis of effects on insect fitness. Ecol Lett 13:506–515.

Bezemer TM, Harvey JA, Cronin JT (2014) Response of Native Insect Communities to Invasive Plants. Annu Rev Entomol 59:119–141. doi: 10.1146/annurev-ento-011613-162104

Bolnick DI, Amarasekare P, Araujo MS, et al (2011) Why intraspecific trait variation matters in community ecology. Trends Ecol Evol 26:183–192. doi: 10.1016/j.tree.2011.01.009

Branco M, Brockerhoff EG, Castagneyrol B, et al (2015) Host range expansion of native insects to exotic trees increases with area of introduction and the presence of congeneric native trees. J Appl Ecol 52:69–77. doi: 10.1111/1365-2664.12362

Branco M, Dhahri S, Santos M, Ben Jamaa ML (2014) Biological control reduces herbivore's host range. Biol Control 69:59–64. doi: 10.1016/j.biocontrol.2013.11.001

Cappuccino N, Carpenter D (2005) Invasive exotic plants suffer less herbivory than noninvasive exotic plants. Biol Lett 1:435–438. doi: 10.1098/rsbl.2005.0341

Carrasco D, Larsson MC, Anderson P (2015) Insect host plant selection in complex environments. Curr Opin Insect Sci 8:1–7. doi: 10.1016/j.cois.2015.01.014

Castagneyrol B, Regolini M, Jactel H (2014) Tree species composition rather than diversity triggers associational resistance to the pine processionary moth. Basic Appl Ecol 15:516–523. doi: 10.1016/j.baae.2014.06.008

D'Costa L, Simmonds MSJ, Straw N, et al (2014) Leaf traits influencing oviposition preference and larval performance of *Cameraria ohridella* on native and novel host plants. Entomol Exp Appl 152:157–164. doi: 10.1111/eea.12211

Demolin G (1969) Comportement des adultes de *Thaumetopoea pityocampa* Schiff.: dispersion spatiale, importance ecologique. Ann For Sci 26:81–102.

Dequeiroz A, Gatesy J (2007) The supermatrix approach to systematics. Trends Ecol Evol 22:34–41. doi: 10.1016/j.tree.2006.10.002

Desurmont GA, Donoghue MJ, Clement WL, Agrawal AA (2011) Evolutionary history predicts plant defense against an invasive pest. Proc Natl Acad Sci 108:7070–7074. doi:10.1073/pnas.1102891108

Forister ML, Wilson JS (2013) The population ecology of novel plant-herbivore interactions. Oikos 122:657–666. doi: 10.1111/j.1600-0706.2013.00251.x

Gilbert GS, Briggs HM, Magarey R (2015) The Impact of Plant Enemies Shows a Phylogenetic Signal. PLoS ONE 10:e0123758. doi: 10.1371/journal.pone.0123758

Gripenberg S, Mayhew PJ, Parnell M, Roslin T (2010) A meta-analysis of preference–performance relationships in phytophagous insects. Ecol Lett 13:383–393. doi: 10.1111/j.1461-0248.2009.01433.x

Harvey JA, Biere A, Fortuna T, et al (2010) Ecological fits, mis-fits and lotteries involving insect herbivores on the invasive plant, *Bunias orientalis*. Biol Invasions 12:3045–3059. doi: 10.1007/s10530-010-9696-9

Hodar JA, Zamora R, Castro J (2002) Host utilisation by moth and larval survival of pine processionary caterpillar *Thaumetopoea pityocampa* in relation to food quality in three *Pinus* species. Ecol Entomol 27:292–301. doi: 10.1046/j.1365-2311.2002.00415.x

Jactel H, Barbaro L, Battisti A, et al (2015) Insect – Tree Interactions in *Thaumetopoea pityocampa*. In: Roques A (ed) Processionary Moths and Climate Change : An Update. Springer Netherlands, Dordrecht, pp 265–310

Jorge LR, Prado PI, Almeida-Neto M, Lewinsohn TM (2014) An integrated framework to improve the concept of resource specialisation. Ecol Lett 17:1341–1350. doi: 10.1111/ele.12347

Keane RM, Crawley MJ (2002) Exotic plant invasions and the enemy release hypothesis. Trends Ecol Evol 17:164–170. doi: 10.1016/S0169-5347(02)02499-0

Leslie AB, Beaulieu JM, Rai HS, et al (2012) Hemisphere-scale differences in conifer evolutionary dynamics. Proc Natl Acad Sci 109:16217–16221. doi: 10.1073/pnas.1213621109

Li S, Daudin JJ, Piou D, et al (2015) Periodicity and synchrony of pine processionary moth outbreaks in France. For Ecol Manag 354:309–317. doi: 10.1016/j.foreco.2015.05.023

Lombardero MJ, Alonso-Rodriguez M, Roca-Posada EP (2012) Tree insects and pathogens display opposite tendencies to attack native vs. non-native pines. For Ecol Manag 281:121–129. doi: 10.1016/j.foreco.2012.06.036

Munkemuller T, Lavergne S, Bzeznik B, et al (2012) How to measure and test phylogenetic signal: How to measure and test phylogenetic signal. Methods Ecol Evol 3:743–756. doi: 10.1111/j.2041-210X.2012.00196.x

Nakadai R, Murakami M (2015) Patterns of host utilisation by herbivore assemblages of the genus *Caloptilia* (Lepidoptera; Gracillariidae) on congeneric maple tree (*Acer*) species. Ecol Entomol 40:14–21. doi: 10.1111/een.12148

Nakadai R, Murakami M, Hirao T (2014) Effects of phylogeny, leaf traits, and the altitudinal distribution of host plants on herbivore assemblages on congeneric *Acer* species. Oecologia 175:1237–1245. doi: 10.1007/s00442-014-2964-0

Nakagawa S, Schielzeth H (2013) A general and simple method for obtaining *R* 2 from generalized linear mixed-effects models. Methods Ecol Evol 4:133–142. doi: 10.1111/j.2041-210x.2012.00261.x

Nakladal O, Uhlikova H (2015) Review of historical outbreaks of the nun moth with respect to host tree species. J For Sci 61:18–26. doi: 10.17221/94/2014-JFS

Pagel M (1999) Inferring the historical patterns of biological evolution. Nature 401:877–884. doi: 10.1038/44766

Paiva MR, Mateus E, Santos MH, Branco MR (2011) Pine volatiles mediate host selection for oviposition by *Thaumetopoea pityocampa* (Lep., Notodontidae). J Appl Entomol 135:195–203. doi: 10.1111/j.1439-0418.2010.01550.x

Paradis E (2012) Analysis of Phylogenetics and Evolution with R. Springer New York, New York, NY

Paradis E, Blomberg S, Bolker B, et al (2015) ape: Analyses of Phylogenetics and Evolution.

Parker IM, Saunders M, Bontrager M, et al (2015) Phylogenetic structure and host abundance drive disease pressure in communities. Nature 520:542–544. doi: 10.1038/nature14372

Parker JD, Burkepile DE, Lajeunesse MJ, Lind EM (2012) Phylogenetic isolation increases plant success despite increasing susceptibility to generalist herbivores: Phylogenetic relatedness and invasion success. Divers Distrib 18:1–9. doi: 10.1111/j.1472 4642.2011.00806.x

Pearse IS, Harris DJ, Karban R, Sih A (2013a) Predicting novel herbivore-plant interactions. Oikos 122:1554–1564. doi: 10.1111/j.1600-0706.2013.00527.x

Pearse IS, Hipp AL (2009) Phylogenetic and trait similarity to a native species predict herbivory on non-native oaks. Proc Natl Acad Sci 106:18097–18102. doi: 10.1073/pnas.0904867106

Pearse IS, Hughes K, Shiojiri K, et al (2013b) Interplant volatile signaling in willows: revisiting the original talking trees. Oecologia 172:869–875. doi: 10.1007/s00442-013-2610-2

Perez-Contreras T, Soler JJ, Soler M (2014) Host selection by the pine processionary moth enhances larval performance: An experiment. Acta Oecologica 55:15–22. doi:10.1016/j.actao.2013.10.006

Pinheiro J, Bates D, Debroy S, Sarkar D (2014) nlme: linear and nonlinear mixed effects models.

Plath M, Dorn S, Riedel J, et al (2011) Associational resistance and associational susceptibility: specialist herbivores show contrasting responses to tree stand diversification. Oecologia 169:477–487. doi: 10.1007/s00442-011-2215-6

Rasmann S, Agrawal AA (2011) Evolution of specialization: a phylogenetic study of host range in the red milkweed beetle (*Tetraopes tetraophthalmus*). Am Nat 177:728–737. doi: 10.1086/659948

R Core Team (2014) R: a language and environment for statistical computing. R fundation for statistical computing, Vienna, Austria

Regolini M, Castagneyrol B, Dulaurent-Mercadal A-M, et al (2014) Effect of host tree density and apparency on the probability of attack by the pine processionary moth. For Ecol Manag 334:185–192. doi: 10.1016/j.foreco.2014.08.038

Revell LJ (2010) Phylogenetic signal and linear regression on species data. Methods Ecol Evol 1:319–329. doi: 10.1111/j.2041-210X.2010.00044.x

Revell LJ (2012) phytools: an R package for phylogenetic comparative biology (and other things). Methods Ecol Evol 3:217–223. doi: 10.1111/j.2041-210X.2011.00169.x

Richardson DM (ed) (2000) Ecology and biogeography of Pinus. Cambridge Univ. Press, Cambridge

Ros N da, Ostermeyer R, Roques A, Raimbault JP (1993) Insect damage to cones of exotic conifer species introduced in arboreta. J Appl Entomol 115:113–133. doi: 10.1111/j.1439-0418.1993.tb00371.x

Schielzeth H (2010) Simple means to improve the interpretability of regression coefficients: Interpretation of regression coefficients. Methods Ecol Evol 1:103–113. doi: 10.1111/j.2041-210X.2010.00012.x

Schlaepfer MA, Runge MC, Sherman PW (2002) Ecological and evolutionary traps. Trends Ecol Evol 17:474–480. doi: 10.1016/S0169-5347(02)02580-6

Smith SA, Beaulieu JM, Donoghue MJ (2009) Mega-phylogeny approach for comparative biology: an alternative to supertree and supermatrix approaches. BMC Evol Biol 9:37. doi: 10.1186/1471-2148-9-37

Srivastava DS, Cadotte MW, MacDonald AAM, et al (2012) Phylogenetic diversity and the functioning of ecosystems. Ecol Lett 15:637–648. doi: 10.1111/j.1461-0248.2012.01795.x

Stamatakis A (2006) RAxML-VI-HPC: maximum likelihood-based phylogenetic analyses with thousands of taxa and mixed models. Bioinformatics 22:2688–2690. doi: 10.1093/bioinformatics/btl446

Stastny M, Battisti A, Petrucco-Toffolo E, et al (2006) Host-plant use in the range expansion of the pine processionary moth, *Thaumetopoea pityocampa*. Ecol Entomol 31:481–490. doi: 10.1111/j.1365-2311.2006.00807.x

Svanback R, Bolnick DI (2007) Intraspecific competition drives increased resource use diversity within a natural population. Proc R Soc Lond B Biol Sci 274:839–844. doi: 10.1098/rspb.2006.0198

Underwood N (2010) Density dependence in insect performance within individual plants: induced resistance to *Spodoptera exigua* in tomato. Oikos 119:1993–1999. doi: 10.1111/j.1600-0706.2010.18578.x

White JA, Whitham TG (2000) Associational susceptibility of cottonwood to a box elder herbivore. Ecology 81:1795–1803.

Whitfeld TJS, Novotny V, Miller SE, et al (2012) Predicting tropical insect herbivore abundance from host plant traits and phylogeny. Ecology 93:S211–S222. doi: 10.1890/11-0503.1

Zovi D, Stastny M, Battisti A, Larsson S (2008) Ecological costs on local adaptation of an insect herbivore imposed by host plants and enemies. Ecology 89:1388–1398. doi:10.1890/07-0883.1

FIGURE CAPTIONS

Figure 1: Relationship between mean tree height, needle width, needle length and PPM attack rate with pine species phylogeny and origin. Pink, green and blue colours refer to pines species from Europe, Asia and North America, respectively. Traits values and mean number of nests per year and per species (PPM) were scaled from 0 to 1. The larger the dot, the bigger the value. Crosses indicate pine species that have never been attacked during the survey.

Figure 2: Temporal pattern of total number of nests (bars) and pine species attacked (dots) by the pine processionary moth (PPM).

Figure 3: Effects of needles width, needles length and tree height on PPM attack. **(A)** Effects of needle width on the probability of PPM attack. Lines represent predictions from GLMM for years as random intercepts. Colour palette refers to PPM population density (and corresponding year). **(B)** Standardized model parameter estimates of year-specific PGLS models showing the effects of tree height, needles length and needles width on the mean number of PPM nests per tree. Vertical bars represent standard errors. Stars indicate coefficients that are significantly different from zero.

Figure 4: Effects of PPM nest density on PPM host range. **(A)** Results of null models comparing the observed (S_{obs}) *vs*. simulated (S_{sim}) number of species attacked by the PPM under the null hypothesis; *k* is proportional to the difference between observed and simulated values. Negative values indicate that the number of attacked species was lower than expected by chance. **(B)** Results of null models comparing the observed (MPD_{obs}) *vs*. simulated (MPD_{sim}) mean phylogenetic distance between species attacked by the PPM under the null hypothesis. To make it consistent with **(A)**, *k* was multiplied by –1 so that positive k values indicate a greater phylogenetic clustering than expected by chance. Simulations were based on

two potential host pools (PHP, see methods). Shaded areas and horizontal dashed lines represent the [-2;2] interval corresponding to expectations under the null hypothesis.

Figure 1

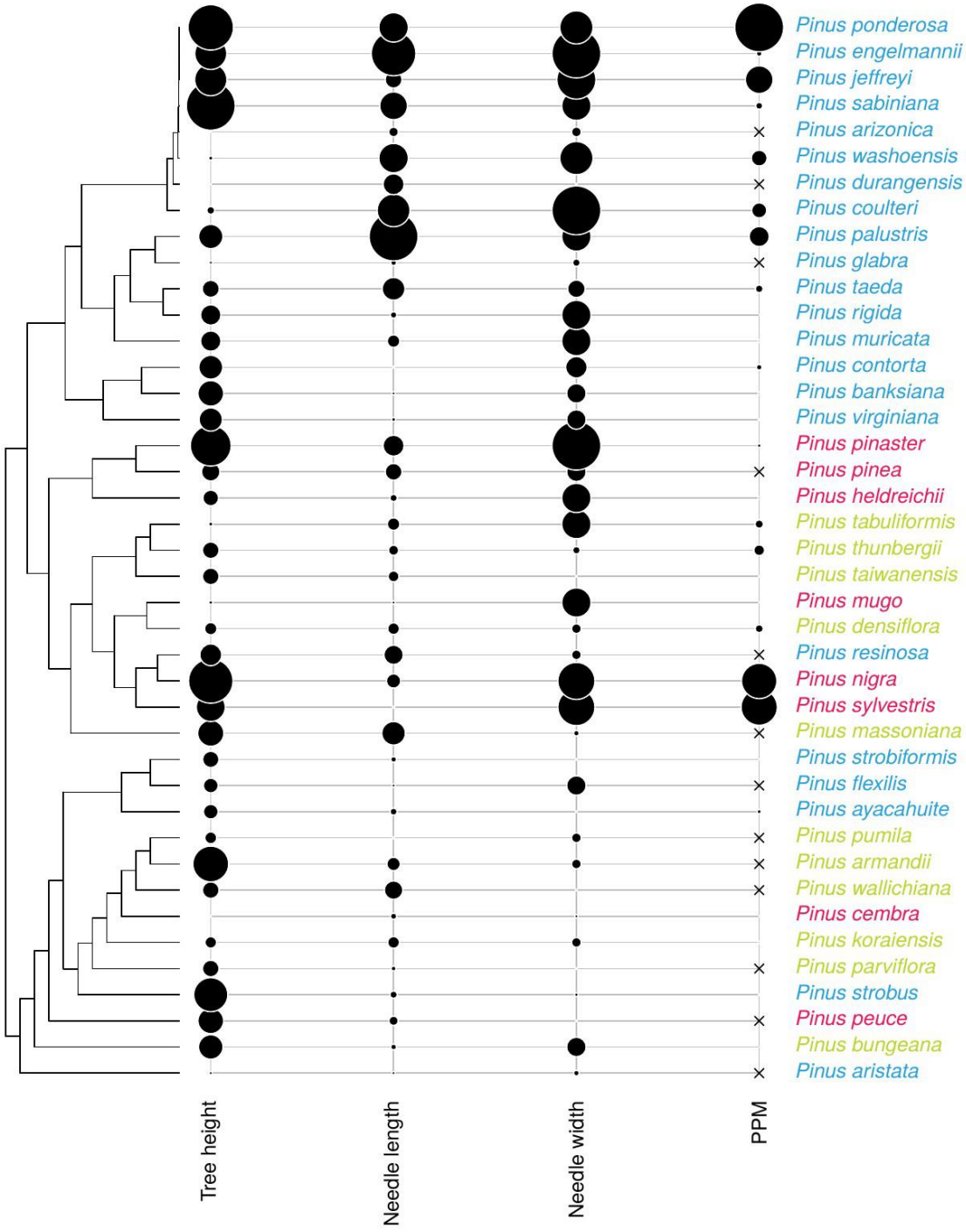

Figure 2

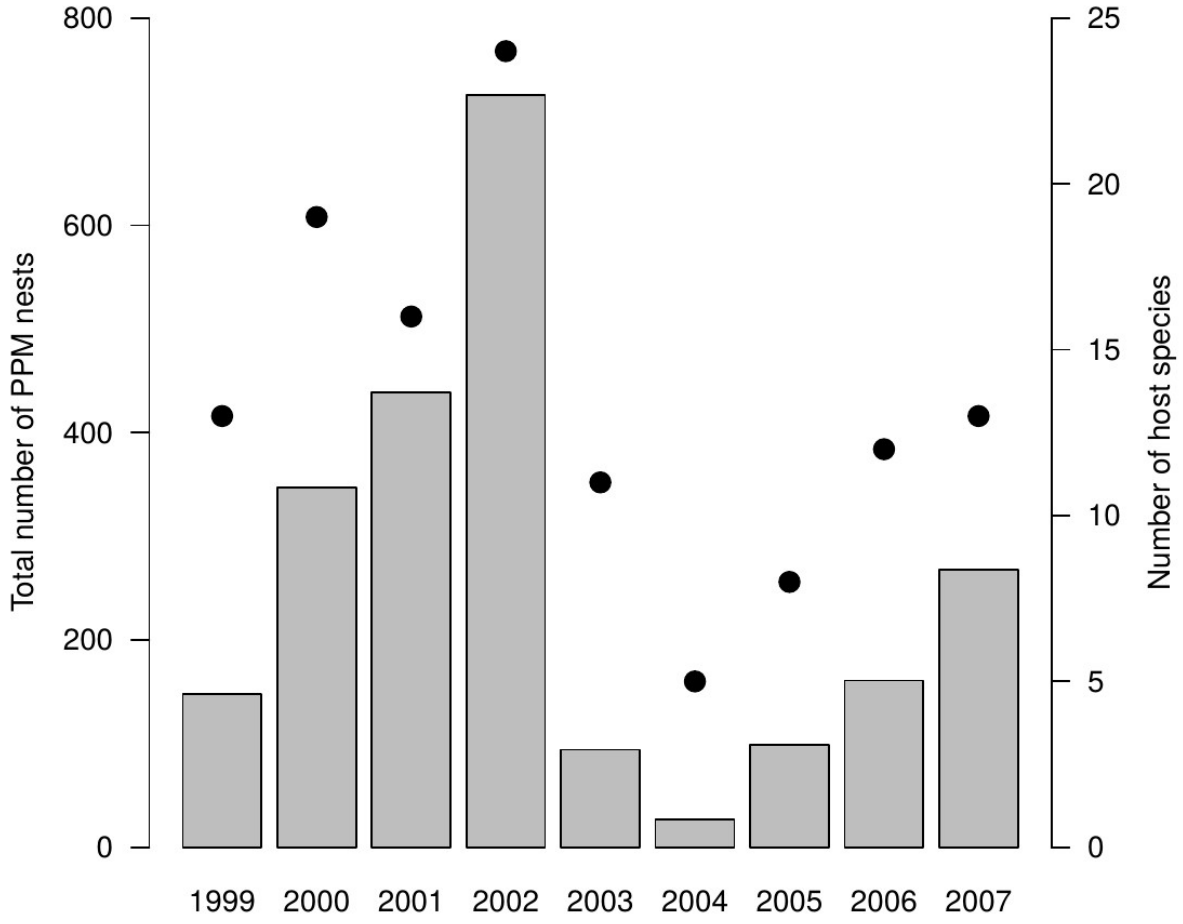
800
600
400
200
0
Total number of PPM nests
25
20
15
10
5
0
Number of host species
1999
2000
2001
2002
2003
2004
2005
2006
2007

Figure 3

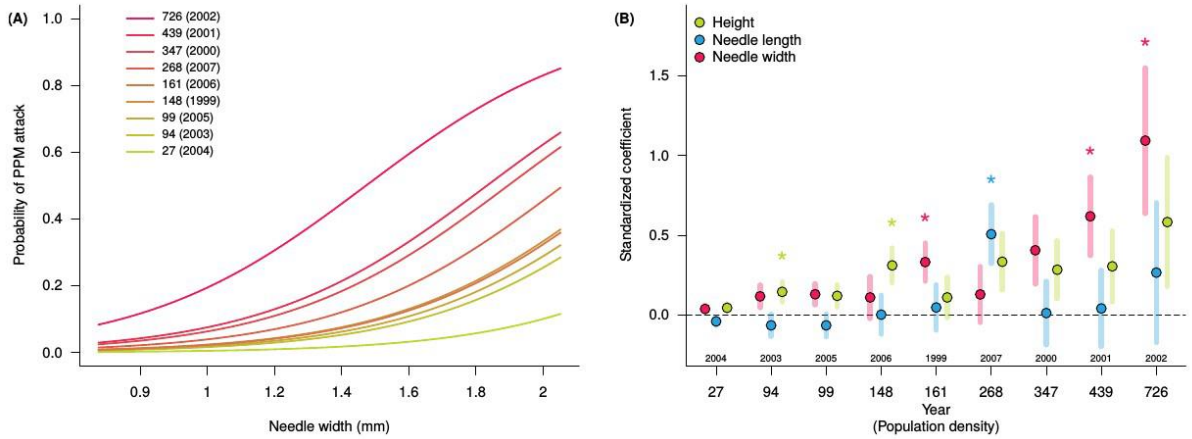

Figure 4

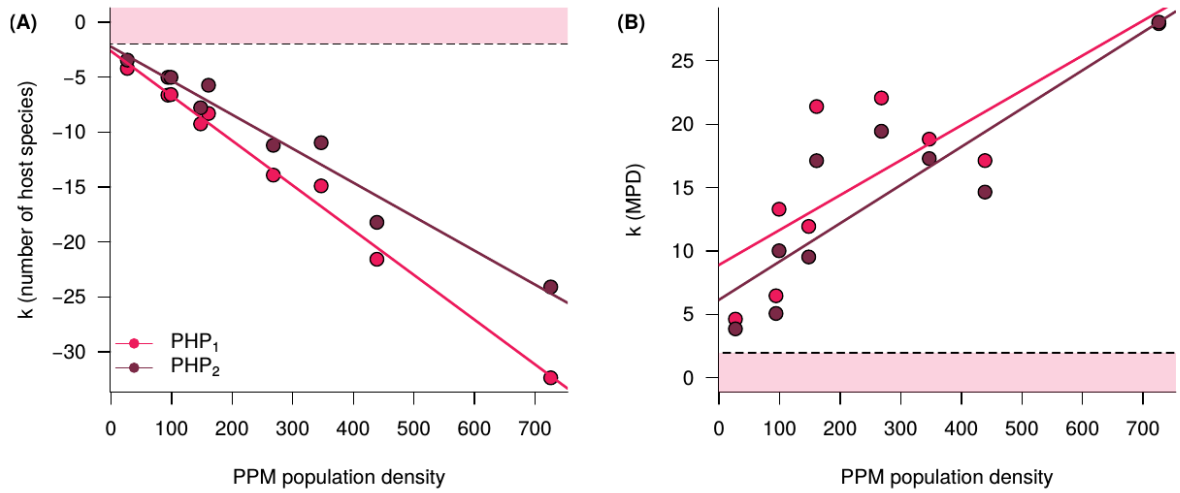

Annex 3. Analysis of genome size evolution and its relationship with hydraulic traits in conifers.

We obtained genome size data (http://data.kew.org/cvalues/) for over 150 species of conifers for which we have measured P_{50}. We tested for a simple correlation between these variables, and found a weak relationship (R^2=0.1). It seems at least that there are limits on genome size in cavitation resistant clades (or that having a large genome limits cavitation resistance). Note the outlier Juniperus chinensis with a duplicated genome (tetraploid). We also reconstructed the evolution of both traits, looking for meaningful trends. Both Callitroidae and Cupressoidae crown groups have high cavitation resistance and small genomes.

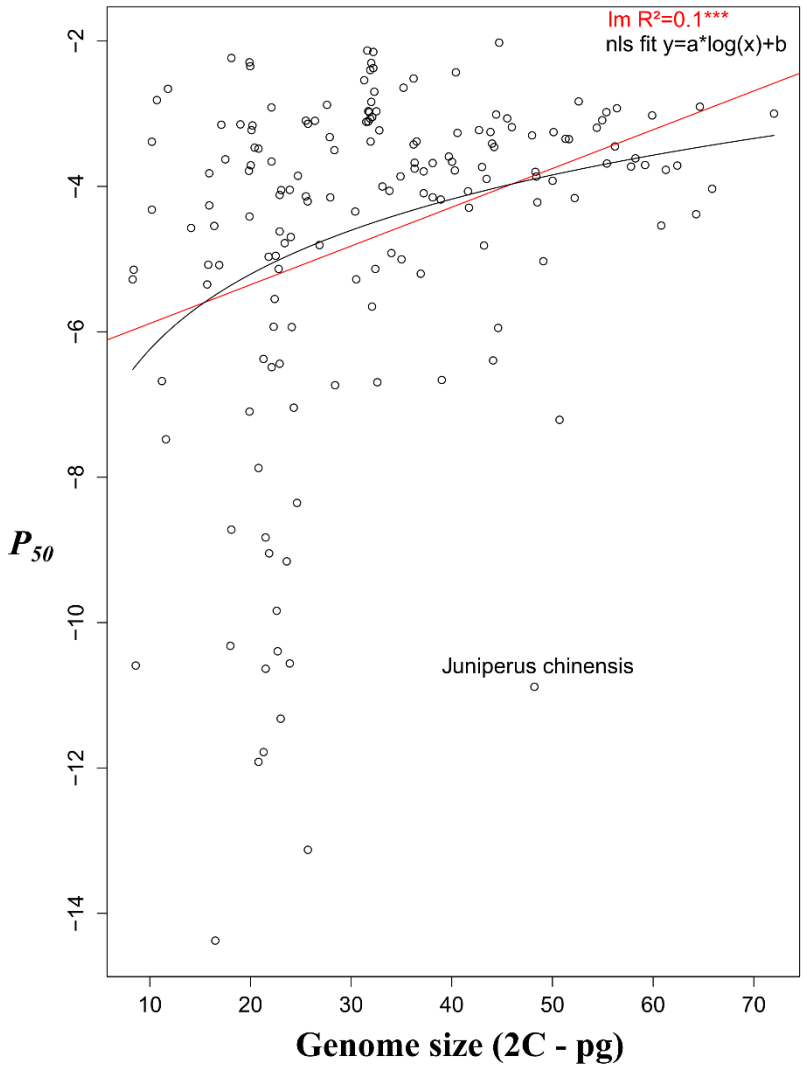

Figure 1. Relationship between cavitation resistance and genome size in conifers. Red line is the linear model, curve is the best fit log function. P_{50} in MPa; genome size is 2 times C-value (or the amount of DNA in the diploid nucleus) in picograms.

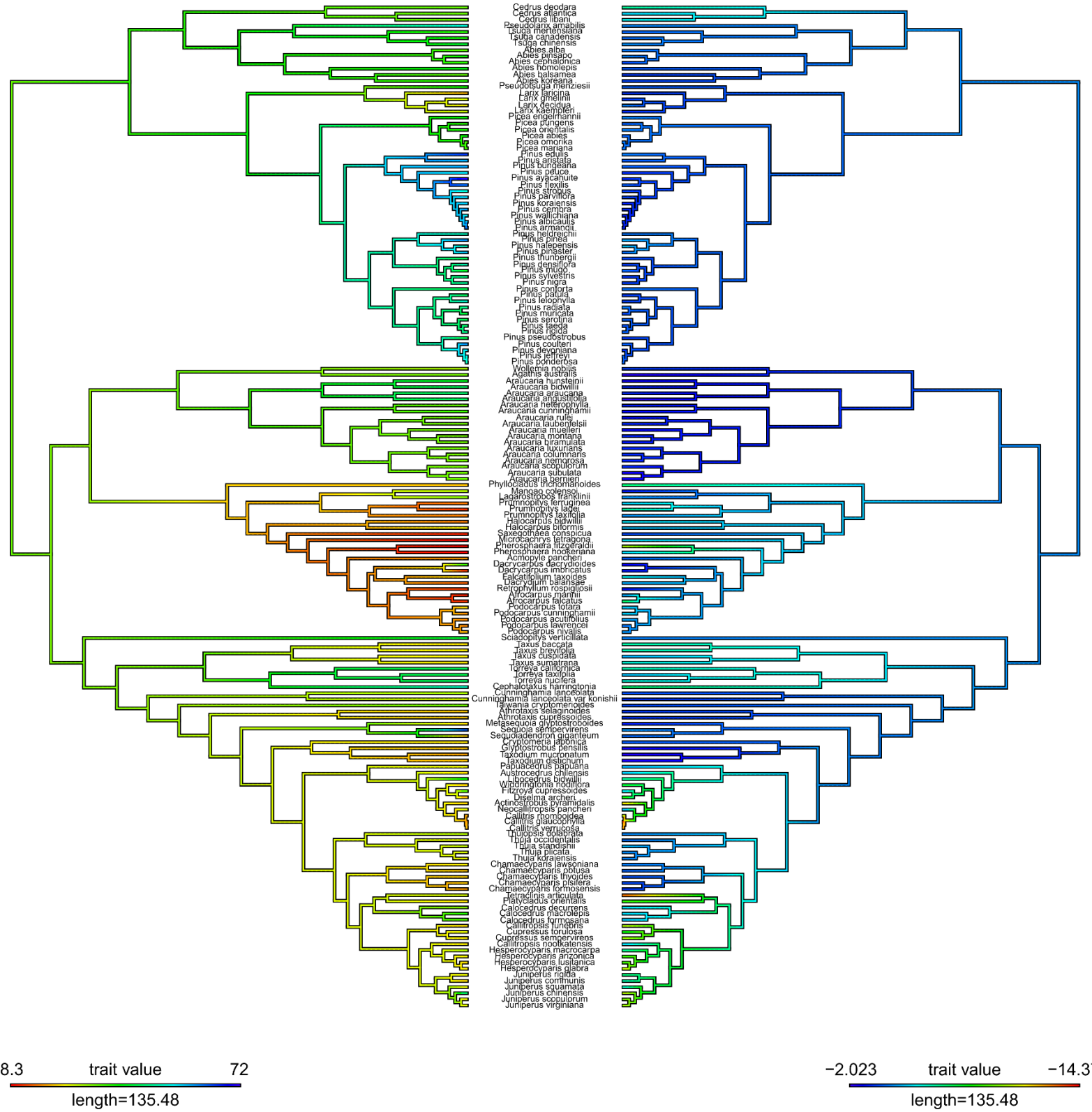

Figure é2. Mirror plot of the evolution of genome size (left) and cavitation resistance (right). The smallest genomes are commonly found in Podocarpaceae, whereas the most cavitation resistant species are in crown groups within Cupressaceae. On the other hand, pines have undergone rapid evolution of the size of their genomes.

Annex 4. Analysis of cavitation resistance using the auteur method (Eastman et al., 2011).

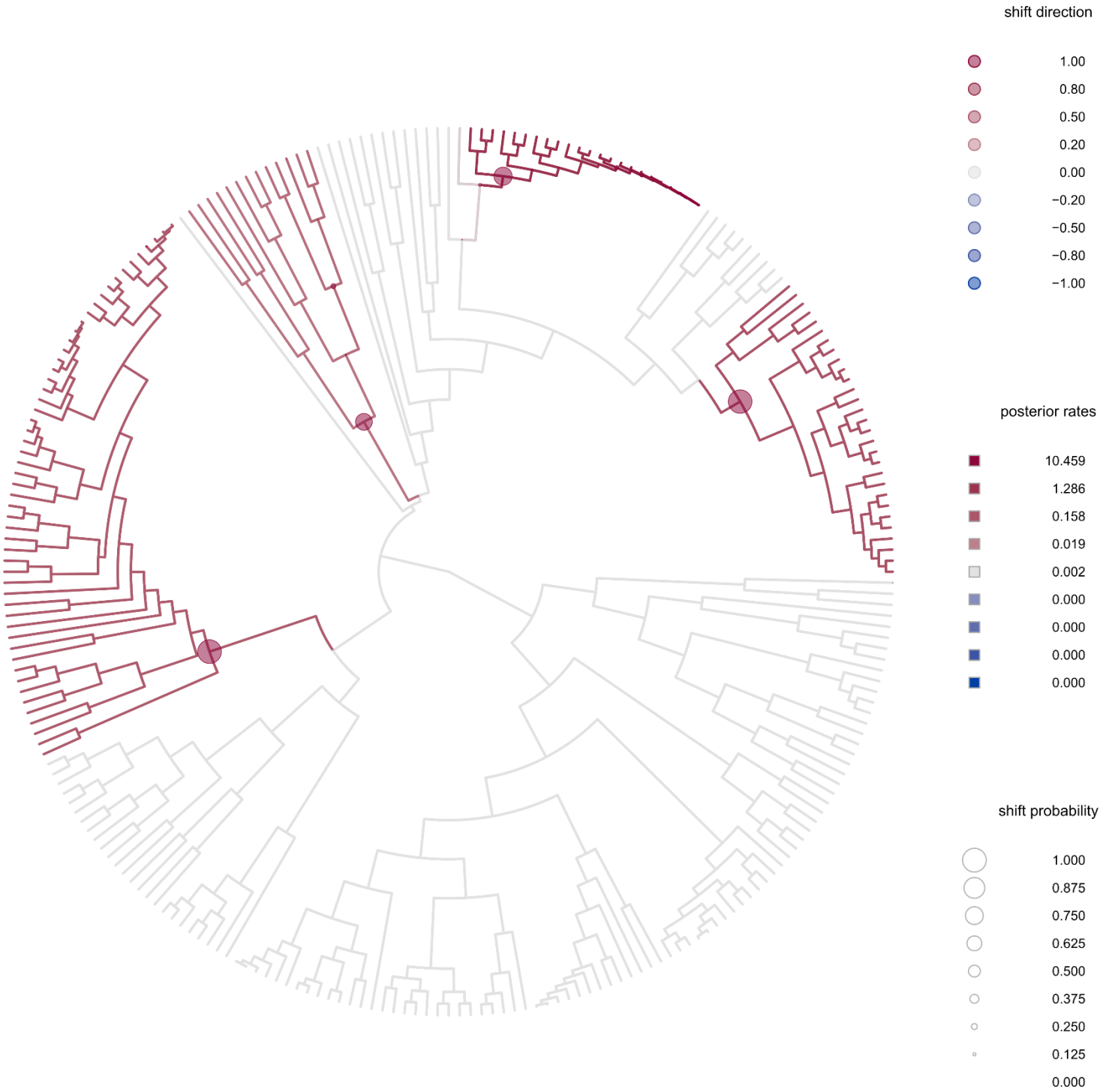

Figure 1. P_{50} evolution in conifers. Posterior rate shifts and branch evolutionary rates from the *auteur* analysis in R. We used the relaxed Brownian motion with shifts algorithm. We recover 4 shifts to faster evolving regimes that concur with the BAMM results presented in Chapter 4 of this thesis.

Annex 5. Examination of the relationship between warts and callitroid thickenings and cavitation resistance in the Callitris clade

Based on data from Heady et al. (1994).

While we did not perform extensive sampling and measurements with SEM, we recovered published data to investigate relationships between sculpturing within tracheids and ecology and physiology in Callitris.

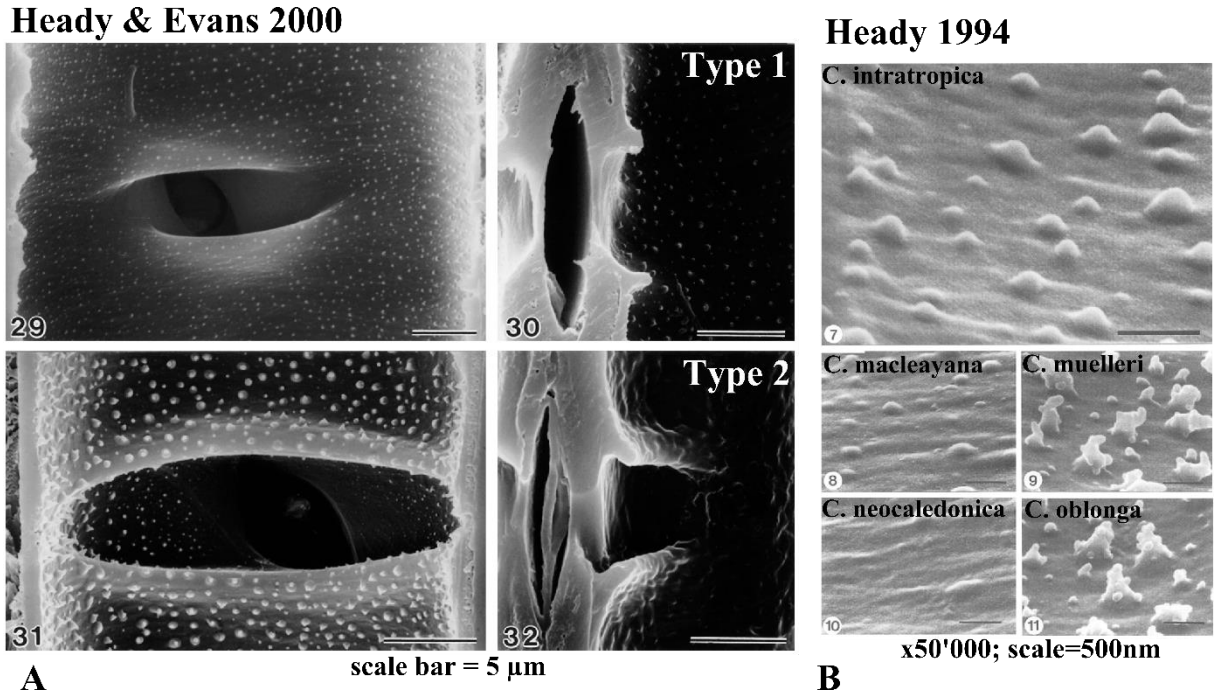

Figure 1. SEM views of **A**) "callitroid thickenings" with the two types identified: top (type 1) with relatively shallow bands that do not reach the tracheid walls, and bottom (type 2) deeper funnelling of the bands which extend across the width of the lumen to reach both radial walls; and B) warts from several species, either small and of simple hemispherical shape (top and left – wet habitat species) or large, convoluted with extending "arms" or nodules (bottom right two photos – drier and/or colder habitats).

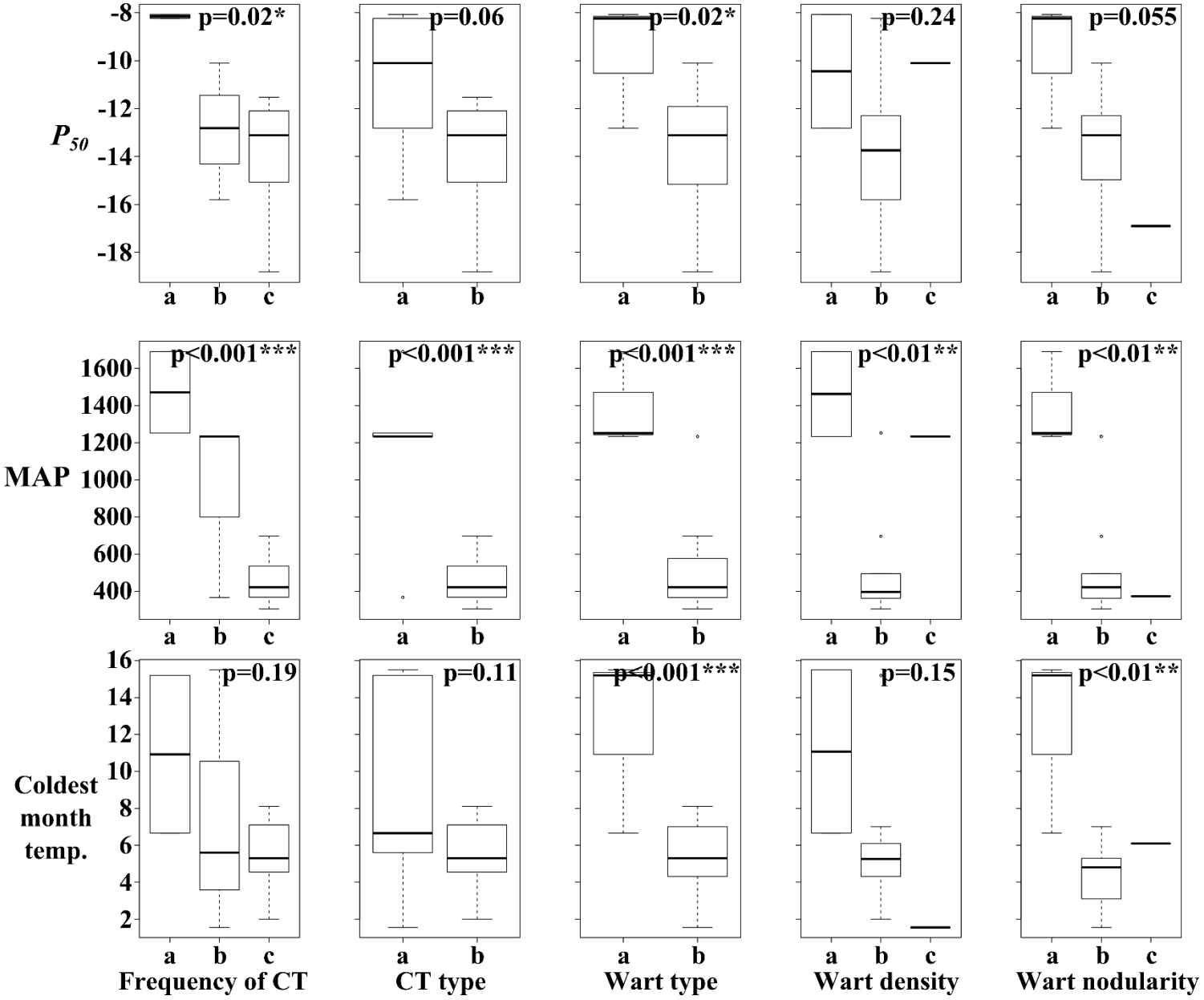

Figure 2. Relationships between P_{50}, Mean annual precipitations (MAP), minimum temperature of the coldest month and "callitroid thickening" and "wart" traits across the *Callitris* clade. P-values reported from anovas in R. Characters are coded as in Piggin et al. 2010: Frequency of CT: a = low (<10% of tracheids with CT); b = intermediate (from 10 to 60%) and c = frequent (over 60%). CT type: a = type 1, b = type 2 (fully reaching both sides of the tracheid). Wart type: a = uniform warts, all small and hemispherical with no nodules; b = not uniform, some nodulated larger warts. Wart density: a = fewer than 1.5 warts per µm²; b = between 1.5 and 3.2 warts per µm²; and c = between 3.2 and 6 warts per µm². Finally, Wart nodularity: a = no nodules; b = 20-60% of warts with nodules; and c = between 60 and 90% of warts with nodules.

Annex 6 : Les conifères, une famille à évolution complexe. Maximilien Larter et Pauline Bouche (Jardins de France 2012 – Hors-série Les conifères font de la résistance)

Les conifères, une famille à évolution complexe

Les conifères font de la résistance par Maximilien Larter et Pauline Bouche

Les plantes à « graines nues » que sont les gymnospermes font partie de la lignée des plantes à graines, au même titre que les angiospermes. Mais de nombreuses différences les distinguent. Souvent considérés comme des végétaux fossiles, les gymnospermes offrent des caractéristiques très intéressantes comme la résistance à la sécheresse. Maximilien Larter et Pauline Bouché nous font entrer dans les dédales de la grande famille des conifères ou plutôt ce groupe composé de sept familles. Mais ce n'est pas qu'un jeu !

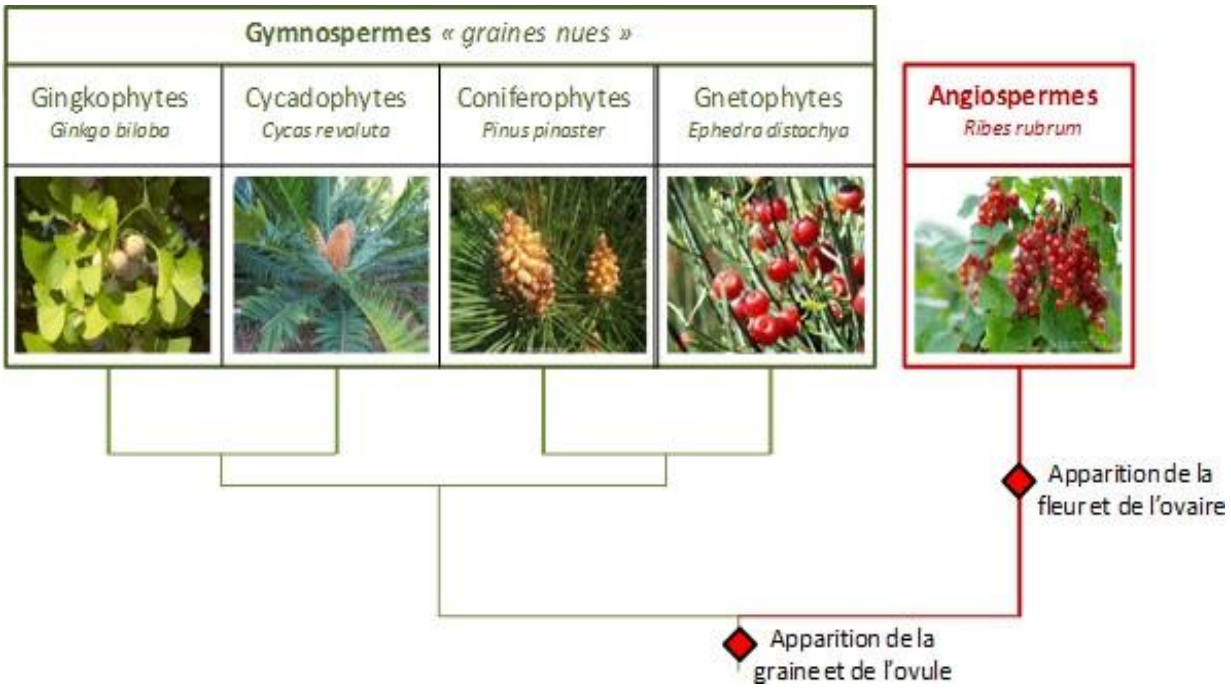

Arbre décrivant les relations entre les groupes de plantes à graines (Spermaphytes). A noter que la position des Cycadophytes et des Gnétophytes (tirées ici de la littérature) est encore débattu entre phylogénéticiens et taxonomistes.

Des aiguilles, des écailles, des cônes, et des trachéides

Si les gymnospermes (Gingkophytes, Coniferophytes, Gnetophytes et Cycadophytes) et les angiospermes appartiennent à la lignée des plantes à graines (spermaphytes) ils n'en sont pas moins radicalement différents.

En effet, les gymnospermes ou littéralement « plantes à graines nues » ne présentent pas de fleur ni de fruit comme les angiospermes, mais des cônes ouverts laissant les ovules et graines qu'ils portent exposées à l'air libre (fig. 1). Si l'on s'attarde sur l'anatomie plus « profonde » de ces plantes on constate que leur système hydraulique, appelé xylème (tuyau qui transporte la sève) est constitué uniquement de trachéides contrairement aux angiospermes dont le xylème comprend à la fois des trachéides et des vaisseaux.

Bien que les critères de distinctions Angiospermes-Gymnospermes semblent clairs, il existe cependant une discordance à propos de l'appartenance des Gnétophytes à la lignée des Gymnospermes – ce sont par exemple *Welwischia mirabilis* (désert de Namibie), *Ephedra distachya* (le Raisin de mer, commun sur les côtes atlantiques françaises) ou encore *Gnetum nodiflorum* (Amérique du Sud). En effet, les Gnétophytes présentent des ressemblances morphologiques avec les Angiospermes telles que la présence de « pseudo fruit ». Autre chose surprenante, le xylème des Gnétophytes est composé de trachéides et de vaisseaux, comme les angiospermes… Sur ces critères morphologiques, nos Gnétophytes seraient donc plus apparentés aux Angiospermes. Mais des analyses moléculaires (voir encadré 1) semblent indiquer que les Gnétophytes seraient un groupe frère des Conifèrophytes confirmant ainsi leur appartenance aux Gymnospermes (fig. 1). Alors d'où viennent ces ressemblances avec les angiospermes ? Il semble que cela résulteraient d'une convergence évolutive de ces deux groupes, c'est-à-dire l'apparition indépendante (dans différentes lignées) de caractères similaires. On cite souvent comme exemple l'évolution des ailes chez les oiseaux et les chauves-souris : ces lignées éloignées (respectivement au sein des dinosaures et des mammifères) ont développé à environ 100 millions d'années d'écart une capacité de vol similaire !

Le grand groupe des conifères

Les relations entre les 7 familles de conifères sont désormais bien connues (fig. 2). La famille des *Pinaceae* (pin, cèdre, mélèze, sapin) occupe une position basale par rapport à toutes les autres familles (c'est la lignée la plus ancienne). Vient ensuite la séparation des *Araucariaceae* (*Araucaria araucana,* le désespoir du singe) et des *Podocarpaceae* (grande famille d'espèces tropicales de l'hémisphère sud, bien souvent à « feuilles » larges). A noter que certains auteurs insèrent une famille supplémentaire au sein de cette dernière famille, les *Phyllocladaceae* (contenant les 5 espèces du genre *Phyllocladus* – originaires des îles d'Asie du Sud-est). Ces espèces sont caractérisés notamment par des excroissances de tige ressemblant (mais d'origine différente) à des feuilles, ce qui justifie selon certains auteurs leur positionnement dans une famille à part. Une seule espèce appartient à la famille des *Sciadopityaceae*, *Sciadopitys verticillata* (le pin parasol du Japon). Les familles *Cephalotaxaceae* et *Taxaceae* (les ifs) sont très proches et sont parfois regroupées, et vient enfin la grande famille des *Cupressaceae* (cyprès, genévrier, thuya, séquoia), seule famille que l'on retrouve dans les deux hémisphères.

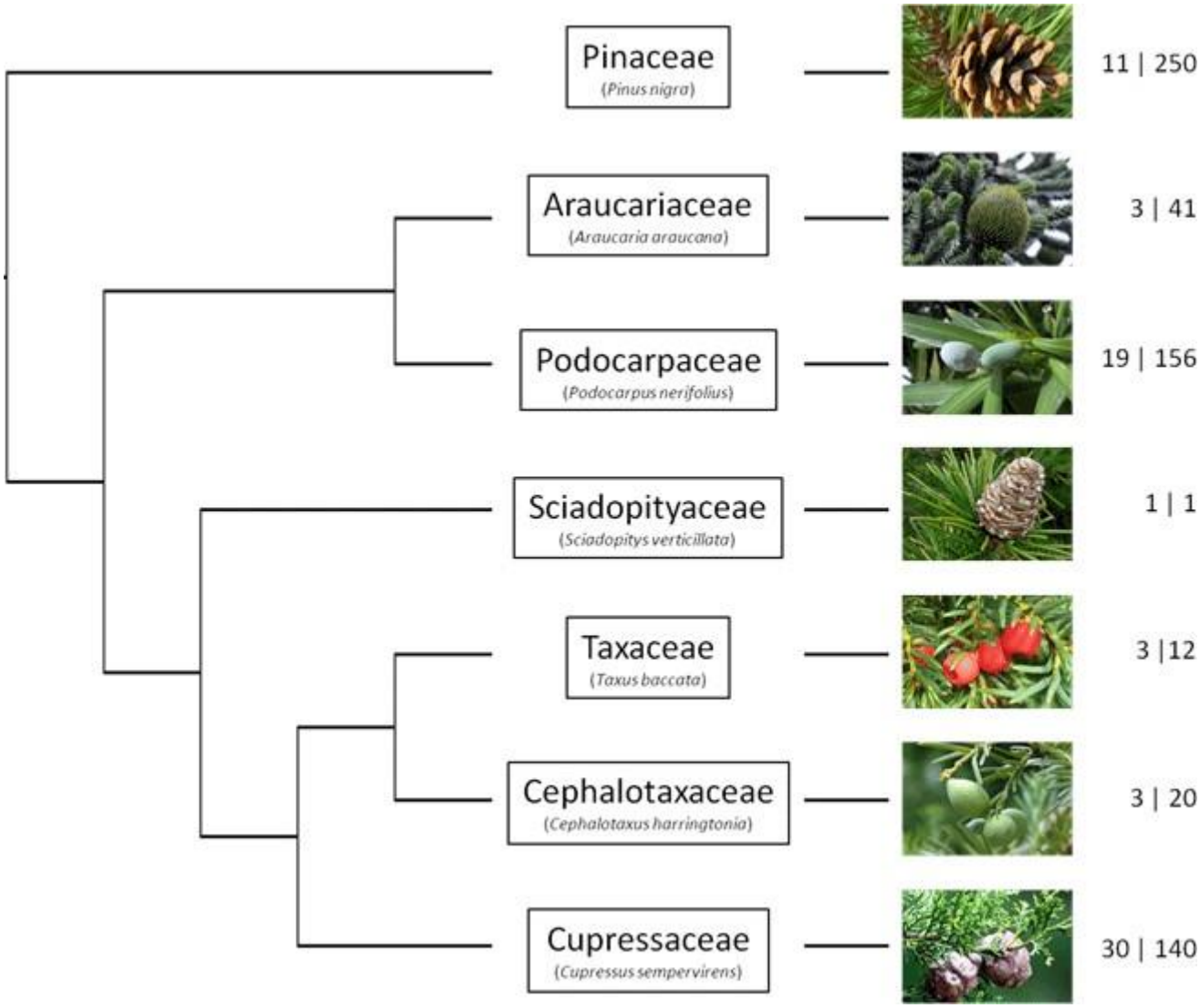

Arbre phylogénétique décrivant les relations entre les 7 familles de conifères. Pour chaque famille un exemple d'espèce typique est donné (en photo) ainsi que leur importance (nombre de genres | nombre d'espèces).

Evolution à une échelle géologique

L'incorporation d'informations tirées de fossiles de plantes dans les phylogénies moléculaires permet d'y ajouter un cadre temporel. On sait par exemple que les premiers fossiles de gymnospermes apparaissent vers la fin du Carbonifère, il y a entre 300 et 310 millions d'années ; ou encore que les premiers cônes typiques de la famille des pins (*Pinaceae*) sont apparus il y a 225 millions d'années. Différentes méthodes ont été élaborées pour mêler ces « calibrations fossiles » et des données moléculaires pour définir des phylogénies dans lesquelles les branches représentent le temps (généralement en millions d'années). Ceci a permis récemment d'apporter de nouvelles connaissances sur l'évolution de différents groupes des plantes.

Le terme de « fossile vivant » décrit un organisme dont la lignée évolutive est ancienne (présence de fossiles de plusieurs dizaines voire centaines de millions d'années) et dont la morphologie actuelle est similaire à ses ancêtres fossilisés. Le cœlacanthe est probablement l'exemple le plus connu de « fossile vivant » : cette espèce de poisson était considérée éteinte avant d'être découverte au milieu du XX^{e} siècle dans l'Océan Indien et sa morphologie n'aurait pas évolué en près de 400 millions d'années. Chez les plantes, le *Ginkgo*, les *Cycas*, et certains conifères (comme le *Wollemia* lien vers l'article sur le Wollemia) ont souvent été qualifiés de « fossiles vivants ». De récentes études moléculaires viennent toutefois contredire ces certitudes.

La lignée des Cycadophytes est ancienne, ayant atteint un niveau maximal de diversité et de dominance durant le Crétacé et le Jurassique (199,6 à 65,5 M d'années). Cependant, Nagalingum *et al*. (2011) ont construit une phylogénie de 199 espèces (sur environ 300) pour ce groupe de plantes, et ont montré que les genres importants (*Cycas*, *Encephalartos*, *Zamia*, *Macrozamia* et *Ceratozamia*) ont subi une diversification rapide et récente, il y a environ 10 M d'années. Les auteurs indiquent que l'émergence des climats modernes vers la fin du Miocène (il y a 5 à 10 M d'années), avec de larges régions tropicales et subtropicales à saison des pluies très marquées pourrait expliquer cette radiation[1].

Des résultats similaires ont été publiés récemment chez les conifères. Leslie *et al*. (2012) ont étudié près de 500 espèces de conifères, et ont montré une diversification récente au cours des 20 derniers millions d'années. Leurs résultats sont d'autant plus intéressants qu'ils montrent que les groupes d'hémisphère nord (*Pinaceae*, et la sous-famille des *Cupressoideae*) seraient d'origine plus récente (< 5 M d'années) que des groupes d'hémisphère Sud (*Araucariaceae*, *Podocarpaceae*, et la sous-famille des *Callitroideae* - entre 5 et 17 M d'années). Ils émettent l'hypothèse que ces différences seraient liées aux cycles de glaciations qui auraient marqué l'hémisphère Nord entraînant l'évolution des plantes pour s'adapter aux changements climatiques.

[1] Diversification plus ou moins rapide d'une lignée, avec notamment une multiplication du nombre d'espèces, l'apparition d'une grande diversité morphologique et l'occupation de nombreux habitats (par exemple la radiation des mammifères à la fin du Crétacé).

Et en termes de résistance à la sécheresse…

De manière générale, des études ont montré que les conifères sont plus résistants à la sécheresse que les angiospermes (Maherali *et al.* 2004). La question qui se pose alors est : quels sont les mécanismes anatomiques et physiologiques à la disposition des arbres pour résister au manque d'eau ? Lors de sécheresses intenses, des bulles d'air se propagent dans les éléments conducteurs du xylème empêchant ainsi le transport de l'eau des racines jusqu'aux feuilles de façon similaire à une embolie pulmonaire. Ce mécanisme appelé cavitation provoque un dysfonctionnement du transport hydrique et peut, à terme, conduire à la mort des organes et de l'arbre. Si l'on observe l'anatomie fine du système de transport de l'eau (le xylème), on constate que l'eau circule à travers des structures poreuses

présentes dans la paroi des éléments conducteurs du xylème appelées « ponctuations » (fig. 3). Chez les espèces à vaisseaux, comme les angiospermes, elles sont constituées uniquement d'un réseau de tresses (microfibrilles) formant une membrane poreuse (fig. 3 – A). Celles des conifères, plus complexes, présentent un épaississement (torus) au centre de la membrane de microfibrilles formant une barrière plus efficace contre le passage de l'air (fig. 3 - B). Lorsqu'un conduit est rempli d'air, le torus agit comme une valve : il est aspiré par l'eau contre la paroi de la trachéide fonctionnelle, et empêche le passage de l'air (fig. 3 – d).

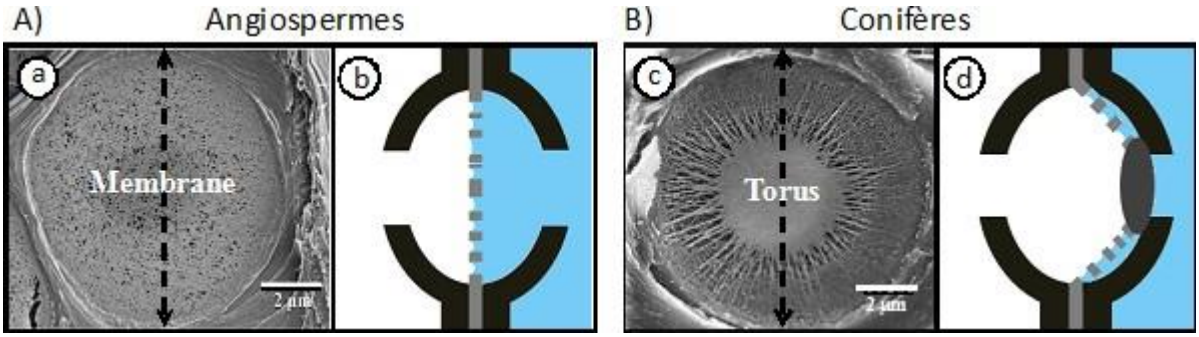

Figure 3 : A. Coupe longitudinale (a) et transversale (b) d'une ponctuation chez les angiospermes avec présence d'une membrane de microfibrilles. B. Coupe longitudinale (c) et transversale (d) d'une ponctuation chez les Conifères avec un torus au centre de la membrane de microfibrilles.

Cette structure très sophistiquée de « sécurité hydraulique » qu'est le torus est apparue chez les gymnospermes modernes (Ginkgo, Gnétales et Conifères) mais est absente chez leurs cousins les Cycadophytes. De manière indépendante, dans des phénomènes d'évolution convergente, 8 genres de 5 familles éloignées d'Angiospermes ont également développés un torus. Des chercheurs bordelais examinent actuellement la résistance à la sécheresse dans des lignées avec et sans torus, pour examiner son rôle dans la protection contre l'embolie dans le système conducteur de la plante.

Afin de caractériser la résistance à la cavitation d'une espèce, les chercheurs utilisent une courbe de vulnérabilité qui correspond à l'évolution du taux d'embolie (cavitation) avec l'augmentation de la sècheresse. Pour cela des branches sont laissées sur la paillasse au laboratoire pendant plusieurs heures pour obtenir différents niveaux de sècheresse. A chaque niveau, le degré d'embolie est mesuré. Ces courbes permettent de déterminer la pression négative[2] qui induit 50% d'embolie dans la branche, aussi appelé P_{50}. Ce paramètre permet ainsi de comparer la résistance à la sécheresse des espèces. Nous savons par ailleurs, que ce seuil de 50% induit la mort des conifères lorsqu'il est atteint en milieu naturel. Pour les valeurs proches de 0 (faiblement négatives, entre -1 et -4 MPa) l'espèce est jugée peu résistante, et à l'inverse à partir de -7 MPa, l'espèce peut tolérer des sécheresses importantes. A titre d'exemple, le cyprès chauve (*Taxodium*) est l'une des espèces les moins résistantes du monde (P_{50} =-2,3 MPa) alors que le record absolue a été mesuré chez une espèce semi-désertique australienne (*Callitris columellaris*, P_{50} =-16 MPa, Delzon *et al*. 2010, Brodribb *et al*. 2010).

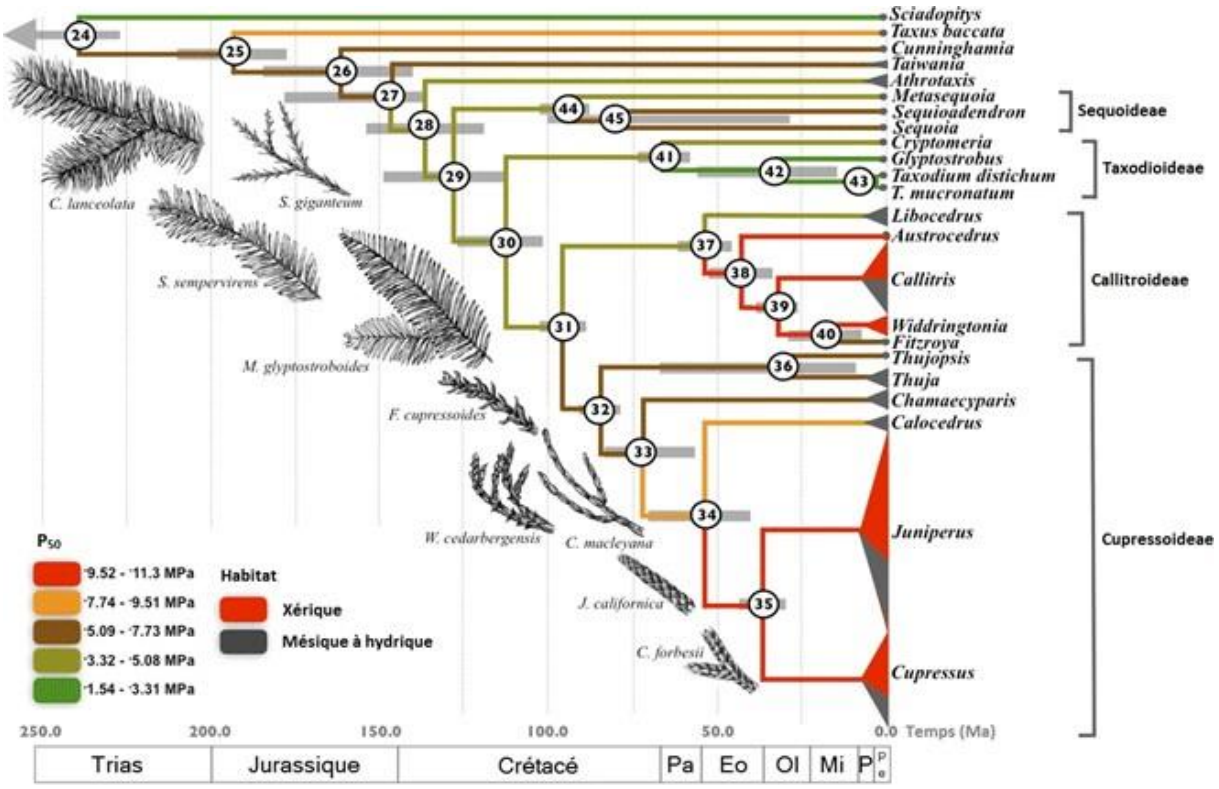

Figure 4 : Phylogénie de la famille des Cupressaceae (tirée de Pittermann et al. 2012) décrivant l'évolution de la résistance à la cavitation au sein de cette famille. La couleur des branches représente la résistance à la cavitation (en rouge les espèces résistantes, et en vert les espèces vulnérables). Les expansions aux extrémités de l'arbre indiquent le nombre d'espèces dans chaque genre, et leur couleur correspond à l'habitat des espèces (en rouge pour les milieux arides, et en gris pour les milieux plus humides) et des exemples de type de feuillages de quelques espèces sont donnés. (Pa = Paléocène, Eo=Eocène, Ol = Oligocène, Mi = Miocène, P = Pliocène, Pe = Pléistocène).

Pittermann *et al*. (2012) ont étudié la résistance à la cavitation chez une vingtaine d'espèces de conifères de la famille des *Cupressaceae*. L'utilisation d'une phylogénie (fig. 4) leur a permis de découvrir que les espèces résistantes à la cavitation sont apparues dans deux groupes séparés géographiquement, les *Callitroideae* (hémisphère Sud) et les *Cupressoideae* (hémisphère Nord), et semble coïncider avec l'apparition de milieux plus arides à la fin de l'Eocène (il y a environ 35 M d'années). Cette adaptation coïncide (i) avec l'évolution des aiguilles en écailles chez ces espèces (principalement *Callitris*, *Cupressus* et *Juniperus*) (ii) et une diversification de ces groupes avec un plus grand nombre d'espèces.

A l'opposé, dans la famille des *Pinaceae*, on observe une stase évolutive, c'est-à-dire que toutes les lignées ont maintenu une faible résistance à la cavitation. Cela peut sembler surprenant puisque ce groupe couvre une large gamme climatique, allant du bassin méditerranéen (*Cedrus libani*) au cercle polaire (*Larix gmelinii*), et des dunes côtières (*Pinus pinaster*) aux sommets des montagnes (*Pinus hartwegii*, l'arbre le plus haut du monde, vivant à plus de 4300 m d'altitude au Mexique). De plus au sein d'une même espèce, comme par exemple chez le pin maritime, les populations d'environnement très sec (Maroc – moins de 500 mm de pluie par an) et plutôt humide (Sud Ouest de la France – jusqu'à 1200

mm) présentent une résistance à la sécheresse similaire (Lamy *et al.* 2011). D'après cette étude, la résistance à la cavitation chez le pin maritime serait « canalisée » : des mécanismes génétiques limiteraient l'effet de nouvelles mutations, maintenant ainsi une résistance identique chez tous les individus provenant pourtant de climats très différents. A l'échelle des Conifères, il semble donc que certaines lignées (notamment au sein des *Cupressaceae*) ont pu se défaire de ces contraintes évolutives. Une équipe de chercheurs européens essaie actuellement d'établir quelles modifications ont permis de lever ces contraintes, en particulier au niveau de l'anatomie du xylème. La compréhension de ces mécanismes évolutifs est essentielle pour prévoir par exemple, la capacité d'adaptation des espèces et donc l'effet du changement climatique sur les écosystèmes forestiers dans les décennies à venir.

> Pour en savoir plus

[2] « Aspirée » à partir des feuilles, l'eau dans la plante circule sous tension (pression négative - phénomène similaire à l'aspiration de l'eau dans un verre avec une paille) : plus le sol est sec ou plus le climat est chaud, plus la plante doit « aspirer » fort pour extraire de l'eau du sol, et donc plus la « pression » dans le xylème est négative !

Annex 7 : Le Pinetum de Bedgebury : « la plus belle collection de conifères du monde ». Maximilien Larter (Jardins de France 2012 – Hors-série Les conifères font de la résistance)

Le Pinetum de Bedgebury : « la plus belle collection de conifères du monde »

Les conifères font de la résistance par Maximilien Larter

Petit frère des « Royal Botanical Gardens » de Kew, ce parc botanique, consacré exclusivement aux conifères, unique au monde vaut vraiment le détour ! Dans une forêt rachetée par la Couronne au début du XX^{e} siècle, le Pinetum est né d'une collaboration entre la Forestry Commission (chargée de gérer les forêts britanniques) et le Jardin Botanique de Kew parce-que la pollution de l'air de la capitale nuisait à la santé de certains conifères.

Le Pinetum de Bedgebury - © S. Delzon

Sous l'aile avisée d'un expert « ès conifères » mondialement reconnu, William Dallimore, la plantation débute en 1925, avec une organisation taxonomique : chaque parcelle regroupe les espèces d'un même genre. Suite à des dégâts considérables (30% de perte) lors de la tempête en 1987, la stratégie bascule vers une gestion plus harmonieuse du paysage : l'objectif est maintenant de mélanger les essences, feuillus et conifères, et de maintenir environ 40% d'espace ouvert. Ceci permet à la fois de mettre en avant les caractéristiques des espèces (port de l'arbre, couleur du feuillage), de maintenir une biodiversité impressionnante (oiseaux, insectes, fleurs, champignons) et de proposer des visites magnifiques au public tout au long de l'année !

Conservation et recherche

L'objectif depuis la création du Pinetum est de maintenir et de développer la plus grande collection de conifères du monde. Environ 200 espèces de conifères (principalement tropicales) ne supportent pas le gel, et donc ne peuvent être plantées à Bedgebury. Toutefois, le parc compte plus de 60% des espèces existantes ! Des expéditions régulières à travers le monde pemettent de récolter des graines, et dans différentes pépinières, les plantes sont soigneusement élevées jusqu'à être plantées dans la zone idéale du Pinetum. En effet, des études très précises du sol et des micro-climats du parc sont réalisées en continu, pour associer chaque plante avec un environnement optimal pour son développement. Plus de la moitié des espèces de conifères du monde sont menacés selon la liste rouge de l'Union internationale pour la conservation de la nature. Les employés du Pinetum récoltent donc des graines d'un maximum de populations pour chaque espèce, et développe pour les espèces les plus menacées de véritables « banques génétiques » vivantes. En effet, certains des individus les plus anciens du site sont issus de populations qui ont maintenant disparues ! Cette ressource est très importante dans l'objectif de restaurer certains écosystèmes détruits par l'activité humaine. En outre, les scientifiques ont un accès privilégié au Pinetum : des chercheurs ont ainsi découvert une variété d'if conservée uniquement à Bedgebury qui contient des taux exceptionnels de *taxol*, composé chimique utilisé pour traiter les cancers ! Notre équipe d'écophysiologie à l'Université de Bordeaux a aussi la chance de collaborer avec l'équipe du Pinetum pour étudier la résistance à la sécheresse des conifères du globe.

Pour le public

Avec des chemins de randonnées pédestres ou cyclistes, des aires de jeux à thème pour les enfants, et des parcours acrobatiques au sommet des arbres pour les plus courageux, le parc propose des activités pour tous les âges et tous les goûts. Le Pinetum s'investit également dans un rôle éducatif et de sensibilisation sur le thème de la conservation de la biodiversité, notamment par le biais de sorties scolaires. Ouvert au public tous les jours de l'année (sauf Noël), le Pinetum de Bedgebury se situe dans le sud-est de l'Angleterre, à moins d'une heure de Londres et de Douvres. Amateurs de plantes et de nature, une visite s'impose !